ZEBRAFISH AS A MODEL FOR ANALYSIS OF SIGNALING PATHWAYS INVOLVED IN CELL GROWTH, PROLIFERATION AND DEVELOPMENT

A THESIS SUBMITTED TO
THE DEPARTMENT OF MOLECULAR BIOLOGY AND GENETICS
AND THE INSTITUTE OF ENGINEERING AND SCIENCE
OF BILKENT UNIVERSITY
IN PARTIAL FULFILLMENT OF THE REQUIREMENTS
FOR THE DEGREE OF DOCTOR OF PHILOSOPHY

By
CEREN SUCULARLI

January 2011

I certify that I have read this thesis and that in my opinion it is fully adequate, in scope, and in quality, as a thesis for the degree of Doctor of Philosophy.

_____
Assist. Prof. Dr. Özlen Konu

I certify that I have read this thesis and that in my opinion it is fully adequate, in scope, and in quality, as a thesis for the degree of Doctor of Philosophy.

_____
Assoc. Prof. Dr. Işık G. Yuluğ

I certify that I have read this thesis and that in my opinion it is fully adequate, in scope, and in quality, as a thesis for the degree of Doctor of Philosophy.

_____
Prof. Dr. Mehmet Öztürk

I certify that I have read this thesis and that in my opinion it is fully adequate, in scope, and in quality, as a thesis for the degree of Doctor of Philosophy.

_____
Assist. Prof. Dr. Sreeparna Banerjee

I certify that I have read this thesis and that in my opinion it is fully adequate, in scope, and in quality, as a thesis for the degree of Doctor of Philosophy.

_____
Assoc. Prof. Dr. Hilal Özdağ

Approved for the Institute of Engineering and Science

_____
Prof. Dr. Levent Onural
Director of the Institute of Engineering and Science

To my mother, Canan Sucularlı
and my brother, Ahmed Enlil Sucularlı

ABSTRACT

Zebrafish as a model for analysis of signaling pathways involved in cell growth, proliferation and development

Ceren Sucularlı
Ph.D. in Molecular Biology and Genetics
Supervisor: Assist. Prof. Dr. Özlen Konu
January 2011

Zebrafish is an emerging and promising model organism to study cancer formation, organogenesis, development, cell signaling, and drug screening applications. Cellular signaling driven by E2F and TOR proteins regulate cell proliferation, growth and development; yet expression of E2F targets and downstream effectors of TOR inhibition have not been studied in zebrafish in detail. In this study, we first demonstrated the conservation of E2F target ortholog expression in zebrafish in response to serum; second our results revealed significant changes in the zebrafish fibroblast cells (ZF4) at the whole transcriptome level upon treatment with rapamycin, an inhibitor of TOR; and third we phenotypically screened zebrafish embryos *in vivo* when exposed to different doses of rapamycin. Our studies showed that as in mammalian cells, ZF4 cells entered into a quiescent state at G1/S phase in the cell cycle, which was reversed by serum stimulation. We showed that serum response of selected E2F target gene orthologs, namely *pcna*, *mybl2*, *tyms*, *mcm7* and *ctgf*, were conserved between zebrafish and mammals. Using microarray analysis, we demonstrated that rapamycin modulated expression of a large number of genes in ZF4 cells with functions ranging from cell cycle to protein synthesis. Similar to previous findings in mammals, rapamycin treatment downregulated expression of proteasomal subunits in zebrafish. Our findings in zebrafish also implicated a moderate increase in expression of ribosomal subunits; this

finding warrants further comparison with mammalian studies. qRT-PCR studies confirmed *dkk1b*, *pah*, *dcc*, *cyp26b1* and *wif1* as being significantly differentially expressed under rapamycin treatment using a time-course experiment. In zebrafish embryos, *in vivo* exposure to rapamycin caused a significant dose-dependent developmental delay and in particular prominent reductions in formation of pigments and cartilage, tissues known to be derived from embryonic neural crest cells. Our study implicates a potential role for TOR in the neural crest formation, differentiation or migration in zebrafish. Our study also clearly establish ZF4 cells as a model to further study signaling pathways involved in cell proliferation, growth and development.

ÖZET

Hücre büyümesi, çoğalması ve gelişiminde rol alan sinyal yolaklarının analizi için Zebrabalığı modeli

Ceren Sucularlı
Doktora Tezi, Moleküler Biyoloji ve Genetik Bölümü
Tez Yöneticisi: Yard. Doç. Dr. Özlen Konu
Ocak 2011

Zebrabalığı, kanser ve organ oluşumunun incelenmesi, gelişim, hücre sinyal yolak analizi ve son zamanlarda da ilaç taramaları için kullanılan, ümit vadeden bir model organizmadır. E2F ve TOR proteinleri tarafından yürütülen hücresel sinyaller, hücre çoğalması, büyüme ve gelişimini kontrol ederler; ancak zebrabalığında E2F hedef proteinlerinin ifadeleri ve TOR inhibisyonunun yolağın alt bileşenleri üzerindeki etkileri, detaylı olarak daha önce çalışılmamıştır. Bu çalışmada, ilk önce E2F hedef ortologlarının ifadelerinin zebrabalığındaki evrimsel korunumu gösterildi; ikinci olarak çalışmalarımız, bir TOR inhibitörü olan rapamisine maruz bırakılan zebrabalığı fibroblast hücre hattında (ZF4) transkriptom düzeyindeki önemli değişiklikleri ortaya çıkardı; üçüncü olarak farklı dozlarda rapamisine maruz bırakılan zebrabalığı embryoları *in vivo* olarak incelendi. Çalışmalarımız, ZF4 hücrelerinin, serum yokluğunda, memeli hücrelerinde olduğu gibi hücre döngüsünün G1/S fazında durgun hale geçtiğini, ve serum eklenmesi ile bu durumun tersine döndüğünü göstermektedir. Seçilen E2F hedef gen ortologlarının (*pcna*, *mybl2*, *tyms*, *mcm7* ve *ctgf*) seruma verdikleri yanıtların zebrabalığı ve memeliler arasında korunmuşluğunu da bulgulamaktayız. Mikrdizin analizi ile, ZF4 hücrelerinde rapamisin tarafından kontrol edilen ve foksiyonları hücre döngüsünden protein sentezine kadar çeşitlenen çok sayıda gen olduğunu gösterdik. Daha önce memelilerde belgelenen bulgulara benzer şekilde, rapamisin, proteasomal alt ünitelerin ifadelerini zebrabalığında da

geriletti. Bulgularımız ayrıca ribosomal alt ünitelerin ifadelerininde az miktarda artış olduğunu göstermekte olup bu bulgunun memeli çalışmaları ile karşılaştırılması öngörülmektedir. qRT-PCR çalışmalarımız ile *dkk1b*, *pah*, *dcc*, *cyp26b1* ve *wif1*'ın ifadelerinin zamana bağlı olarak rapamisin uygulaması ile istatistiksel olarak anlamlı bir şekilde değiştiği doğrulanmıştır. Zebrabalığı embryolarında *in vivo* rapamisin uygulaması gelişimde doza bağlı olarak gerçekleşen bir gerilemeye ve özellikle embryonik nöral krest hücrelerinden geliştiği bilinen pigment ve kıkırdak hücrelerinde belirgin azalmalara neden olmuştur. Çalışmalarımız, TOR'un nöral krest oluşumu, farklılaşması veya göçünde potansiyel bir etkisi olduğuna işaret etmektedir. Sonuç olarak çalışmalarımız, zebrabalığını, hücre çoğalması, büyümesi ve gelişimde rol alan sinyal yolaklarını çalışmak için önemli bir model olarak ortaya çıkarmaktadır.

ACKNOWLEDGEMENTS

I would like to thank Dr.Özlen Konu for her support, faith and guidance throughout my PhD study. I am deeply thankful to her for sharing knowledge of science and of life with me. Her guidance helped me to improve myself. She was always positive and supportive.

I am very thankful to Dr. Mehmet Öztürk for sharing his valuable ideas and knowledge with me and to Dr.Işık Yuluğ for her support and kind help throughout my PhD study. I also would like to thank all the academic members of the department of Molecular Biology and Genetics at Bilkent University. I would thank to Dr. Hilal Özdağ for her scientific support. I thank to Dr. Michelle Adams for her support.

I thank Onur Kaya, Rumeysa Bıyık, Ahmet Raşit Öztürk, Muammer Üçal and Gizem Ölmezer for their support and friendship. They have been not only group members but also closest friends. I thank Koray Doğan Kaya for sharing his knowledge with me. I thank Ertuğrul Dalkıç and Cem Kuşcu for their contribution in development of zebrafish as a model. I thank Şerif Şentürk for his help with Western Blotting and PI analyses.

I would like to thank all the graduate students of Molecular Biology and Genetics department for their friendship and scientific support. I thank to Iraz Toprak Aydın and Bala Gür-Dedeoğlu for their warm friendship and for sharing their knowledge with me. I deeply thank to Hande Koçak for always being there for me. I am grateful to Tolga Acun, Elif Uz, Ayça Arslan Ergül, Zeynep Tokçaer Keskin, Fatma Ayaloğlu Bütün, Ece Terzioğlu Kara, Kubilay Demir, Gülçin Çakan Akdoğan, Aynur Kaya Çopur, Nilüfer Sayar and Chigdem Aydın Mustafa for their support and friendship.

I would deeply want to thank my mother, Canan Sucularlı for her support, love and care through my life. None of this would happen without her.

I thank my brother, Ahmet Enlil Sucularlı for being the joy of my life. Finally, I want to thank my grandmother for her support and faith.

I would like to thank TÜBİTAK, Scientific and Technological Research Council of Turkey; this thesis was supported by grants from TÜBİTAK to Dr. Özlen Konu and to Dr. Mehmet Öztürk. I would like to thank Bilkent University for providing me with a PhD scholarship. I thank to Dr. Carl Neumann and EMBL Heidelberg, The European Molecular Biology Laboratory for hosting me to conduct my *in vivo* experiments.

TABLE OF CONTENTS

ABSTRACT iii
ÖZET v
ACKNOWLEDGEMENTS vii
TABLE OF CONTENTS ix
LIST OF FIGURES xiv
LIST OF TABLES xix
ABBREVIATIONS xx
Chapter 1. INTRODUCTION 1
1.1 Zebrafish as model organism 1
1.1.1 Zebrafish embryo 1
1.1.2 Zebrafish cell line, ZF4 3
1.2 Serum starvation/replenishment in molecular biology studies 3
1.3 E2F signaling 5
1.3.1 pcna 6
1.3.2 mybl2 7
1.3.3 tyms 7
1.3.4 mcm7 8
1.3.5 ctgf 9
1.4 Rapamycin 10
1.4.1 Rapamycin as an inhibitor of cellular signaling 10
1.4.2 Mechanisms of rapamycin action 11
1.4.3 Rapamycin in cell viability and apoptosis, autophagy 13
1.4.4 Microarray 15
1.4.4.1 Brief introduction about microarrays 15
1.4.4.2 Zebrafish microarrays 17
1.4.4.3 Transcriptome studies of rapamycin treatment 17
1.4.5 Selected E2F target orthologs and rapamycin 19
1.4.5.1 pcna 19
1.4.5.2 mybl2 19
1.4.5.3 tyms 20

1.4.5.4 mcm7 20
1.4.5.5 ctgf 20
Chapter 2. AIMS AND STRATEGY 21
Chapter 3. MATERIALS & METHODS 23
3.1 Materials 23
3.1.1 General reagents 23
3.1.2 Oligonucleotides 23
3.1.3 Antibodies 24
3.1.4 Western Blotting materials 24
3.1.5 Photography, spectrophotometer and autoradiography 25
3.1.6 Kits 25
3.1.7 Cell lines and Tissue culture reagents 26
3.1.8 Microarray 26
3.2 General Solutions and Media. 26
3.2.1 Cell culture solutions 26
3.2.2 Cell proliferation solutions 27
3.2.3 Cell cycle analysis solution 27
3.2.4 Western Blotting solutions 28
3.3 Methods 29
3.3.1 General Methods 29
3.3.1.1 Total RNA extraction 29
3.3.1.2 cDNA synthesis 30
3.3.1.3 Real-time qRT-PCR analysis 30
3.3.1.3.1 Primer design 30
3.3.1.3.2 Real-time qRT-PCR 30
3.3.1.4 Protein Extraction, Detection and Western Blotting 31
3.3.1.4.1 Protein extraction from tissue culture cells 32
3.3.1.4.2 Quantification of protein concentrations 32
3.3.1.4.3 Western Blotting 33
3.3.2 Cell Culture techniques 35
3.3.2.1 Cell lines 35
3.3.2.2 Cell line maintenance 35

3.3.2.3 Cryopreservation of cell lines 35
3.3.2.4 Serum starvation/replenishment experiments 36
3.3.2.5 Rapamycin treatment experiments 36
3.3.3 MTT Assay 37
3.3.4 BrdU Assay 37
3.3.5 Cell Cycle Analysis 38
3.3.6 Cell Death Detection Analysis 38
3.3.7 Microarray Analysis 39
3.3.7.1 The assessment of quantity and quality of RNA 39
3.3.7.2 Amplification, hybridization and scanning 39
3.3.7.3 Quality control of the arrays 40
3.3.7.4 Normalization 40
3.3.7.5 Obtaining differentially expressed genes 40
3.3.7.6 Gene Ontology analyses 41
3.3.8 Phylogenetic analysis of E2F pathway genes 41
3.3.9 In vivo Zebrafish embryo experiments 43
3.3.9.1 Zebrafish embryo strain 43
3.3.9.2 Rapamycin treatment to zebrafish embryo 43
3.3.9.3 Morphological measurements 44
3.3.9.4 Histological examinations of intestinal system 44
3.3.9.5 Hematoxylen-eosin staining 44
3.3.9.6 Alcian blue staining 45
3.3.10 Statistical Analyses 45
Chapter 4. RESULTS 47
4.1 The effect of serum starvation/replenishment on ZF4 cells 47
4.1.1 Cell viability analysis of serum starved/replenished ZF4 cells 47
4.1.1.1 Cell viability analysis of serum-starved ZF4 cells 47
4.1.1.2 Cell number counts of the ZF4 cells used for dose-serum response real-time qRT-PCRs 48
4.1.1.3 Cell viability analysis of serum replenished ZF4 cells 49
4.1.1.4 Cell number counts of the ZF4 cells used for 24h serum replenishment real-time qRT-PCRs 50

4.1.2 Cell proliferation analysis of serum starved/replenished ZF4 cells 51
4.1.3 Cell cycle analysis of serum starved/replenished ZF4 cells 52
4.1.4 The effect of serum starvation on translation 56
4.2 The effect of serum starvation/replenishment on E2F target gene expression 56
4.2.1 Pcna 57
4.2.2 Mybl2 59
4.2.3 Tyms 62
4.2.4 Mcm7 65
4.2.5 Ctgf 68
4.3 The effect of rapamycin treatment on ZF4 cells 70
4.3.1 Cell viability analysis of rapamycin treated ZF4 cells 71
4.3.2 Cell proliferation analysis of rapamycin treated ZF4 cells 71
4.3.3 Cell Death Analysis of Rapamycin Treated ZF4 cells 72
4.3.4 Cell cycle analysis of rapamycin treated ZF4 cells 73
4.3.5 Cell number counts of ZF4 cells used in the microarray study 74
4.4 Transcriptome analysis of rapamycin exposed ZF4 cells 75
4.4.1The quality control of RNA samples 75
4.4.2 The quality control of arrays 77
4.4.3 Normalization 78
4.4.4 Identification of differentially expressed genes after rapamycin exposure 81
4.4.5 KEGG pathway analysis of differentially expressed genes 83
4.4.6 Gene Ontology analysis of differentially expressed genes 84
4.4.7 Confirmation of microarray results 88
4.4.7.1 Selection of genes 88
4.4.7.2 Real-time qRT-PCR confirmation 88
4.4.8 The effect of rapamycin on E2F target genes 92
4.5 The effect of rapamycin on zebrafish embryo: in vivo studies 93
4.5.1 Effect of rapamycin on zebrafish body development 93
4.5.2 Effect of rapamycin on intestinal system 96
4.5.3 Effect of rapamycin on pigmentation 96

4.5.3.1 Melanophore pigmentation delay in response to rapamycin treatment 97
4.5.3.2 Iridophores in response to rapamycin treatment 97
4.5.4 Effect of rapamycin on cartilage development 98
Chapter 5. DISCUSSION 99
5.1 Serum response of E2F target genes in zebrafish 99
5.2 The effect of rapamycin treatment on gene expression of ZF4 cells and on zebrafish embryo 103
5.2.1 The effect of rapamycin treatment on gene expression of ZF4 cells 103
5.2.1.1 The effect of rapamycin treatment on ZF4 cell cycle progression 103
5.2.1.2 The effect of rapamycin treatment on gene expression in ZF4 cells, microarray analysis 105
5.2.1.3 Confirmation of microarray results by real-time qRT-PCR 107
5.2.2 The effect of rapamycin treatment on zebrafish embryogenesis and larval development 111
5.3 Zebrafish as a model for conserved gene expression signal profiling 114
Chapter 6. FUTURE PERSPECTIVES 116
6.1 E2F target gene regulation in zebrafish 116
6.2 Identification of conserved signatures in response to rapamycin in different species 117
6.3 In vivo rapamycin experiments with zebrafish embryos 117
REFERENCES 119

LIST OF FIGURES

Figure 4. 1 MTT analysis of ZF4 cells treated with 0%, 1%, 3% and 10% FBS supplemented media for 24 h. 48

Figure 4. 2 Cell counts of ZF4 cells used for real-time qRT-PCR analysis..... 48

Figure 4. 3 MTT analyses of 6 and 24 h serum replenished ZF4 cells 49

Figure 4. 4 Cell counts of ZF4 cells used for 24 h serum relplenishment real-time qRT-PCR. 50

Figure 4. 5 Representative presentation of BrdU incorporation of serum replenished ZF4 cells..... 51

Figure 4. 6 BrdU incorporation of 24 h serum starved and then 24 h serum replenished (24h rep.) ZF4 cells. 52

Figure 4. 7 Cell cycle analysis of 24 and 48 h serum starved cells and 24 h serum starved and then 24 h serum replenished (24h Rep.) ZF4 cells..... 54

Figure 4. 8 Cell cycle analyses of 24 h starved ZF4 cells at low confluency. . 55

Figure 4. 9 The activity of phospho-p70S6 kinase in 24 h serum starved ZF4 cells..... 56

Figure 4. 10 Phlyogenetic tree of Pcna protein sequence..... 57

Figure 4. 11 The real-time qRT-PCR results of *pcna* expression in serum starved cells for 24 h.. 58

Figure 4. 12 The real-time qRT-PCR results of *pcna* expression in 24 h serum starved and then 6 h serum replenished ZF4 cells (6 h rep.). 59

Figure 4. 13 The real-time qRT-PCR results of *pcna* expression in 24 h serum replenished ZF4 cells. 59

Figure 4. 14 Phlyogenetic tree of Mybl2 protein sequence. 60

Figure 4. 15 The real-time qRT-PCR results of *mybl2* expression in serum starved cells.. 60

Figure 4. 16 The real-time qRT-PCR results of *mybl2* gene expression in 30 h serum starved and in 24 h serum starved then 6 h serum replenished cells.. ... 61

Figure 4. 17 The real-time qRT-PCR results of *mybl2* gene expression in 24 h serum replenished ZF4 cells. 62

Figure 4. 18 Phlyogenetic tree of Tyms protein sequence.. 62

Figure 4. 19 The real-time qRT-PCR results of *tyms* expression in serum starved cells.. 63

Figure 4. 20 The real-time qRT-PCR results of *tyms* gene expression in 6 h serum replenished ZF4 cells.. 64

Figure 4. 21 The real-time qRT-PCR results of *tyms* gene expression 24 h serum replenished ZF4 cells. 64

Figure 4. 22 Phlyogenetic tree of Mcm7 protein sequence. 65

Figure 4. 23 The real-time qRT-PCR results of *mcm7* expression in serum starved cells. 65

Figure 4. 24 The real-time qRT-PCR results of *mcm7* gene expression in 6 h serum replenished ZF4 cells.. 66

Figure 4. 25 The real-time qRT-PCR results of *mcm7* gene expression in 24 h serum replenished ZF4 cells.. 67

Figure 4. 26 Western Blot analysis of Mcm7 protein in response to serum starvation or replenishment.. 68

Figure 4. 27 Phylogenetic tree of Ctgf protein sequence. 68

Figure 4. 28 The real-time qRT-PCR results of *ctgf* expression in serum starved cells. 69

Figure 4. 29 The real-time qRT-PCR results of *ctgf* expression in 6 h serum replenished ZF4 cells. 69

Figure 4. 30 The real-time qRT-PCR results of *ctgf* gene expression in 24 h serum replenished ZF4 cells. 70

Figure 4. 31 MTT analyses of 100 nM rapamycin treated or control ZF4 cells.. 71

Figure 4. 32 BrdU staining of 100 nM rapamycin treated ZF4 cells.. 72

Figure 4. 33 Cell Death Detection (CDD) of rapamycin treated ZF4 cells..... 73

Figure 4. 34 Cell cycle analyses of 48 h 100 nM rapamycin or equivalent of DMSO treated ZF4 cells. 74

Figure 4. 35 Attached cell number counts of rapamycin treated cells. 75

Figure 4. 36 The RNA degradation plot of the RNA samples used for the microarrays. 77

Figure 4. 37 Relative Log Expression (RLE) and Normalized Unscaled Standard Error (NUSE) plots of the chips used in the experiment..... 78

Figure 4. 38 Boxplot presentation of the arrays before normalization (raw data). 79

Figure 4. 39 MVA plots of the arrays before normalization. 80

Figure 4. 40 Boxplot presentation of the arrays after normalization..... 80

Figure 4. 41 MVA plots of the arrays after normalization. 81

Figure 4. 42 Cluster presentation of the differentially expressed genes.. 83

Figure 4. 43 The correlation between microarray and real-time qRT-PCR results for selected genes. 89

Figure 4. 44 The selected genes for confirmation that were significantly upregulated by rapamycin in real-time qRT-PCR analysis. 90

Figure 4. 45 The genes whose expressions were detected as upregulated by microarray analysis, but cannot be confirmed by real-time qRT-PCR analysis. 91

Figure 4. 46 The selected genes for confirmation that were downregulated by rapamycin in real-time qRT-PCR analysis. 92

Figure 4. 47 The effect of rapamycin treatment on zebrafish embryo development. 94

Figure 4. 48 The graphical presentation of time- and dose- dependent treatments.. 95

Figure 4. 49 Representative presentation of measurements. 95

Figure 4. 50 The effect of rapamycin on digestive tract development.. 96

Figure 4. 51 The effect of rapamycin treatment on melanophore pigmentation at 4 dpf. 97

Figure 4. 52 The iridophores on the yolk of the 5 dpf rapamycin or DMSO treated zebrafish embryo.. 98

Figure 4. 53 5 and 6 dpf 10 μM rapamycin treated embryos strained with alcian blue. 98

LIST OF TABLES

Table 3. 1 List of primer pairs and the primer efficiencies of used in the experiments 24

Table 3. 2 BSA dilutions for standard curve preparation. 33

Table 3. 3 Amino acid sequences used to generate phylogenetic trees 42

Table 4. 1 The experimental conditions, concentrations and RIN values of RNA samples used in the microarray experiments 76

Table 4. 2 The number of probe ids in different significance parameters 82

Table 4. 3 The KEGG results from DAVID of upregulated genes with rapamycin treatment 84

Table 4. 4 The KEGG results from DAVID of downregulated genes with rapamycin treatment 84

Table 4. 5 The Gene Ontology (GO) results for cellular component (CC) category of up and down genes after rapamycin treatment (DAVID). 85

Table 4. 6 The Gene Ontology (GO) results for biological process (BP) category of up and down genes after rapamycin treatment (DAVID). 86

Table 4. 7 The Gene Ontology (GO) results for molecular function (MF) category of up and down genes after rapamycin treatment (DAVID). 87

Table 4. 8 Log2 fold change ratios of microarray and real-time qRT-PCR results of selected genes. 89

Table 4. 9 The effect of rapamycin on E2F target gene expression based on ZF4 microarray analysis. 93

ABBREVIATIONS

ZF4	Zebrafish embryonic fibroblast cell line
E2F1	E2F transcription factor 1
mTOR	Mechanistic target of rapamycin
pRb	Retinoblastoma 1
pcna	Proliferating cell nuclear antigen
mybl2	Myeloblastosis oncogene-like 2
tyms	Thymidylate synthase
mcm7	Minichromosome maintenance complex component 7
ctgf	Connective tissue growth factor
eIF4E	Eukaryotic translation initiation factor 4E
4E-BP1	Eukaryotic translation initiation factor 4E binding protein 1
S6K1	Ribosomal protein S6 kinase
mRNA	Messenger RNA
cDNA	Complementary DNA
RMA	Robust Multichip Average
PVDF	Polyvinylidene Difluoride
FBS	Fetal bovine serum
BrdU	5-bromo-2-deoxyuridine
DAPI	4',6-diamidino-2-phenylindole
MTT	3-(4,5-dimethylthiazole-2-yl)-2.5-diphenyltetrazolium bromide
PI	Propidium Iodide
CDD	Cell Death Detection
DMSO	Dimethyl sulfoxide
RLE	Relative Log Expression
NUSE	Normalized Unscaled Standard Error
CC	Cellular component

MF	Molecular function
BP	Biological process
ddc	Dopa decarboxylase
cyp26b1	Cytochrome P450, family 26, subfamily b, polypeptide 1
pah	Phenylalanine hydroxylase
dkk1b	Dickkopf 1b
wif1	Wnt inhibitory factor 1
bambia	BMP and activin membrane-bound inhibitor (Xenopus laevis) homolog a
foxm1	Forkhead box M1
tagln2	transgelin 2
mmp9	matrix metalloproteinase 9
b2m	beta-2-microglobulin
ef1a	elongation factor 1-alpha

Chapter 1. INTRODUCTION

1.1 Zebrafish as model organism

1.1.1 Zebrafish embryo

The zebrafish has been used as a valuable model in molecular biology studies because of its ease of maintenance and molecular conservation with higher organisms (Barbazuk et al., 2000). A healthy female fish may lay hundreds of eggs; the embryos are easy to visualize and manipulate because they are large in size, transparent and have a short generation time (Wixon, 2000). The mutant zebrafish strains are available to explore the genes required for the development in large scale genetic screens (Driever et al., 1996). Zebrafish is a convenient model to also study organogenesis by visualizing mutations affecting specific organs; such as kidney (Chen et al., 1996; Drummond et al., 1998), heart, and cardiovascular system, liver and intestine (Chen et al., 1996; Pack et al., 1996).

More recently, the zebrafish has been used as a model organism in cancer. The tumor formation in zebrafish may develop naturally (Smolowitz et al., 2002), upon treatment with chemicals (Feitsma and Cuppen, 2008) or by xenotransplantation (Lee et al., 2005; Nicoli et al., 2007). The conservation between human and zebrafish tumors was shown at the molecular level by high-throughput transcriptome analysis (Lam et al., 2006; Ung et al., 2009). The short development time and the existence of mutant strains also make zebrafish as an important and rising model for drug screening (Taylor et al., 2010; Wang et al., 2010).

The zebrafish has also emerged as a valuable model organism to study craniofacial cartilage development and pigment pattern formation (Barrallo-Gimeno et al., 2004; Ellies et al., 1997; Parichy, 2006; Yelick and Schilling, 2002). Zebrafish have the similar craniofacial elements with higher vertabrate counterparts. In zebrafish the pharyngeal skeleton, jaw and branchial arches, arise from the cranial neural crest cells that develop from dorsal and lateral regions of the neural ectoderm then migrate

to pre-determined locations (Yelick and Schilling, 2002). Pigment cells are also derived from neural crest cells, except for the retinal pigment epithelium, which is derived from the neural epithelium (Dupin and Le Douarin, 2003). In mammals neural crest cells give rise to only one type of pigment cell, melanocytes. However, in zebrafish, pigments consist of black melanophores, yellow xanthophores and silver iridophores (Hirata et al., 2003; Parichy, 2006). Melanophores become visible around 25 hpf in the retinal epithelium of zebrafish embryo and migrate to anterior of the trunk and the posterior of the head. Xanthophores become visible at the posterior of the head as yellow marks. Iridophores appear on the eye as silver spots. Xanthophore and iridophores start to appear during hatching period (Kelsh et al., 1996).

Zebrafish has been used to understand the cellular signaling components of the regulatory pathways of development and disease, such as Wnt, TGF-β, TOR, PTK, and BMP and FGF signaling (Kan et al., 2009; Kim et al., 1999; Lemeer et al., 2007; Makky et al., 2007; Pyati et al., 2005; Shin et al., 2007). Since it is simple to generate transgenic fish, *in vitro* findings can easily be extended to *in vivo* fish models. One example of this is the identification of the PTK signaling profiles with zebrafish peptide arrays and discovery of functions with the zebrafish embryos using knock down of PTKs with morpholinos (Lemeer et al., 2007). Another example combines findings from human cell lines with an *in vivo* zebrafish model. The activation by polycystin of Wnt signaling, whose mutations caused autosomal dominant polycystic kidney disease, was shown in human embryonic kidney cells then the inhibition of GSK-3β by polycystin and its effect on phenotype have been shown in zebrafish embryos (Kim et al., 1999). The similarity of mammalian and zebrafish liver generation and the role of WNT, BMP and FGF signaling in liver regeneration have also been shown in a zebrafish model with expression studies and by generating transgenic zebrafish (Kan et al., 2009). The first *in vivo* presentation of the requirement of BMP and FGF signaling for hepatic specification was shown in zebrafish (Shin et al., 2007). The activation of Wnt signaling in neural crest development also was identified in zebrafish embryos by monitoring the neural crest induction at different time points in transgenic fish, expressing Wnt inhibitor, Tcf (Lewis et al., 2004).

1.1.2 Zebrafish cell line, ZF4

Zebrafish embryonic fibroblast cell line, ZF4, was generated from 1 day-old zebrafish embryo for use in gene expression studies (ATCC, CRL-2050; (Driever and Rangini, 1993)). The ZF4 cells have been used to compare overlapping segments of zebrafish and mouse cell chromosomes (Ekker et al., 1996), to investigate the effect of heat and cold shock on zebrafish heat shock proteins (Airaksinen et al., 2003), to identify the function of the genes, such as *ATM* (Garg et al., 2004), *lamin B2* (Gruber et al., 2005), *Tip-1* (Besser et al., 2007), *XBP-1*(Hu et al., 2007), *TNF-alpha* (Roca et al., 2008) and to assess the effects of chemical treatments on gene expression (Long et al., 2011). The effect of serum replenishment for 6 h after 24 h serum starvation on global gene expression of zebrafish has also been investigated using ZF4 and PAC2 cells (He et al., 2006); however, the molecular response of ZF4 cells to 24 and 48 h serum starvation and 24 h replenishment has not been identified in this study. Accordingly, ZF4 cells provide ample opportunity to compare cell signaling components with humans with respect to sequence and expression.

1.2 Serum starvation/replenishment in molecular biology studies

Tissue culture cells require addition of serum to the culture media. Serum provides growth factors, nutrients, vitamins and amino acids that are lacking in the plain media of the tissue culture cells (Gstraunthaler, 2003). Insufficiency of these factors in the culture conditions affects the growth of the cells and causes a reversible cell cycle arrest (quiescence) (Demidenko and Blagosklonny, 2008). Lack of serum in the culture media also affects the number of the proliferating cells. In a study with normal human fibroblasts, the decrease in the cell number was observed in the cells cultured with serum free media. The number of the cells continued to decrease as the time of the treatment increased (0 to 10 days) (Nakatani et al., 2008). However, the duration of the treatment of serum starvation should be assessed carefully, since serum starvation may induce apoptosis (Kues et al., 2000).

Serum starvation is an appropriate model to study cell cycle progression, since serum starvation arrests cells at G0/G1 phase of the cell cycle (Bettuzzi et al., 1999; Goissis et al., 2007; Khammanit et al., 2008; Kues et al., 2000; Vackova et al., 2003). Previous studies with fibroblast cell lines from various species, such as human, porcine and canine showed that serum starvation (24 h to 5 day) causes an increase in the cell number at G0/G1 phase, while it decreases cells entering the S and G2/M phases of the cell cycle (Bettuzzi et al., 1999; Goissis et al., 2007; Khammanit et al., 2008; Kues et al., 2000; Vackova et al., 2003). These changes in cell cycle distribution of cells may be reversible; serum replenishment may restore the effects of serum deprivation while the duration of starvation is critical to generate reversible growth arrest (Bettuzzi et al., 1999; Kues et al., 2000).

The growth factor depletion exerts its effect on transcription (please see section 1.3) and translation of the genes which are regulatory for G1 to S phase progression (Brunn et al., 1997; Hidalgo and Rowinsky, 2000).

The transcription of several genes required for G1 to S phase transition are regulated by the E2F transcription factor family (Linhart et al., 2005). The role of E2F1 transcription factor in S phase progression has been shown in quiescent cells: overexpression of E2F1 facilitates the S phase entry in growth arrested cells (Johnson et al., 1993). In serum starved and then replenished human T98G neuroblastoma cells the increase in *E2F1* mRNA expression was observed at the transition from G1 to S phase (Kherrouche et al., 2006).

The translation of the genes required for the progression of G1 to S phase is mediated by the mTOR pathway (Hidalgo and Rowinsky, 2000). mTOR (mechanistic Target of Rapamycin) pathway is responsive to the changes in growth factors and nutrients (Edinger and Thompson, 2002). Thus treating cells with no serum inactivates TOR and causes a decrease in phosphorylation of S6, which is also observed in rapamycin treatment (Demidenko and Blagosklonny, 2008). Starvation also causes a decrease in phosphorylation of S6 (Demidenko and Blagosklonny, 2008). Rapamycin treatment has a similar affect with serum starvation on the phosphorylation of 4E-BP1, which is phosphorylated by mTOR, in HEK 293 cells (Gingras et al., 1998).

1.3 E2F signaling

The E2F transcription factors are important regulators of G1/S phase of the cell cycle. The regulatory regions of E2F target genes have been conserved in a wide range of species, including fruitfly, zebrafish, fugu, green spotted puffer fish, chicken, rat, mouse, dog and human (Duronio et al., 1995; Linhart et al., 2005).

The E2F/DP transcription factor complex is a major downstream target of the pRB tumor-suppressor pathway. The E2F/DP heterodimer drives cell proliferation under the control of the pRb family proteins, pRB, p107 and p130 (Dyson, 1998). The hypophosphorylated pRB-bound E2F/DP heterodimer represses transcription of E2F target genes in quiescent cells. After stimulation with mitotic signals, the cyclin/cdk complex phosphorylates pRB; when hyperphosphorylated, pRB releases E2F and the E2F/DP heterodimer induces transcription of the responsive genes (Cayirlioglu and Duronio, 2001; Muller and Helin, 2000; Nevins, 2001).

The genes controlled by the E2F/DP complex are involved in DNA repair, differentiation, apoptosis and development (Bracken et al., 2004; Cayirlioglu and Duronio, 2001; DeGregori and Johnson, 2006; DeGregori et al., 1995a; Duronio et al., 1995; Ishida et al., 2001; Polager et al., 2002; Stevaux and Dyson, 2002). These genes are either the regulators of cell cycle such as *cyclin E*, *cyclin A*, *B-Myb*, *E2F1*, and *p107* and the cyclin-dependent kinases (Cdks) or have roles in DNA replication such as ribonucleotide reductase, DNA polymerase, the origin recognition complex (ORC), thymidine kinase, and dihydrofolate reductase (Cayirlioglu and Duronio, 2001; Ishida et al., 2001; Stevaux and Dyson, 2002).

The E2F transcription factors are also important regulators involved in the transition from the quiescent state into the cell cycle (DeGregori et al., 1995b; Smith et al., 1996). A DNA microarray analysis performed with mouse embryonic fibroblasts overexpressing E2F1 or E2F2 revealed that many of the genes induced by E2Fs were regulated at the G1/S phase of the cell cycle (Ishida et al., 2001). In another study performed with rat fibroblast cells that were made quiescent by serum-

starvation, overrepression of E2F3 or E2F1 forced cells to re-enter the S phase from the G1 phase through upregulation of genes involved in DNA replication, DNA repair and mitosis (Polager et al., 2002). These studies strongly emphasized the importance of the roles E2Fs play in regulating the transition from the G1 to S phase in cell cycle in the context of serum response.

1.3.1 pcna

Proliferating cell nuclear antigen (pcna) is a cofactor of DNA polymerase delta and an important component of DNA replication in eukaryotic cells. Pcna is also involved in DNA repair (Essers et al., 2005).

The relationship between serum starvation/E2F regulation and *Pcna* expression has been shown in many studies; *PCNA* carries a binding site in its regulatory region and is a direct target of E2F1, and this region is transcriptionally activated during the transition from G1 to S phase (Lee et al., 1995). In mouse embryonic fibroblast (MEF) cells, *Pcna* expression was increased in the S phase entry after serum stimulation following serum starvation (Hurford et al., 1997). In NIH 3T3 (mouse embryonic fibroblast) cell line serum starvation caused a cell cycle arrest, while in these cells overxpression of *Pcna* overcame the growth arrest and cells continued to proliferate (Fukami-Kobayashi and Mitsui, 1999). The decrease in *Pcna* mRNA expression after 40 h serum starvation and following an increase in the expression after serum stimulation has also been shown the Chinese hamster ovary cell line (CHOK1) (Liu et al., 1995).

PCNA protein has been used as a cell proliferation marker in bovine aortic endothelial cells, and PCNA negative cells were addressed as apoptotic after serum deprivation and hypoxia (Hogg et al., 1999). In zebrafish embryonic intermediate cell mass (ICM) and in adult kidney cells, *pcna* has also been stated as a cell proliferation marker. In 24 hpf zebrafish embryos, *pcna* expression was observed in the highly proliferative sites, such as brain, spinal cord and ICM (Leung et al., 2005).

1.3.2 mybl2

MYBL2 (Myeloblastosis oncogene-like 2, B-Myb) belongs to a transcriptional factor family consisting of three members named as A-Myb, B-Myb and C-Myb (Nomura et al., 1988).

E2F transcription factors have an important role in the regulation of *MYBL2* expression; the promoter region of *MYBL2* carries binding sites for E2F1, E2F2, E2F3 and E2F4. E2F4 negatively regulates the *MYBL2* expression in the early G1 phase, while E2F1, E2F2 and E2F3 replace the E2F4 at the late G1 and increase the expression of *MYBL2* as shown in serum starved (synchronized) and then serum stimulated T98G human glioblastoma cells and mouse cells (Takahashi et al., 2000). Also in normal human bone marrow fibroblast cells, *MYBL2* mRNA expression increased in serum-stimulated cells that were serum starved for 48 h (Scortechini et al., 1999). The serum-stimulated increase in *Mybl2* expression has also been shown in the quiescent mouse embryonic fibroblast cells, the increase in *Mybl2* mRNA was detected after serum stimulation in these cells (Tominaga et al., 2004).

The *mybl2* expression is required for zebrafish development, the loss of *mybl2* results in necrosis in central nervous system in the 1 dpf (days post fertilization) zebrafish embryo (Amsterdam et al., 2004). The zebrafish *mybl2* is also critical for G2/M progression; in the zebrafish *crash&burn* (*crb*) mutant which carries a loss of function mutation in *mybl2*, the delayed entry to G2/M was observed and accompanied with genomic instability and increased cancer susceptibility (Shepard et al., 2005).

1.3.3 tyms

The TYMS (thymidylate synthase) is an important component of DNA synthesis and proliferation. TYMS enzyme generates TTP (thymidine 5’-triphosphate)

precursor which is required for DNA replication by converting dUMP (deoxyuridine 5'-monophosphate) to dTMP (thymidine 5'-monophosphate) (Conrad, 1971).

The TYMS is a direct target of E2F1. The E2F1 and E2F4 binding sites have been detected in the promoter region of human *TYMS* gene by using ChIP analysis (Weinmann et al., 2002).

Long-term serum starvation decreased the Tyms activity in mouse 3T6 fibroblast cells, which was reversed by serum stimulation, the increased protein activity was observed during the S phase of the cell cycle (Navalgund et al., 1980). Serum stimulation also increased the *Tyms* expression in mouse embryonic fibroblast cell line, NIH 3T3 (Saxena et al., 2009).

The *tyms* expression in zebrafish embryo is apparent in the 1-cell stage and persists through the 72 hpf (hours post fertilization). The *tyms* expression is required for proper zebrafish development; loss of *tyms* expression causes an arrest in the development of head and tail of the zebrafish embryo (Du et al., 2006).

1.3.4 mcm7

Minichromosome maintenance complex component 7, Mcm7, together with the other Mcm family proteins (Mcm2-6) is the component of a pre-replicative complex (pre-RC), which is required to initiate and elongate the replication during the S phase (Blow and Dutta, 2005).

The *MCM7* is a direct target of E2F transcription factors; the promoter region of human *MCM7* gene carries E2F binding sites (Suzuki et al., 1998).

The serum response and MCM7 relation has previously been shown for human cells. In the MCF7 breast cancer cell line, serum stimulation increased the MCM7 protein levels, peaking after 2, 4 and 6 h of stimulation (Rizwani et al., 2009). In

human and mouse cells made quiescent by contact inhibition, the decrease in Mcm7 protein levels was apparent (Stoeber et al., 2001).

In the developing zebrafish embryo the *mcm* gene expression was observed in the highly proliferative sites (Ryu and Driever, 2006). In the retina of zebrafish embryo the decrease in *mcm5* caused an aberrant cell cycle progression and increased apoptosis (Ryu et al., 2005). Although the role and expression of *mcm5* on cell cycle progression was investigated in zebrafish, the expression of *mcm7* has not been previously studied to our knowledge.

1.3.5 ctgf

CTGF (Connective tissue growth factor) is a member of the CCN (ctgf/cyr61/nov) family. CTGF has important roles in extracellular matrix formation, cell proliferation and migration (Moussad and Brigstock, 2000).

The response of *Ctgf* expression to serum starvation/replenishment may be cell type specific. In serum-starved human mesangial cells the *Ctgf* expression was decreased after 24 and 48 h of starvation, while serum stimulation increased the *Ctgf* mRNA expression transiently; the expression of mRNA peaked after 2 h of stimulation and gradually decreased as the stimulation continues (Goppelt-Struebe et al., 2001). However, according to GEO microarray expresion profile analysis, the expression *CTGF* increased after 3 days of serum starvation in human T98G cancer cells (Cam et al., 2004).

CTGF is not a direct target of E2F transcription factors as shown by expreriments performed with cycloheximide treatments. The *CTGF* expression was negatively regulated by E2Fs, the mRNA levels of *CTGF* decreased in the E2F1, E2F2 and E2F3 overexpressing human osteosarcoma (U2OS) cells (Muller et al., 2001).

The *ctgf* expression was shown to be important for zebrafish embryonic development, especially of the notochord (Chiou et al., 2006). The requirement of *Ctgf* expression in development was also conserved in the mouse model. In the mouse, *Ctgf* was required for the extracellular matrix production in cartilage, and loss of *Ctgf* caused severe cartilage defects (Ivkovic et al., 2003).

1.4 Rapamycin

1.4.1 Rapamycin as an inhibitor of cellular signaling

mTOR (mechanistic target of rapamycin) is a serine/threonine kinase which is a member of the phosphoinositide 3-kinase related kinase (PIKKs) protein family. The PIKKs are regulatory kinases of the cell cycle progression, DNA damage and repair, and DNA replication (Sarkaria et al., 1998).

The mTOR regulates cell proliferation and growth in response to nutrients and growth factors through regulation of translation. Translation initiation is controlled through two pathways by mTOR. In the first pathway, mTOR directly phosphorylates Thr389 of S6K1. Activation of S6K1 increases the translation of ribosomal proteins and translation factors. In the second pathway mTOR phosphorylates and inactivates 4E-BP suppressor proteins (Huang et al., 2003; Kim and Novak, 2007). The 4E-BP suppressor protein is the inhibitor of eukaryotic translation initiation factor 4E (eIF4E). After phosphorylation and inactivation by mTOR binding, 4E-BP dissociates from eIF4E and free eIF4E initiate translation (Dufner and Thomas, 1999; Fingar et al., 2002; Gingras et al., 1998; Panwalkar et al., 2004).

Nutrients, growth factors, hypoxia and low energy affect the mTOR response in human cells (Arsham et al., 2003; Brugarolas et al., 2004; Dennis et al., 2001; Edinger and Thompson, 2002; Scott et al., 1998). Growth factors activate mTOR via PI3K/Akt pathway. Stress, hypoxia and low energy conditions lead to inactivation of mTOR by activating TSC1/TSC2 complex that are the upstream inhibitors of mTOR

and are also targets of Akt after growth factor and nutrient stimulation (Hay and Sonenberg, 2004; Wullschleger et al., 2006).

Function of tor protein is highly conserved between species from yeast to human (Wullschleger et al., 2006). The sequence and the expression of tor in zebrafish have been recently identified. The whole-mount *in situ* hybridization studies showed the ubiquitous expression of zebrafish tor from the single cell stage to 24 hpf. Between 24 and 48 hpf the expression was detected in the head, brain, eyes and brancial arches. After 4 dpf, the expression of zebrafish tor persisted only in head and eyes (Makky et al., 2007). Makky and colleagues also showed that the rapamycin treatment arrested the digestive tract development, and caused a weak developmental delay overall (Makky et al., 2007).

1.4.2 Mechanisms of rapamycin action

Rapamycin is an immunosuppresive, antifungal and antitumor agent; and the inhibitor of the mechanistic target of rapamycin (mTOR) (Martel et al., 1977; Vezina et al., 1975). Rapamycin inhibits mTOR by forming a complex with FKBP12. The rapamycin-FKBP12 complex binds to mTOR and prevents mTOR from initiating translation (Sabers et al., 1995; Tsang et al., 2007).

Rapamycin shows its effect on growth inhibition in various cell types, including B-cell lymphoma (Wanner et al., 2006), breast cancer (Mosley et al., 2007; Yu et al., 2001), leukemia (Mayerhofer et al., 2005), colon adenocarcinoma (Guba et al., 2005) and hepatocarcinoma cells (Zhang et al., 2007).

Rapamycin treatment arrests cell at the G1 phase of the cell cycle from yeast to human in various cell types (Albers et al., 1993; Decker et al., 2003; Gorshtein et al., 2009; Metcalfe et al., 1997; Zhang et al., 2007; Zinzalla et al., 2007). In the 48 h serum-starved human osteosarcoma cell line, MG-63, rapamycin treatment arrested cells at early G1 phase even after serum stimulation (Albers et al., 1993).

Rapamycin exerts its effect on cell cycle progression by inhibiting transcription or translation of regulatory genes, such as *cyclin D1*, *pcna*, *cyclin E* (Hashemolhosseini et al., 1998; Nelsen et al., 2003). Rapamycin has also been shown to prevent the accumulation of *cyclin D1* mRNA after serum stimulation of serum-starved NIH 3T3 fibroblasts and decreased the Cdk4 kinase activity and pRb phosphorylation (Hashemolhosseini et al., 1998). In rat pituitary tumor cell line, GH3, rapamycin prevented the pRb phosphorylation and following E2F activity, and decreased the mRNA and protein levels of cyclin E and cdk2, which are regulated by E2F, but did not change the cyclin D1 protein levels (Gorshtein et al., 2009). Also in human IL-2-dependent T-cell line, Kit225, rapamycin treatment decreased E2F1 activity (Brennan et al., 1999). Rapamycin not only affects the activity of E2F/Rb pathway by regulating the pRb phosphorylation, it also downregulates the transcription of *E2F1*. The expression of *E2F1* was downregulated in primary human CASMCs after 100 ng/ml rapamycin treatment for 48 h. In these cells rapamycin treatment also decreased the expression E2F target genes; such as *cyclin-D3* and *CDK4*, which are the regulators of cell cycle (Zohlnhofer et al., 2004). In addition, overexpression of *cyclin D1* and *E2F1* rescued cells from arresting at G1 and stimulates S phase transition in rapamycin treated rat hepatocytes (Nelsen et al., 2003).

An increase in the number of cells in the G1 phase after rapamycin treatment has been shown in many cell types, as explained above. However, for example, in OVCAR4 and OVCAR5 ovarian cancer lines, 100 ng/ml rapamycin treatments for 48 h did not change the cell numbers in G1 phase of the cell cycle (Altomare et al., 2004). Rapamycin treatment also had no effect on the cell number of the cell cycle phases in rapamycin insensitive WB311 rat epithelial cell line, although treatment decreased the phosphorylation of S6 and 4E-BP1 as it did in rapamycin sensitive cells (Jimenez et al., 2009). The phospho-p70S6 kinase protein levels were decreased after rapamycin treatment for 24 h in a dose dependent manner in human malignant glioma cell lines U87-MG, T98G, and U373-MG, although the latter one was rapamycin insensitive (Takeuchi et al., 2005). These might indicate phosphorylation levels of p70S6 kinase and 4E-BP1 may not be indicative of rapamycin sensitivity.

Previous studies exemplified the sensitivity of zebrafish to rapamycin. The growth of adult caudal fin was negatively affected from rapamycin treatment, whereas the juvenile caudal fin was not (Goldsmith et al., 2006). 400 nM rapamycin treatment caused an arrest on the digestive tract development at the primitive gut tube stage and in general a weak developmental delay up to 72 hpf in zebrafish embryo (Makky et al., 2007). The effect of rapamycin on zebrafish model has also been demonstrated from the 8-cell stage to 28 hpf zebrafish embryos. Rapamycin treated embryos mimicked embryonic growth–associated protein (EGAP) morphants with a developmental delay, vessel defects and cardiac failure (Wenzlau et al., 2006). However, rapamycin induced cell signaling has not yet been studied at the transcriptome level in zebrafish embryos or cell lines.

1.4.3 Rapamycin in cell viability and apoptosis, autophagy

The growth arrest at G1 phase induced by rapamycin treatment was explained in section 1.4.2. Rapamycin also has outcomes on cell viability and cell death in different organisms.

Rapamycin may induce apoptosis or may protect cells from apoptosis by inducing autophagy (Ravikumar et al., 2006; Tirado et al., 2005). According to MTT assay based cell proliferation analysis, rapamycin treatment decreased cell viability in MIN-6 insulinoma cells in a dose-dependent manner starting from 24 h of exposure; 10 nM and 100 nM rapamycin treatment for 19 h induced apoptosis in those cells (Bell et al., 2003). In JN-DSRCT-1 cell line, a model for desmoplastic small round cell tumors, rapamycin induced apoptosis and decreased viable cell number in a dose-dependent manner via inducing pro-apoptotic Bax and reducing anti-apoptotic Bcl-xL protein levels and leading to caspase-3 activation (Tirado et al., 2005).

In human rhabdomyosarcoma cells, rapamycin exposure also induced apoptosis which could be rescued by IGF-I treatment (Hosoi et al., 1999). Huang et al. proposed that rapamycin induces apoptosis but not G1 arrest under serum starvation in p53 deficient human rhabdomyosarcoma cell lines, Rh1 and Rh30 (Huang et al., 2003;

Huang et al., 2001). In these cells serum starvation and rapamycin treatment increased the number of cells at G1 phase of the cell cycle, however did not change expression of the cell cycle regulators; such as *cyclin D1*, *cyclin E* and *cyclin A*, representing continuing cell cycle progression. BrdU incorporation also confirmed these results; 97% of the rapamycin treated cells (100 nM for 24 h) continued to incorporate the BrdU, accompanied with the increase in apoptotic cell number. When the cells were transfected with p53 carrying plasmid, the number of the apoptotic cells were decreased and G1 induced growth arrest increased (Huang et al., 2001). Also in wild type mouse embryonic fibroblast cells, MEFs, under serum starvation, rapamycin did not induce apoptosis but decreased BrdU incorporated cell number, while in *p53*-/- and *p21*-/- MEFs, rapamycin induced apoptosis and only slightly decreased the BrdU incorporated cell number, proposing in p53 intact cells rapamycin treatment caused a G1 arrest but not apoptosis, while in *p53*-/- and *p21*-/- MEF cells, rapamycin induced apoptosis since cells continued to proliferate (Huang et al., 2001).

The apoptotic and anti-apoptotic functions of rapamycin may depend on the cell type. In vascular smooth muscle cells (VSMCs) of injured rat arteries, rapamycin rescued VSMCs from apoptosis by preventing the activity of caspase-3/7 (Reddy et al., 2008). In primary human coronary artery smooth muscle cells, CASMCs, rapamycin treatment reduced the basal and H_2O_2-induced apoptosis compared to control CASMCs. The activity of caspase-3 was inhibited by rapamycin in these cells, suggesting the decrease in apoptosis to some extent was a result of caspase-3 activity inhibition (Zohlnhofer et al., 2004). In the African Green Monkey SV40-transformed kidney fibroblast cell line, Cos-7, rapamycin treatment for 48 h before induction of apoptosis, protected cells from undergoing apoptosis. This protection was prevented when autophagy inhibitor, 3MA was used. Also in a *Drosophila* model, rapamycin treatment prior to apoptotic agent treatment increased the survival ratio of wild type *Drosophila*, but not the *Atg1*, the gene specific for autophagy, mutants (Ravikumar et al., 2006). Rapamycin treatment prior to apoptosis induction decreased the activated caspase-3 and caspase-9 in rat pheochromocytoma cell line PC12 (Ravikumar et al., 2006). In the wild-type yeast model, rapamycin induced autophagy, but not in *Atg1* mutants (Alvers et al., 2009). The upregulation of autophagy has also been observed in 3 dpf zebrafish embryos after 24 h rapamycin treatment (He et al., 2009). The induction of autophagy was also investigated in human malignant glioma cell lines,

e.g., rapamycin sensitive U87-MG, T98G, and rapamycin insensitive U373-MG, rapamycin induced autophagy in the rapamycin sensitive cell lines, while had no effect on the rapamycin insensitive cell line (Takeuchi et al., 2005).

1.4.4 Microarray

1.4.4.1 Brief introduction about microarrays

High-throughput microarray analysis have been used to analyze the expression of the genes in various organisms in response to chemical treatments, cancer formation and disease (Golub et al., 1999; Kittleson et al., 2004; Lock et al., 2002; Martyniuk et al., 2007; Mirnics et al., 2000; Ramaswamy et al., 2001; Ross et al., 2000; Walker et al., 2006; Xiao et al., 2005). Microarrays are also convenient tools to compare the conserved pathways or signatures involved in disease formation or cellular functions in different species (Hancock and Lessnick, 2008; Kobayashi et al., 2010b; Lam et al., 2006; Shepard et al., 2005). Several types of arrays are available for different purposes, such as protein microarrays to explore protein-protein interactions (MacBeath and Schreiber, 2000), antibody microarrays for detection of antigens (Chaga, 2008), tissue microarrays for prognostic and therapeutic approaches (Kononen et al., 1998) and DNA microarrays for gene expression, copy number and SNP analysis (Hacia et al., 1999; Pollack et al., 1999; Schena et al., 1995).

In principle, DNA microarray chips consist of cDNA or fragmented oligonucleotid sequences, specific for the coding or non-coding parts of the DNA sequences, attached on a solid surface. The RNA extracted from the subjects are reverse transcribed to cDNA and sometimes further transcribed to cRNA which are then hybridized to cDNA or oligonucleotid sequences on the microarray chips. The hybridization process generates a signal which is detected with special scanners. The expression value coming from the intensity of the signal is used for analysis (Lipshutz et al., 1999; Schena et al., 1995). In order to compare the expression changes between different chips, normalization and preprocessing of the data are required.

The preprocessing of the microarray data consists of background correction, normalization and summarization (Gautier et al., 2004). In background correction step, the background noise is removed from the signal of the probes. Normalization removes the chip effects, background noises, or batch effects, thus only biological difference is valued (Bolstad et al., 2003). Normalization is performed in order to correct the technical differences, thus leaves only the biological differences. The last step of preprocessing is summarization. One or more probe sets on the chips represents genes, and one probe set consist of 11 to 20 probes in Affymetrix chips. Summarization step combines the signal intensities of probes and generates one expression value for a probe set (Gautier et al., 2004). Different techniques have been used to preprocess and normalize the microarray data, such as MAS 5.0 (Hubbell et al., 2002), dChip (Li and Hung Wong, 2001) and RMA (Irizarry et al., 2003). Another important subject emerges here is the annotation of probe sets, i.e., associating probe sets with their related transcript names, gene information, homology information or gene ontology. NetAffx (Liu et al., 2003) and BioMart (Durinck et al., 2005) are preferable tools to annotate probe sets.

After preprocessing and normalization, the expression values of DNA microarray probe sets can be further analyzed in order to obtain differentially expressed genes between treatments/diseases/tumors and their related controls. The differentially expressed genes between conditions are filtered according to selected criteria, which may be fold change differences, p values according to selected test statistics, false discovery rates or combination of them (Chen et al., 2007; Olson, 2006).

The functional annotations of differentially expressed genes are also performed in order to identify the pathways affected and molecular and biological function of the genes. Several web-based tools are available to for functional annotations, such as DAVID (Dennis et al., 2003; Huang da et al., 2009), FatiGO (Al-Shahrour et al., 2004) of Babelomics (http://babelomics.bioinfo.cipf.es/functional.html), MGI (http://www.informatics.jax.org/function.shtml), WebGestalt (http://bioinfo.vanderbilt.edu/webgestalt/) and PathwayMiner (http://www.biorag.org/pathway.html).

Since microarray data are complex and the information coming from analyses is extensive, programs that analyze, store and interpret the data are required. Several tools are available to analyze microarray data, such as R programming language (http://cran.t-project.org) and Bioconductor packages (Gentleman et al., 2004), GeneSpring (http://www.genomics.agilent.com), Ingenuity Pathways Analysis (http://www.ingenuity.com/) and BRB Array tools (http://linus.ncbi.nih.gov/BRB-ArrayTools.html).

1.4.4.2 Zebrafish microarrays

Although there are different microarray platforms available for zebrafish model (Peterson and Freeman, 2009; Wardle et al., 2006), the most widely used one is Affymetrix GeneChip® Zebrafish Genome Array (Santa Clara, CA, USA; http:www.affymetrix.com/products/arrays/specific/zebrafish.affx).

Zebrafish microarrays have been used to understand different mechanisms effecting the expression of the organism. The effect of chemicals (Carney et al., 2006; Henry et al., 2007; Hoffmann et al., 2006; van Boxtel et al., 2008; Xiong et al., 2008), diseases, such as cancer (Lam et al., 2006; Langenau et al., 2007; MacInnes et al., 2008; Ung et al., 2009) or infections (Meijer et al., 2005) on gene expression have been surveyed by microarrays in zebrafish. Furthermore, the comparative microarray analyses between zebrafish and human tumors helped understand the conserved signatures in cancers (Lam et al., 2006; Langenau et al., 2007; Ung et al., 2009).

1.4.4.3 Transcriptome studies of rapamycin treatment

The cDNA or tissue microarray analyses contributed to understanding of the molecular mechanisms that were affected by the rapamycin treatment (Jimenez et al., 2010; Mousses et al., 2001).

The effect of rapamycin treatment on gene expression has been studied in various organisms and cell lines by high-throughput transcriptome analysis. A common gene set obtained from meta-analysis of human breast cancer cell line, MDA-MB-468, treated with DMSO or 100 nM rapamycin for 24 h, and MDA-MB-468 xenografts in nude female mice treated with DMSO or 15 mg/kg rapamycin for 24 h or 3 weeks, has been shown to be important in prognosis of the breast cancer (Akcakanat et al., 2009). In xenographs rapamycin treatment affected the genes regulating immune response and metabolism (Akcakanat et al., 2009). The effect of rapamycin treatment was also investigated in rapamycin sensitive, WB-F344; rapamycin insensitive, WB311 and intermediate sensitive, GN5 and H5D, rat epithelial cell lines. The genes involved in cell cycle, cell death and energy pathways were affected in all cell lines. Aminoacyl-tRNA biosynthesis, ribosome, cell cycle and carbohydrate metabolisms were affected in the rapamycin sensitive cell line, WB-F344, while oxidative phosphorylation, amino acid metabolism and cell communication changed in the rapamycin insensitive cell line, WB311 (Jimenez et al., 2009). In TSC2-/- murine embryonic fibroblast cells 20 nM rapamycin treatment for 14 h repressed the mitochondrial genes (Cunningham et al., 2007).

Microarray analysis performed with polysome-bound mRNAs is an efficient way to assess the effect of rapamycin on translation (Grolleau et al., 2002). In this respect, a microarray study performed with rapamycin-treated human E6–1 Jurkat T cell line for 4 h searched for the effect of rapamycin on transcription by using poly A mRNAs and translation by using only polysome-bound mRNAs. This study showed that rapamycin treatment affects both transcription and translation of the genes. Rapamycin treatment induced the transcription of negative regulators of cell cycle, and repressed the positive regulators of cell proliferation. Translation of ribosomal proteins, proteasome subunits and elongation factors were inhibited by rapamycin treatment (Grolleau et al., 2002). In another microarray study with human lung fibroblast cell line, MRC-5, the effect rapamycin treatment (100 nM for 30 min) had on translation initiation was investigated; rapamycin upregulated the mRNAs with anti-apoptotic functions, downregulated the ribosomal protein and elongation factor mRNAs (Genolet et al., 2008). Also in yeast model the transcriptional and translational effects of rapamycin were investigated; the transcription and translation of genes involved in oxidative phosphorylation, proteasome subunits, TCA cycle and

energy metabolism were upregulated by rapamycin, while transcription and translation of ribosomal proteins, rRNA processing, RNA polymerases and translation initiation factors were downregulated by rapamycin (Preiss et al., 2003).

Rapamycin treatment repressed the genes coding for cytoplasmic and mitochondrial ribosomal proteins, tRNA synthetases and the components of translation in *Candida albicans* (Bastidas et al., 2009). In another study with yeast strains showed that genes involved in ribosome and protein synthesis, transcription and RNA processing and cell cycle regulation were affected from rapamycin treatment (Butcher et al., 2006). 100 nM rapamycin treatment for 2 h in *Saccharomyces cerevisiae* strain BY4741 downregulated genes coding for ribosomal proteins and nucleotide synthesis, while upregulated genes coding for energy metabolism and autophagy; 4 to 6 h treatment decreased the expression of lipid metabolism genes, while increasing the expression of genes responsible from amino acid and vitamin synthesis (Fournier et al., 2010).

1.4.5 Selected E2F target orthologs and rapamycin

1.4.5.1 pcna

In primary human CASMCs after 100 ng/ml rapamycin treatment for 48 h decreased the expression of *pcna* (Zohlnhofer et al., 2004). In murine T lymphocytes, rapamycin decreased IL-2 induced Pcna expression (Feuerstein et al., 1995). Rapamycin treatment also decreased the Pcna expression in human keratinocyte stem cells (Javier et al., 1997), in rabbit lens epithelium cells (rLECs) (Liu et al., 2010).

1.4.5.2 mybl2

There are not many studies showing the response of *mybl2* expression to rapamycin. However, it has been shown that *mybl2* expression was downregulated in

primary human CASMCs after 100 ng/ml rapamycin treatment for 48 h (Zohlnhofer et al., 2004). Also in mouse mammary epithelium, NMuMG, cells 100 ng/ml rapamycin treatment for 24 h decreased the Mybl2 protein levels (Law et al., 2002).

1.4.5.3 tyms

48 h rapamycin treatment also decreased the *tyms* expression in primary human CASMCs (Zohlnhofer et al., 2004). In many human gastric cancer cell lines, rapamycin and also RAD001 (a rapamycin analogue) downregulated both the mRNA and protein levels of *tyms* (Lee et al., 2010; Shigematsu et al., 2010).

1.4.5.4 mcm7

mcm7 expression decreased in primary human CASMCs after 100 ng/ml rapamycin treatment (Zohlnhofer et al., 2004). Also in rat aortic smooth muscle cells (RASMC), rapamycin treatment decreased the mRNA and protein levels of Mcm7 (Bruemmer et al., 2003).

1.4.5.5 ctgf

The effect of rapamycin on ctgf expression may be cell type dependent. Since, different outcomes have been observed in different cell types. Rapamycin treatment did not affect the *CTGF* mRNA expression in bovine mammary epithelial cell line, MAC-T (Zhou et al., 2008). However, 50 ng/ml rapamycin treatment starting from 8 h increased the CTGF protein levels in rat glomerular mesangial cells (Osman et al., 2009). In normal keratinocytes (NK) and keloid keratinocytes (KK), rapamycin treatment decreased CTGF protein levels (Khoo et al., 2006).

Chapter 2. AIMS AND STRATEGY

Zebrafish have been used widely as a model organism in molecular biology and genetics studies due to its short generation time, easy maintenance, and visualization and manipulation of the transparent embryos (Wixon, 2000). Adult and embryonic and larval fish have been used to understand and study disease formation, such as cancer, organogenesis and embryonic development, and drug screening for therapeutic approaches (Driever et al., 1996). ZF4 cell line derived from zebrafish embryos (Driever and Rangini, 1993) has been used to explore the regulatory cellular signaling components of growth and proliferation in combination with the zebrafish adults and embryos (Gruber et al., 2005). Previously zebrafish model has been used to explore the components of the regulatory pathways of growth and proliferation, such as Wnt, TGF-β, TOR, PTK, and BMP and FGF signaling (Kan et al., 2009; Kim et al., 1999; Lemeer et al., 2007; Makky et al., 2007; Pyati et al., 2005; Shin et al., 2007). E2F and mTOR signaling are two of the main regulatory pathways in cell growth, proliferation and disease formation. However, the expression and conserved modulation of E2F and mTOR signaling pathway targets have not been studied in zebrafish model before.

Our aim in this study has been a) to understand the conservation of E2F signaling targets in zebrafish in the context of sequence and expression, which has not been studied before in zebrafish and b) to explore the role of mTOR in cell growth and development in zebrafish embryos and on global gene expression of the zebrafish cell line ZF4.

In order to study the selected pathways in zebrafish, we used the modulators of these pathways, serum starvation/replenishment for E2F pathway and rapamycin for mTOR pathway. Serum starvation by generating a reversible growth arrest at G0/G1 phase of the cell cycle is an easy and appropriate model to study the alterations of E2F target gene expression (Bettuzzi et al., 1999; Goissis et al., 2007; Khammanit et al., 2008; Kues et al., 2000; Vackova et al., 2003). Rapamycin is an inhibitor of mTOR

pathway; rapamycin forms a complex with FKBP12 and this complex binds and prevents mTOR activity (Sabers et al., 1995; Tsang et al., 2007).

First we asked whether ZF4 cells a) were responsive to serum starvation/replenishment and also to the rapamycin treatment at the cellular level and b) behave as mammalian cells. We performed multiple cellular assays, i.e., cell viability assay, MTT; cell proliferation assay, BrdU; cell cycle analysis, propidium iodide staining; and apoptosis assay, CDD, to explore the cellular response of ZF4 cells to serum starvation and rapamycin treatment.

Second we asked whether E2F target genes responded to serum fluctuations in the same manner with their mammalian counterparts. In order to answer this question, we selected the zebrafish counterparts of five known mammalian E2F target gene orthologs, either positively or negatively regulated by E2F in mammals. We searched for the sequence and expression conservation of selected genes in zebrafish. For sequence conservation, the sequences of selected genes from various species, including mammals and fish species were obtained from NCBI and Ensembl data bases, aligned by ClustalW and phlygenetic analysis was performed with Mega4. Phylogenetic analysis revealed the evolutionary conservation of selected genes in several organisms including mammals and fish species. For expression analysis, selected gene expressions were investigated in serum starved ZF4 cells, to show the dose-dependent gene expression changes and 6 or 24 h serum replenished ZF4 cells, to show whether their expression is restored in ZF4 cells as in mammalian cells with real-time qRT-PCR. To investigate expression of mTOR pathway components in ZF4 cells, we used high-throughput microarray analysis.

Rapamycin treatment has been shown to effect the general development and organ formation in various organisms (Makky et al., 2007; Moriyama et al., 2010; Oldham et al., 2000). Third we asked whether and in which context rapamycin treatment affects the zebrafish development in a dose-dependent manner. To explore the effect of rapamycin on zebrafish embryo development, we exposed zebrafish embryos to varying doses of rapamycin and monitored the general development of zebrafish embryos starting from 1 dpf to 5 dpf.

Chapter 3. MATERIALS & METHODS

3.1 Materials

3.1.1 General reagents

The chemicals used in the laboratory were obtained from Sigma-Aldrich (St. Louis, MO, U.S.A), Farmitalia Carlo Erba (Milano, Italy), Merck (Schucdarf, Germany), Riedel-de Haën (Germany) and Gibco (Carlsbad, CA, USA). Rapamycin was purchased from Calbiochem (Darmstald, Germany). BrdU was purchased from Sigma (St. Louis, MO, USA). DAPI was obtained from Roche (Germany).

3.1.2 Oligonucleotides

The oligonucleotides used in the real-time qRT-PCR were synthesized and supplied from Iontek Inc. (Istanbul, Turkey) and from Integrated RNA technologies (IDT; Leuven, Belgium). The list of the primers, the expected product sizes and the primer efficiencies were given in **Table 3.1**.

Table 3. 1 List of primer pairs and the primer efficiencies of used in the experiments

Gene Name	Forward primer (5'-3')	Reverse primer (5'-3')	Primer Efficiency
mybl2	CCCACACTGAAGGAGGTGAT	CTCCTTTACTGCCCTTGCTG	1.89
pcna	AGCCTGTCATCTGTGGGATT	TGGTAAAGCTAAGGCCCAAA	1.85
mcm7	GAGATTTACGGCCATGAGGA	GGTGTACTGACTGCGTGGAG	2
tyms	TGCTAACGGCTCCAGAGAGT	CATGATGATCCTTCGGTCCT	1.86
ctgf	ACCAATGACAACCGTGAGTG	GGTAGTGGTACAGCCGGAAA	1.78
ef1a	CCCTGGACACAGAGACTTCA	CAGCCTCAAACTCACCAACA	1.81
foxm1	GACACATGACCCTGAAGGAGA	AGAGTGAGACAGCGGTTTGC	1.9
pah	TGTGGGTATCGTGAGGACAA	GGAGCTGTGGCGAATGTACT	1.75
cyp26b1	CAACACGGGACAAGAGCTG	CCCATAAGAACCTTACGCACA	1.92
tagln2	GCTGGTACAGTGGATCGTCA	TGGATCTTCTTCACAGGCTTT	1.98
ddc	CCTGCCTGTACGGAGCTAGA	CTGGATCAGCCTGACGATTT	1.85
bambia	TTTGCATGACCTCACACACC	CGGAACCACACCTCTTTAGC	1.91
dkk1b	CGCTATTAAAGTCGGTTCAGG	TTGCACTGGAGACAGACACC	1.89
wif1	CAGACTCTGCGTTCTTTGGA	GGATGGTCACCTCAAATGCT	1.86
mmp9	CAAGACATTCGACGGAGACC	TGCTTTCCCGAAAGAGATCA	2
b2m	TTCTTTGTCTGCTGTACATCACTG	TGCTTGGTGTCCGACATAAC	1.95

3.1.3 Antibodies

The phospho-p70S6 kinase (Thr 386) primary antibody, p70S6 kinase primary antibody and HRP-conjugated secondary antibody was obtained from Cell Signaling Technology (Danvers, MA, USA). Mcm7 primary antibody was purchased from Santa Cruz Biotechnology (Santa Cruz, CA, USA) and α -Tubulin was purchased from Calbiochem (Darmstadt, Germany). Horseradish peroxidase (HRP)-conjugated goat anti-mouse secondary antibody was obtained from Sigma (St. Louis, MO, USA).

3.1.4 Western Blotting materials

The protein transfer materials, Immobilen P transfer (PVDF) membrane was from Roche (Germany) and 3mm filter paper was from Whatman International Ltd. (Madison, WI, USA).

The protein detection kits, ECL+ Western Blot Detection Kit and SuperSignal West Femto were purchased from Amersham GE Healthcare Life and Sciences (Buckinghamshire, UK) and Thermo Scientific (Northumberland, UK), respectively. Protein size marker, PageRuler Prestained protein ladder was obtained from MBI Fermentas (Ontario, Canada).

3.1.5 Photography, spectrophotometer and autoradiography

The Kodak (Rochester, NY, USA) films were used for the autoradiography of the proteins and were developed by Hyperprocessor (Amsderdam, UK). The protein concentration was measured by Beckman Du640 Spectrophotometer from Backman Instruments (Fullerton, CA, USA). Nucleic acid concentrations were measured by Nanodrop ND-1000 Spectrophotometer from Thermo Fisher Scientific (Wilmington, DE, USA). Agilent 2100 Bioanalyzer (Agilent Technologies, Santa Clara, CA, USA) was used to assess the RNA quality for microarray analysis. µQuant™ Microplate Spectrophotometer was used to measure ELISA based MTT assay (BioTek, Winooski, VT, USA). Digital fluorescent microscopy images of BrdU assays were obtained from Zeiss, AX10 Imager A1 (Germany). The zebrafish embryo images were taken with Leica MZ16FA Stereo microscope (Solms, Germany).

3.1.6 Kits

Total RNA was isolated using SV total RNA isolation kit (Promega, Madison, WI, USA) and used for both microarray analysis and real time RT-PCR analysis. The cDNA synthesized by using RevertAid first strand cDNA synthesis kit (MBI Fermentas, Ontario, Canada) and for the cDNA amplification the DyNAmo HS SYBR-green kit (Finnzymes, Espoo, Finland) was used. Vybrant MTT Cell Proliferation Assay Kit was purchased from Molecular Probes (Darmstadt, Germany).

3.1.7 Cell lines and Tissue culture reagents

ZF4, zebrafish embryonic fibroblast cell line was purchased from ATCC (Manassas, VA, USA). D-MEM/F-12 (1:1), FBS (fetal bovine serum), Penicillin/Streptomycin (10,000 U/mL Penicillin, 10,000 μg/mL Streptomycin) and trypsin without EDTA were supplied from HyClone (Logan, UT, USA).

3.1.8 Microarray

Affymetrix zebrafish GeneChips (Affymetrix, Santa Clara, CA) were used for microrray analysis.

3.2 General Solutions and Media.

3.2.1 Cell culture solutions

D-MEM/F-12 medium: D-MEM/F-12 (1:1) was supplemented with 10% FBS and 1% Penicillin/Streptomycin. Stored at 4ºC, warmed to room temperature prior to use. Serum starvation medium was prepared as follows; D-MEM/F-12 (1:1) was supplemented with 0%, 0.1%, 1% or 3% FBS with 1% Penicillin/Streptomycin. Stored at 4ºC, warmed to room temperature prior to use.

Rapamycin solution: Powder rapamycin was dissolved in DMSO to prepare 5 mM final concentration of stock solution. For cell culture treatments, 5 mM rapamycin was mixed with complete media to make 100 nM working concentration. For cell culture expreriments the final concentration of DMSO in culture medium is 0.002%. For *in vivo* rapamycin treatments, 5 mM rapamycin was mixed with embryo medium to make 400 nM, 2 μM, 10 μM and 20 μM working concentration and for *in vivo* experiments final concentration of DMSO in embryo medium are 0.008%, 0.04%, 0.2% and 0.4%, respectively.

PBS stock solution (10X): 80g NaCl, 2g KCl, 11.5g $Na_2HPO_4.7H_2O$, and 2g KH_2PO_4 dissolved in ddH_2O to a final concentration of 1 liter.

PBS Working solution (1XPBS): 10X PBS was diluted to 1X with ddH2O. pH was adjusted to 7.4.

Freezing solution: 5% DMSO and 95% complete media were mixed and used freshly.

3.2.2 Cell proliferation solutions

5-bromo-2-deoxyuridine (BrdU) staining stock solution: Powder BrdU was dissolved in ddH_2O to prepare 10 mg/ml stock concentration.

BrdU staining working solution: 9.2 µl BrdU from stock solution was mixed with 10 ml complete media (30 µM).

4',6-diamidino-2-phenylindole (DAPI): Powder DAPI was dissolved in dd H_2O to prepare 0.1-1 µg/ml working solution.

3-(4,5-dimethylthiazole-2-yl)-2.5-diphenyltetrazolium bromide (MTT) solution: Each vial of powder MTT was dissolved in 1 ml 1X PBS to prepare working solution.

3.2.3 Cell cycle analysis solution

Propidium Iodide (PI) staining solution: 50 µg/ml PI, 0.1 mg/ml RNase A and 0.05% TritonX-100 were mixed in 1 ml 1X PBS to prepare working solution.

3.2.4 Western Blotting solutions

NP40 lysis Buffer: 50 mM Tris.Cl pH: 8.0, 150 mM NaCl, 1% NP-40 and 1X protease inhibitor mix was mixed in ddH2O.

Bradford Working Solution: 10 mg powder Coomassie brilliant blue was dissolved in 10 ml 85% phosphoric acid-5 ml 95% ethanol mix and completed to 1 liter with ddH_2O. Filtered with whatman paper. Stored in dark at +4ºC.

Cracking Buffer (2X protein loading buffer): 50 mM Tris.HCl at pH 6.8, 2 mM EDTA at pH 6.8, 1% SDS, 10% glycerol and 0.02% Bromophenol blue was mixed and 1% Beta-mercaptoethanol was added prior to use.

1.5 M Tris-HCl (PH: 8.8): 54.45 g Tris base was dissolved in 150 ml ddH2O. After PH was adjusted with 1N HCl, the volume is completed to 300 ml with ddH2O. Stored at +4ºC.

1 M Tris-HCl (PH: 6.8): 12 g Tris base was dissolved in 60 ml ddH2O. After PH was adjusted with 1N HCl, the volume is completed to 100 ml with ddH2O. Stored at +4ºC.

10% SDS: 10 g SDS was dissolved in 100 ml ddH2O.

30% Acrylamide solution: 145 g acrylamide and 5 g bisacrylamide were dissolved in 500 ml ddH2O and filtered. Stored in dark at +4ºC.

10% APS: 0.15 g APS was dissolved in 1 ml of ddH2O to prior to use.

5X Running Buffer: 15 g Tris.base, 95 g glycine and 50 ml 10% SDS were mixed in ddH2O to a final volume of 1 liter.

Semi-dry Transfer Buffer: 2.5 gr Glycine, 5.8 gr Tris base, 3.7 ml 10% SDS and 200 ml MeOH were mixed in ddH_2O to a final volume of 1 liter.

TBS stock solution (10XTBS): 12.19 g Tris base, 87.76 g NaCl were dissolved in ddH_2O to a final volume of 1 liter. pH was adjusted to 8.

TBS working solution (1XTBS): 10X TBS was diluted to 1X with ddH_2O.

TBS-T: 0.1% Tween 20 was dissolved in 1X TBS.

Blocking Solution: 5 g powder non-fat milk was dissolved in 100 ml 0.1% TBS-T.

3.3 Methods

3.3.1 General Methods

3.3.1.1 Total RNA extraction

Total RNA were isolated from ZF4 cells for quantitative assessment of gene expression, microarray analyses and following confirmatory real-time qRT-PCRs. Cells were trypsinized and centrifuged at 1200 rpm for 3 min. The medium was aspirated before washing with ice-cold PBS. The PBS was aspirated and cells were snap frozen in liquid nitrogen and stored at -80 ºC for later use. Total RNA was isolated using SV total RNA isolation kit according to the manufacturer's recommendations (Promega, Madison, WI, USA) and used for both microarray analysis and real-time qRT-PCR analysis. The RNA concentration was assessed with the NanoDrop ND-1000 spectrophotometer (Thermo Fisher Scientific, Wilmington, DE, USA) at a ratio of absorbance at 260 nm to 280 nm. The integrity of the RNA samples for microarray analysis was measured by Agilent 2100 Bioanalyzer (Agilent Technologies, Santa Clara, CA, USA). RNA samples were stored in -80ºC.

3.3.1.2 cDNA synthesis

First-stand cDNA synthesis was performed with Revert Aid First strand cDNA synthesis kit according to manufacturer's instructions (MBI Fermentas, Ontario, Canada).

3.3.1.3 Real-time qRT-PCR analysis

3.3.1.3.1 Primer design

Primers used in real-time qRT-PCR experiments were designed by using Primer 3 v.0.4.0 (http://frodo.wi.mit.edu) and purchased from Iontek (Istanbul, Turkey) and Integrated RNA technologies (IDT; Leuven, Belgium). Intron spanning primers were designed from consecutive exons. Gene specificity was assured with blasting primer sequences in zebrafish genome by using ENSEMBL (http://www.ensembl.org/Multi/blastview). The primer sequences used in serum starvation/replenishment and rapamycin microarray confirmation studies was presented in **Table 3.1**.

3.3.1.3.2 Real-time qRT-PCR

The real-time qRT-PCR analysis was performed with primer pairs supplemented in **Table 3.1** to identify the effect of serum fluctuations or rapamycin on the expression of selected gene sets. The real-time qRT-PCR analysis was performed using DyNAmo HS SYBR-green kit (Finnzymes, Espoo, Finland) on iCycler (Bio-Rad, Hercules, CA, USA) thermocycler. For each amplification 10 µl SYBR Green Mix (2X), 20 pmol/µl forward and reverse primers (0.5 µl each) and 8 µl autoclaved ddH_2O was mixed and completed with 1 µl (1:5 diluted) cDNA template to 20 µl qPRC mix. For avoiding evaporation 10 µl mineral oil was added to cover the

surface of the PCR mix. The amplification conditions were as follows; 10 min at 95ºC; 45 cycles of 30s of 95 ºC, 30s of 62 ºC (for *tyms*, *mcm7* and *mybl2*) or 60 ºC (for *ctgf*, *pcna*, *ef1a*, *b2m*, *mmp9*, *cyp26b1*, *ddc*, *dkk1b*, *pah*, *tagln2*, *foxm1*, *bambia*, *wif1*), 30s of 72 ºC and final extension at 72 ºC for 10 min. Real-time qRT-PCR runs of each gene was performed with biological and technical duplicates for serum starvation/replenishment experiments, while three biological replicates and two technical duplicates were applied for rapamycin experiment samples. The iCycler iQ Optical System Software (version 3.021, BioRad, Hercules, CA, USA) provides the melting curves and the threshold cycles of the runs. The melting curves were used to assure a single product was obtained for each sample and the threshold cycle (Ct) was used to calculate the expression change of the selected genes. The expression changes were calculated with an efficiency method; a modified formula of $2^{-\Delta\Delta Ct}$ (Pfaffl, 2001), in which the expressions of selected genes were normalized according to the expression of the housekeeping genes and the mean of the expressions of control samples. The following formula was used to calculate the expression change of selected genes;

$$(E_{target})^{\Delta CtTarget\ (control\text{-}sample)} / (E_{ref})^{\Delta CtReference\ (control\text{-}sample)}$$

The 10-fold serial cDNA dilutions for each primer pair was used for the detection of primer efficiency (E). The formula to calculate the primer efficiencies is;

$$E=10^{[-1/slope\ of\ the\ dilution\ curve]}$$

The reference control genes were observed as the least changed genes from the test conditions. For serum fluctuations *ef1a* and for rapamycin treatments *b2m* were used as reference genes (McCurley and Callard, 2008).

3.3.1.4 Protein Extraction, Detection and Western Blotting

3.3.1.4.1 Protein extraction from tissue culture cells

The cells were collected in the falcon tubes by trypsinization. After removal of culture media, cell pellets washed with ice-cold 1XPBS. 1XPBS were disposed after centrifugation at 1200 rpm for 3 min at 4°C. The cell pellets were immediately frozen by liquid nitrogen and stored at -80°C for later use.

For protein extraction cell pellets in falcons were placed in ice. NP40 lysis buffer (please see in 3.2.4) was prepared and added, 4-5 volumes of cell pellets, on top of the cell pellets in the falcon tubes. The cells were lysed by vortexing at every 5 min for half an hour on ice. The lysates were centrifuged at 13000 rpm for 30 min at $+4^{o}$C. The supernatant was transferred in a fresh tube and stored at -80°C for later use.

3.3.1.4.2 Quantification of protein concentrations

The protein concentrations were detected with Bradford assay. Bradford solution was prepared as explained in section 3.2.5. The protein concentrations were calculated by comparing the absorbance values of cell lysates with the known BSA standard curve concentrations (absorbance vs. BSA concentration). The BSA stock was prepared fresh by dissolving 1 mg BSA in 1 ml of ddH2O to make 1mg/ml BSA. The different BSA concentrations were prepared according to **Table 3.2.** The OD595 λm values were obtained and plotted on a standard curve graph. 2 µl of each protein sample were mixed with the 900 µl of Bradford working solution and the volume completed to 1 ml with the 98 µl of ddH2O. The blank was prepared by mixing 2µl of NP40-lysis buffer with the 900 µl of Bradford working solution and 98 µl of ddH2O. The protein concentrations were measured at OD_{595} λm and calculated by using the BSA standard curve.

Table 3. 2 BSA dilutions for standard curve preparation.

Sample	1	2	3	4	5	6	7
Bradford solution(µl)	900	900	900	900	900	900	900
BSA (1mg/ml) (µl)	0	1	2	4	8	16	32
ddH2O (µl)	100	99	98	96	92	84	68

3.3.1.4.3 Western Blotting

SDS polyacrylamide gel electrophoresis: 5% Stacking gel and 10% or 15% separating gel according to protein size were prepared as follows:

5% stacking gel;

dH_2O	5.5 ml
30% Acrylamide mix	1.3 ml
1.0 M Tris, pH=6.8	1 ml
10% SDS	80 µl
10% APS	80 µl
TEMED	8 µl

10% separating gel;

dH_2O	5.9 ml
30% Acrylamide mix	5 ml
1.5 M Tris, pH=8.8	3.8 ml
10% SDS	150 µl
10% APS	150 µl
TEMED	6 µl

An equal amount of proteins from each sample was obtained and mixed with cracking buffer containing 1% β-mercaptoethanol to complete the volume to 20 µl. Proteins were denaturated by boiling in the water for 5 min. Before loading on the gel, proteins were centrifuged. Fermentas PageRuler Protein size marker was also loaded on the gel to follow the proteins. Proteins were run at 80V during the stacking gel and 120V during the separating gel. According to the protein size to be detected, runs were terminated.

Transferring proteins to PVDF membrane: The proteins were transferred from gel to membrane by a semi-dry transfer process for phospho-p70S6 kinase and p70S6 kinase protein level analyses or by wet-transfer for mcm7 and alpha-tubulin. PVDF membrane was cut slightly larger than the expected gel size. Before incubation in semi-dry transfer buffer, the membrane was placed into 100% methanol for 30 seconds, then transferred into ddH_2O and incubated for 2 min by vigorously shaking. 4 whatman papers were cut as the same size of the membrane and placed into the semi-dry transfer buffer. Before transfer the gel was washed with ddH_2O and waited in semi-dry transfer buffer. For the transfer a sandwich of 2 whatman papers, the membrane and the gel and the rest of the 2 Whatmans were stacked. Transfer was performed at 160mA for 30-45 min.

The immunological detection of transferred proteins: After the transfer the membrane was washed with 1XTBS-T for 5 min. Membrane was blocked in 5% non-fat blocking solution for 1 h with gentle agitation. After blocking, the membrane was extensively washed for 3X15 min with 1XTBS-T. The primary antibody solutions were prepared by adding the recommended antibody concentrations in 5% BSA added TBS-T. After overnight primary antibody incubation at 4ºC, the membrane was washed for 3X15 min with 1XTBS-T. Secondary antibodies were prepared in 5% non-fat blocking solution according to the recommended antibody concentrations. After 1h secondary antibody incubation at room temperature, membrane washed for 3X15 min with 1XTBS-T. Then the membrane was treated with ECL+ western blot detection kit for 5 min. To detect the chemiluminescence, the membrane was exposed to X-ray films.

3.3.2 Cell Culture techniques

3.3.2.1 Cell lines

Zebrafish embryonic fibroblast cells, ZF4 (ATCC, CRL-2050), were derived from 1-day-old zebrafish embryos (Driever and Rangini, 1993). ZF4 cells are adherent fibroblast cells.

3.3.2.2 Cell line maintenance

ZF4 cells were grown in D-MEM/F-12 (1:1) including 10% FBS and 1% Penicillin/Streptomycin at 28ºC with no air. Medium was changed every 3 to 4 days depending on the level of confluency. For subculturing, the growth medium was aspirated and the cells were washed with 1XPBS twice before trypsin solution was added to the flasks. After the cells were detached from the surface of the flasks, the fresh medium was added. The cells were transferred to tubes and centrifuged at 1200 rpm for 3 min. The medium was aspirated and the cells were dispersed in fresh medium and separated into new flasks. The culture media and PBS were kept at 4 ºC; trypsin was kept at -20 ºC. All the solutions were warmed to room temperature for ZF4 cells before use.

3.3.2.3 Cryopreservation of cell lines

The exponentially growing cells were pelleted after trypsinization and re-suspended with freezing medium. The cryotubes were stored at -80 ºC overnight and transferred to the liquid nitrogen tank for long term storage. Freezing medium for ZF4 cells is a complete growth medium supplemented with 5% (v/v) DMSO as suggested by ATCC (http://www.atcc.org). The frozen cells were re-cultured after thawing the cells at RT. The incompletely thawed cells were mixed with fresh growth medium in a larger tube and centrifuged at 1500 rpm for 5 minutes at room temperature. The

medium was aspirated and the cells were re-suspended with fresh complete growth medium and plated.

3.3.2.4 Serum starvation/replenishment experiments

Serum-starvation experiments were performed by plating 3 x 10^6 ZF4 cells in 75-T flasks for 24 h followed by the addition of media containing a pre-determined amount of FBS (i.e., 0%, 1%, 3% and 10%). For serum-replenishment experiments, ZF4 cells at a density of 3.75 x 10^6 in 150-T flasks were incubated for 24 and 48 h with 0.1% or 10% FBS-containing media and 24 h serum-starved cells were re-incubated with 10% FBS media for another 24 h. For 6 h serum-replenishment experiments, ZF4 cells at a density of 3 x 10^6 in 75-T flasks were incubated for 24 h with 0.1% FBS-containing media and then re-incubated with 0.1% or 10% FBS-containing media for 6 h. Cells were counted following trypsin (without EDTA; HyClone, Logan, UT, USA) treatment with hemocytometer and cell pellets were preserved in liquid nitrogen until later use.

3.3.2.5 Rapamycin treatment experiments

For microarray experiments, 5.5 x 10^6 ZF4 cells were cultured in 150-T flasks in triplicates. Cells were treated with 100 nM final concentration of rapamycin (Calbiochem, Darmstadt, Germany) and DMSO as control for two days before collection and counting of cells. 5 x 10^6 cells were used for RNA isolation for microarray studies. To confirm the microarray data by real-time qRT-PCR analysis an independent set of rapamycin treatment experiment was used. For rapamycin treatment experiments, 5 x 10^6 ZF4 were seeded in 75-T flasks in triplicates; and cells were incubated with 100 nM final concentration of rapamycin or equivalent of DMSO for 6 or 48 h before collection for ZF4. Cells were counted following trypsin (without EDTA; HyClone, Logan, UT, USA) treatment with hemocytometer and cell pellets were preserved in liquid nitrogen until later use.

3.3.3 MTT Assay

For different serum levels; 0%, 1%, 3% and 10% FBS treatment, 2 x 10^4ZF4 cells were incubated in triplicates for 24 h in 96-well microplates. For rapamycin experiments 2 x 10^4 ZF4 cells were treated with 100 nM rapamycin or equivalent of DMSO for 48 h. MTT (3-(4,5-dimethylthiazole-2-yl)-2.5-diphenyltetrazolium bromide) assay was performed according to the manufacturer's protocols (Vybrant MTT Cell Proliferation Assay Kit, Molecular Probes, V-13154, Germany). MTT, reduced to an insoluble formazan dye by mitochondrial enzymes associated with metabolic activity, provides a reliable cellular assay for predicting viable cells (Mosmann, 1983). The MTT experiment performed by adding 10 µl MTT solution to 100 µl treatment medium, 4 h before the end of the treatment duration. ZF4 cells were incubated in the 28 ºC incubator for 4 h with MTT solution. The cell culture medium including MTT solution was removed by inverting the plate in order to avoid cell loss. 50 µl DMSO was added to each well. After 1-2 min DMSO was mixed gently and incubated for 10 min. The absorbancy at 540 nm was read with µQuant™ Microplate Spectrophotometer (BioTek, Winooski, VT). The results from triplicate measurements were normalized to the blanks and averaged.

3.3.4 BrdU Assay

BrdU (5-bromo-2-deoxyuridine) staining was performed to estimate the effect of test conditions on cell proliferation. BrdU is a synthetic analog of tymidine and incorporated in DNA of proliferating cells during DNA replication. Therefore, BrdU incorporation is used to detect the proliferating cells. For serum starvation/replenishment experiments 5 x 10^4 ZF4 cells were cultured in 6-well plates and serum starved for 48 h with 0.1% FBS including media. Serum replenishment was performed with treating 24 h serum starved cell with complete media for another 24 h. For rapamycin treatments 5 x 10^4 ZF4 cells were cultured in 6-well plates and treated with 100 nM rapamycin or DMSO for 48 h. For BrdU staining cells were incubated with 30 µM BrdU for 24h and then fixed with 70% ice cold ethanol for 10 min. After fixation, cells were treated with 2N HCl for 20 min. Prior to incubation with an α-BrdU antibody (1:500 in 2% FBS in PBS; Dako, Denmark) for 1 h, cell were blocked

with 10% FBS/PBS for 1 h. After α-BrdU antibody, cells were incubated with α - mouse secondary antibody (1:750 in 2% FBS; Invitrogen, Carlsbad, CA, USA) for 1 h at RT. DAPI staining was used as counterstain to visualize all the nuclei. The digital fluorescent microscopy images were taken for all the samples using Zeiss, AX10 Imager A1 (Germany). Multiple fields were counted, averaged and plotted.

3.3.5 Cell Cycle Analysis

The cell cycle analysis of serum starvation/replenishment samples were performed by seeding 3 x 10^6 ZF4 cells in 100 mm petri dishes. For serum starvation experiments cells were treated either with 0.1 % or with 10% FBS including media for 24 and 48 h. For serum replenishment experiments 24 h serum starved cells in 0.1% FBS including media were treated with 10% FBS including media for another 24 h. The cell cycle analysis of 100 nM rapamycin treated ZF4 cells was performed by culturing 5 x 10^5 ZF4 cells in 6-well petri plates. ZF4 cells were treated with 100 nM rapamycin, DMSO including media or culture media for 48 h at 28ºC. After treatments, cells were fixed in a 70% EtOH/PBS solution for 15 min on ice. The propidum iodide staining was carried out by incubating cells with PI staining solution (a final concentration of 50µg/ml PI, and 100µg/ml RnaseA in PBS) at 37ºC in dark for 40 min. Propidium iodide staining is used to detect the percent cell numbers at each cell cycle stage (Krishan, 1975). For rapamycin experiments attached and non-attched cells were collected, however for serum starvation/replenishment experiments only attached cells were collected for the cell cycle analysis. For serum starvation/replenishment samples, 3 x 10^4 cells and for rapamycin treated samples, 1 x 10^4 cells were analyzed by Becton Dickson FACScalibur (USA).

3.3.6 Cell Death Detection Analysis

The effect of rapamycin on apoptosis was detected with Cell Death Detection ELISA^{PLUS} (CDD, Roche, Germany). In principle, CDD assay specifically detects

mono and oligonucleasomes (histone-associated DNA fragments) in the cell lysate. 2 x 10^4 ZF4 cells were cultured in 96 well plates, treated with 100nM rapamycin or equivalent of DMSO or culture media for 48 h at 28ºC. Cell lysates were prepared and placed into the streptavidin-coated plates provided with the kit. Cell lysates incubated with an immunoreagent composed of anti-histon biotin together with anti-DNA-POD (anti-DNA peroxidase) for 2 h at RT. Anti-histone biotin antibody binds to streptavidin-coated plates and captures the nucleosomes by their histones, while anti-DNA-POD binds to DNA in the nucleasomes. The anti-histone recognizes the H1, H2A, H2B, H3, and H4 histones from several species. After washing, the ABTS solution, the substrate, was added and the absorbancy was assessed with μQuant™ Microplate Spectrophotometer (BioTek, Winooski, VT) at 405 nm using 490 nm as reference.

3.3.7 Microarray Analysis

3.3.7.1 The assessment of quantity and quality of RNA

For microarray analysis, 3 rapamycin and 2 DMSO (vehicle control) RNA samples were prepared as explained in section 3.3.2.5. Before hybridization on chips, the quantity and quality of total RNAs were assessed by using Agilent 2100 BioAnalyzer (Agilent Technologies, Santa Clara, CA, USA). The RIN values and rRNA ratios [28s/18s] were supplemented in **Table 4.1.** After hybridization on chips, the quality of RNAs were assessed by using the using the affy (Gautier et al., 2004) and affyPLM (Bolstad, 2005; Brettschneider, 2007) packages of Bioconductor (Gentleman et al., 2004) in the R 2.10.1 (http://cran.t-project.org).

3.3.7.2 Amplification, hybridization and scanning

The Affymetrix zebrafish GeneChips (Affymetrix, Santa Clara, CA, USA; http:www.affymetrix.com/products/arrays/specific/zebrafish.affx) were used for

microarray analysis. The total RNA conversion to complementary DNA (cDNA) (Superscript II kit; Invitrogen, Carlsbad, CA, USA), the *in vitro* transcription to biotin-labeled cRNA (antisense RNA) and the following cRNA fragmentation (Ambion, Austin, TX, USA) and lastly hybridization to Affymetrix zebrafish GeneChips were performed under the supervision of Dr. Hilal Ozdag from Ankara University, Ankara. The results were quantified using a GeneChip scanner (Affymetrix, Santa Clara, CA, USA).

3.3.7.3 Quality control of the arrays

The quality control of arrays was assessed using the *affy* (Gautier et al., 2004) and *affyPLM* (Bolstad, 2005; Brettschneider, 2007) packages of Bioconductor (Gentleman et al., 2004) in the R 2.10.1 (http://cran.t-project.org). The two methods in *affyPLM* package, Relative Log Expression (RLE) and the Normalized Unscaled Standard Error (NUSE) methods were used to evaluate the CEL files.

3.3.7.4 Normalization

The CEL files were converted to gene expression values by BRB-Array tools version 3.8.0 (http://linus.ncbi.nih.gov/BRB-ArrayTools.html; developed by Dr. Richard Simon and the BRB-ArrayTools Development Team). The data were normalized using the RMA normalization (Robust multiple array normalization) (Bolstad et al., 2003; Irizarry et al., 2003) with background correction, quantile normalization and calculating the expression values using median-polish algorithms.

3.3.7.5 Obtaining differentially expressed genes

The differentially expressed genes in response to rapamycin treatment were identified by using the Class Comparison Tools of BRB-array tools; the significance

threshold value was set to p=0.05. Univariate tests were performed to select the differentially expressed genes between groups giving the p-values, FDRs and fold changes of the significant genes. The upregulated and downregulated probe sets in response to rapamycin exposure in the differentially expressed gene set were also marked by class comparison tool.

3.3.7.6 Gene Ontology analyses

The gene ontology (GO) terms for biological process (BP), molecular function (MF) and cellular component (CC) analysis and KEGG pathway analysis for the upregulated and downregulated probesets were performed using Fisher's exact test in DAVID (Dennis et al., 2003; Huang da et al., 2009).

3.3.8 Phylogenetic analysis of E2F pathway genes

The evolutionary conservation of selected E2F target genes within different species was assessed with phylogenetic analysis. The protein sequences of Pcna, Mybl2, Tyms, Mcm7 and Ctgf for different species were extracted from NCBI (http://www.ncbi.nlm.nih.gov/) and ENSEMBL (http://www.ensembl.org/index.html) databases. The amino acid sequences were aligned using Clustal W (Thompson et al., 1994). MEGA version 4 (Tamura et al., 2007) was used to generate the bootstrapped neighbor-joining phylogenetic trees. The species and their abbreviations used in trees were as follows: human (Hs), rat (Rn), mouse (Mm), chicken (Gg), cow (Bt), salmon (Ss), stickleback (Ga), green spotted puffer fish (Tn), zebrafish (Dr), western clawed frog (Xt), fugu (Tr) and medaka (Ol). The amino acid sequences used in generating trees were supplemented in **Table 3.3**.

Table 3. 3 Amino acid sequences used to generate phylogenetic trees

Pcna protein seq.	Accession Number
rat	NP_071776.1
mouse	NP_035175.1
human	NP_002583.1
chicken	NP_989501.1
zebrafish	NP_571479.1
western clawed frog	NP_001007921.1
cow	NP_001029666.1
fugu	ENSTRUP00000036585
medaka	ENSORLP00000003669
stickleback	ENSGACP00000007613
green spotted puffer fish	ENSTNIP00000018432
Tyms protein seq.	**Accession Number**
human	NP_001062.1
rat	NP_062052.1
mouse	NP_067263.1
zebrafish	NP_571835.1
western clawed frog	NP_001072852.1
fugu	ENSTRUP00000004951
stickleback	ENSGACP00000005414
medaka, transcript 1	ENSORLP00000013876
medaka, transcript 2	ENSORLP00000013877
Mybl2 protein seq.	**Accession Number**
mouse	NP_032678.1
human	NP_002457.1
rat	NP_001100006.1
zebrafish	NP_001003867.2
chicken	NP_990649.1
cow	NP_001068916.1
medaka	ENSORLP00000014540
stickleback, grXII	ENSGACP00000008012
stickleback, grXVII	ENSGACP00000014242
green spotted puffer fish, ch9	ENSTNIP00000004055
green spotted puffer fish, ch11	ENSTNIP00000010146
Mcm7 protein seq.	**Accession Number**
human isoform 1	NP_005907.3
human isoform 2	NP_877577.1
mouse	NP_032594.1
western clawed frog	NP_998877.1
rat	NP_001004203.3
zebrafish	NP_997734.1
cow	NP_001020516.2
fugu	ENSTRUP00000037145

medaka	ENSORLP00000000656
stickleback	ENSGACP00000021654
green spotted puffer fish	ENSTNIP00000018801
Ctgf protein seq.	**Accession Number**
mouse	NP_034347.2
rat	NP_071602.1
human	NP_001892.1
chicken	NP_989605.1
zebrafish	NP_001015041.1
western clawed frog	NP_001015042.1
cow	NP_776455.1
salmon	NP_001133471.1
fugu	ENSTRUP00000034594
green spotted puffer fish	ENSTNIP00000013889
medaka, transcript 1	ENSORLP00000022627
medaka, transcript 2	ENSORLP00000022629
medaka, transcript 3	ENSORLP00000022630

3.3.9 In vivo Zebrafish embryo experiments

3.3.9.1 Zebrafish embryo strain

The *in vivo* rapamycin experiments were performed with the Tupfel long fin (TLF, previous name; Tuebingen long fin), a wild type zebrafish strain, having homozygous mutations for leo^{t1} and lof^{dt2}. leo^{t1} gene mutation is recessive and cause spotting in adult fish. lof^{dt2} mutation is dominant homozygous and results in long fins (http://zfin.org).

3.3.9.2 Rapamycin treatment to zebrafish embryo

Shield stage healthy zebrafish embryos were collected and transferred into 96-well plates, each well contained 3 embryos. At this point, a final concentration of 2 µM, 10 µM and 20 µM rapamycin or equivalent of DMSO was added to embryo

medium. Zebrafish embryos were collected at 1, 2, 3, 4 and 5 dpf (days post fertilization) for further examination.

3.3.9.3 Morphological measurements

Zebrafish embryos were visualized with Leica MZ16FA Stereo microscope. The body length of rapamycin or vehicle (DMSO) treated zebrafish embryos at indicated time points were assessed with Image-J (version 1.38) in millimeters.

3.3.9.4 Histological examinations of intestinal system

Zebrafish embryos were treated with 400 nM rapamycin or equivalent of DMSO for 8 days in 96-well plates. 8 dpf rapamycin or DMSO treated embryos were collected and fixed in 4% PFA (paraformaldehyde)/PBS for 1h at RT; washed twice in PBS each for 5 min; and incubated in 20% sucrose/PBS overnight at 4ºC. Zebrafish embryos were taken out from the sucrose and placed in plastic molds (Molding Cups, Polysciences Inc., Eppelheim, Germany) and the sucrose was cleaned out of the embryos. Embryos were covered with Tissue Tek (O.C.T. Compound, Plano, Wetzlar, Germany) in sagital orientation. Embryo containing molds were placed on dry ice for about 20 min to harden Tissue Tek. The plastic molds were removed and 10-12 µm sections were cut. The pieces were placed on to a slide and leaved at RT to dry.

3.3.9.5 Hematoxylen-eosin staining

Cryosectioned samples were stained with hematoxylen and eosin to visualize the tissues. The slides were stained with Hayer's hematoxylen (Sigma, St. Louis, MO, U.S.A) for 2 min and washed 5 min under the tap water; and stained with eosin (Sigma, St. Louis, MO, U.S.A) for 1 min and washed with H_2O. Before being incubated with 100% EtOH, slides were treated with first 70% EtOH and later 96%

EtOH. At last slides were treated with xylol or Poti-histol for 5 min. The sections on slides were covered with entalan and coverslips were placed on the sections; left overnight to dry; and visualized by Leica DC500 High-resolution Digital Camera System (Cambridge, UK).

3.3.9.6 Alcian blue staining

Zebrafish embryos were treated with 10 µM rapamycin or DMSO for 5 and 6 days. Embryos were collected and fixed in 4% PFA overnight at 4ºC. Removed from the PFA and transferred to 70% EtOH for 10 min. Embryos were stained overnight with 0.1 mg Alcian blue in 0.1 N HCl at RT. After staining, embryos were rinsed in H_2OT (tap water with 0.1% Tween-20) twice for 5 min. The pigmentation was removed by bleaching the embryos in solution containing 10 µl 30% H_2O_2 and 100 µl 10% KOH in 890 µl H_2OT for 30 min at 37ºC; and washed twice in H_2OT for 5 min. Embryos were rinsed with 300 µl saturated borate in 600 µl H_2OT. The tissues covering the cartilage were removed by digestion with 0.25 mg/ml trypsin and 300 µl saturated borate in 600 µl H_2OT for 30 min; and again washed twice in H_2OT for 5 min. Then they were rinsed in 25% glycerol/75% H_2O. Zebrafish were transferred to 50% glycerol/50% H_2O and then to 75% glycerol/25% H_2O. Embryos were stored at RT or 4ºC.

3.3.10 Statistical Analyses

The Minitab software release 13.20 (Minitab Inc., State College, PA, USA) was used to analyze the significance of real-time qRT-PCR, MTT, BrdU and PI staining results. One-way ANOVA test with Fisher's pairwise comparisons was performed to analyze dose effect in serum starvation or replenishment samples. Two-way ANOVA test was used to test the significance between dose and time effect in serum replenishment (between 24 and 48 h) and rapamycin treatments (between 6 and 24 h). General linear model was performed to detect the significance of *in vivo* zebrafish experiments; dose and exposure time dependent rapamycin effect on body

length was assessed. The graphs were generated by GraphPad Prism 5 software (GraphPad Software, San Diego, CA, USA).

Chapter 4. RESULTS

4.1 The effect of serum starvation/replenishment on ZF4 cells

4.1.1 Cell viability analysis of serum starved/replenished ZF4 cells

The MTT, cell viability assay was performed in order to assess the effect of 24, 30 and 48 h serum starvation on ZF4 cells. The recovery of the living cell number after 6 and 24 h serum replenishment following 24 h serum starvation was also investigated with MTT assay.

4.1.1.1 Cell viability analysis of serum-starved ZF4 cells

The effect of serum starvation on viable cell number was assessed by treating ZF4 cells with reducing serum concentrations for 24 h. MTT analysis reflected the decrease in the number of the living cells as the serum concentration in the media decreases (**Figure 4.1**).

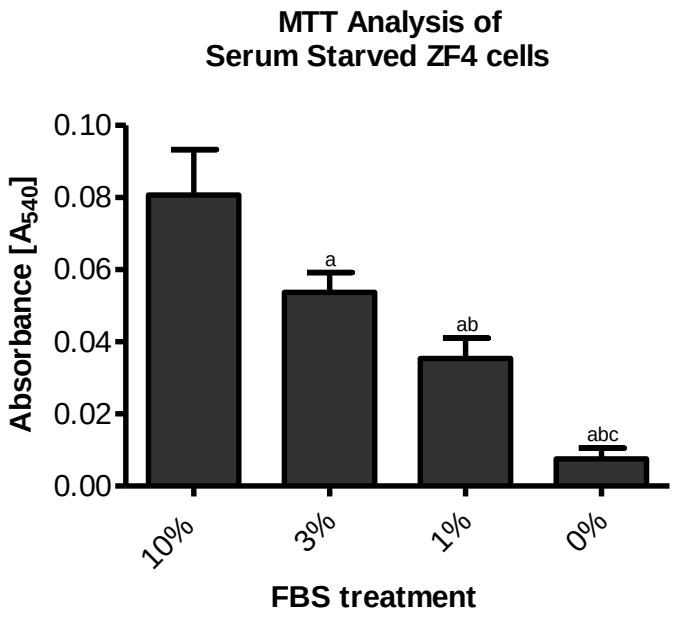

Figure 4. 1 MTT analysis of ZF4 cells treated with 0%, 1%, 3% and 10% FBS supplemented media for 24 h. Pair-wise analysis was performed according to Fisher's multiple comparisons in One-way ANOVA (One-way ANOVA; $p \leq 0.001$ for % FBS, [a], [b], [c] represents the significance at $p \leq 0.05$ from 10%, 3%, and 1% FBS, respectively).

4.1.1.2 Cell number counts of the ZF4 cells used for dose-serum response real-time qRT-PCRs

The cell numbers of ZF4 cells used for dose-dependent serum starvation experiments were counted after tyrpsinization. As explained in the Materials- Methods section of this thesis, 3 x 10^6 ZF4 cells were treated with pre-determined amount of FBS (i.e., 0%, 1%, 3% and 10%) for 24 h, in duplicates, in order to detect the serum dose-dependency of ZF4 cells. After treatments, cells were collected and counted to observe the concordance with the MTT analysis and attached cell numbers (**Figure 4.2**). The numbers of the cells used for serum starvation real-time qRT-PCRs were highly correlated with MTT results (**Figure 4.1**).

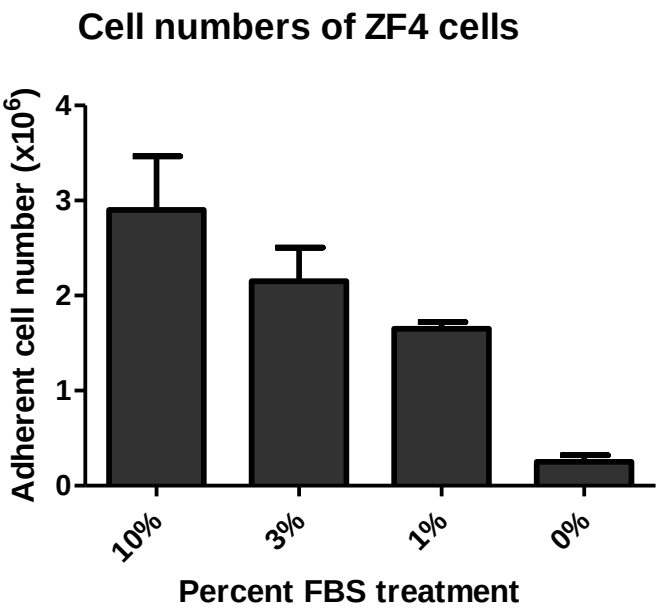

Figure 4. 2 Cell counts of ZF4 cells used for real-time qRT-PCR analysis. ZF4 cells were treated with variying doses (i.e., 0%, 1%, 3% and 10%) of serum including media for 24 h, in duplicates. Cells were collected and counted with hemocytometer after trypsinization. The RNA extracts of these cells used for real-time qRT-PCR analysis.

4.1.1.3 Cell viability analysis of serum replenished ZF4 cells

The decrease in the viable cell number after serum starvation was reversible. Serum replenishment gradually increased the living ZF4 cells. The number of the viable cells after 6 h serum replenishment increased significantly (**Figure 4.3-A**). After 24 h serum replenishment the viable cell number was reached to the number of the control cells that were cultured in the 10% FBS including media (**Figure 4.3-B**).

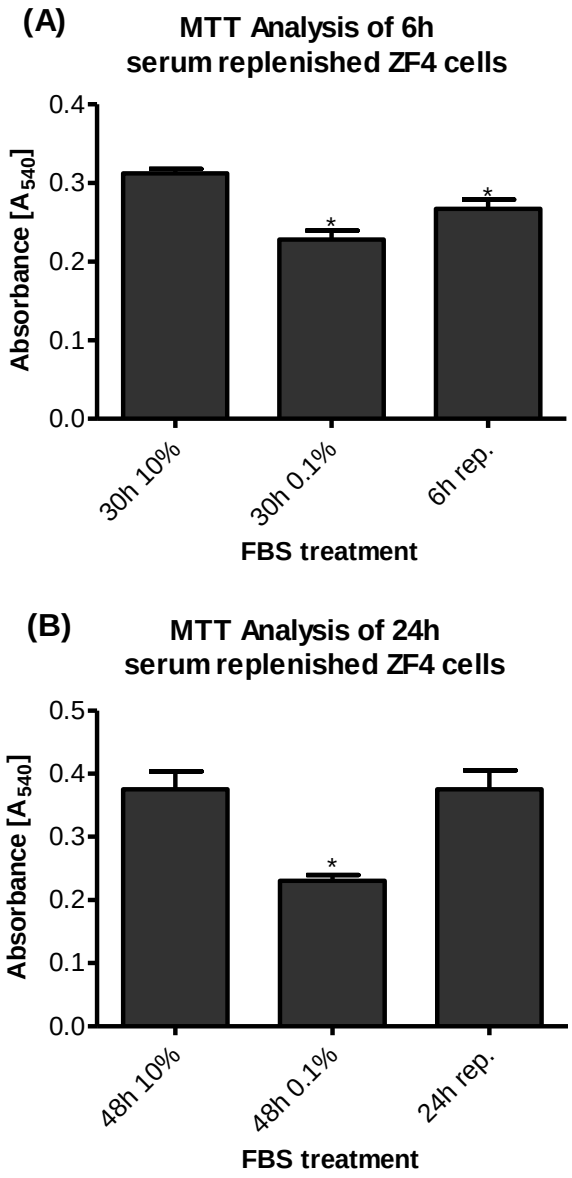

Figure 4. 3 MTT analyses of 6 and 24 h serum replenished ZF4 cells (A) ZF4 cells were serum starved for 30 h with 0.1% FBS including media or serum starved for 24 h and replenished with culture media for 6 h. One-way ANOVA was performed to test the significance (One-way ANOVA; $p \leq 0.001$). **(B)** ZF4 cells were serum starved with 0.1% FBS including media for 48 h. 24 h serum replenishment was performed with culturing 24 h serum starved cells with culture media for another 24 h. One-way

ANOVA was performed to test the significance (One-way ANOVA; $p \leq 0.001$). * represents the significance at $p \leq 0.05$ according to Fisher's multiple comparisons.

4.1.1.4 Cell number counts of the ZF4 cells used for 24h serum replenishment real-time qRT-PCRs

The cell numbers of ZF4 cells used for 24 h serum replenishment experiments were counted after tyrpsinization. The experitmental set up was explained in the Materials and Methods section. After treatments, cells were collected and counted to observe the concordance with the MTT analysis and attached cell numbers (**Figure 4.4**).

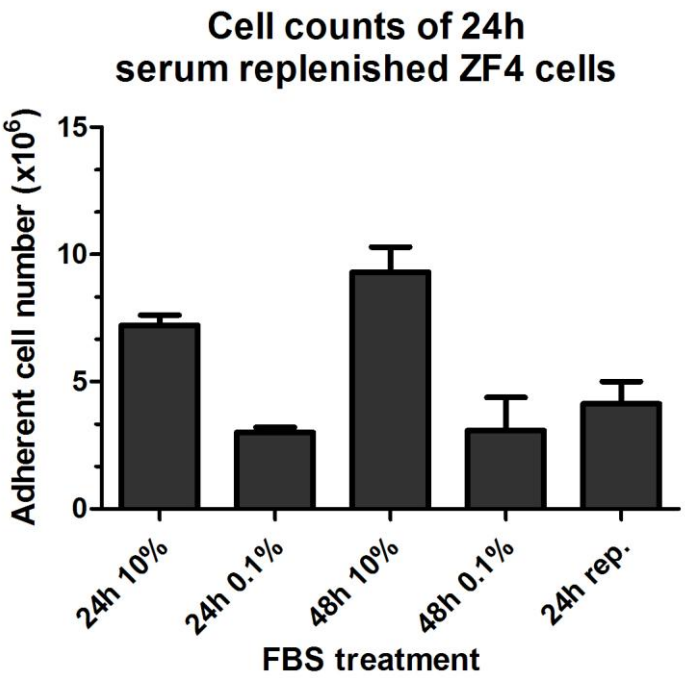

Figure 4. 4 Cell counts of ZF4 cells used for 24 h serum relplenishment real-time qRT-PCR. ZF4 cells were serum starved with 0.1% FBS including media for 24 or 48 h. 24 h serum replenishment was performed with culturing 24 h serum starved cells with culture media for another 24 h. Cells were collected and counted with hemocytometer after trypsinization. The RNA extracts of these cells used for real-time qRT-PCR analysis.

4.1.2 Cell proliferation analysis of serum starved/replenished ZF4 cells

The MTT analysis revealed that serum starvation decreased the cell number in ZF4 cells, which was reversed after serum replenishment. To assess the proliferative capacity of the serum-starved/-replenished cells, BrdU staining was performed with the cells that were starved for 48 h, or starved for 24 h and cultured with serum containing media for another 24 h. The cells that were proliferating was significantly decreased after 48 h serum starvation, however serum replenishment increased the proliferating cell number (**Figure 4.5-4.6**).

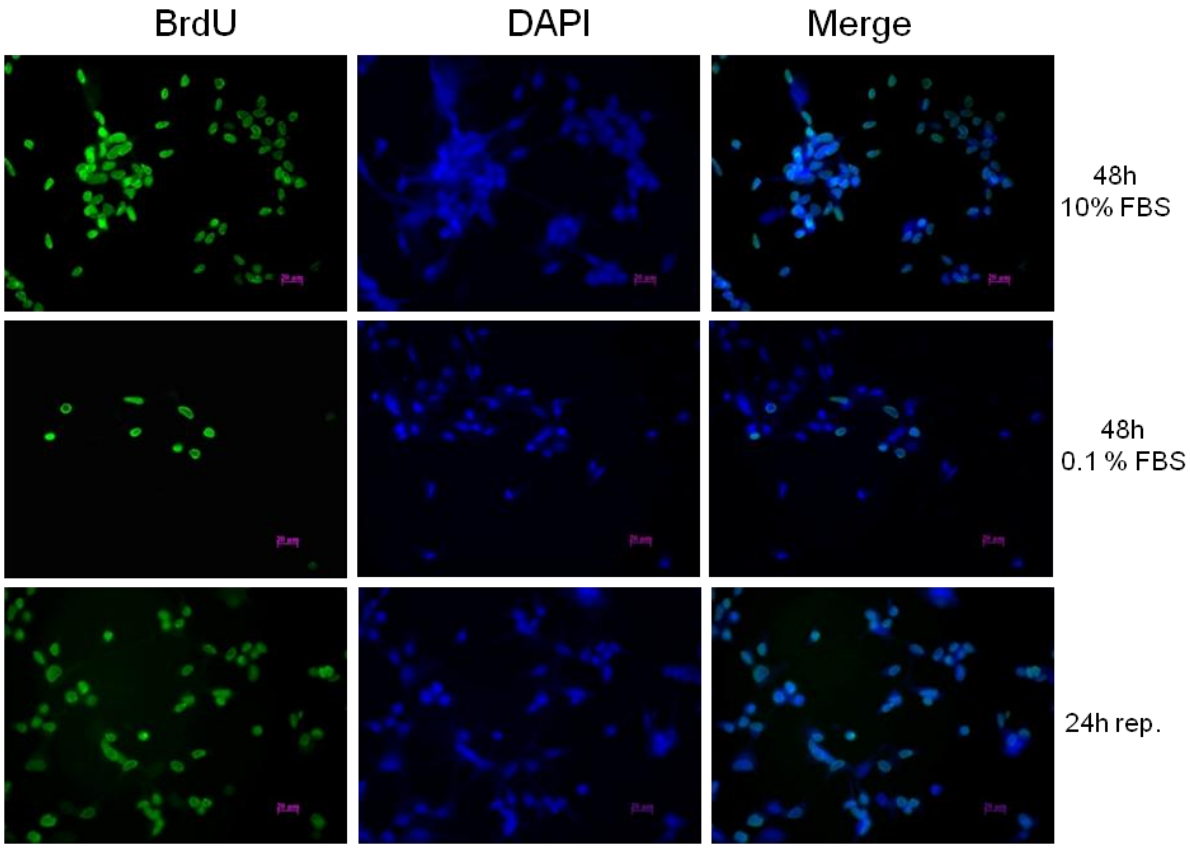

Figure 4. 5 Representative presentation of BrdU incorporation of serum replenished ZF4 cells. ZF4 cells were either serum starved for 48 h in 0.1% FBS supplemented media or serum starved for 24 h and then incubated with 10% FBS including culture media for another 24 h; 24 h serum replenishment (24h Rep.) group. BrdU incorporated nuclei were visualized as green stained and DAPI was used to stain the nuclei of viable cells. The magnification was 40x for all the figures and the scale bars marks the distance of 20 μm.

Our results were consistent with the previous reports. In a previous study with porcine fetal fibroblasts, serum starvation with 0.2% FCS decreased the percent BrdU positive cell number from 90% to 2% after 48 h of starvation. The percent BrdU positive cells were decreased as the time of starvation increases (Kues et al., 2000). In our study after 48h of starvation, percent BrdU positive cells were decreased from 99% to 11%, and serum replenishment for 24 h following a 24 h starvation increased the proliferating cell number to 72% (**Figure 4.6**).

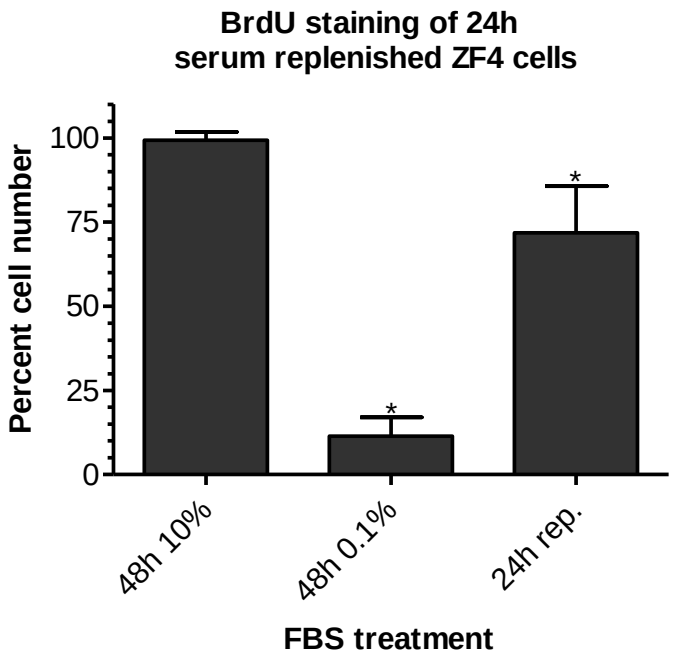

Figure 4. 6 BrdU incorporation of 24 h serum starved and then 24 h serum replenished (24h rep.) ZF4 cells. The BrdU positive cells were corrected to DAPI stained nuclei for the multiple areas counted and the mean of percent cell number was plotted. One-way ANOVA was performed to test the significance with Fisher's multiple comparisons (One-way ANOVA; $p \leq 0.001$). *indicates significance at $p \leq 0.05$.

4.1.3 Cell cycle analysis of serum starved/replenished ZF4 cells

In order to detect the affect of serum starvation/replenishment in cell cycle status of ZF4 cells, we performed PI staining to detect the percentage of the cells at different cell cycle stages. Serum starvation causes an increase in G0/G1 phases and a decrease in the S and G2/M phases of the cell cycle in mammalian fibroblast cell lines (Bettuzzi et al., 1999; Goissis et al., 2007; Khammanit et al., 2008; Kues et al., 2000;

Vackova et al., 2003) which recovered by serum addition to culture media (Bettuzzi et al., 1999). The percentage of the cells at G0/G1 phase of the cell cycle significantly increased in both the 24 h and 48 h serum-starved ZF4 cells, while the percentage of the cells at S and G2/M phases decreased. The growth arrest caused by serum starvation was reversible; after serum addition to 24 h serum-starved ZF4 cells, the cell percentage at the S and G2/M phases increased significantly (**Figure 4.7**). This increase in S phase represents a synchronization event in ZF4 cells.

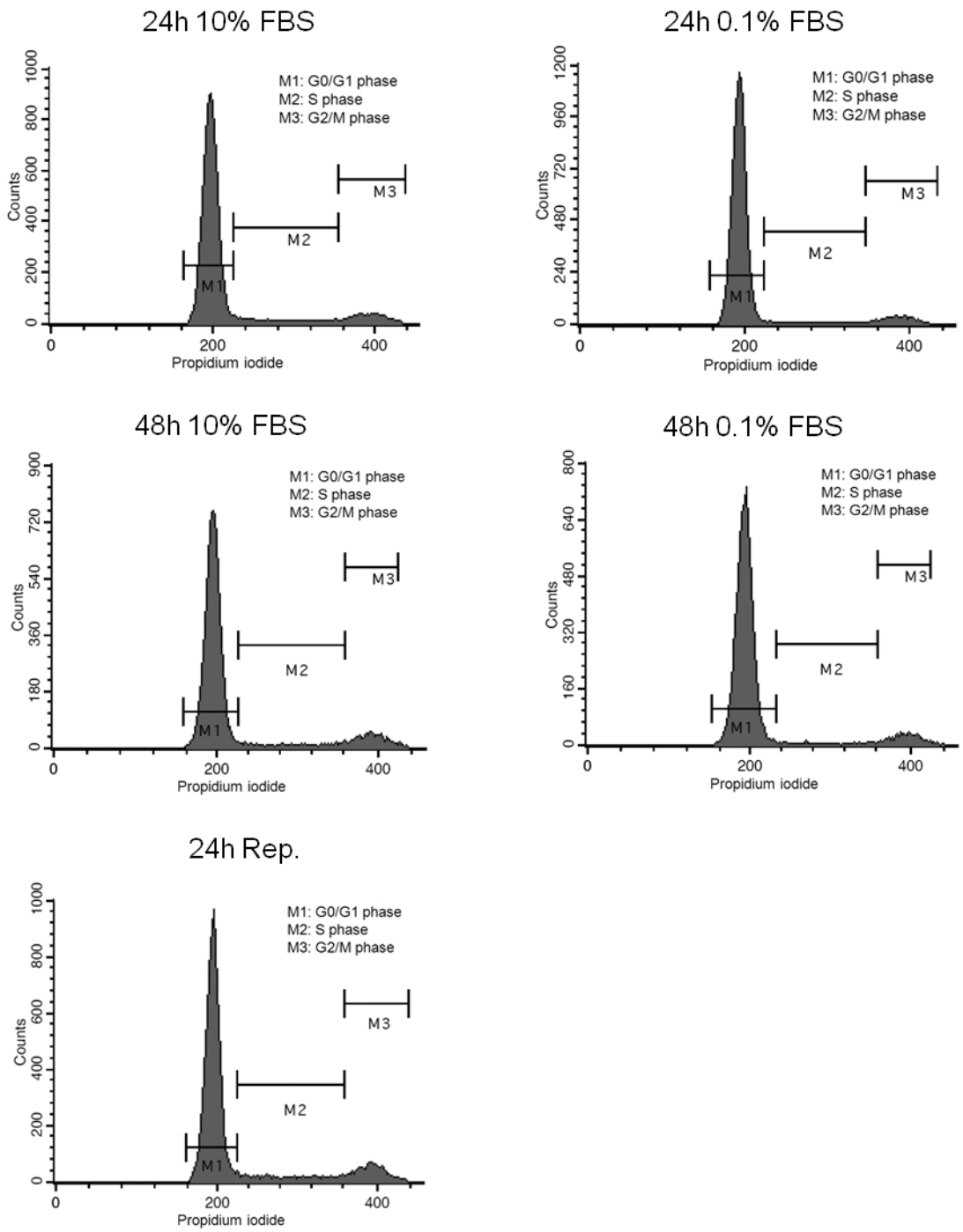

	24h 10% FBS	24h 0.1% FBS	48h 10% FBS	48h 0.1% FBS	24h Rep.
G0/G1	85.40 ± 0.12	91.48 ± 0.26*	85.24 ± 0.86	91.22 ± 0.02*	80.66 ± 0.28#*
S	6.44 ± 0.60	2.25 ± 0.05*	5.90 ± 0.28	2.32 ± 0.42*	8.27 ± 0.24#*
G2/M	8.35 ± 0.49	6.35 ± 0.21*	8.75 ± 1.04	6.28 ± 0.45	11.25 ± 0.11#

Figure 4. 7 Cell cycle analysis of 24 and 48 h serum starved cells and 24 h serum starved and then 24 h serum replenished (24h Rep.) ZF4 cells. 3 X 10^6 ZF4 cells were cultured in 100 mm petri dishes and serum starvation and replenishment was performed as for indicated time points. The mean percentage of cells at G0/G1, S, G2/M phases of cell cycle was presented with ± standard deviation. (One-way

ANOVA between 24 h 0.1%-10%; G0/G1, p=0.001; S, p=0.01; G2/M, p=0.034; between 48 h 0.1%-10% and 24h replenishment; G0/G1, p=0.001; S, p=0.001; G2/M, p=0.011). * represents the significant difference from 10% FBS at $p \leq 0.05$ at corresponding time points. # represents the significant difference from 0.1% FBS at 48 h time point.

Since the confluency of the cells also affect the cell percentage at cell cycle phases (de Barros et al., 2010), we performed another cell cycle analysis with the ZF4 cells seeded at low confluency (**Figure 4.8**). PI staining showed that when cells were seeded at a lower confluency, the percentage of the cells at the G0/G1 phase is less than cells seeded at higher confluency at 10% FBS group. However in the 24 h 0.1% FBS cultured group the difference at cell cycle phases were very similar to the cells cultured at a higher confluency (**Figure 4.7-4.8**).

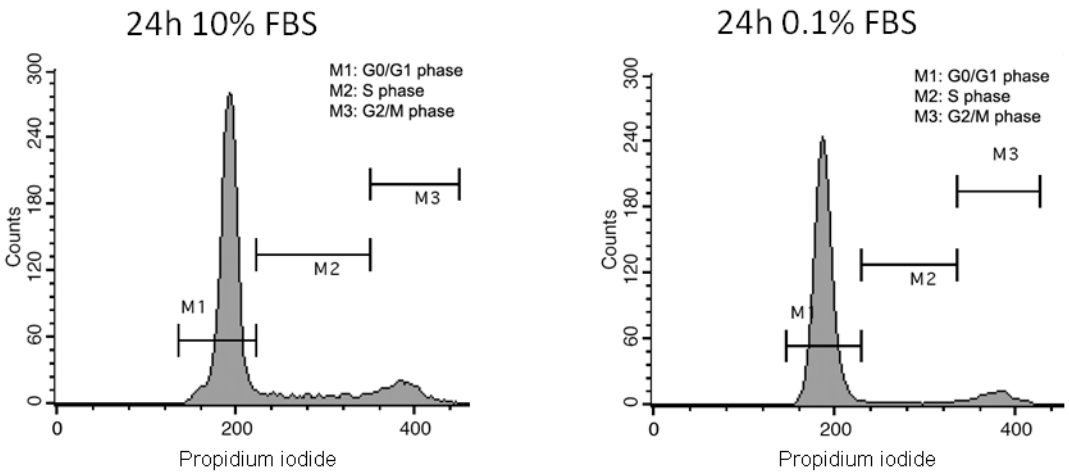

	24h 10% FBS	24h 0.1% FBS
G0/G1	78.71	90.34
S	9.90	1.72
G2/M	11.58	7.98

Figure 4. 8 Cell cycle analyses of 24 h starved ZF4 cells at low confluency. 1.5 X 10^6 ZF4 cells were cultured in 100 mm petri dishes and serum starved with 0.1% FBS supplemented media for 24 h. The mean percentage of cells at G0/G1, S, G2/M phases of cell cycle was presented with ± standard deviation. At each event, 1 X 10^4 cells were analyzed by Becton Dickinson FACScalibur.

4.1.4 The effect of serum starvation on translation

The effect of serum starvation on proteins synthesis was assessed by surveying the phospho-p70 S6 kinase protein levels in serum-starved ZF4 cells. Phosphorylation of p70 S6 kinase protein on Thr389 is a regulatory step in protein translation (Jefferies et al., 1997; Pullen and Thomas, 1997). Serum starvation decreased the phosphorylated p70 S6 kinase proteins in ZF4 cells, which represents the negative effect of serum starvation on protein translation (**Figure 4.9**).

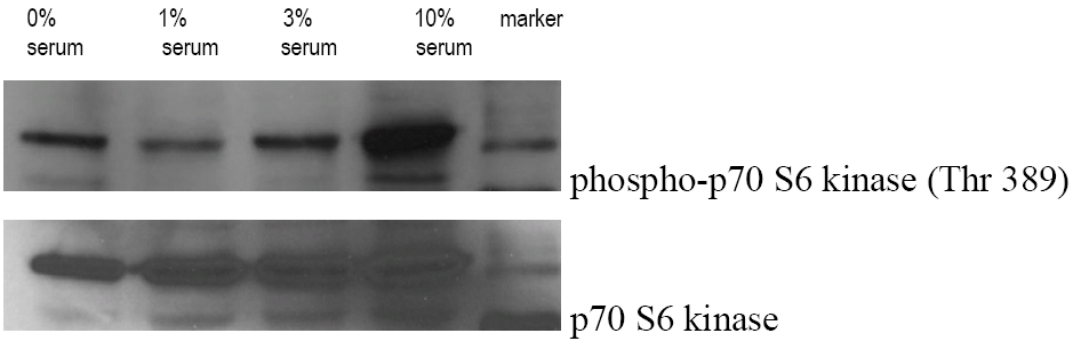

Figure 4. 9 The activity of phospho-p70S6 kinase in 24 h serum starved ZF4 cells. ZF4 cells were serum starved with 0%, 1% and 3% FBS including media. The phospho-p70 S6 kinase (Thr389) protein levels were investigated with western blot. The equal loading was tested with total p70 S6 kinase.

4.2 The effect of serum starvation/replenishment on E2F target gene expression

We selected the zebrafish orthologs of five known mammalian E2F target genes to study the molecular and functional conservation in zebrafish (Bracken et al., 2004). The selected genes; *pcna*, *mybl2*, *tyms*, *mcm7* and *ctgf* expression was investigated in serum-starved and -replenished ZF4 cells. The sequence conservation of selected genes was surveyed with phylogenetic analysis.

4.2.1 Pcna

The evolutionary conservation of Pcna was searched by comparing the amino acid sequences of Pcna in mammalian and fish species. The zebrafish Pcna sequence was closer to fish Pcna sequences, while mammalian, chicken and western clawed frog PCNA amino acid sequences were more similar (**Figure 4.10**).

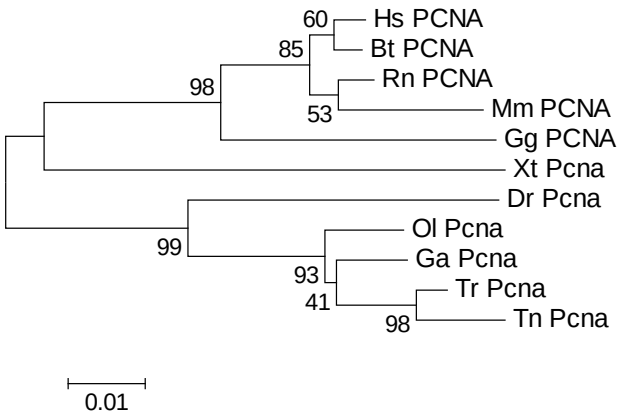

Figure 4. 10 Phlyogenetic tree of Pcna protein sequence. Species; human (Hs), rat (Rn), mouse (Mm), chicken (Gg), cow (Bt), stickleback (Ga), green spotted puffer fish (Tn), zebrafish (Dr), western clawed frog (Xt), fugu (Tr) and medaka (Ol). Scale bar =0.01 substitutions per site.

As in their mammalian counterparts (Hurford et al., 1997; Liu et al., 1995), the zebrafish *pcna* expression decreased after 24 h of serum starvation. The gradual decrease in the expression was significant at 0% FBS treated cells (**Figure 4.11**).

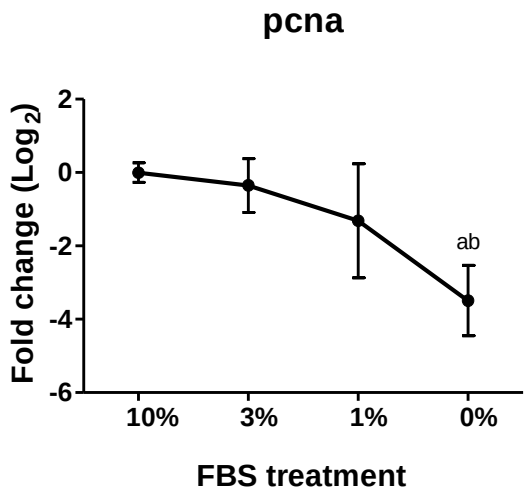

Figure 4. 11 The real-time qRT-PCR results of *pcna* expression in serum starved cells for 24 h. ZF4 cells were serum starved for 24 h with 0%, 1% or 3% FBS containing media. The fold change difference from 10% FBS control was calculated. The log2 based fold changes were plotted and used to test the significance by one-way ANOVA (*pcna*, p=0.077). [a] indicates the significance to 10% FBS at $p \leq 0.05$, [b] indicates the significance to 3% FBS at $p \leq 0.05$.

Serum stimulation reversed the decrease in *pcna* expression. The expression of pcna was rescued starting from the 6 h serum stimulation (**Figure 4.12**) and after 24 h serum replenishment the *pcna* mRNA levels reached to the mRNA levels of control cells (**Figure 4.13**).

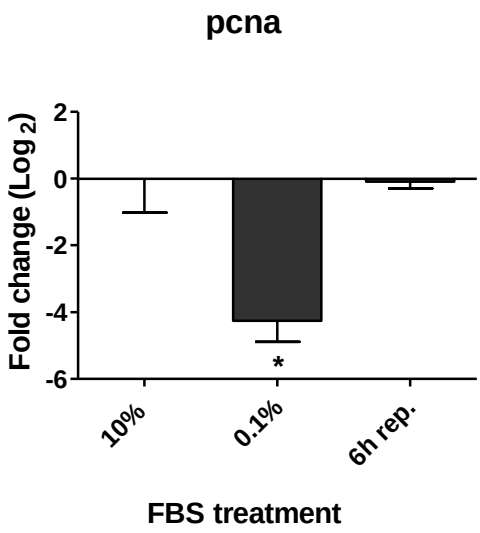

Figure 4. 12 The real-time qRT-PCR results of *pcna* expression in 24 h serum starved and then 6 h serum replenished ZF4 cells (6 h rep.). The real-time qRT-PCR results were normalized to the 30 h 10%-FBS treatment. One-way ANOVA with Fisher's multiple comparison results showed the significant changes between groups (One-way ANOVA; *pcna*, p=0.014). * represents significance at p≤0.05.

According to two way ANOVA analysis, the decrease in *pcna* expression at 0.1% FBS group was significant and independent of time (**Figure 4.13**, *pcna*, Two-way ANOVA, $P_{dose} = 0.001$, $P_{time} = 0.276$).

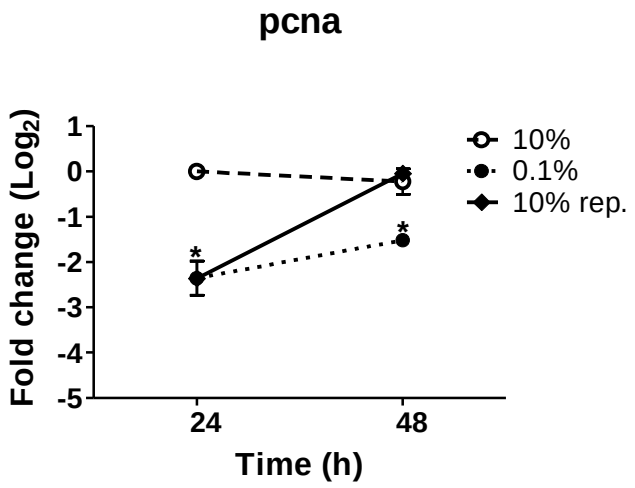

Figure 4. 13 The real-time qRT-PCR results of *pcna* expression in 24 h serum replenished ZF4 cells. The real-time qRT-PCR results were normalized to the 24 h 10%-FBS treatment values. One-way ANOVA results showed the significant changes between groups (One-way ANOVA; 24 h serum starvation, *pcna*, p=0.013; 48 h serum starvation and 24 h serum replenishment, *pcna*, p=0.005). * represents significance at p≤0.05.

4.2.2 Mybl2

The fish Mybl2 amino acid sequences were clustered together in the phylogenetic tree, while mammalian and chicken MYBL2 amino acid sequences formed another cluster (**Figure 4.14**). The protein product of the transcripts on chromosome 11 in green spotted puffer fish, and on group XVII in stickleback were more conserved than the products of the other transcripts (**Figure 4.14**).

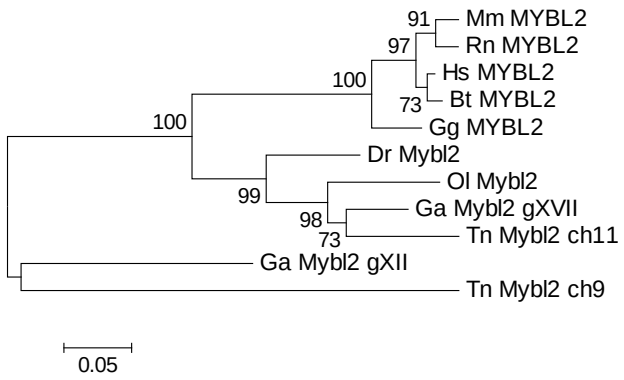

Figure 4. 14 Phlyogenetic tree of Mybl2 protein sequence. Species; human (Hs), rat (Rn), mouse (Mm), chicken (Gg), cow (Bt), stickleback (Ga), green spotted puffer fish (Tn), zebrafish (Dr) and medaka (Ol). Scale bar =0.05 substitutions per site.

Serum starvation caused a significant decrease in *mybl2* mRNA expression as shown by real-time qRT-PCR analysis. The decrease was significant at both 1% and 0% FBS treated cells but not in 3% FBS treated cells (**Figure 4.15**).

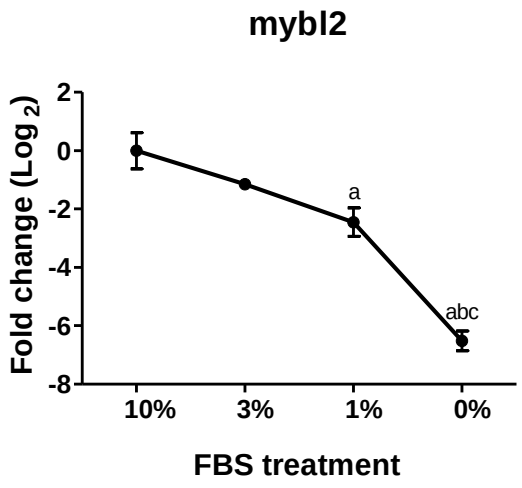

Figure 4. 15 The real-time qRT-PCR results of *mybl2* expression in serum starved cells. The fold change difference from 10% FBS control was calculated. One-way ANOVA with Fisher's multiple comparisons was performed to test the significance (*mybl2*, $p \leq 0.001$). [a] indicates the significance to 10% FBS at $p \leq 0.05$, [b] indicates the significance to 3% FBS at $p \leq 0.05$, [c] indicates the significance to 1% FBS at $p \leq 0.05$.

Serum stimulation for 6 and 24 h after 24 h of serum starvation increased the *mybl2* expression to the basal levels (**Figure 4.16-4.17**).

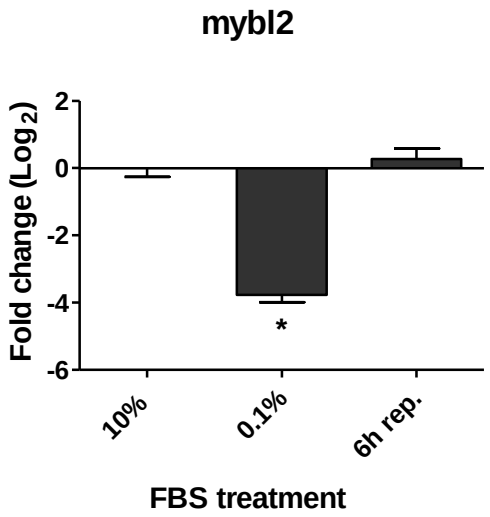

Figure 4. 16 The real-time qRT-PCR results of *mybl2* gene expression in 30 h serum starved and in 24 h serum starved then 6 h serum replenished cells. The real-time qRT-PCR results were normalized to the 30 h 10%-FBS treatment. (One-way ANOVA; *mybl2*, p=0.001). * represents significance at $p \leq 0.05$.

The decreased expression of *mybl2* at 0.1% FBS treatment was significant and independent of time (**Figure 4.17**, Two-way ANOVA, *mybl2*, $P_{dose} \leq 0.001$, $P_{time} = 0.212$).

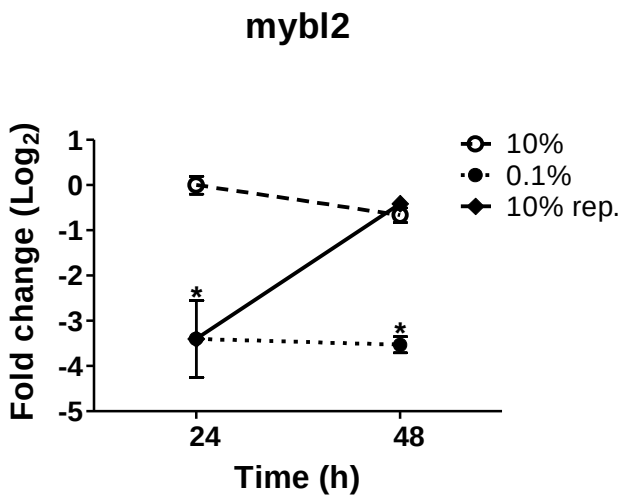

Figure 4. 17 The real-time qRT-PCR results of *mybl2* gene expression in 24 h serum replenished ZF4 cells. The real-time qRT-PCR results were normalized to the 24 h 10%-FBS treatment. One-way ANOVA results showed the significant changes between groups (One-way ANOVA; 24 h serum starvation, *mybl2*, p=0.031; 24 h serum replenishment, *mybl2*, p≤0.001). * represents significance at p≤0.05.

4.2.3 Tyms

The mammalian TYMS proteins were more similar, thus they clustered together, while fish Tyms sequences were formed another branch in the phylogenetic tree (**Figure 4.18**).

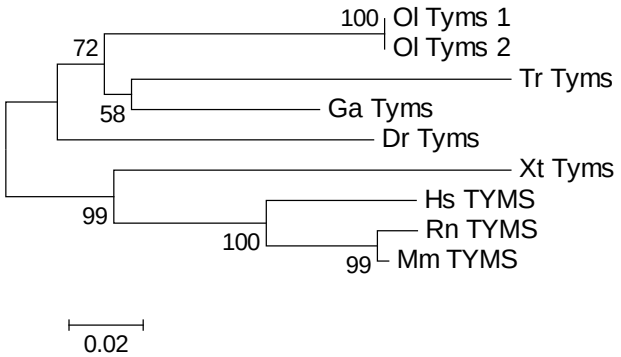

Figure 4. 18 Phlyogenetic tree of Tyms protein sequence. Species; human (Hs), rat (Rn), mouse (Mm), stickleback (Ga), zebrafish (Dr), western clawed frog (Xt), fugu (Tr) and medaka (Ol). Scale bar =0.02 substitutions per site.

Zebrafish *tyms* expression was serum responsive as in mouse fibroblast cells (Navalgund et al., 1980), serum starvation caused a significant decrease in *tyms* mRNA expression (**Figure 4.19**). Serum replenishment for 6 and 24 h increased the *tyms* mRNA expression in ZF4 cells (**Figure 4.20-4.21**) as in mouse cells (Saxena et al., 2009). The decrease in expression of *tyms* for 24 and 48 serum starved cells were significant and independent of time (**Figure 4.21**, Two-way ANOVA, *tyms*, P_{dose} = 0.001, P_{time} = 0.558).

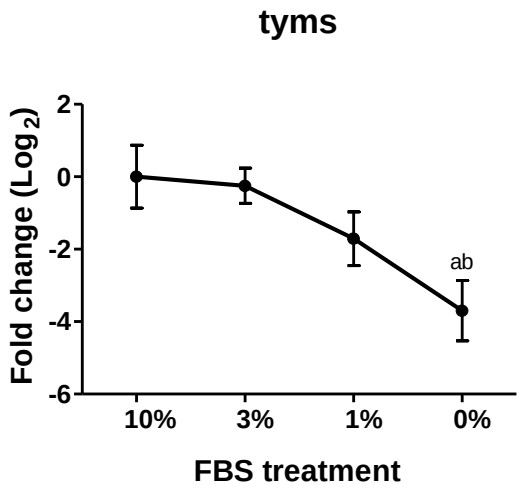

Figure 4. 19 The real-time qRT-PCR results of *tyms* expression in serum starved cells. The fold change difference from 10% FBS control was calculated (One-way ANOVA, *tyms*, p=0.024). [a] indicates the significance to 10% FBS at $p \leq 0.05$, [b] indicates the significance to 3% FBS at $p \leq 0.05$.

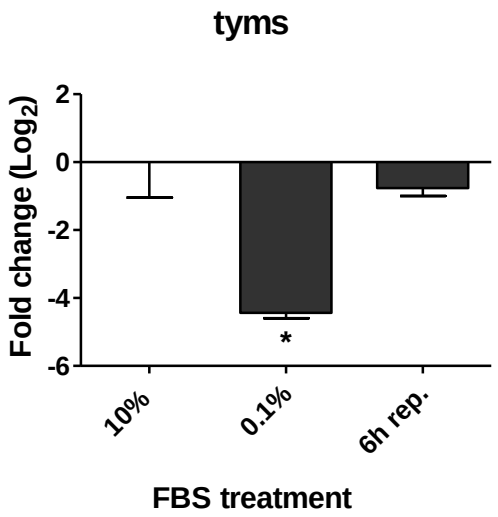

Figure 4. 20 The real-time qRT-PCR results of *tyms* gene expression in 6 h serum replenished ZF4 cells.The real-time qRT-PCR results were normalized to the 30 h 10% FBS (One-way ANOVA; 6 h replenishment, *tyms*, p=0.011). * represents significance at p≤0.05.

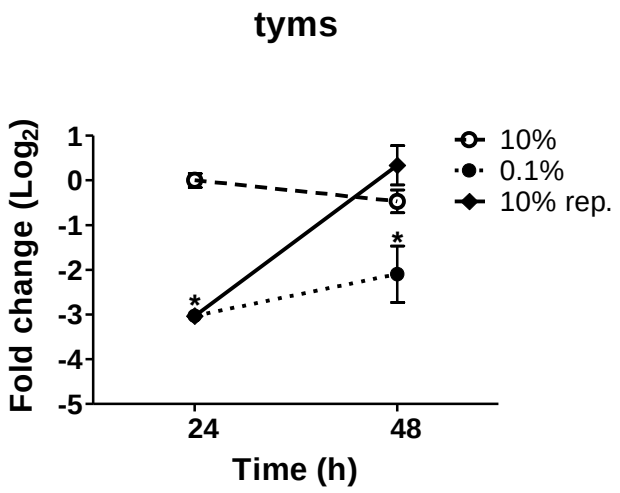

Figure 4. 21 The real-time qRT-PCR results of *tyms* gene expression 24 h serum replenished ZF4 cells. The real-time qRT-PCR results were normalized to the 24 h 10% FBS treatment. The log2 based fold changes were calculated and plotted. One-way ANOVA results showed the significant changes between groups (24 h serum starvation, *tyms*, p=0.002; 24 h serum replenishment, *tyms*, p=0.03). * represents significance at p≤0.05.

4.2.4 Mcm7

The amino acid sequence of zebrafish Mcm7 was clustered together with fish counterparts (**Figure 4.22**).

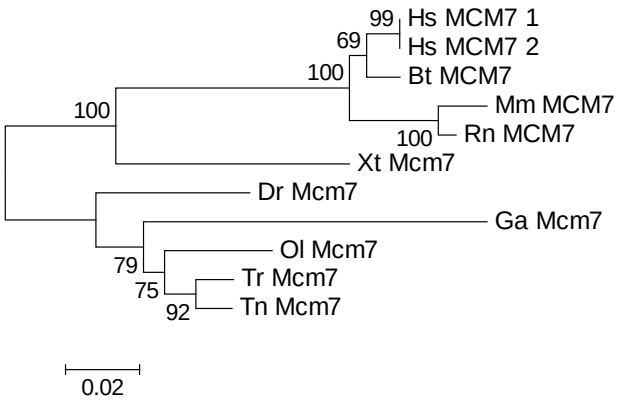

Figure 4. 22 Phlyogenetic tree of Mcm7 protein sequence. Species; human (Hs), rat (Rn), mouse (Mm), cow (Bt), stickleback (Ga), green spotted puffer fish (Tn), zebrafish (Dr), western clawed frog (Xt), fugu (Tr) and medaka (Ol). Scale bar =0.02 substitutions per site.

Serum starvation caused a significant decrease in *mcm7* mRNA expression. The decrease was significant at both 1% and 0% FBS treatment groups (**Figure 4.23**).

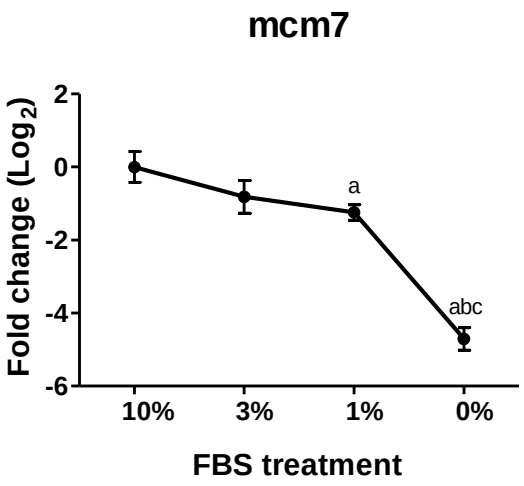

Figure 4. 23 The real-time qRT-PCR results of *mcm7* expression in serum starved cells. The fold change difference from 10% FBS control was calculated (One-way ANOVA, *mcm7*, p=0.001). [a]

indicates the significance to 10% FBS at p≤0.05, [b] indicates the significance to 3% FBS at p≤0.05, [c] indicates the significance to 1% FBS at p≤0.05.

6 h serum stimulation following 24 h serum starvation did not rescue the *mcm7* expression according to the real-time qRT-PCR analysis, yet an increase in the mRNA levels was observed (**Figure 4.24**). 24 h serum stimulation significantly increased the *mcm7* mRNA levels; the *mcm7* expression after serum stimulation significantly exceeded the *mcm7* expression in the 48 h 10% FBS treated control cells (**Figure 4.25**).

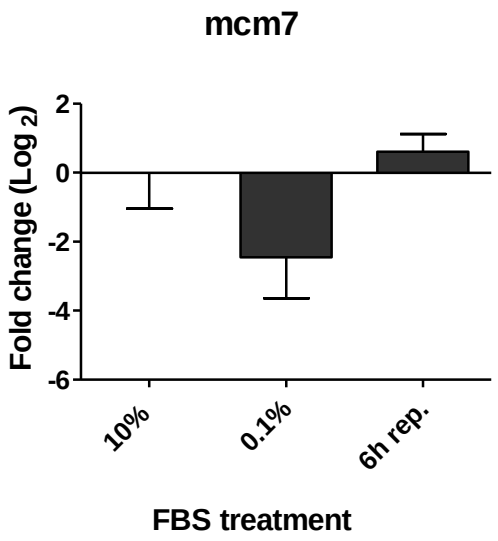

Figure 4. 24 The real-time qRT-PCR results of *mcm7* gene expression in 6 h serum replenished ZF4 cells. The real-time qRT-PCR results were normalized to the 30 h 10% FBS treatment (One-way ANOVA; 6 h replenishment, *mcm7*, p=0.095). * represents significance at p≤0.05.

According to two-way ANOVA analysis the decreased expression of *mcm7* in 24 and 48 h serum starved cells was significant and independent of time (**Figure 4.25**, Two-way ANOVA, *mcm7*,$P_{dose} \leq 0.001$,$P_{time} = 0.576$).

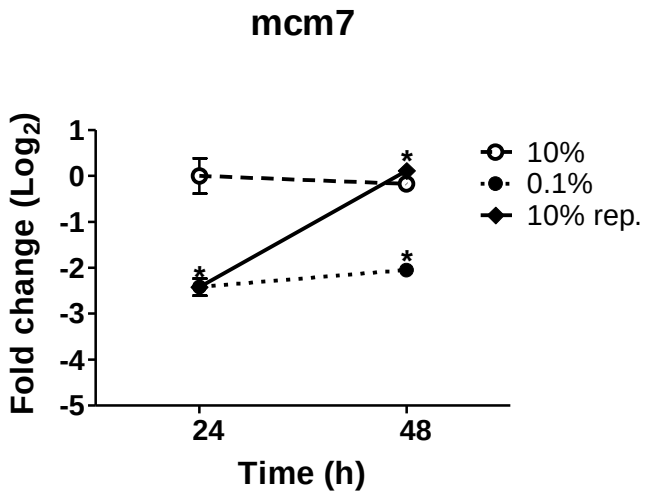

Figure 4. 25 The real-time qRT-PCR results of *mcm7* gene expression in 24 h serum replenished ZF4 cells.The real-time qRT-PCR results were normalized to the 24 h 10% FBS treatment values in 24 h replenishment samples. One-way ANOVA results showed the significant changes between groups (24 h serum starvation, *mcm7*, p=0.015; 24 h serum replenishment, *mcm7*, p≤0.001). * represents significance at p≤0.05.

The serum response trend observed in mRNA levels was conserved also in the protein levels. Serum starvation decreased the Mcm7 protein, while serum replenishment increased the Mcm7 protein levels starting from the 6 h (**Figure 4.26**).

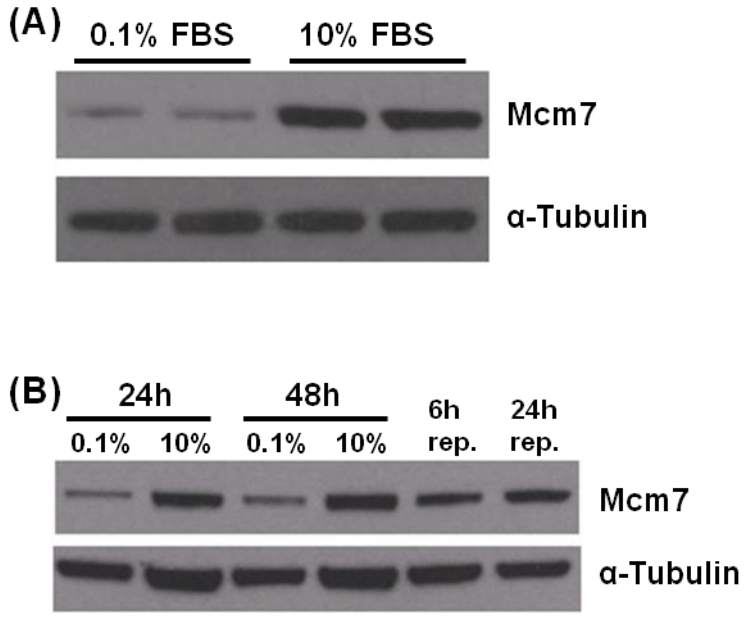

Figure 4. 26 Western Blot analysis of Mcm7 protein in response to serum starvation or replenishment. **(A)** Mcm7 protein levels in 24 h serum starved ZF4 cells. **(B)** Mcm7 protein in 24 and 48 h serum starved or 24 h serum starved and then 6 or 24 h serum replenished ZF4 cells.

4.2.5 Ctgf

The zebrafish Ctgf amino acid sequence was closer to salmon, and this group was clustered together with fish Ctgf amino acid sequences as the other selected E2F target genes (**Figure 4.27**).

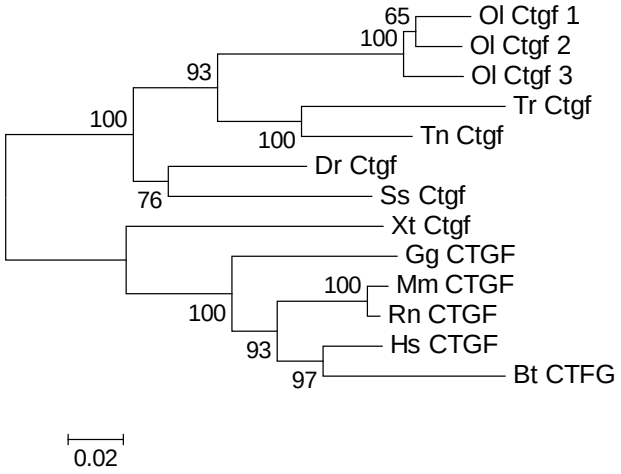

Figure 4. 27 Phylogenetic tree of Ctgf protein sequence. Species; human (Hs), rat (Rn), mouse (Mm), chicken (Gg), cow (Bt), salmon (Ss), green spotted puffer fish (Tn), zebrafish (Dr), western clawed frog (Xt), fugu (Tr) and medaka (Ol). Scale bar =0.02 substitutions per site.

According to Fisher's pair-wise comparisons *ctgf* expression gradually increased in cells cultured with 1% and 3% FBS including media in ZF4 cells (**Figure 4.28**) as in human cells (Cam et al., 2004). A significant decrease in expression was observed at 0% FBS treated cells, yet the decrease was not significant between 0% FBS and 10% FBS treated cells (**Figure 4.28**). The response to serum starvation was time-dependent according to two-way ANOVA analysis, but significant at both 24 and 48 h serum starved cells (**Figure 4.30**, *ctgf*, $P_{dose} \leq 0.001$, $P_{time} = 0.01$).

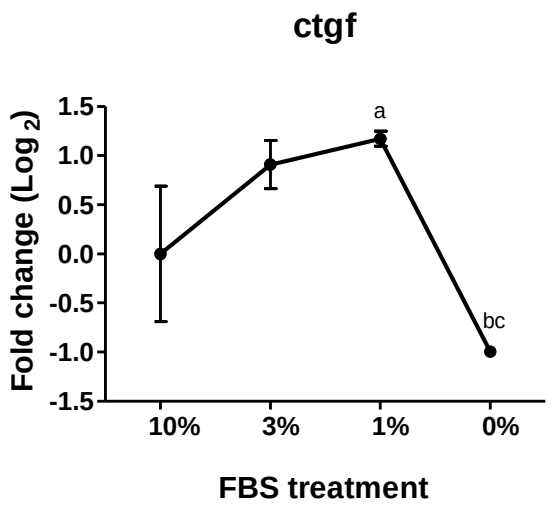

Figure 4. 28 The real-time qRT-PCR results of *ctgf* expression in serum starved cells.The fold change difference from 10% FBS control was calculated (One-way ANOVA, *ctgf*, p=0.013). [a] indicates the significance to 10% FBS at p≤0.05, [b] indicates the significance to 3% FBS at p≤0.05, [c] indicates the significance to 1% FBS at p≤0.05.

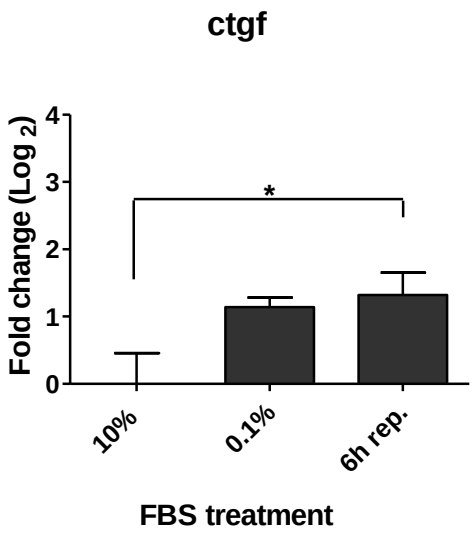

Figure 4. 29 The real-time qRT-PCR results of *ctgf* expression in 6 h serum replenished ZF4 cells. The real-time qRT-PCR results were normalized to the 30 h 10%-FBS treatment values in 6 h replenishment samples (One-way ANOVA; 6 h replenishment, *ctgf*, p=0.053). * represents significance in dose comparisons at p≤0.05.

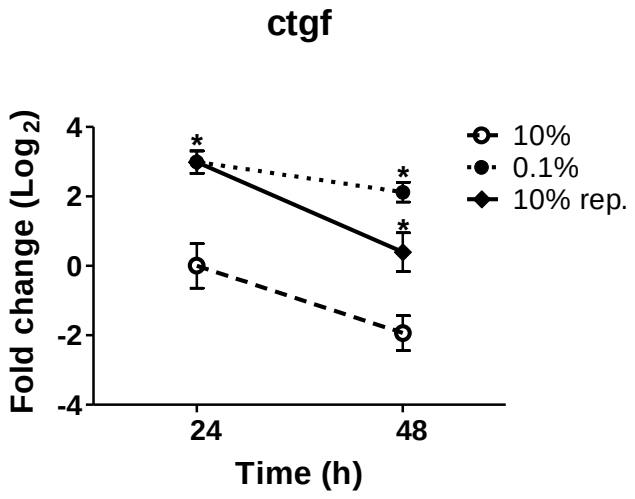

Figure 4. 30 The real-time qRT-PCR results of *ctgf* gene expression in 24 h serum replenished ZF4 cells. The real-time qRT-PCR results were normalized to the 24 h 10%-FBS treatment values in 24 h replenishment samples. The log2 based fold changes were calculated and plotted. One-way ANOVA results showed the significant changes between groups (24 h serum starvation, *ctgf*, p=0.028; 24 h serum replenishment, *ctgf*, p=0.007). * represents significance in dose comparisons at $p \leq 0.05$.

4.3 The effect of rapamycin treatment on ZF4 cells

Previously, the effects of rapamycin on cell cycle, cell proliferation, cell viability and death have been searched in different organisms (Albers et al., 1993; Altomare et al., 2004; Decker et al., 2003; Gorshtein et al., 2009; Jimenez et al., 2009; Metcalfe et al., 1997; Ravikumar et al., 2006; Zinzalla et al., 2007). However, characterization of rapamycin effect on zebrafish cell lines has not been performed previously. Before analyzing the gene expression response by qRT-PCR to rapamycin exposure in ZF4 cells, we investigated the cellular response of ZF4 cells to rapamycin treatment. Cell viability after rapamycin treatment was assessed by MTT analysis. BrdU incorporation assay and PI staining were performed to test whether rapamycin caused cell cycle arrest in ZF4 cells. Rapamycin may arrest cells at G1 phase of the cell cycle, and cause a growth arrest, or cells may continue proliferating after rapamycin treatment (Altomare et al., 2004; Bell et al., 2003; Jimenez et al., 2009; Tirado et al., 2005). Previous studies also state the role of rapamycin on cell death and autophagy (Ravikumar et al., 2006; Tirado et al., 2005); we also detected a decrease in

apoptosis in rapamycin treated cells by CDD analysis and the cell number in subG1 phase of cell cycle was lower as compared to DMSO (vehicle control).

4.3.1 Cell viability analysis of rapamycin treated ZF4 cells

According to MTT analysis, rapamycin treatment did not change the living cell number in ZF4 cells as compared to DMSO (vehicle) and culture media controls (**Figure 4.31**).

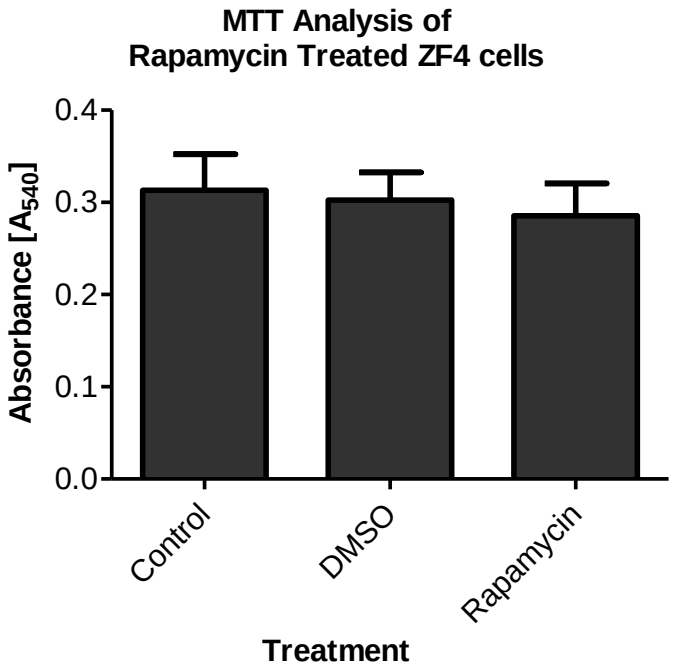

Figure 4. 31 MTT analyses of 100 nM rapamycin treated or control ZF4 cells. ZF4 cells were treated with 100 nM rapamycin or equivalent of DMSO (vehicle control) or 10% FBS including plain culture media for 48 h. One-way ANOVA was performed to test the significance (p=0.470).

4.3.2 Cell proliferation analysis of rapamycin treated ZF4 cells

Rapamycin treatment has also no statistically significant effect on proliferating cell number in ZF4 cells although a decreasing trend was recorded (p = 0.141). After rapamycin treatment ZF4 cells continued entering S phase (**Figure 4.32**).

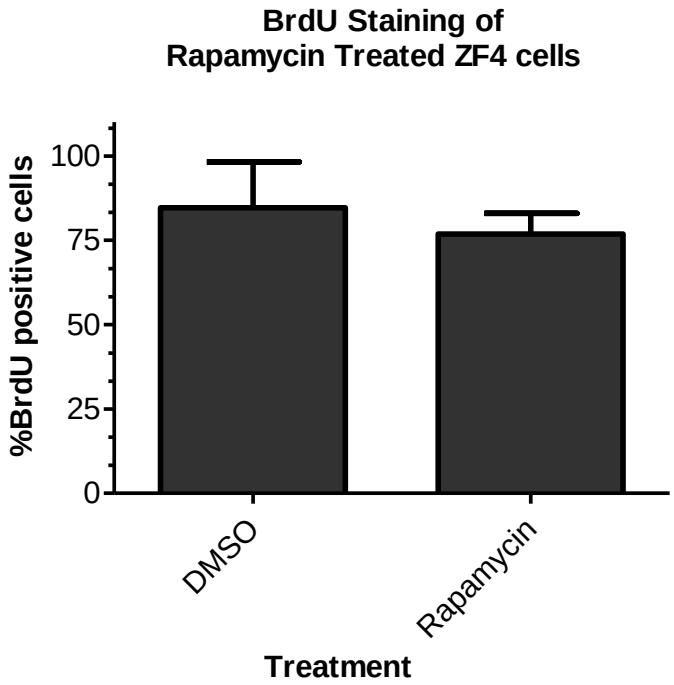

Figure 4. 32 BrdU staining of 100 nM rapamycin treated ZF4 cells. ZF4 cells were treated with 100 nM rapamycin or equivalent of DMSO for 48 h. Percent BrdU positive cells were calculated by correcting BrdU positive cells to DAPI stained nuclei. One-way ANOVA was performed to test the significance (p=0.141).

4.3.3 Cell Death Analysis of Rapamycin Treated ZF4 cells

In ZF4 cells, rapamycin treatment did not decrease the cell viability and proliferation (**Figure 4.31-4.32**). Interestingly, cell death detection analysis showed that rapamycin significantly decreased the basal apoptosis in ZF4 cells (**Figure 4.33**).

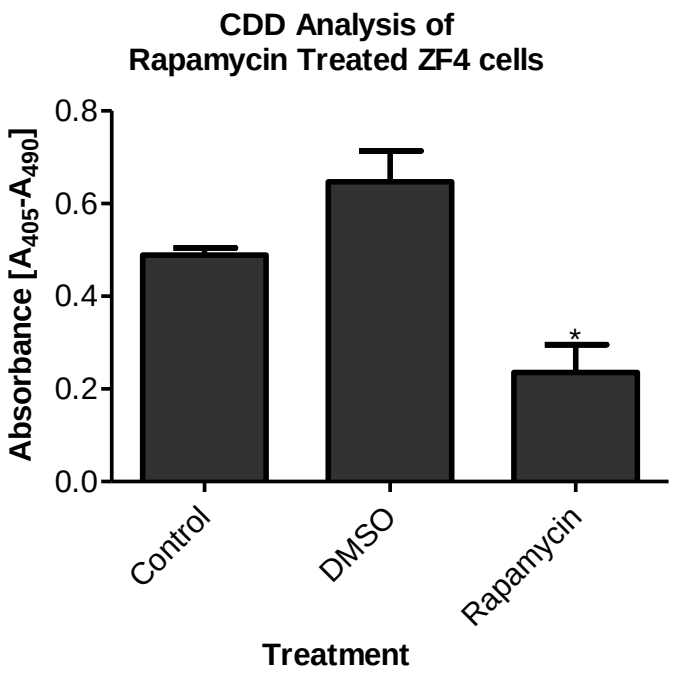

Figure 4. 33 Cell Death Detection (CDD) of rapamycin treated ZF4 cells. ZF4 cells were treated with 100 nM rapamycin, DMSO or culture media for 48 h. One-way ANOVA with Fisher's multiple comparisons were performed to test the significance (p=0.01). * represents significance at $p \leq 0.05$.

4.3.4 Cell cycle analysis of rapamycin treated ZF4 cells

Cell cycle analysis confirmed that rapamycin did not cause cell cycle arrest in ZF4 cells, since no significant increase was observed in G0/G1 phase as in BrdU analysis. Rapamycin treated cells entered S phase as in DMSO control. A decreasing trend in subG1 phase, indicating apoptotic cell population, was also detected in rapamycin treated samples ($p = 0.394$), although this decrease seemed statistically insignificant as a result of high variation in the rapamycin samples. As previously reported, rapamycin may reduce the basal apoptosis in cells (Zohlnhofer et al., 2004). CDD and cell cycle analysis of ZF4 cells in response to rapamycin treatment were also in the same direction with that previous report (**Figure 4.33-4.34**).

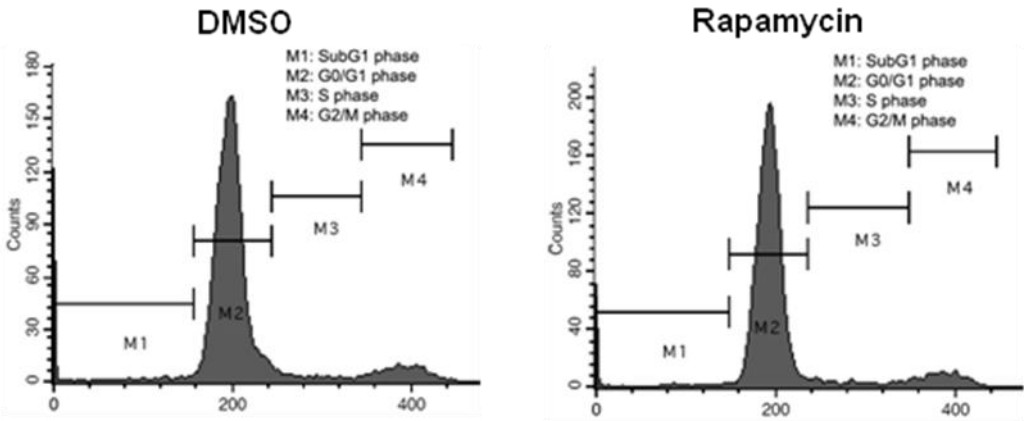

	DMSO	Rapamycin
subG1	8.43 ± 1.97	5.67 ± 3.47
G0/G1	79.22 ± 1.48	81.07 ± 3.05
S	5.06 ± 0.81	5.03 ± 1.56
G2/M	7.47 ± 1.19	8.41 ± 0.53

Figure 4. 34 Cell cycle analyses of 48 h 100 nM rapamycin or equivalent of DMSO treated ZF4 cells. The mean percentage of cells at subG1, G0/G1, S and G2/M phases of cell cycle was presented with ± standard deviation. One-way ANOVA with Fisher's multiple comparisons were made to test the significance.

4.3.5 Cell number counts of ZF4 cells used in the microarray study

Before performing the microarray study with ZF4 cells, ZF4 cells were treated with decreasing concentrations of rapamycin for 48 h and attached cells were counted with hemocytometer (**Figure 4.35**). The cells we used for counting were from the same passage lineage with the cells used in the microarray (passage15 for cell counts and passage 16 for microarray analysis); however, no MTT, BrdU, or PI analyses were performed with these ZF4 cells used in the microarray study. On the other hand, the assays reported in 4.3.1-4.3.4 in the above sections were performed on ZF4 cells from a later lineage.

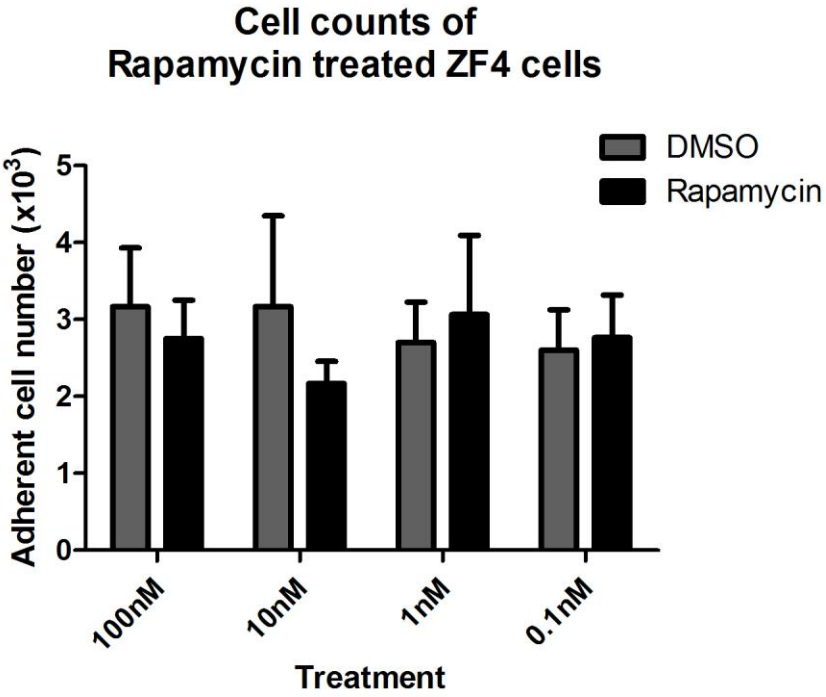

Figure 4. 35 Attached cell number counts of rapamycin treated cells. 3 x 10^4 ZF4 cells were seeded in 24-well plates. After 24 h of culturing ZF4 cells were treated with 100, 10, 1 and 0.1 nM of rapamycin or equivalent of DMSO for 48 h.

4.4 Transcriptome analysis of rapamycin exposed ZF4 cells

The global gene expression response to rapamycin treatment was detected with high-throughput microarray analysis. ZF4 cells were treated with 100 nM rapamycin for 48 h and extracted RNA samples were used for microarray analysis.

4.4.1The quality control of RNA samples

The RNA integrity, rRNA Ratio (28s / 18s) and RNA concentrations were measured by using Agilent 2100 BioAnalyzer before hybridization. The high integrity of RNA is essential for proper analysis of gene expression in both microarray analysis and RT-PCR experiments and Agilent 2100 BioAnalyzer provides the RIN (RNA

integrity numbers) for the RNA samples. RIN values closer to 10 mean the RNA is intact for that sample (Schroeder et al., 2006). The RIN values of RNA samples for rapamycin and DMSO controls ranged between 8.7-9.1 and rRNA Ratio (28s / 18s) between 1.7-2, representing the high integrity of RNAs (**Table 4.1**).

Table 4. 1 The experimental conditions, concentrations and RIN values of RNA samples used in the microarray experiments

Sample Name	Treatment	Duration of Treatment	Concentration of RNA	rRNA Ratio [28s / 18s]	RIN value
1-1 rap	rapamycin	48h	238 ng/µl	1.9	8.7
2-1 rap	rapamycin	48h	246 ng/µl	1.8	8.8
1-3 rap	rapamycin	48h	379 ng/µl	1.8	8.9
1-2 dmso	DMSO	48h	215 ng/µl	2.0	9.1
1-4 dmso	DMSO	48h	449 ng/µl	1.7	8.9

After hybridization on chips, the quality of RNA and arrays were assessed by using *affy* and *affyPLM* packages of Bioconductor in R 2.10.1.

Since RNA degradation starts at the 5’ end of the mRNA, the mean intensities of the probes at the 5’ end is lower. If the slope of the degradation plot is high, it means there is high degradation in mRNAs of that chip. If the ends of 5’ and 3’ are close, the slope of the plot is lower, meaning lower rate of degradation (Gautier et al., 2004; Wilson et al., 2004). The slopes and appearance of the lines also should be similar among the experiments (Archer et al., 2006; Gautier et al., 2004). The RNA degradation plot for DMSO and rapamycin treated samples represented that there was no outlier among the chips, the pattern and the slopes of the chips were similar, and thus all the chips could further be analyzed (**Figure 4.36**).

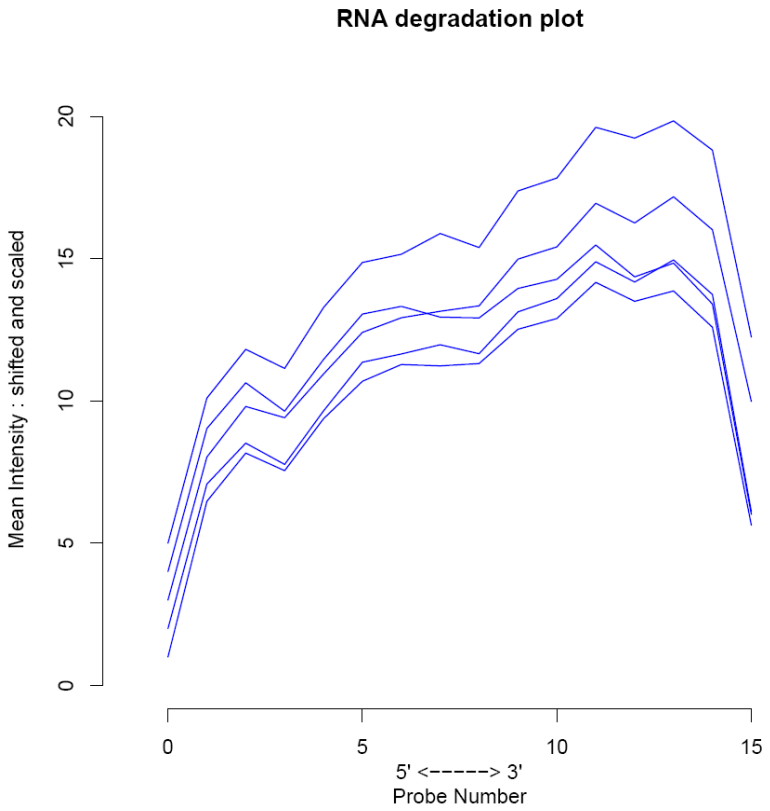

Figure 4. 36 The RNA degradation plot of the RNA samples used for the microarrays. This plot shows the mean intensities (shifted and scaled) from 5' to the 3' of the mRNA and each blue line represents a chip.

4.4.2 The quality control of arrays

The quality of the arrays was surveyed by using *affyPLM* package of Bioconductor. AffyPLM package was used to detect whether any chip in the experiment was problematic and should not be used for further analysis.

RLE and NUSE are the two quality assessment tools of *affyPLM* package. In the microarray analysis, it is expected that only a small proportion of genes are affected by treatments and the rest of the genes remains unaffected. In the RLE plot, the RLE values are expected to be 0 or close to be 0. They indicate that any probe in any chip does not significantly deviate from the median value of that particular probe calculated based on all chips.

NUSE (Normalized Unscaled Standard Error) is another quality control measure found in *affyPLM* package. It is expected that median values of standard errors to be 1. If any chip is aberrant (median values, 1.05 or higher); then that chip might be excluded from the analysis (Jones et al., 2006).

The RLE and NUSE plots of the chips used in the rapamycin microarray fulfilled the required criteria (**Figure 4.37**).

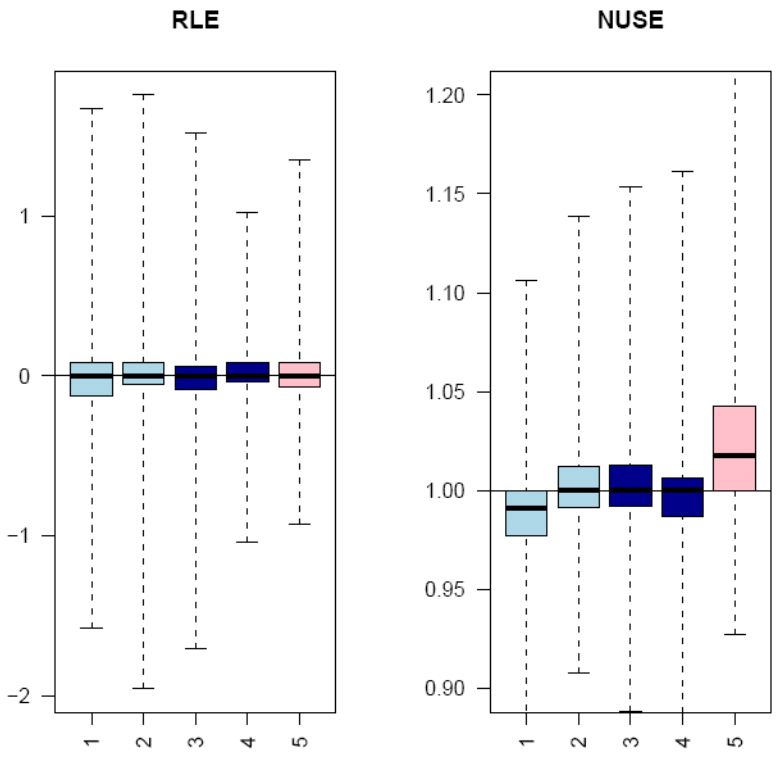

Figure 4. 37 Relative Log Expression (RLE) and Normalized Unscaled Standard Error (NUSE) plots of the chips used in the experiment.

4.4.3 Normalization

The raw data were normalized in order to avoid the differences that arise from array handling, batches, labeling, rather than the biological ones. The expression values of each probe id were obtained upon RMA normalization (Irizarry et al., 2003). The medians of each array lined up similarly after normalization (**Figure 4.38-4.40**).

MVA plots before and after normalization also indicated that normalization helped standardize medians and the distribution of differences along the 0 midline (**Figure 4.39-4.41**).

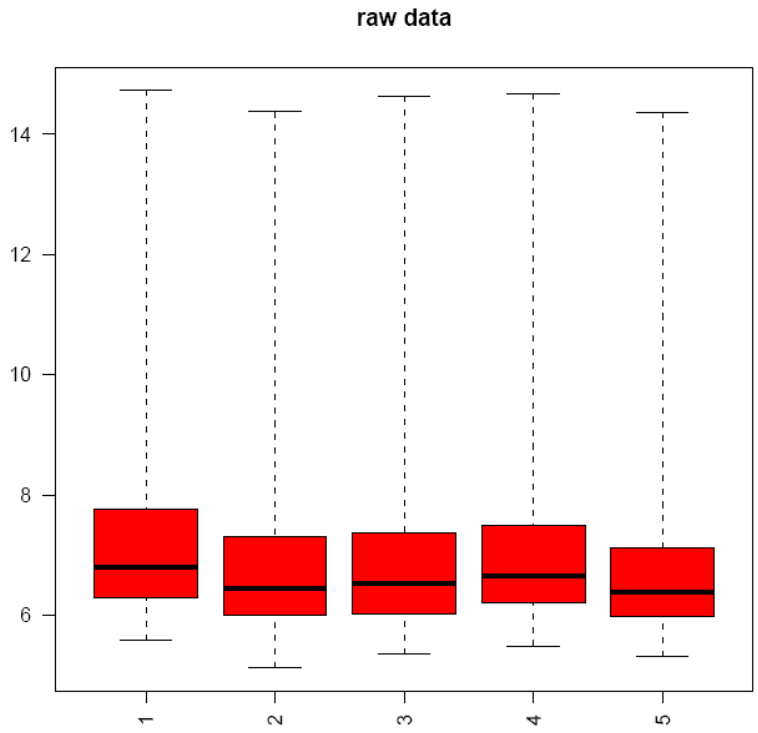

Figure 4. 38 Boxplot presentation of the arrays before normalization (raw data). Each red box represents the range of the values from 50% of the probes in an array. The x axis shows the array numbers and the y axis is the log2 intensities of the arrays.

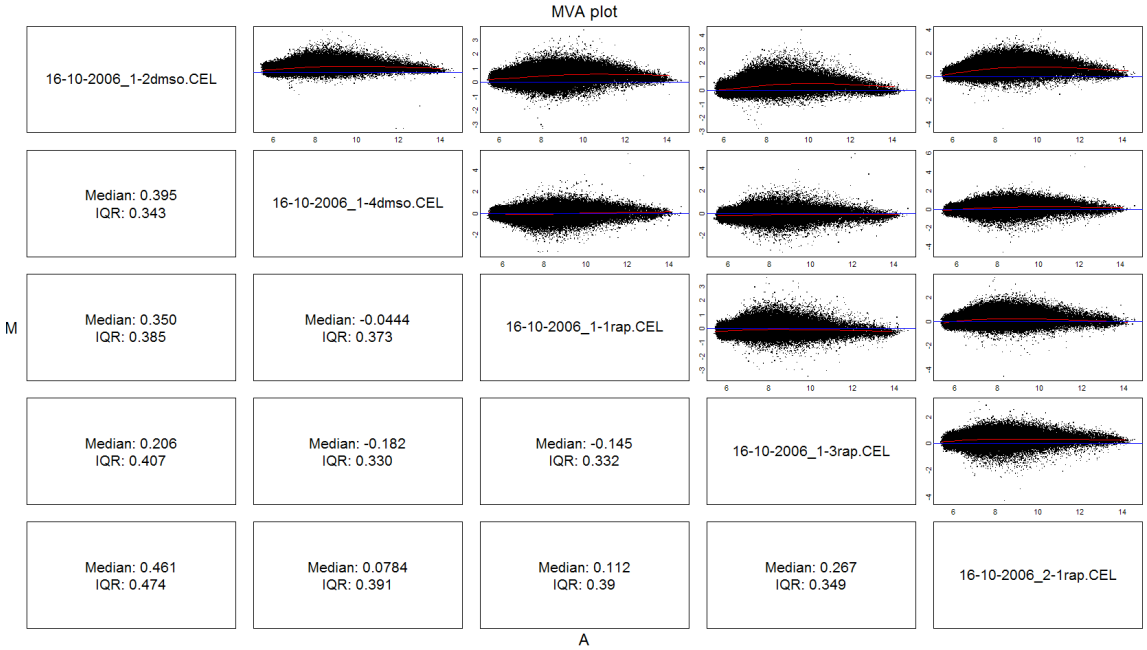

Figure 4. 39 MVA plots of the arrays before normalization. The log2 intensities of each array were compared to the median of log2 intensities of all arrays. It is expected that the distribution of the log 2 intensities to be around 0 at M axis.

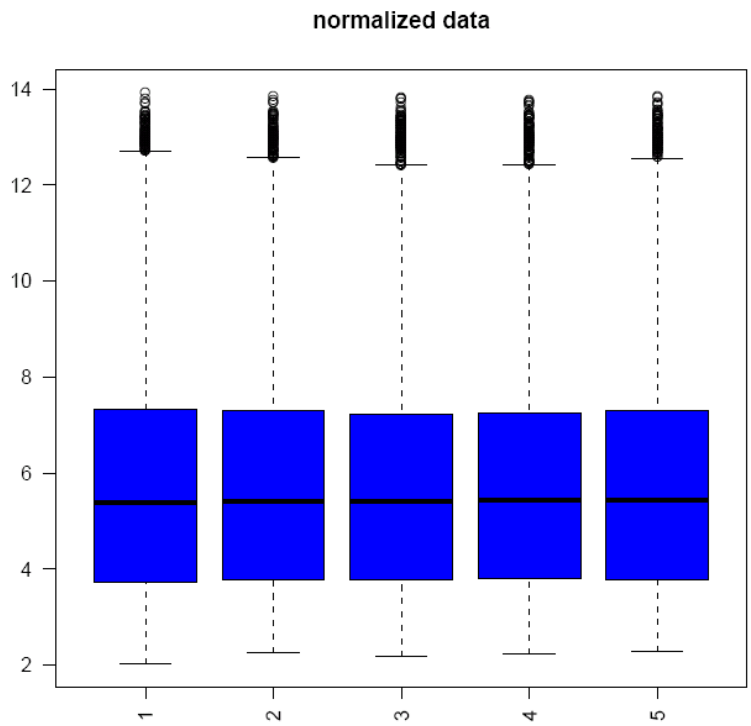

Figure 4. 40 Boxplot presentation of the arrays after normalization.

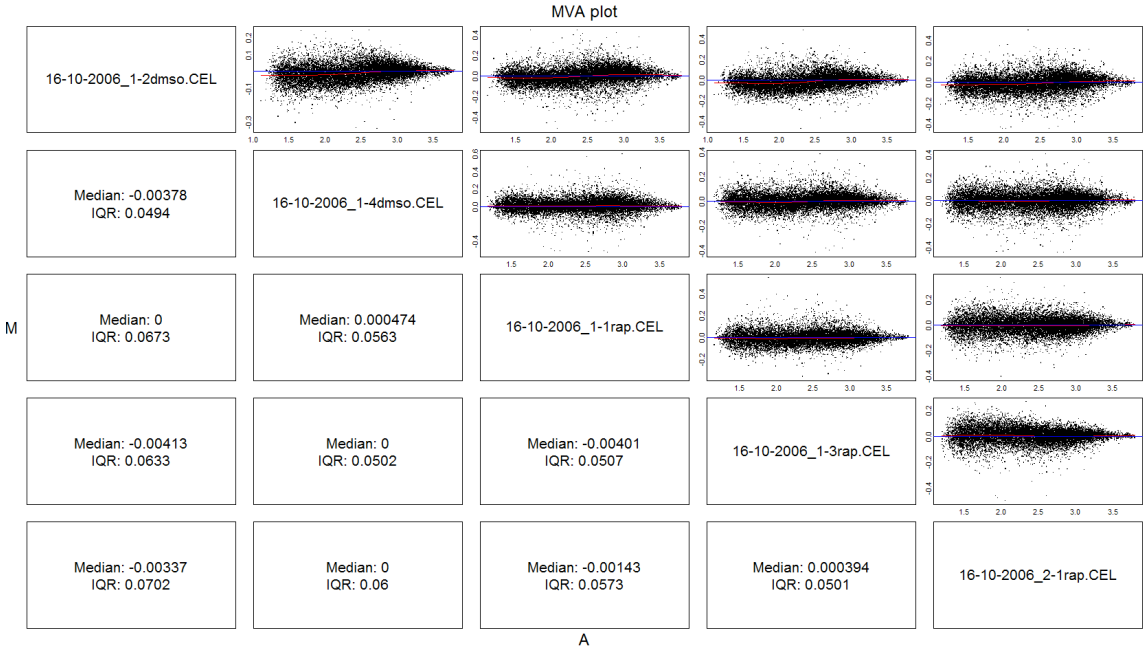

Figure 4. 41 MVA plots of the arrays after normalization.

4.4.4 Identification of differentially expressed genes after rapamycin exposure

The differentially expressed genes between rapamycin and DMSO control were obtained with *class comparison* function of BRB array tools (p=0.05), which uses a random variance model for univariate tests and computes a p-value for each probe set (Wright and Simon, 2003). 2185 probe ids (i.e., 904 probe ids upregulated and 1281 probe ids downregulated, among 15.600 probe ids) were detected as significantly modulated between rapamycin and DMSO groups (**Figure 4.39**). We did not perform multiple test correction so that more genes could be included to identify functional clusters more efficiently. At a level p<0.05, a high number of probesets were identified as being affected by rapamycin, thus some of which are likely to be false posivites. However, in the literature, it states that high FDRs might be used for identification of pathways since strict p-values will lead to shrinkage of the gene lists (Gold et al., 2009). Furthermore, we plan on comparing differentially expressed genes from multiple studies for determining core pathways affected by rapamycin. However, we demonstrate herein that applying different parameters to detect significant gene lists provided different numbers of significant genes (**Table 4.2**).

Table 4. 2 The number of probe ids in different significance parameters

Selected parameters	Total number of probe ids	The number of upregulated probe ids	The number of downregulated probe ids
p value= 0.05	2185	904	1281
p value= 0.001	210	76	134
max. proportion of FDRs=0.3 CI%= 70%	432	150	282
max. proportion of FDRs=0.3 CI%= 80%	30	12	18
max. proportion of FDRs=0.5 CI%= 70%	432	150	282
max. proportion of FDRs=0.5 CI%= 80%	156	59	97
fold change=2	48	25	23
fold change=1.5	353	174	179

CI, confidence interval which gives the confidence level of false discovery rates; max. allowed proportion of FDRs, maximum allowed proportion of false-positive genes.

A cluster analysis performed with Cluster program (Eisen et al., 1998) and visualized by JavaTreeview (Saldanha, 2004) showed that rapamycin and DMSO samples were grouped together within their class although there existed more variability among the rapamycin treated samples (**Figure 4.42**).

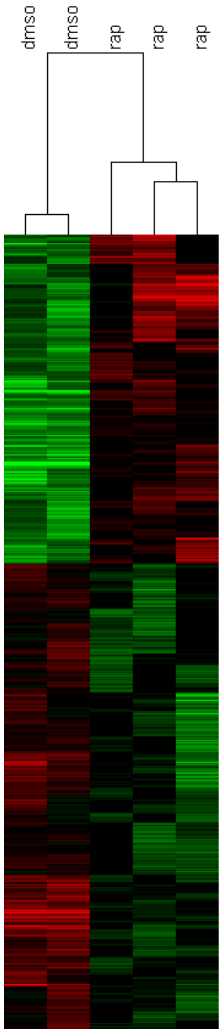

Figure 4. 42 Cluster presentation of the differentially expressed genes. According to class comparison analysis of BRB array tools, 2185 genes were identified as differentially expressed between rapamycin and DMSO groups (p=0.05).

4.4.5 KEGG pathway analysis of differentially expressed genes

The functional analysis of the differentially expressed genes was performed with DAVID (Dennis et al., 2003; Huang da et al., 2009). According to KEGG pathway results, along with other genes, upregulated genes coded for the ribosomal proteins, while downregulated genes coded for the subunits of proteasome (**Table 4.3-4.4**). The downregulation of the genes coding for proteasomal subunits were consistent with the previous reports showing a similar pattern (Grolleau et al., 2002).

Table 4. 3 The KEGG results from DAVID of upregulated genes with rapamycin treatment

Term	p-value	Benjamini	Zebrafish Array Affy id	Gene Name
Ribosome	1,8E-5	2,6E-2	Dr.4091.1.S1_at	ribosomal protein l8
			Dr.17536.2.S1_a_at	ribosomal protein l3
			Dr.876.1.S1_at	ribosomal protein l5a
			Dr.15443.2.S1_at	ribosomal protein l10a
			Dr.1338.1.S1_at	ribosomal protein l28-like
			Dr.14110.1.A1_at	zgc:73262
			Dr.1208.1.S1_at	chromosome 15 open reading frame 15 (h. sapiens)
			Dr.1324.1.S1_at	ribosomal protein s5
			Dr.24671.1.S1_at	ribosomal protein l27
			Dr.18282.2.S1_at	ribosomal protein s7

Table 4. 4 The KEGG results from DAVID of downregulated genes with rapamycin treatment

Term	p-value	Benjamini	Zebrafish Array Affy id	Gene Name
Proteasome	4,7E-4	5,2E-2	Dr.11843.1.S1_at	proteasome (prosome, macropain) subunit, beta type, 6
			Dr.3054.1.A1_at	proteasome (prosome, macropain) 26s subunit, atpase, 4
			Dr.15385.1.S1_at	zgc:110330
			Dr.10120.1.S1_at	proteasome (prosome, macropain) subunit, alpha type, 6b
			Dr.786.1.S1_at	proteasome (prosome, macropain) subunit, alpha type, 2
			Dr.10596.1.S1_at	proteasome (prosome, macropain) subunit, alpha type, 4
			Dr.1375.1.S1_at	proteasome (prosome, macropain) 26s subunit, atpase, 1a
			Dr.20627.1.S1_at	proteasome (prosome, macropain) subunit, beta type, 5
			Dr.15038.1.S1_at	proteasome (prosome, macropain) subunit, beta type, 1
			Dr.20156.1.S1_at	proteasome (prosome, macropain) subunit, alpha type,5
			Dr.5594.1.S1_at	proteasome (prosome, macropain) subunit, beta type, 3
			Dr.9622.1.S1_at	zgc:92726
			Dr.3143.1.S1_at	proteasome (prosome, macropain) 26s subunit, atpase, 3

4.4.6 Gene Ontology analysis of differentially expressed genes

The upregulated genes were predominantly located in the intracellular non-membrane-bound organelles and ribosome (according to CC), and were involved in gene expression and translation, regionalization and pattern specification (according to BP), and functioned in nucleic acid binding and as structural constituents of ribosome (according to MF) (**Table 4.5-4.6-4.7**).

The downregulated genes by rapamycin were mainly located in the cytoplasm, chromosome, endoplasmic reticulum, proteasome and mitochondrion (according to CC), had roles in catabolic and metabolic processes, DNA damage and repair response (according to BP), and functioned in oxidoreductase and ion- or cation-transporter activity (according to MF) (**Table 4.5-4.6-4.7**).

Table 4. 5 The Gene Ontology (GO) results for cellular component (CC) category of up and down genes after rapamycin treatment (DAVID).

Category (for up genes in rapamycin)	**Term**	**Gene Count**	**P-Value**	**Benjamini**
CC	intracellular non-membrane-bound organelle	40	3,3E-6	6,9E-4
CC	non-membrane-bound organelle	40	3,3E-6	6,9E-4
CC	ribosome	17	2.0E-5	2.7E-3
Category (for down genes in rapa)	**Term**	**Gene Count**	**P-Value**	**Benjamini**
CC	cytoplasmic part	102	8,7E-11	3,6E-8
CC	cytoplasm	136	4,9E-10	1,0E-7
CC	intracellular part	236	3,3E-9	4,6E-7
CC	cytosol	22	9,1E-8	9,4E-6
CC	intracellular organelle part	67	4,9E-7	3,4E-5
CC	organelle part	67	4,9E-7	3,4E-5
CC	proteasome core complex (sensu Eukaryota)	11	8,0E-7	4,7E-5
CC	proteasome complex (sensu Eukaryota)	11	1,9E-6	1,0E-4
CC	intracellular	257	2,3E-6	1,1E-4
CC	endoplasmic reticulum	25	2,3E-6	1,1E-4
CC	intracellular organelle	178	2,7E-5	1,0E-3
CC	organelle	178	2,8E-5	9,8E-4
CC	intracellular membrane-bound organelle	153	1,9E-4	6,0E-3
CC	membrane-bound organelle	153	1,9E-4	6,0E-3
CC	intracellular non-membrane-bound organelle	48	2,4E-4	6,6E-3

CC	non-membrane-bound organelle	48	2,4E-4	6,6E-3
CC	mitochondrion	25	4,7E-4	1,1E-2
CC	chromosome	17	1,1E-3	2,6E-2
CC	envelope	17	1,5E-3	3,3E-2

Table 4. 6 The Gene Ontology (GO) results for biological process (BP) category of up and down genes after rapamycin treatment (DAVID).

Category (for up genes in rapamycin)	**Term**	**Gene Count**	**P-Value**	**Benjamini**
BP	regionalization	19	1,2E-6	2,6E-3
BP	gene expression	84	1,6E-6	1,8E-3
BP	translation	23	3,1E-5	2,3E-2
BP	pattern specification process	19	5,8E-5	3,2E-2
BP	regulation of biological process	85	8,4E-5	3,7E-2

Category (for down genes in rapamycin)	**Term**	**Gene Count**	**P-Value**	**Benjamini**
BP	catabolic process	48	3,4E-11	7,8E-8
BP	macromolecule catabolic process	38	2,8E-10	3,2E-7
BP	cellular catabolic process	38	4,0E-10	3,0E-7
BP	cellular macromolecule catabolic process	28	3,6E-9	2,0E-6
BP	metabolic process	346	6,2E-8	2,8E-5
BP	intracellular transport	38	1,2E-6	4,4E-4
BP	protein catabolic process	23	1,6E-6	5,2E-4
BP	cellular localization	41	2,2E-6	6,4E-4
BP	coenzyme metabolic process	24	6,1E-6	1,5E-3
BP	biopolymer catabolic process	24	6,1E-6	1,5E-3
BP	alcohol catabolic process	15	8,7E-6	1,8E-3
BP	hexose metabolic process	17	1,2E-5	2,2E-3
BP	monosaccharide metabolic process	17	1,4E-5	2,5E-3
BP	glucose metabolic process	15	1,4E-5	2,3E-3
BP	hexose catabolic process	14	1,7E-5	2,5E-3
BP	monosaccharide catabolic process	14	1,7E-5	2,5E-3
BP	glucose catabolic process	14	1,7E-5	2,5E-3
BP	cellular carbohydrate catabolic process	15	1,8E-5	2,3E-3
BP	DNA metabolic process	35	1,9E-5	2,3E-3
BP	establishment of cellular localization	38	2,1E-5	2,4E-3
BP	carbohydrate catabolic process	15	3,5E-5	3,8E-3
BP	carboxylic acid metabolic process	28	6,8E-5	7,0E-3
BP	organic acid metabolic process	28	6,8E-5	7,0E-3

BP	response to stress	30	9,3E-5	8,8E-3
BP	modification-dependent protein catabolic process	13	1,0E-4	9,1E-3
BP	ubiquitin-dependent protein catabolic process	13	1,0E-4	9,1E-3
BP	cellular protein catabolic process	13	1,0E-4	9,1E-3
BP	modification-dependent macromolecule catabolic process	13	1,0E-4	9,1E-3
BP	proteolysis involved in cellular protein catabolic process	13	1,0E-4	9,1E-3
BP	cellular carbohydrate metabolic process	21	1,3E-4	1,0E-2
BP	cofactor metabolic process	31	1,7E-4	1,2E-2
BP	response to DNA damage stimulus	16	2,0E-4	1,4E-2
BP	coenzyme biosynthetic process	18	2,1E-4	1,5E-2
BP	protein localization	36	2,3E-4	1,5E-2
BP	generation of precursor metabolites and energy	38	2,4E-4	1,5E-2
BP	alcohol metabolic process	18	2,4E-4	1,5E-2
BP	macromolecule localization	36	2,5E-4	1,5E-2
BP	glycolysis	11	3,2E-4	1,9E-2
BP	microtubule-based movement	11	3,9E-4	2,3E-2
BP	cytoskeleton-dependent intracellular transport	11	3,9E-4	2,3E-2
BP	DNA repair	15	4,3E-4	2,3E-2
BP	carbohydrate metabolic process	29	4,9E-4	2,6E-2

Table 4. 7 The Gene Ontology (GO) results for molecular function (MF) category of up and down genes after rapamycin treatment (DAVID).

Category (for up genes in rapa)	**Term**	**Gene Count**	**P-Value**	**Benjamini**
MF	nucleic acid binding	103	3,5E-6	4,7E-3
MF	structural constituent of ribosome	17	1,1E-5	7,3E-3

Category (for down genes in rapa)	**Term**	**Gene Count**	**P-Value**	**Benjamini**
MF	catalytic activity	300	2,4E-17	3,3E-14
MF	oxidoreductase activity	77	2,7E-10	1,8E-7
MF	threonine endopeptidase activity	11	1,4E-6	6,3E-4
MF	hydrogen ion transmembrane transporter activity	17	4,9E-6	1,7E-3
MF	carbon-carbon lyase activity	12	1,9E-5	5,2E-3
MF	monovalent inorganic cation transmembrane transporter activity	17	3,3E-5	7,7E-3
MF	inorganic cation transmembrane transporter activity	21	4,0E-5	7,7E-3
MF	lyase activity	19	9,8E-5	1,6E-2

4.4.7 Confirmation of microarray results

4.4.7.1 Selection of genes

In order to confirm microarray results we prepared another experimental set-up with ZF4 cells, in which ZF4 cells were treated with 100 nM rapamycin or DMSO for 48 h as in the microarray analysis and we added an additional treatment time point, 6 h, to visualize time dependent response of the genes to rapamycin. In this experiment, ZF4 cells were from a later passage than those used for the rapamycin microarray experiment. We selected 9 genes, 7 of them were upregulated and 2 of them were downregulated by rapamycin treatment, for real-time qRT-PCR confirmations (**Table 4.8**). The genes that were selected for confirmation were among the genes which have high fold change differences, low p-values and FDRs.

4.4.7.2 Real-time qRT-PCR confirmation

Of the 9 genes, we confirmed five; among these four were upregulated (**Figure 4.44**) and one was downregulated (**Figure 4.46-A**). These genes were *ddc, cyp26b1, dkk1b, wif1, and pah,* respectively. Although, only 5 genes were confirmed by real-time qRT-PCR analysis, the log2 fold changes of all the selected genes were highly correlated and tend to behave in the same direction given the high Pearson correlation coefficient (0.791) (**Figure 4.43**). Since the qRT-PCR experiment was performed with a different batch of ZF4 cells from a later passage than those used for microarray studies, the inability to detect significant differential expression for *bambia*, *foxm1*, *tagln2*, and *mmp9* suggests that there might be batch effects.

Table 4. 8 Log2 fold change ratios of microarray and real-time qRT-PCR results of selected genes.

Gene Symbol	Microarray				Real-time qRT-PCR	
	Probe id	Log2 fold change	p-value	FDR	Log2 fold change at 48 hours	p-value One-way ANOVA
ddc	Dr.26319.1.A1_at	1.11	≤0.001	0.01	0.93	0.004
	Dr.861.1.S1_at	0.81	≤0.001	0.03		
cyp26b1	Dr.180.1.A1_at	1.05	≤0.001	0.03	1.62	0.001
	DrAffx.2.62.S1_at	0.83	≤0.001	0.03		
	Dr.26342.1.A1_at	1.09	≤0.001	0.06		
	Dr.180.2.A1_at	0.69	0.01	0.2		
pah	Dr.4171.1.A1_at	-1.34	≤0.001	0.01	-1.08	0.004
dkk1b	Dr.8056.1.S1_at	1.98	≤0.001	0.01	3.40	≤0.001
wif1	Dr.3690.1.S1_at	0.98	≤0.001	0.01	0.92	0.003
bambia	Dr.7919.1.S1_at	1.18	≤0.001	0.03	0.55	0.153
foxm1	Dr.17623.1.S1_at	-1.14	≤0.001	0.01	-0.45	0.129
tagln2	Dr.2363.1.S1_at	0.62	≤0.001	0.04	0.43	0.166
mmp9	Dr.967.1.S1_at	1.46	≤0.001	0.01	0.20	0.412

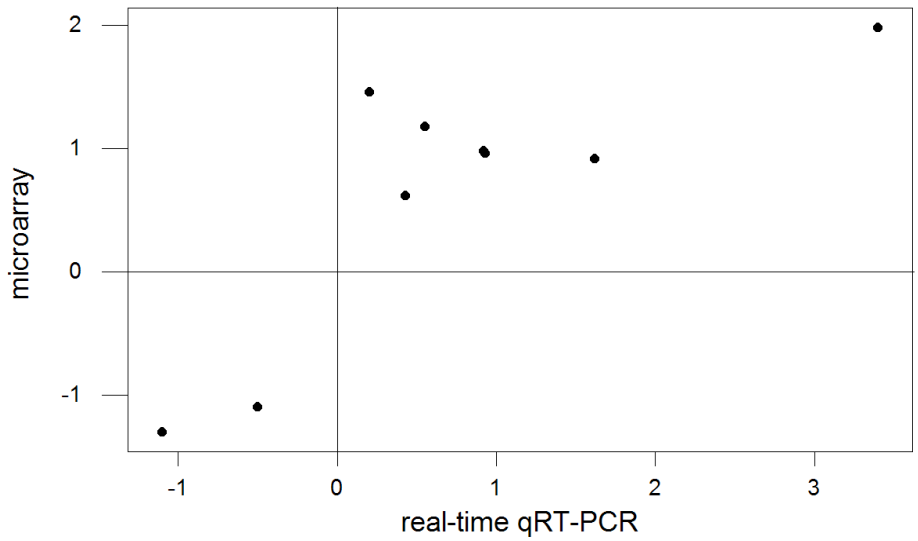

Figure 4. 43 The correlation between microarray and real-time qRT-PCR results for selected genes. The Pearson correlation coefficient was calculated in Minitab (The Pearson correlation coefficient= 0.791 and P Value = 0.011).

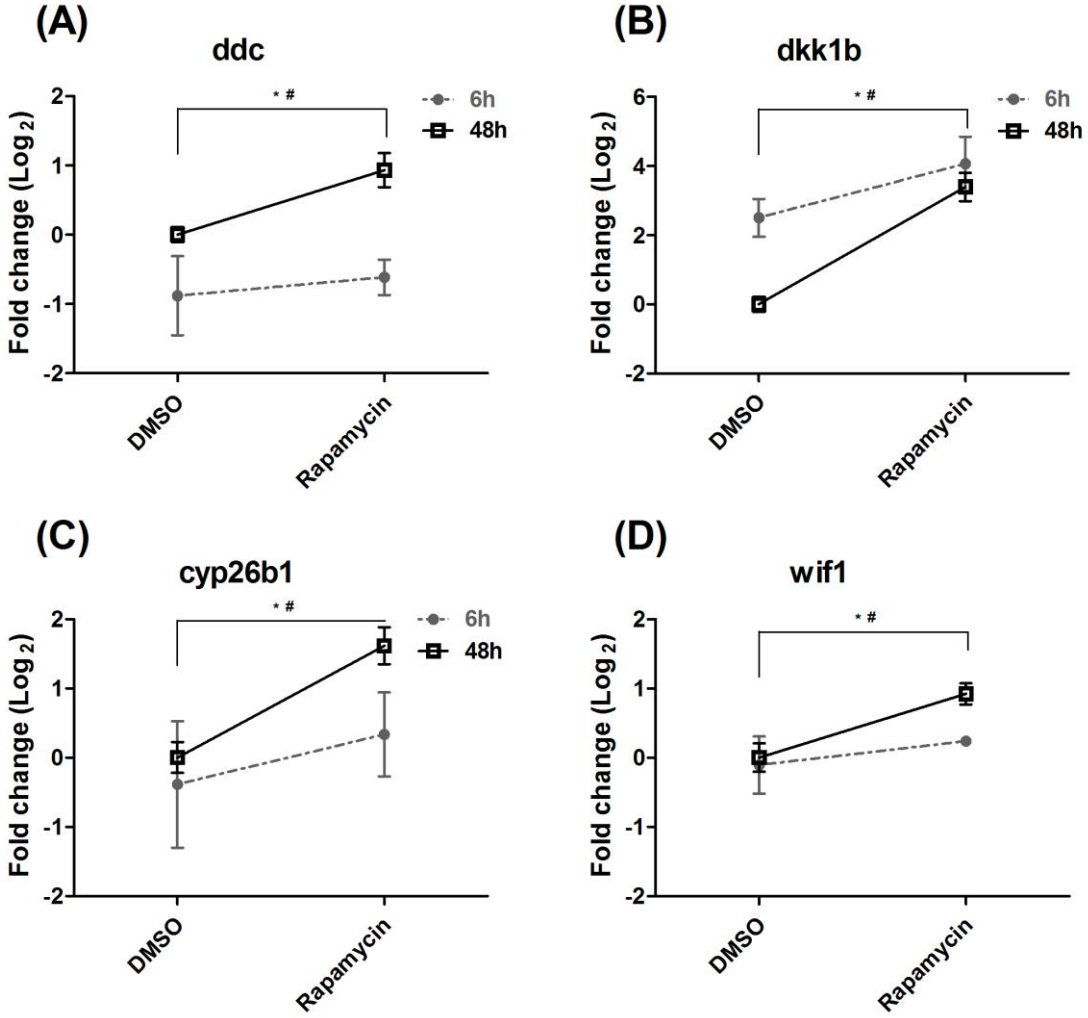

Figure 4. 44 The selected genes for confirmation that were significantly upregulated by rapamycin in real-time qRT-PCR analysis. **(A-D)** ZF4 cells treated with 100 nM rapamycin or equivalent of DMSO either for 6 or 48 h. The data was normalized to 48 h DMSO treatment. The log2 based fold changes were plotted and used to test the significance by two-way ANOVA to test the significance between treatment and time (Two-way ANOVA, *ddc*, $p_{treatment}$= 0.022, p_{time}≤0.001; *dkk1b*, $p_{treatment}$≤0.001, p_{time}=0.004; c*yp26b1*, $p_{treatment}$=0.008, p_{time}=0.039; *wif1*, $p_{treatment}$=0.004, p_{time}=0.039). * represents the significant response to rapamycin and # represents the significant difference between 6-48h.

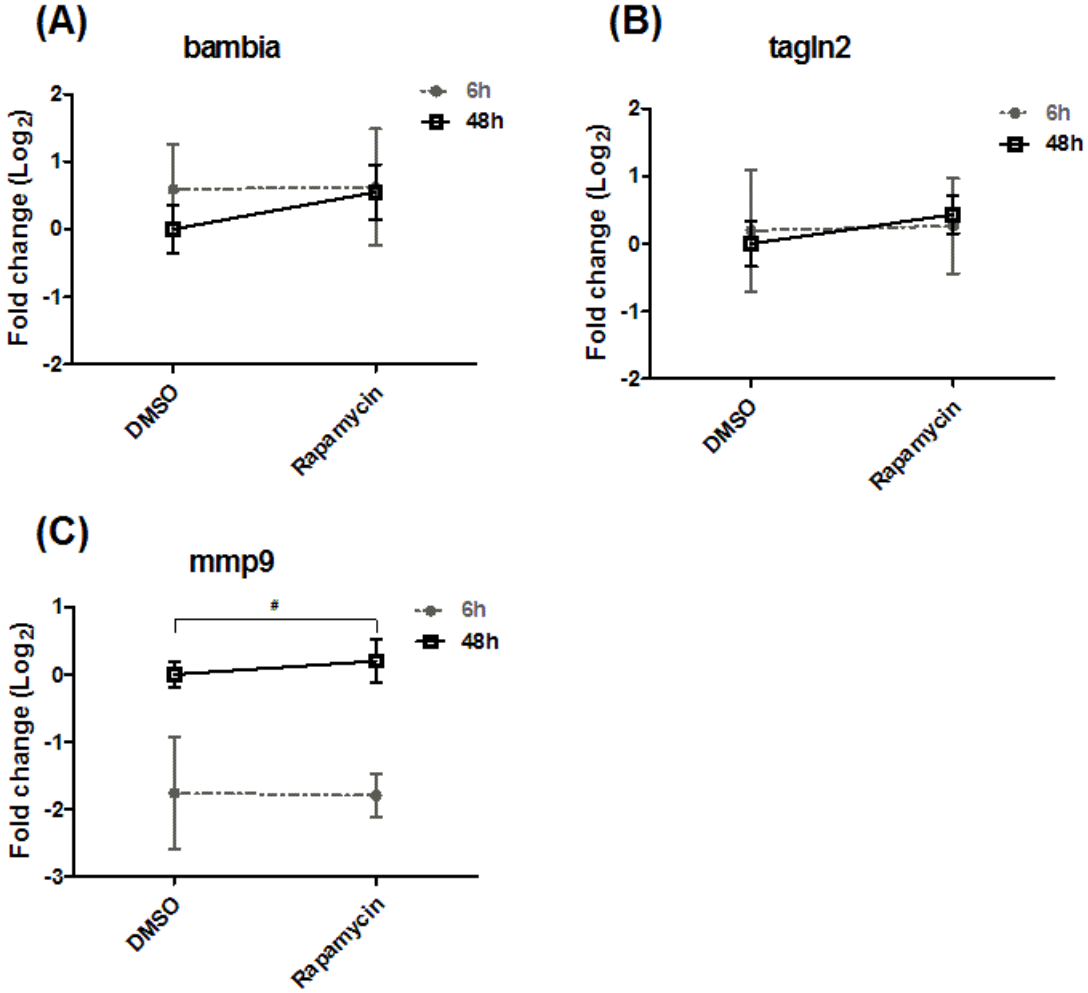

Figure 4. 45 The genes whose expressions were detected as upregulated by microarray analysis, but cannot be confirmed by real-time qRT-PCR analysis. **(A-C)** ZF4 cells treated with 100 nM rapamycin or equivalent of DMSO either for 6 or 48 h. The data was normalized to 48h DMSO treatment. The log2 based fold changes were plotted and used to test the significance by two-way ANOVA to test the significance between treatment and time (Two-way ANOVA, *bambia*, $p_{treatment}$= 0.420, p_{time}=0.362; *tagln2*, $p_{treatment}$=0.482, p_{time}=0.972; *mmp9*, $p_{treatment}$=0.765, p_{time}≤0.001). $^{\#}$ represents the significant difference between 6-48 h.

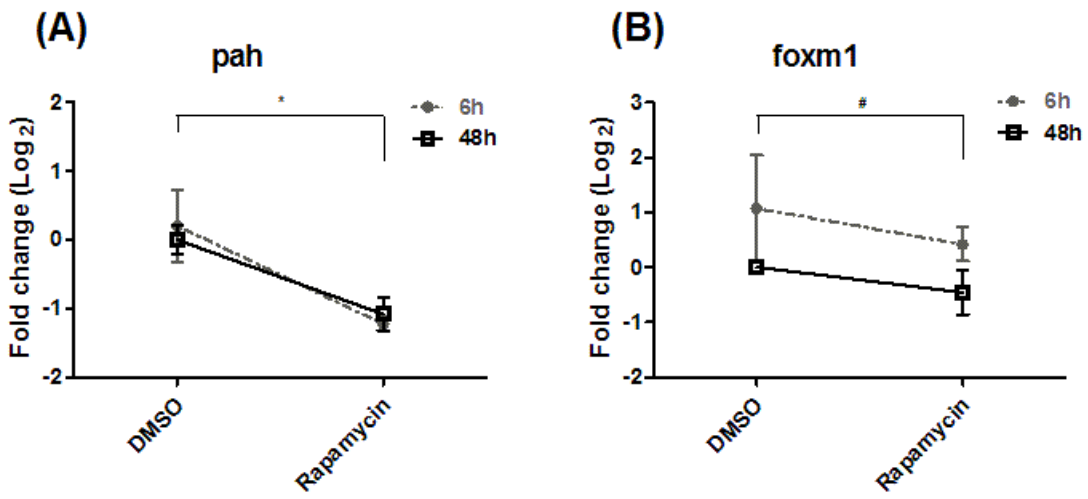

Figure 4. 46 The selected genes for confirmation that were downregulated by rapamycin in real-time qRT-PCR analysis. **(A-B)** ZF4 cells treated with 100 nM rapamycin or equivalent of DMSO either for 6 or 48 h. The data was normalized to 48 h DMSO treatment. The log2 based fold changes were plotted and used to test the significance by two-way ANOVA to test the significance between treatment and time (Two-way ANOVA, *pah*, $p_{treatment} \leq 0.001$, $p_{time}=0.884$; *foxm1*, $p_{treatment}=0.098$, $p_{time}=0.010$). * represents the significant response to rapamycin and # represents the significant difference between 6-48 h.

4.4.8 The effect of rapamycin on E2F target genes

We have shown that E2F target genes, *pcna*, *mybl2*, *tyms*, *mcm7* and *ctgf* were behaved in the similar direction to serum fluctuations as the mammalian homologs. In order to investigate whether *pcna*, *mybl2*, *tyms*, *mcm7* and *ctgf* expressions also behave similarly with the mammalian counterparts in response to rapamycin, we extracted the expression profiles from our microarray analysis. According to microarray data only *pcna* and *mybl2* expression seemed to be affected from rapamycin, while the others were not responsive (**Table 4.9**). Previous studies showed that rapamycin treatment decreases the expression of *mybl2* and *pcna* in mammalian cells (Javier et al., 1997; Law et al., 2002; Zohlnhofer et al., 2004) as in ZF4 cells.

Table 4. 9 The effect of rapamycin on E2F target gene expression based on ZF4 microarray analysis.

Gene Symbol	Probe id	Log2 fold change	p-value	FDR
pcna	Dr.1348.1.S1_at	-0.36	≤0.001	0.13
mybl2	Dr.17421.1.A1_at	-0.70	0.002	0.11
tyms	Dr.1047.1.S1_at	-0.04	0.75	0.92
mcm7	Dr.1055.1.S1_at	-0.11	0.40	0.74
ctgf	Dr.10431.1.S1_at	0.53	0.11	0.48

4.5 The effect of rapamycin on zebrafish embryo: in vivo studies

4.5.1 Effect of rapamycin on zebrafish body development

In order to observe the effect of rapamycin treatment on the development of zebrafish embryo, we treated zebrafish embryos with increasing doses of rapamycin for different time points. Our results suggested that rapamycin caused a significant delay in the development of the zebrafish embryo in a dose- and time- dependent manner (**Figure 4.47-4.48**). Rapamycin treated embryos morphologically had bigger yolks and shorter body size. The effect of rapamycin on body size was more apparent at 10 and 20 μM treatments, although 2 μM treatment also had significant effect on the body size (**Figure 4.48**).

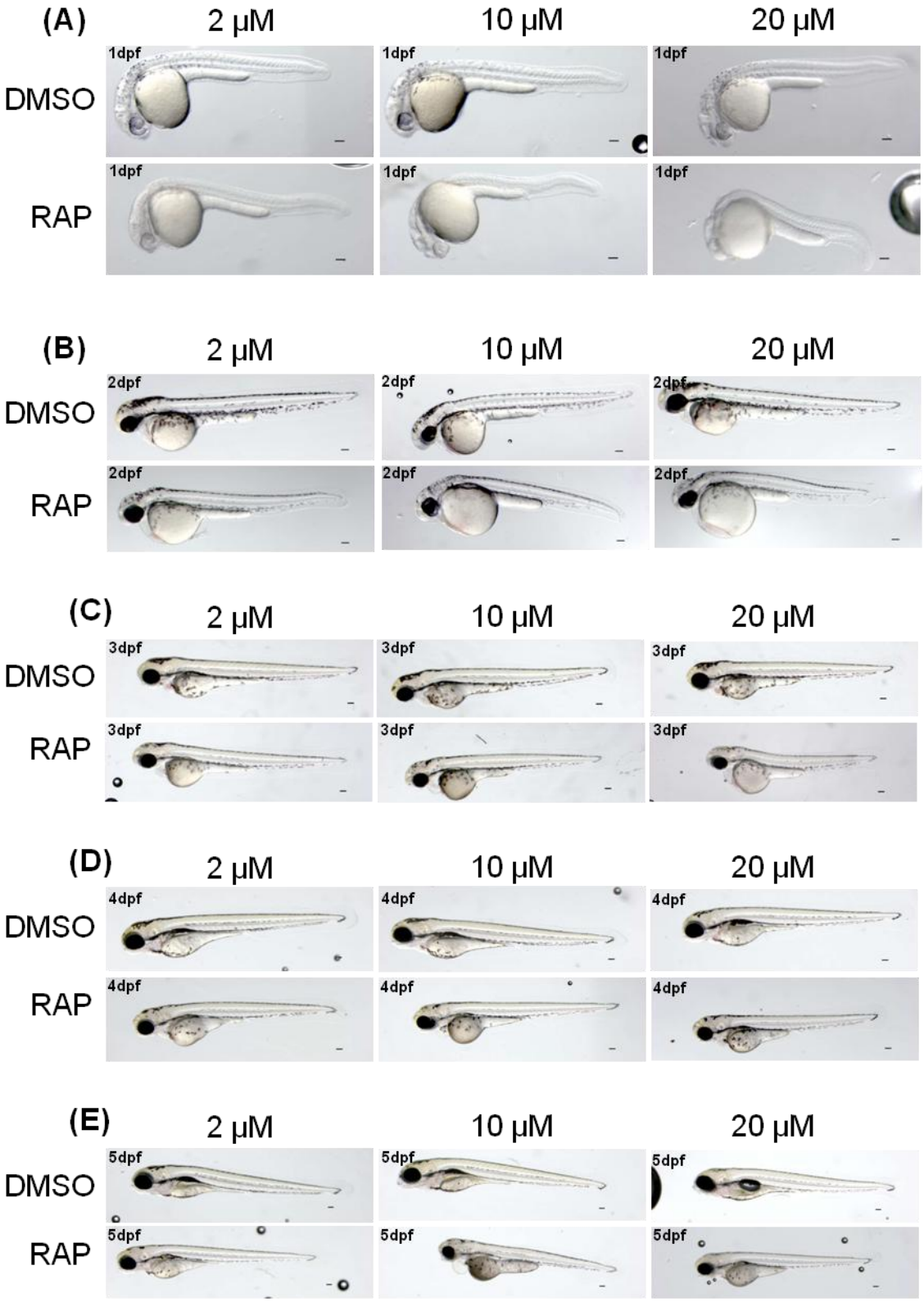

Figure 4. 47 The effect of rapamycin treatment on zebrafish embryo development. **(A-E)** Shield stage zebrafish embryos were treated with 2 µM, 10 µM and 20 µM rapamycin or equivalent of DMSO and collected with indicated time points. All the treatments were performed with duplicates or triplicates. Scale bars marks the distance of 100 µm for all the pictures.

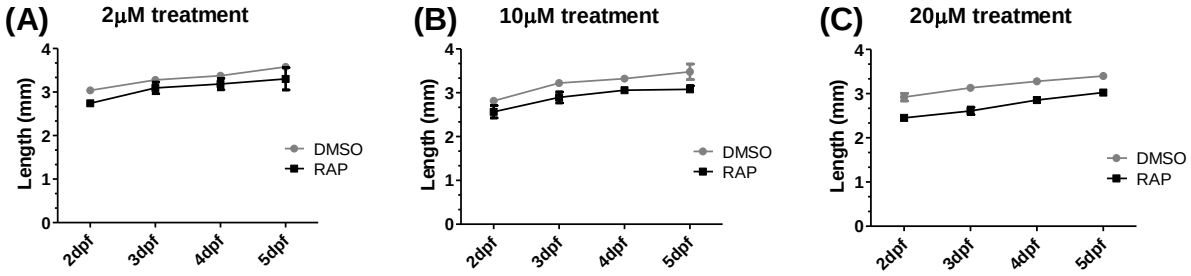

Figure 4. 48 The graphical presentation of time- and dose- dependent treatments. The lengths of the fish were measured from the tip of the head to the end of notochord in milimetres, averaged and plotted against the time of development. Whiskers represent the standard deviation among embryos. The ANOVA analysis for dose- and time- dependent response to rapamycin was performed to test the significance (General Linear Model; $p_{dose} \leq 0.001$; $p_{time} \leq 0.001$, $p_{rapamycin} \leq 0.001$).

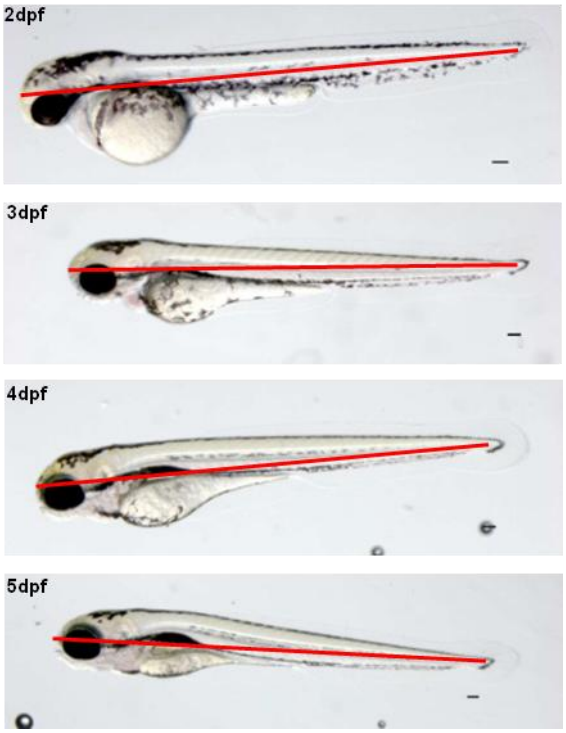

Figure 4. 49 Representative presentation of measurements. The body length of the zebrafish was measured as shown in figures above from 2 to 5 dpf. The meaurements were performed using Image-J software. Since embryos at 1dpf were not completely flexed they were not used for analyzing the trend for body size. The start and end point of measurements were shown with a red line. Measurements were made from diencephalon to the tip of notochord at 2dpf; and from the tip of the snout to the tip of notochord at 3 dpf, 4 dpf and 5 dpf.

4.5.2 Effect of rapamycin on intestinal system

Previously, Makky and colleagues have shown that rapamycin treatment caused a weak general developmental delay but mainly arrested digestive tract development at 400 nM (Makky et al., 2007). We also confirmed these results; zebrafish embryos were treated with 400 nM rapamycin, and at 8 dpf we observed an arrest in the digestive tract development (**Figure 4.50**).

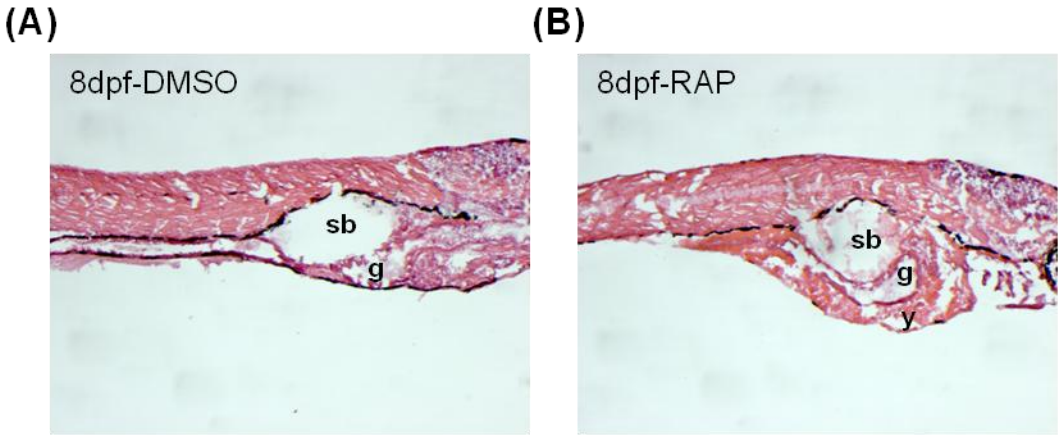

Figure 4. 50 The effect of rapamycin on digestive tract development. **(A)** DMSO embryos at 8 dpf cryosectioned and hematoxylin-eosin stained. The digestive tract formed properly. **(B)** 400 nM rapamycin treated 8 dpf embryos. Digestive tract formation was arrested. sb, swim bladder; g, gut; y, yolk.

4.5.3 Effect of rapamycin on pigmentation

Rapamycin not only arrested general development, it also affected the pigmentation and cartilage development of zebrafish embryos. Neural crest cells give rise to cartilage components (Yelick and Schilling, 2002) and pigment cells in zebrafish (Parichy, 2006).

The zebrafish have 3 kinds of pigments; black melanophores, yellow xanthophores and silver iridophores (Hirata et al., 2003; Parichy, 2006). Rapamycin particularly affected melanophores and iridophores.

4.5.3.1 Melanophore pigmentation delay in response to rapamycin treatment

We observed an apparent reduction in the melanophore pigmentation of rapamycin treated embryos starting from 24 hpf to 5 dpf (**Figure 4.47-51**). Melanocytes seemed to fail migrating ventrally and slowed migration laterally. In 24 hpf embryos treated with rapamycin, almost no pigmentation was observed for all the doses tested (**Figure 4.47**). The pigmentation was fainter from head to tail in the rapamycin treated embryos and the migration of melanocytes to the yolk and horizontal myoseptum was apparently delayed in the 2 and 3 dpf treatment groups. The delay of melanocyte migration to yolk and horizontal myoseptum persisted through the 4 and 5 dpf larvae (**Figure 4.47)**.

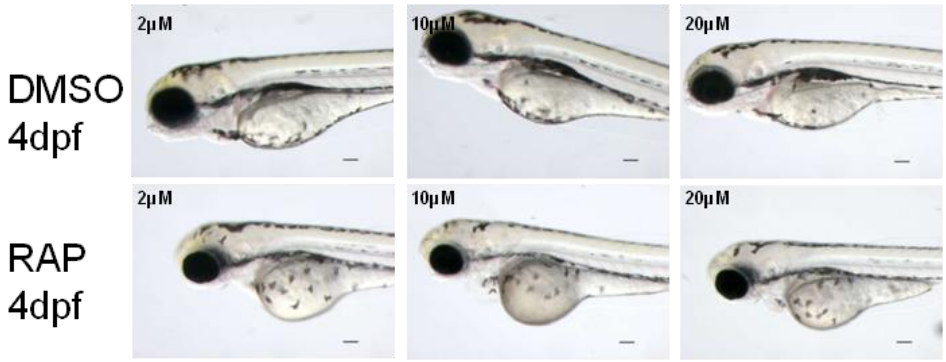

Figure 4. 51 The effect of rapamycin treatment on melanophore pigmentation at 4 dpf. Scale bars represent the distance of 100 μm for all the pictures.

4.5.3.2 Iridophores in response to rapamycin treatment

The iridophore pigmentation was also responsive to rapamycin treatment in the zebrafish embryo. In the 5 dpf zebrafish embryo, rapamycin treatment arrested the iridophore migration to the yolk of the embryo (**Figure 4.52**).

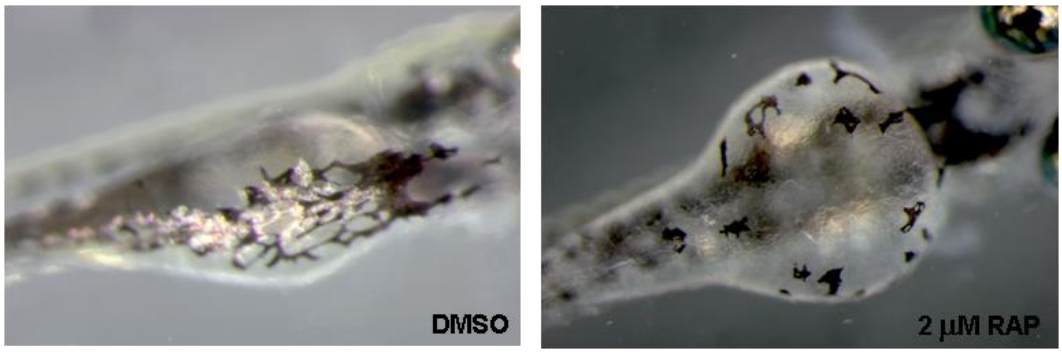

Figure 4. 52 The iridophores on the yolk of the 5 dpf rapamycin or DMSO treated zebrafish embryo. The silver light pigments are the iridophores accompanied with the black melanophores.

4.5.4 Effect of rapamycin on cartilage development

The cartilage components were shorter in the rapamycin treated embryos for both 5 and 6 dpf. The branchial arches were barely stained in the 5 dpf rapamycin treated embryos as compared to their control counterparts. In the 6 dpf rapamycin treated embryos the alcian blue staining of the branchial arches were more apparent (**Figure 4.53**).

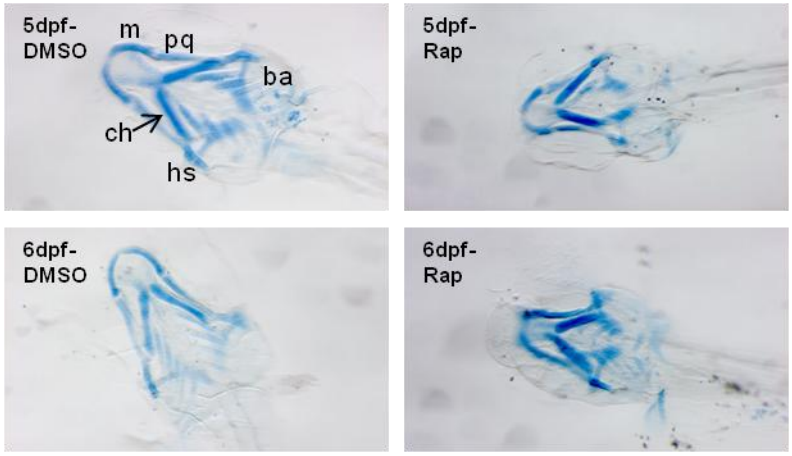

Figure 4. 53 5 and 6 dpf 10 µM rapamycin treated embryos strained with alcian blue. The ventral view of alcian blue stained embryos were presented. m, meckel's cartilage; pq, palatoquadrate; ch, ceratohyal; hs, hyosymplectic; ba, branchial arches.

Chapter 5. DISCUSSION

Comparing the conserved expression patterns between species, such as human and zebrafish, helps us understand and explore the role of a particular signaling pathway with roles in cell proliferation and cancer formation (Lam et al., 2006; Ung et al., 2009).

Zebrafish is an emerging model for cell signaling, cancer and development studies. In this study, we surveyed the expression changes of zebrafish orthologs of the known mammalian E2F transcription factor targets and of the mTOR pathway target genes in zebrafish model for the first time. We have shown that cell proliferation and cell cycle stages of ZF4 cells were significantly affected by the serum starvation and replenishment treatments, as in mammalian cells as well as that the rapamycin treatment diminished the basal apoptosis in ZF4 cells, although cell proliferation remained unaffected. We also reported on for the first time the global gene expression change that includes significant modulations in ribosomal and proteaosomal components. The delay rapamycin caused on the development of organs with a neural crest origin, i.e., cranial cartilage elements and pigmentation, are also intriguing aspects of our findings and require further expoloration both *in vitro* and *in vivo*.

5.1 Serum response of E2F target genes in zebrafish

Serum starvation/replenishment is an effective way to study the cell cycle and mitogen dependency of cancer cells (DeGregori et al., 1995b; Nakashima et al., 2005; Porter et al., 2003; Smith et al., 1996). The genes whose expressions were regulated by serum response in fibroblast cells have also been shown to be regulated in various epithelial cancer types. Therefore, the conserved serum response signatures in fibroblast cells are important for epithelial cancer prognosis (Chang et al., 2004). Microarray studies have been used to characterize the conserved serum response signatures in human cancers and zebrafish cell lines (Cam et al., 2004; He et al.,

2006). In various cell types from different species serum starvation causes a reversible cell cycle arrest at G0/G1 phase of the cell cycle, which may be reversed by serum replenishment (Bettuzzi et al., 1999; Goissis et al., 2007; Khammanit et al., 2008; Kues et al., 2000; Vackova et al., 2003). Serum depletion as an inducer of cell cycle arrest is also an appropriate model to study the gene expression changes of cell cycle regulatory proteins (Brunn et al., 1997; Hidalgo and Rowinsky, 2000). E2F transcription factor family regulates the expression of genes involved in the G1 to S phase of the cell cycle progression (Linhart et al., 2005). Accordingly, the serum starvation/replenishment model was chosen to investigate the regulation of E2F target gene expressions in ZF4 cell line.

Before the gene expression was surveyed in zebrafish cells, the cellular response of ZF4 cells to serum fluctuations was investigated. After serum starvation, we found that the viable cell number decreased in ZF4 cells in a dose-dependent manner. The decrease in viable cell number persisted up to 30 and 48 h exposure; Serum starvation also decreased the proliferating cell number in ZF4 cells. After 48 h of serum starvation the cell number entering S phase significantly decreased in ZF4 cells as observed by BrdU and PI staining. 24 and 48 h serum starvation caused a growth arrest at G1 phase of the cell cycle; the percent cell number significantly increased in G0/G1 phase, while it significantly decreased in S and G2/M phases according to PI staining. Serum stimulation for 24 h reversed the effects of serum starvation. The viable cell number significantly increased upon 6 and 24 h serum stimulation. Also the percent cell number entering S phase was restored with 24 h serum stimulation as shown by the BrdU and PI analysis. Our results were consistent with previous studies performed with mammalian fibroblast cell lines, in which serum starvation caused an increase the cell number at G0/G1 phase, and a decrease at S and G2/ phases, which may be reversed by serum stimulation (Bettuzzi et al., 1999; Goissis et al., 2007; Khammanit et al., 2008; Kues et al., 2000; Vackova et al., 2003). Our results clearly showed that serum starvation caused G0/G1 arrest in ZF4 cells. However according to 24 h dose dependent serum starvation MTT assay results; serum starvation may induce cell death in ZF4 cells as the level of serum decrease in the media. The cell number counts were highly correlated with MTT results for the 24 h serum starved cells under differing doses of serum treatment (0, 1, 3% FBS). Since only attached cells were used for MTT, BrdU and cell cycle analysis, the effect of

serum starvation on different types of cell death in ZF4 cells remains unknown and need to be futher studied. However, it is apparent that the most of the remaining cells after serum starvation for 24 hours go into a state of G1 arrest, and then recover to the original levels with the addition of serum within 24 hours based on the MTT, BrdU and PI analyses from the serum replenishment experiments. Furthermore, the amount of cell death may depend on the passage number the ZF4 cells in and/or the duration of the serum starvation (48 h).

The zebrafish orthologs of *mcm7*, *pcna*, *mybl2*, *tyms*, and *ctgf* whose expressions known to be directly or indirectly regulated by E2F transcription factors in mammals have been selected to study whether the E2F target gene response is conserved in zebrafish (Lee et al., 1995). The selected genes are also important components of DNA repair, replication and cell cycle progression (Essers et al., 2005).

The phylogenetic analysis showed the evolutionary conservation of the selected genes in several species. Our phylogenetic analysis with protein sequences of selected genes confirmed that they were orthologous genes and showed sequence conservation between species. As expected the zebrafish orthologs of selected E2F target genes clustered with their fish counterparts, while the mammalian homologs clustered together. The expression of *mcm7*, *pcna*, *mybl2*, *tyms*, and *ctgf* were investigated in 24 h serum-starved ZF4 cells with 0%, 1%, and 3% FBS including media. Our results showed that serum starvation caused a significant decrease in gene expressions of *mcm7*, *pcna*, *mybl2* and *tyms* in a dose-dependent manner as in the mammalian cells. *ctgf* expression significantly increased at 1% FBS treated cells, although 0% FBS treated cells were not different from 10% FBS.

The effect of serum replenishment also was surveyed in 24, 30 and 48 h serum-starved ZF4 cells. Following a 24 h serum starvation, ZF4 cells were serum replenished either for 6 or 24 h and the changes in gene expression were observed with real-time qRT-PCR. *pcna* and *mybl2* expressions significantly decreased in 24, 30 and 48 h serum-starved ZF4 cells. After 6 and 24 h replenishment, the expressions of *pcna* and *mybl2* were back to basal levels. *tyms* expression significantly decreased in 24 and 30 h serum-starved ZF4 cells according to Fisher's multiple comparisons. In

6 and 24 h serum replenished ZF4 cells, the expression of *tyms* significantly increased. The *mcm7* expression significantly decreased at 24 and 48 h serum-starved ZF4 cells. *mcm7* expression completely recovered, also overtopped the basal levels after 24 h serum replenishment. Previously the change in MCM7 protein levels in response to serum starvation and replenishment have been shown in human and mouse cells (Rizwani et al., 2009). We also investigated the change in Mcm7 protein levels in response to serum starvation for 24 and 48 h and serum replenishment for 6 and 24 h following 24 h serum starvation. Consistent with real-time qRT-PCR results, 24 and 48 h serum starvation decreased, and not 6 h but 24 h of serum replenishment restored the Mcm7 protein levels, although both at 6 and 24 h of replenishment an increase in protein levels have been observed. The *ctgf* expression significantly increased in 24 and 48 h serum-starved ZF4 cells, however 24 h serum replenishment was not enough to decrease the *ctgf* expression to basal levels.

Previously, the serum responsiveness of the selected genes has been shown in higher organisms. The increase in *Pcna* expression has been shown in quiescent mouse embryonic fibroblast cells, MEFs, and Chinese hamster ovary cell line, CHOK1s, after serum stimulation (Hurford et al., 1997). The *Mybl2* expression decreased in serum-starved T98G human glioblastoma cells, mouse embryonic fibroblast cells and in normal human bone marrow fibroblast cells and increased after serum stimulation (Takahashi et al., 2000). Serum stimulation increased the *Tyms* expression in serum-starved mouse 3T6 fibroblast cells and mouse embryonic fibroblast cells, NIH 3T3 (Saxena et al., 2009). *MCM7* has also been shown to be serum modulated; in breast cancer and mouse cells, serum starvation decreased and serum stimulation increased MCM7 protein levels (Rizwani et al., 2009). The *Ctgf* expression in response to serum fluctuations varied; in human mesangial cells *Ctgf* expression behaved like the other selected genes, while in human T98G cancer cells, serum starvation increased the *Ctgf* expression (Goppelt-Struebe et al., 2001).

In conclusion, the expression of selected E2F target gene orthologs, responded to serum fluctuations as they did in the mammalian cells.

5.2 The effect of rapamycin treatment on gene expression of ZF4 cells and on zebrafish embryo

5.2.1 The effect of rapamycin treatment on gene expression of ZF4 cells

5.2.1.1 The effect of rapamycin treatment on ZF4 cell cycle progression

mTOR (mechanistic target of rapamycin) is a serine/threonine kinase and a member of phosphoinositide 3-kinase related kinase (PIKKs) protein family, which are the regulators of cell cycle progression, DNA damage and repair, and DNA replication (Sarkaria et al., 1998). In human cells, mTOR pathway is responsive to changes in nutrients, growth factors, hypoxia and energy (Arsham et al., 2003; Brugarolas et al., 2004; Dennis et al., 2001; Edinger and Thompson, 2002; Scott et al., 1998).

mTOR activity is negatively regulated by rapamycin, which is naturally an immunosuppressive, antifungal and antitumor reagent (Martel et al., 1977; Vezina et al., 1975). Rapamycin by blocking mTOR pathway, one of the major regulatory pathways in the cells, interferes with the cell cycle progression in different cell lines (Albers et al., 1993; Decker et al., 2003; Gorshtein et al., 2009; Metcalfe et al., 1997; Zhang et al., 2007; Zinzalla et al., 2007). Rapamycin treatment has important outcomes in the cell proliferation, viability, apoptosis and autophagy. As in serum starvation, rapamycin treatment induces a growth arrest at the G0/G1 phase of the cell cycle in human, rat, murine and yeast cells (Albers et al., 1993; Decker et al., 2003; Gorshtein et al., 2009; Metcalfe et al., 1997; Zhang et al., 2007; Zinzalla et al., 2007). However, in some cell lines rapamycin treatment may not induce a cell cycle arrest at G0/G1 phase thus they are rapamycin insensitive; and cells continue to proliferate (Altomare et al., 2004). Rapamycin has both apoptotic and anti-apoptotic functions probably regulating anti-apoptotic and pro-apoptotic genes and caspase activity (Ravikumar et al., 2006; Tirado et al., 2005). Rapamycin induced apoptosis and decreased cell viability has been observed in human and mouse cell lines (Tirado et

al., 2005). On the contrary, rapamycin has been shown to be protective against apoptosis induction in some human, monkey, rat cell line models and in fruitfly (Reddy et al., 2008).

In ZF4 cells, we did not observe any significant difference in cell cycle progression after rapamycin treatment. 100 nM rapamycin treatment for 48 h did not change the viable cell number according to MTT analysis. Rapamycin had also no effect on proliferating cell number according toBrdU and PI staining; we could not detect a significant difference in the cell number entering S phase. Interestingly, rapamycin treatment decreased the basal apoptosis in ZF4 cells. Cell death detection analysis (CDD) showed that rapamycin treated cells were less apoptotic than both DMSO (vehicle) and control cells cultured with 10% FBS including media. As in ZF4 cells, in primary human coronary artery smooth muscle cells, rapamycin treatment decreased the basal and also H_2O_2-induced apoptosis as compared to control cells (Zohlnhofer et al., 2004). However, we could not confirm the effect of rapamycin on cell death in the cell cycle analysis performed with PI staining. Although the percent cell number at subG1 phase in rapamycin treated cells were lower when compared to DMSO treated cells, the decrease was insignificant because of the high variation observed for rapamycin samples at the subG1 phase. Our results showed that rapamycin has no quantifiable effect on cell cycle progression of ZF4 cells based on BrdU and PI analyses, and yet is likely to be anti-apoptotic. However, in order to show the effect of rapamycin on apoptosis more effectively apoptosis should be induced in ZF4 cells and the apoptotic cell number in the rapamycin treated and control cells should be quantified. Furthermore, it should be considered that ZF4 cells might develop resistance to rapamycin over time. Thus the ability of ZF4 cells also to undergo G1 arrest or to become apoptotic/antiapoptotic might depend on their source, and passage duration and number.

5.2.1.2 The effect of rapamycin treatment on gene expression in ZF4 cells, microarray analysis

Rapamycin treatment affects cellular growth by regulating the transcription and translation of the cell cycle regulatory genes, such as *cyclin D1*, *cyclin D3*, *pcna*, *cyclin E*, *E2F1* and *cdk2* (Hashemolhosseini et al., 1998; Nelsen et al., 2003). In addition to studying single gene expressions in response to rapamycin treatment, the high-throughput microarray analyses have been performed to understand the effect of rapamycin treatment on global gene expression. The differentially expressed genes do not only help researchers to understand conserved regulatory pathway between different species, can also be used for prognostic approaches (Akcakanat et al., 2009).

According to microarray analysis with yeast strains *Candida albicans* and *Saccharomyces cerevisiae* strain BY4741, rapamycin treatment downregulated the genes coding for ribosomal proteins, tRNA synthetases and the components of translation (Fournier et al., 2010), and upregulated the genes coding for energy metabolism and autophagy (Fournier et al., 2010).

Rapamycin might affect expression of certain genes independent or dependent of the sensitivity status of cells to rapamycin. According to a microarray study performed with different rat cell lines, the genes encoding for the energy metabolism, cell cycle progression and death have been observed to be responsive to rapamycin treatment in the rapamycin sensitive (WB-F344), insensitive (WB311) and intermediate sensitive (GN5 and H5D) cell lines. On the other hand, in the rapamycin sensitive cell line, aminoacyl-tRNA biosynthesis, ribosome, cell cycle and carbohydrate metabolism were affected from rapamycin treatment, while in rapamycin insensitive cell lines, oxidative phosphorylation, amino acid metabolism and cell communication were affected from rapamycin treatment (Jimenez et al., 2009).

In addition to analysis of gene transcription, the effect of rapamycin treatment on gene translation has also been studied with a microarray approach via polysome-bound mRNAs (Grolleau et al., 2002). Rapamycin treatment respressed the translation

of ribosomal proteins, proteasome subunits and elongation factors in human E6–1 Jurkat T cells (Grolleau et al., 2002). In human lung fibroblast cells, MRC-5, mRNAs with anti-apoptotic functions were upregulated and mRNAs of ribosomal proteins and elongation factors were downregulated with rapamycin treatment (Genolet et al., 2008).

The effect of rapamycin on gene expression has not been investigated previously in zebrafish thus we used Affymetrix GeneChip® Zebrafish Genome Array to profile ZF4 cells that were treated with 100 nM rapamycin treatment or equivalent of DMSO for 48 h. The quality of arrays also fulfilled the required criteria and there was not any aberrant chip in the experiments according to NUSE and RLE graphs. By using BRB Array tools, the raw data was normalized and the differentially expressed genes were identified. Differentially expressed genes were selected with a random variance model for univariate tests (Wright and Simon, 2003). Among 15,610 probes, 2185 of them were differentially expressed between rapamycin and DMSO (p=0.05). The KEGG pathway and functional analysis of the differentially expressed genes were performed by DAVID.

The genes encoding for the ribosomal proteins, and components of gene expression and translation, regionalization and pattern specification were upregulated by rapamycin. The genes involved in proteasome structure, catabolic and metabolic processes, DNA damage and repair responses were downregulated by rapamycin. Consistent with our results, the transcriptional and translational downregulation of protesome subunits by rapamycin has been shown in human E6–1 Jurkat T cells (Grolleau et al., 2002). We also observed consistent but mild downregulation of close to 90% of the mitochondrial ribosomal proteins in rapamycin treated cells; this result is also in accord with previous studies showing the downregulation of mitochondrial ribosomes (Bastidas et al., 2009; Cunningham et al., 2007). Although in yeast model and some human cell lines (Fournier et al., 2010) rapamycin treatment downregulates ribosomal proteins, in ZF4 cells rapamycin treatment upregulated ribosomal proteins. According to our analysis, the increase in the ribosomal proteins was mild; the increase ranged between 0.2-0.4 log2 fold change, but was consistent. The observed increase in ribosomal protein expression might be related with the inhibition of their translation, thus accumulation of mRNAs.

The increased ribosomal protein expression might be related with the secondary roles of ribosomal proteins. In addition to their conserved roles in protein synthesis, ribosomal proteins have been shown to involved in the cell survival and apoptosis (Chen and Ioannou, 1999). In adult zebrafish, heterozygous mutations in ribosomal proteins increased the rate of tumor formation, and ribosomal subunits have been proposed as haploinsufficient tumor suppressor genes (Amsterdam et al., 2004). Human 23K ribosomal protein also functions as an inhibitor of cell proliferation (Chen et al., 1998). In Jurkat cells constitutively active RPL7 (ribosomal protein L7) caused a cell cycle arrest at G1 phase and induced apoptosis (Neumann and Krawinkel, 1997). In human WI38 both overexpression and inhibition of RPL23 (ribosomal protein L23), stabilized p53 and induced growth arrest (Jin et al., 2004). Ribosomal subunits may also be involved in cell cycle progression; the overexpression of ribosomal protein L35a in Jurkat cells protected from indution of apoptosis (Lopez et al., 2002); over-expression of another ribosomal protein L36a increased cell proliferation, also L36a has been found to be overexpressed in hepatocellular carcinoma cases and cell lines (Kim et al., 2004).

As shown previously, types of ribosomal subunits may induce or repress cell growth in different cells. In ZF4 cells, slight but consistent increase in ribosomal protein expression might serve as a protector of apoptosis.

5.2.1.3 Confirmation of microarray results by real-time qRT-PCR

In order to confirm the microarray results with real-time qRT-PCR, 9 genes; either significantly upregulated or downregulated by rapamycin treatment according to microarray analysis, have been selected. The selected genes were *wif1*, *dkk1b*, *bambia*, *ddc*, *cyp26b1*, *pah*, *mmp9*, *tagln2* and *foxm1*. For confirmation analysis an independent rapamycin experimental setup was performed, in which ZF4 cells were treated with 100 nM rapamycin for 6 and 48 h. As a result, we confirmed the increase in *ddc*, *cyp26b1*, *dkk1b*, and *wif1* expressions and the decrease in *pah* expression in response rapamycin treatment by real-time qRT-PCR; however we could not detect a

significant change in other four selected genes in response to rapamycin treatment. Yet, the log2 fold changes for all the selected genes were in the same direction and were signficantly correlated between the microarray and real-time qRT-PCR results (Pearson correlation coefficient=0.791, P-Value = 0.011).

Validation of microarray results with real-time qRT-PCR is reliable (Dallas et al., 2005). Thus, there might be several reasons why some of the genes identified in the microarray study were not confirmed in the following qRT-PCR study (i.e., the expression changes observed for the *bambia*, *foxm1*, *tagln2*, and *mmp9* were not significant in qRT-PCR study while they were significant according to the microarray analysis). One such reason might be that ZF4 cells used for the microarray and those used for the qRT-PCR experiments were from different passages thus might have displayed different levels of sensitivity to rapamycin. Another possibility could be that the exact amount of change in the gene expression from the microarray study may not be reflected in real-time qRT-PCR analyses. It is also possible that the correlation of microarray results with real-time qRT-PCR results may be poorer for the genes exhibiting low fold change differences (<1.5) while the correlation is expected to be higher in the genes with high fold change differences (>1.5) (Dallas et al., 2005). In our study, we selected our microarray validation genes among the genes with significantly high fold changes. However, even among these genes, the fold change differences do not exceed 2/-1.8 log2 fold, since rapamycin affected the degree of expression moderately, according to our study. Indeed, the log2 fold changes of the genes that could not be confirmed by real-time qRT-PCR were 1.46/-1.14 between rapamycin and DMSO samples. Although real-time qRT-PCR analysis is known to be more sensitive than the microarray analyses, around a 70% match with real-time qRT-PCR and microarray results has been frequently reported (Morey et al., 2006; Rajeevan et al., 2001).

The p-value of selected genes also plays an important role in the high correlation of the microarray and real-time qRT-PCR results. Genes with low p-values, such as 0.0001 showed higher correlation than the genes with high p-values (Morey et al., 2006). However, the discrepancies between our microarray and real-time qRT-PCR results probably have not emerged from the selected p-value criteria, since all our selected genes have significantly low p-values (<0.001). Discrepancies

might also result from the false positive microarray results due to differential hybridization or probeset specificity or alternative splicing. It has been reported in the literature that although the selected genes seem to be highly differentially expressed genes, they may be still false positive and not differentially expressed (Wright and Simon, 2003).

Among the genes confirmed by qRT-PCR, only *DKK1* was shown to be a target for rapamycin previously in human cells to our knowledge thus we show for the first time the effect of rapamycin on *dkk1b*, *wif1*, *ddc*, *cyp26b1*, and *pah* expression in zebrafish. Further studies are needed to generalize whether these genes are common targets of rapamycint treatment. Below, information on function and expression of genes significantly affected by rapamycin in zebrafish are provided.

WIF1 (WNT inhibitory factor 1) is a Wnt antagonist protein. Wif1 inhibits Wnt signaling by directly binding to Wnt proteins and preventing their binding to Wnt receptors (Hsieh et al., 1999). *WIF1* expression was downregulated in human prostate, breast, non-small cell lung and bladder tumors (Wissmann et al., 2003). The sequence of wif1 is also highly conserved between zebrafish, *Xenopus* and human. *wif1* was expressed in zebrafish embryo in the notochord at the 15-somite-stage, the epiphysis and ventral midbrain at the 24 hpf zebrafish (Hsieh et al., 1999). *Wif1* involved in CNS and limb development in mouse model (Hu et al., 2008; Witte et al., 2009). The effect of rapamycin on *WIF-1* expression has not been shown previously.

DKK1 (dickkopf homolog 1) is a member of the dickkopf family (Krupnik et al., 1999). Dkk1 is secreted protein and inhibits Wnt signaling by preventing the formation LRP5/6–Wnt–Frizzled complex (Brott and Sokol, 2002; Kawano and Kypta, 2003). Dkk1 has a conserved function in various species as a Wnt signaling inhibitor including zebrafish (Fedi et al., 1999; Glinka et al., 1998; Krupnik et al., 1999; Shinya et al., 2000; Wu et al., 2000). *dkk1b* expression is observed in zebrafish embryos starting from blastula stage and persisted. Zebrafish dkk1 protein has a major role in the anterior nervous system and axial mesondoderm formation (Hashimoto et al., 2000). *dkk1* regulates and required for head formation in Xenopus (Glinka et al., 1998). In human keratinocytes, DKK1 was involved in pigmentation and thickness of

skin (Yamaguchi et al., 2008). The role of *DKK1* in cancer formation has also been shown in various human cancers, such as Wilms' tumors, lung cancers, hepatocellular carcinomas, hepatoblastomas, esophageal squamous cell carcinomas and myelomas, in which *DKK1* was upregulated, and colorectal cancers, in which *DKK1* was downregulated (Gonzalez-Sancho et al., 2005; Patil et al., 2005; Tian et al., 2003; Wirths et al., 2003; Yamabuki et al., 2007). Recently, the effect of rapamycin treatment on *DKK1* expression was shown in human cells; rapamycin treatment or silencing mTOR by shRNA treatment increased the *DKK1* expression in primary human endothelial cells (Kobayashi et al., 2010a).

DDC (dopa decarboxylase) is an enzyme, which is involved in catecholamine biosynthesis (Blaschko, 1942). In human cells DDC decarboxylates L-DOPA to dopamine, and L-5-hydroxytryptophan to serotonin (Lovenberg et al., 1962). DDC has been found to be overexpressed in prostate cancer (Avgeris et al., 2008). The relation of *DDC* with Parkinsons' Disease has also been shown; the combination of DDC inhibitors and L-Dopa has been used in the treatment of Parkinsons' Disease. The *ddc* expression was detected in the dopaminergic neurons of the juvenile zebrafish brains (Filippi et al., 2010). The effect of rapamycin on *DDC* expression has not been shown.

The CYP26B1 (cytochrome P450, family 26, subfamily B, polypeptide 1) is involved in retinoic acid metabolism; this enzyme converts all-*trans*-Retinoic acid into 4-oxo-RA, 4-OH-RA, and 18-OH-RA. *CYP26B1* is expressed in various normal human tissues according to multi-tissue RNA dot blot analysis (White et al., 2000). But the higher expression is detected in the cerebellum of the brain tissue (Trofimova-Griffin and Juchau, 2002; White et al., 2000). The expression of mouse *Cyp26B1* is detected in many developing tissues such as, limbs, spinal cord, spleen, kidney and cartilage elements (Abu-Abed et al., 2002). Zebrafish *cyp26b1* also functions in metabolizing retinoic RA and is expressed in zebrafish embryo from 8-10 hpf. *Cyp26b1* expression was observed in developing zebrafish embryo in the neural tissues, such as eyes and some parts of brain including cerebellum and diencephalon, pectoral fin which is the homolog of forelimbs, pharyngeal arches and otic vesicle until 48 hpf (Zhao et al., 2005). The expression profiles in different organisms

highlight the importance of *Cyp26b1* in embryonic development. The effect of rapamycin on *CYP26B1* expression has not been shown previously.

PAH (phenylalanine hydroxylase) gene encodes for a protein involved in phenylalanine catabolism, the enzyme is responsible for conversion of phenylalanine to tyrosine (Kobe et al., 1999). The deficiency of metabolizing phenylalanine causes the genetic disorder, phenylketonuria and one of the factors of this disease is deficiency of PAH enzyme (Folling, 1934; Jervis, 1947; Parker, 1979). The role of this enzyme in melanogenesis has been shown (Schallreuter and Wood, 1999). In developing zebrafish embryo, *pah* expression was observed in the central nervous system and kidney at 18 and 24 hpf (Song et al., 2004). The effect of rapamycin on *PAH* expression has not been shown previously.

5.2.2 The effect of rapamycin treatment on zebrafish embryogenesis and larval development

Zebrafish is a preferable and widely used model organism in molecular biology, organ development, cancerogenesis, drug screening, and developmental studies (Chen et al., 1996; Drummond et al., 1998).

Previously, the sensitivity of zebrafish model to rapamycin has been shown in the zebrafish embryos and adults (Goldsmith et al., 2006). A mild developmental delay in embryonic development and arrest in the digestive tract development were observed up to 72 hpf in zebrafish embryo, after 400 nM rapamycin treatment (Makky et al., 2007). The developmental delay induced by rapamycin was accompanied with vessel defects and cardiac failure in zebrafish embryos from the 8-cell-stage to 26 hpf (Wenzlau et al., 2006). Rapamycin treatment (400 nM for 2 days) suppressed lymphangiogenesis, formation of the growth of lymphatic vessels, also in 26 hpf zebrafish embryo as in mammalian models (Flores et al., 2010). phospho-p70S6 kinase protein levels were responsive to rapamycin treatment in zebrafish embryos as in mammals; phospho-p70S6 kinase protein levels were decreased in 500 nM rapamycin treated zebrafish embryos (DiBella et al., 2009). Rapamycin-induced

autophagy has been detected in 3 dpf zebrafish embryos (He et al., 2009), the induction of autophagy by rapamycin has previously been shown in mammals and fruitfly (Ravikumar et al., 2006). However, the dose-dependent effect of rapamycin on the development of zebrafish neural crest derived tissues such as melanocytes and cranial cartilage has not been studied.

In order to explore the effects of rapamycin on zebrafish embryo development, shield stage embryos were treated with 2, 10 and 20 μM rapamycin provided in the embryo medium, for a duration of 1 day to 5 day. We observed that 400 nM rapamycin treatment arrested the development of digestive tract as previously shown (Makky et al., 2007). According to our results rapamycin caused a general delay in zebrafish developmental in a dose-dependent manner starting from 1 dpf to 5 dpf. Interestingly, rapamycin treatment caused a detention in pigmentation and cartilage development in larvae. We observed a delay in both the melanophore and iridophore pigmentation in the rapamycin treated group. Recently, the negative effect of rapamycin on melanocyte pigmentation has been shown in *Xenopus* model (Moriyama et al., 2010) supporting our findings in zebrafish embryos. We demonstrated that the cartilage elements were also shorter and pharyngeal arches stained less in the rapamycin treated embryos as compared to the control fish. These defects in cartilage elements accompanied with reduced pigmentation have previously been shown in different zebrafish mutants (Neuhauss et al., 1996), but not in rapamycin treated zebrafish. Previously, the inhibitory effect of rapamycin treatment on the general development and developing bone and cartilage has been reported in rat and chicken models and mouse embryonic carcinoma cells, ATDC5 (Alvarez-Garcia et al., 2007; Alvarez-Garcia et al., 2010; Nishigaki et al., 2002; Oh et al., 2001; Sanchez and He, 2009). Rapamycin treatment inhibited the chondrogenic differentiation of chick bud mesenchymal cells by repressing the formation of cartilage nodules (Oh et al., 2001). In rat model, rapamycin treatment repressed chondrocyte proliferation in the growth-plate, caused aberrant chondrocyte growth (Alvarez-Garcia et al., 2007). In conclusion, rapamycin treatment might interfere with chondrogenic differentiation in vertebrates, the dose-dependent delay we reported in cartilage element formation in zebrafish model, might also be a result of a delay in chondrogenic differentiation.

Although the inhibitory effects of rapamycin treatment in pigment formation or migration have not been shown previously in zebrafish, the link between S6 kinase and pigment cells was shown in *Drosophila*. As explained in the introduction part of this thesis, rapamycin treatment is known to cause a decrease in S6 kinase phosphorylation, hence a decrease in S6 kinase activity (Demidenko and Blagosklonny, 2008). Particularly interesting is that in *Drosophila* S6 kinase mutants, the absence of red pigments has been observed (Montagne1999). However, in senescent retinal pigment epithelium (RPE) cells, rapamycin treatment inhibited senescence markers (Chen et al., 2010). Our results suggest that rapamycin might affect formation and/or migration of pigment cells and restricts them dorsally to the yolk; and these effects might involve changes in the S6 kinase activity. These results require further study yet implicate rapamycin as a possible teratogen and point to a need for further assessment in use during pregnancy.

In our study, we observed an increase in *dkk1b* expression and a decrease in *pah* and *ddc* expressions in the rapamycin treated ZF4 cells. The involvement of these genes in pigmentation has been shown in different organisms. Overexpression of DKK1 has been shown to supress the melanocyte growth and proliferation in human keratinocytes (Yamaguchi et al., 2004; Yamaguchi et al., 2008; Yamaguchi et al., 2007). DDC provides dopamine by conversion from dopa, which in turn can be used for melanin formation and thus is involved in the color formation (e.g., butterfly wings (Koch et al., 1998)). PAH supplies tyrosine for melanin production and contributes to melanogenesis (Schallreuter and Wood, 1999). In our study, we detected upregulation of *dkk1b* and downregulation of *pah* in ZF4 cells, which were modulated in the expected direction for observing a defect in pigmentation patterns. However, our results were obtained in ZF4 cells thus the expression of these genes also should be investigated in rapamycin treated embryos to confirm these initial findings.

Cartilage and pigment cells are derived from the neural crest cells (Yelick and Schilling, 2002). Our results suggest that rapamycin might negatively affect particulary the neural crest cell derivatives, namely cranial cartilages and pigment cells. In zebrafish, the neural crest cells are formed at the border of the neural plate during gastrulation and give rise to pigment cells, cartilage components and cells of

the peripheral nervous system (Lister, 2002). However, the pigment cells in the retinal epithelium are derived from the neural epithelium not from the neural crest cells (Dupin and Le Douarin, 2003). The delayed melanophore and iridophore pigmentation in the horizontal myoseptum and yolk, but not in the eye of the rapamycin treated embryos may also indicate that the effect of rapamycin might be specific to neural crest derivatives. A similar situation with pigmentation was observed in *Xenopus* embryos treated with rapamycin further supporting our findings (Moriyama et al., 2010).

In further support of our findings in relationship to the interaction between neural crest cells and rapamycin treatment, we searched the literature for rapamycin and neural crest derived tumor related studies. Malignant peripheral nerve sheath tumors (MPNST) derived from NF1 (Neurofibromatosis type 1) patients have also been thought to derive from the neural crest cells. Peviously, rapamycin derivative, RAD001 were shown to be protective for the tumor formation in MPNST xenografts in mice. RAD001 treatment also decreased the growth of several MPNST cell lines (Johansson et al., 2008). These suggest that rapamycin might be particularly beneficial for neural crest derived tumor regression and warrant further study.

5.3 Zebrafish as a model for conserved gene expression signal profiling

We have established ZF4 cell line in zebrafish as a quiescence model. Two types of potential quiescent inducing stimuli were used: serum deprivation and rapamycin exposure. Both of these agents were shown to be potent growth inhibitors in mammals. Our findings showed that serum starvation in zebrafish indeed has similar consequences in terms of G1/S arrest while rapamycin did not seem to have an effect on cell proliferation. On the other hand, ZF4 cells exhibited anti-apoptotic response when treated with rapamycin and this might compensate for a potential delay in cell growth/proliferation. These findings are novel and set ZF4 as a potentially phylogenetically conserved vertebrate cell line model for expression signaling pathway comparisons across taxa. We have used *b2m* and *ef1a* as reference genes and performed a series of qRT-PCR experiments to demonstrate serum responsiveness and rapamycin sensisitivity of ZF4 cells. Our findings revealed conserved expression

patterns for *pcna*, *mybl2*, *tyms*, *mcm7* and *ctgf* in zebrafish as observed for mammals. We have identified several novel genes that were affected by rapamycin exposure, namely, *dkk1b*, *pah*, *dcc*, *wif1* and *cyp26b1* which were not previously studied in zebrafish in this context and/or associated with rapamycin sensitivity. Furthermore, exposure of zebrafish embryos to different doses of rapamycin revealed novel phenotypes not previously shown in zebrafish. Among these were reductions and delays in pigmentation and cartilage development. These neural crest derivatives have been identified as affected by rapamycin dose-dependently for the first time in the zebrafish model, although general growth retardation has been observed in invertebrates and in vertebrates including zebrafish when exposed to rapamycin.

Chapter 6. FUTURE PERSPECTIVES

6.1 E2F target gene regulation in zebrafish

In our study, we have shown that ZF4 cell line is an appropriate model to study E2F target gene expression in response to serum fluctuations as in mammalian cells (Takahashi et al., 2000).

However, in order to show that selected E2F target genes are also regulated by E2F1, the zebrafish E2F1 gene needs to be cloned and sequenced. The E2F1 gene sequence has not been identified in zebrafish. We performed preliminary studies to find a possible ortholog of human E2F1 gene in zebrafish. The sequencing of the putative E2F1 sequence and its overexpression or depletion studies would be helpful to search for the E2F1 regulation in zebrafish cells. Indeed, in mammalian fibroblast cell lines, overexpression of E2F1 mediated the progression to S phase in quiescent cells (Ishida et al., 2001). The overexpression of E2F1 in serum-starved ZF4 cells, and monitoring cell cycle progression and selected E2F1 target gene expression could be performed in ZF4 cells to explore a conservatory role for E2F1 between species. Also the function of E2F1 in zebrafish development can be investigated by silencing E2F1 in zebrafish embryos. The role on E2F1 in regeneration of tissues, such as liver and fin can be easily applied in zebrafish models.

Furthermore, mammalian *mcm7*, *pcna*, *mybl2* and *tyms* genes have binding sites to E2F1 in their promoter regions (Lee et al., 1995). However, there is no detailed information about regulation of these genes in zebrafish by E2F1. Our future studies will include searching of the promoter regions of zebrafish *mcm7*, *pcna*, *mybl2* and *tyms* for E2F binding sites.

We also have shown that in zebrafish model the selected E2F target genes behave in the same manner as their mammalian counterparts which may indicate the conserved role of the selected genes in cell cycle regulation also in zebrafish. As being

crucial regulator of cell cycle, the deregulation of E2F signaling pathway components has been observed in various cancers. The overexpression of *MCM7* have been observed in prostate cancer and associated with reoccurrence of the cancer after the treatment (Ren et al., 2006). High expression of MCM proteins have been detected in different carcinomas, including kidney, bladder and colon (Freeman et al., 1999). *PCNA* expression has been shown to be predictive in the metastasis of breast cancers (Schonborn et al., 1995). The high expression of *TYMS* has been associated with the decrease in overall survival in colorectal cancer (Popat et al., 2004). Loss of *mybl2* expression increased cancer susceptibility in zebrafish (Shepard et al., 2005). The high *CTGF* expression has been shown to be correlated with extended survival in lung cancers (Chen et al., 2007).The overexpression of these genes can easily be applied to zebrafish embryo model, the formation of tumors could be monitored and therapeutic approaches can be tested *in vivo*, since using zebrafish model for drug screening is an emerging and promising field (Taylor et al., 2010; Wang et al., 2010).

6.2 Identification of conserved signatures in response to rapamycin in different species

We have shown that rapamycin significantly affected a large number of transcripts; among these rapamycin upregulated ribosomal protein expressions, while downregulated the genes encoding proteasome subunits according to our microarray results. The observation of increase in ribosomal protein expression is a novel finding to our knowledge. It is known that mutations, causing the loss of ribosomal proteins contribute to tumor formation in zebrafish (Amsterdam et al., 2004) thus upregulation of ribosomal proteins by rapamycin might be a coping mechanism for tumor formation. Currently, we are performing a meta-analysis to assess whether expression profile upon rapamycin exposure is conserved from invertebrates to vertebrates based on existing microarray studies in flies, mice, rats, and humans.

6.3 In vivo rapamycin experiments with zebrafish embryos

In rapamycin treated embryos, we observed a delay in general embryonic development, cartilage formation and pigmentation. Further studies are planned for the morphometric analysis of zebrafish embryos using multivariate techniques and automated image analysis. In the near future we also plan on further studying the expression of known markers of cartilage formation and neural crest cells, e.g., *dlx2*, *sox9a* and *sox9b* in 10 and 36 hpf rapamycin treated and control embryos by *in situ* hybridization (Chiang et al., 2001; Li et al., 2002). *Sox9* expression is crucial for cartilage development as shown in mouse and zebrafish (Bi et al., 1999; Chiang et al., 2001; Yan et al., 2002) and zebrafish has two *sox9* genes, which are the orthologs of human *SOX9*; *sox9a* and *sox9b* (Chiang et al., 2001). Although both *sox9a* and *sox9b* are important for cartilage formation, their expression patterns overlap or differ in adult and embryos of zebrafish (Chiang et al., 2001). In 24 hpf zebrafish embryo both genes are expressed in parts of the brain, and in the head region. At this point only *sox9a* is expressed in the cranial mesenchyme, at the time of hatching *sox9b* is also expressed. Both genes are expressed during chondrogenesis of the head and pectoral fin. In the tissues of adult zebrafish, *sox9a* is expressed in brain, pectoral fin, kidney, muscle and testis, while *sox9b* expression is restricted only in ovary tissue (Chiang et al., 2001). *sox9b* is a neural crest marker of the developing zebrafish. The expression of *sox9b* is observed in the midbrain, hidbrain and trunk neural crest precursors at the 11-12 hpf zebrafish embryo and proposed as a marker of cranial and trunk neural crest precursor cells (Li et al., 2002). In the 14 hpf embryos *sox9*a is expressed in the otic placode, while sox9b is expressed in the cranial and trunk premigratory neural crest, eye and ear. *sox9b* expression in cranial neural crest cells is higher than *sox9a* expression. *sox9b* mutation causes a reduction in the pharyngeal arches and cranial cartilages, while in *sox9a* mutants the cartilage elements are more affected in 4 dpf zebrfish embryos (Yan et al., 2005). The pigmentation is also effected by *sox9b* mutation. Only in *sox9b* mutants but not in *sox9a* mutants, iridophore pigmentation is decreased, and melanocytes become less condensed (Yan et al., 2005). Our preliminary results show that *sox9b* expression might be reduced or delayed in rapamycin treated zebrafish embryos (data not shown) is in accord with the phenotype observed in rapamycin treated embryos, i.e., a delay but not a severe effect on cartilage development and reduction in melanocyte and iridophore pigmentation. Studies are in progress to confirm these preliminary results.

REFERENCES

Abu-Abed, S., MacLean, G., Fraulob, V., Chambon, P., Petkovich, M., Dolle, P., 2002. Differential expression of the retinoic acid-metabolizing enzymes CYP26A1 and CYP26B1 during murine organogenesis. Mech Dev 110, 173-177.

Airaksinen, S., Jokilehto, T., Rabergh, C.M., Nikinmaa, M., 2003. Heat- and cold-inducible regulation of HSP70 expression in zebrafish ZF4 cells. Comp Biochem Physiol B Biochem Mol Biol 136, 275-282.

Akcakanat, A., Zhang, L., Tsavachidis, S., Meric-Bernstam, F., 2009. The rapamycin-regulated gene expression signature determines prognosis for breast cancer. Mol Cancer 8, 75.

Al-Shahrour, F., Diaz-Uriarte, R., Dopazo, J., 2004. FatiGO: a web tool for finding significant associations of Gene Ontology terms with groups of genes. Bioinformatics 20, 578-580.

Albers, M.W., Williams, R.T., Brown, E.J., Tanaka, A., Hall, F.L., Schreiber, S.L., 1993. FKBP-rapamycin inhibits a cyclin-dependent kinase activity and a cyclin D1-Cdk association in early G1 of an osteosarcoma cell line. J Biol Chem 268, 22825-22829.

Altomare, D.A., Wang, H.Q., Skele, K.L., De Rienzo, A., Klein-Szanto, A.J., Godwin, A.K., Testa, J.R., 2004. AKT and mTOR phosphorylation is frequently detected in ovarian cancer and can be targeted to disrupt ovarian tumor cell growth. Oncogene 23, 5853-5857.

Alvarez-Garcia, O., Carbajo-Perez, E., Garcia, E., Gil, H., Molinos, I., Rodriguez, J., Ordonez, F.A., Santos, F., 2007. Rapamycin retards growth and causes marked alterations in the growth plate of young rats. Pediatr Nephrol 22, 954-961.

Alvarez-Garcia, O., Garcia-Lopez, E., Loredo, V., Gil-Pena, H., Rodriguez-Suarez, J., Ordonez, F.A., Carbajo-Perez, E., Santos, F., 2010. Rapamycin induces growth retardation by disrupting angiogenesis in the growth plate. Kidney Int 78, 561-568.

Alvers, A.L., Wood, M.S., Hu, D., Kaywell, A.C., Dunn, W.A., Jr., Aris, J.P., 2009. Autophagy is required for extension of yeast chronological life span by rapamycin. Autophagy 5, 847-849.

Amsterdam, A., Nissen, R.M., Sun, Z., Swindell, E.C., Farrington, S., Hopkins, N., 2004. Identification of 315 genes essential for early zebrafish development. Proc Natl Acad Sci U S A 101, 12792-12797.

Archer, K.J., Dumur, C.I., Joel, S.E., Ramakrishnan, V., 2006. Assessing quality of hybridized RNA in Affymetrix GeneChip experiments using mixed-effects models. Biostatistics 7, 198-212.

Arsham, A.M., Howell, J.J., Simon, M.C., 2003. A novel hypoxia-inducible factor-independent hypoxic response regulating mammalian target of rapamycin and its targets. J Biol Chem 278, 29655-29660.

Avgeris, M., Koutalellis, G., Fragoulis, E.G., Scorilas, A., 2008. Expression analysis and clinical utility of L-Dopa decarboxylase (DDC) in prostate cancer. Clin Biochem 41, 1140-1149.

Barbazuk, W.B., Korf, I., Kadavi, C., Heyen, J., Tate, S., Wun, E., Bedell, J.A., McPherson, J.D., Johnson, S.L., 2000. The syntenic relationship of the zebrafish and human genomes. Genome Res 10, 1351-1358.

Barrallo-Gimeno, A., Holzschuh, J., Driever, W., Knapik, E.W., 2004. Neural crest survival and differentiation in zebrafish depends on mont blanc/tfap2a gene function. Development 131, 1463-1477.

Bastidas, R.J., Heitman, J., Cardenas, M.E., 2009. The protein kinase Tor1 regulates adhesin gene expression in Candida albicans. PLoS Pathog 5, e1000294.

Bell, E., Cao, X., Moibi, J.A., Greene, S.R., Young, R., Trucco, M., Gao, Z., Matschinsky, F.M., Deng, S., Markman, J.F., Naji, A., Wolf, B.A., 2003. Rapamycin has a deleterious effect on MIN-6 cells and rat and human islets. Diabetes 52, 2731-2739.

Besser, J., Leito, J.T., van der Meer, D.L., Bagowski, C.P., 2007. Tip-1 induces filopodia growth and is important for gastrulation movements during zebrafish development. Dev Growth Differ 49, 205-214.

Bettuzzi, S., Astancolle, S., Guidetti, G., Moretti, M., Tiozzo, R., Corti, A., 1999. Clusterin (SGP-2) gene expression is cell cycle dependent in normal human dermal fibroblasts. FEBS Lett 448, 297-300.

Bi, W., Deng, J.M., Zhang, Z., Behringer, R.R., de Crombrugghe, B., 1999. Sox9 is required for cartilage formation. Nat Genet 22, 85-89.

Blaschko, H., 1942. The activity of l(-)-dopa decarboxylase. J Physiol 101, 337-349.

Blow, J.J., Dutta, A., 2005. Preventing re-replication of chromosomal DNA. Nat Rev Mol Cell Biol 6, 476-486.

Bolstad, B.M., Collin, F, Brettschneider, J, Simpson, K, Cope, L, Irizarry, R.A, Speed, T.P., 2005. Quality Assessment of Affymetrix GeneChip Data in Bioinformatics and Computational Biology Solutions Using R and Bioconductor. Gentleman R, Carey V, Huber W, Irizarry R, and Dudoit S. (Eds.), Springer, New York.

Bolstad, B.M., Irizarry, R.A., Astrand, M., Speed, T.P., 2003. A comparison of normalization methods for high density oligonucleotide array data based on variance and bias. Bioinformatics 19, 185-193.

Bracken, A.P., Ciro, M., Cocito, A., Helin, K., 2004. E2F target genes: unraveling the biology. Trends Biochem Sci 29, 409-417.

Brennan, P., Babbage, J.W., Thomas, G., Cantrell, D., 1999. p70(s6k) integrates phosphatidylinositol 3-kinase and rapamycin-regulated signals for E2F regulation in T lymphocytes. Mol Cell Biol 19, 4729-4738.

Brettschneider, J., Collin, F, Bolstad, B.M, Speed, T.P., 2007. Quality assessment for short oligonucleotide arrays. Technometrics. .

Brott, B.K., Sokol, S.Y., 2002. Regulation of Wnt/LRP signaling by distinct domains of Dickkopf proteins. Mol Cell Biol 22, 6100-6110.

Bruemmer, D., Yin, F., Liu, J., Kiyono, T., Fleck, E., Van Herle, A.J., Law, R.E., 2003. Rapamycin inhibits E2F-dependent expression of minichromosome maintenance proteins in vascular smooth muscle cells. Biochem Biophys Res Commun 303, 251-258.

Brugarolas, J., Lei, K., Hurley, R.L., Manning, B.D., Reiling, J.H., Hafen, E., Witters, L.A., Ellisen, L.W., Kaelin, W.G., Jr., 2004. Regulation of mTOR function in response to hypoxia by REDD1 and the TSC1/TSC2 tumor suppressor complex. Genes Dev 18, 2893-2904.

Brunn, G.J., Hudson, C.C., Sekulic, A., Williams, J.M., Hosoi, H., Houghton, P.J., Lawrence, J.C., Jr., Abraham, R.T., 1997. Phosphorylation of the translational repressor PHAS-I by the mammalian target of rapamycin. Science 277, 99-101.

Butcher, R.A., Bhullar, B.S., Perlstein, E.O., Marsischky, G., LaBaer, J., Schreiber, S.L., 2006. Microarray-based method for monitoring yeast overexpression

strains reveals small-molecule targets in TOR pathway. Nat Chem Biol 2, 103-109.

Cam, H., Balciunaite, E., Blais, A., Spektor, A., Scarpulla, R.C., Young, R., Kluger, Y., Dynlacht, B.D., 2004. A common set of gene regulatory networks links metabolism and growth inhibition. Mol Cell 16, 399-411.

Carney, S.A., Chen, J., Burns, C.G., Xiong, K.M., Peterson, R.E., Heideman, W., 2006. Aryl hydrocarbon receptor activation produces heart-specific transcriptional and toxic responses in developing zebrafish. Mol Pharmacol 70, 549-561.

Cayirlioglu, P., Duronio, R.J., 2001. Cell cycle: Flies teach an old dogma new tricks. Curr Biol 11, R178-181.

Chaga, G.S., 2008. Antibody arrays for determination of relative protein abundances. Methods Mol Biol 441, 129-151.

Chang, H.Y., Sneddon, J.B., Alizadeh, A.A., Sood, R., West, R.B., Montgomery, K., Chi, J.T., van de Rijn, M., Botstein, D., Brown, P.O., 2004. Gene expression signature of fibroblast serum response predicts human cancer progression: similarities between tumors and wounds. PLoS Biol 2, E7.

Chen, F.W., Davies, J.P., Ioannou, Y.A., 1998. Differential gene expression in apoptosis: identification of ribosomal protein 23K, a cell proliferation inhibitor. Mol Genet Metab 64, 271-282.

Chen, F.W., Ioannou, Y.A., 1999. Ribosomal proteins in cell proliferation and apoptosis. Int Rev Immunol 18, 429-448.

Chen, J.J., Wang, S.J., Tsai, C.A., Lin, C.J., 2007. Selection of differentially expressed genes in microarray data analysis. Pharmacogenomics J 7, 212-220.

Chen, J.N., Haffter, P., Odenthal, J., Vogelsang, E., Brand, M., van Eeden, F.J., Furutani-Seiki, M., Granato, M., Hammerschmidt, M., Heisenberg, C.P., Jiang, Y.J., Kane, D.A., Kelsh, R.N., Mullins, M.C., Nusslein-Volhard, C., 1996. Mutations affecting the cardiovascular system and other internal organs in zebrafish. Development 123, 293-302.

Chen, Y., Wang, J., Cai, J., Sternberg, P., 2010. Altered mTOR signaling in senescent retinal pigment epithelium. Invest Ophthalmol Vis Sci 51, 5314-5319.

Chiang, E.F., Pai, C.I., Wyatt, M., Yan, Y.L., Postlethwait, J., Chung, B., 2001. Two sox9 genes on duplicated zebrafish chromosomes: expression of similar transcription activators in distinct sites. Dev Biol 231, 149-163.

Chiou, M.J., Chao, T.T., Wu, J.L., Kuo, C.M., Chen, J.Y., 2006. The physiological role of CTGF/CCN2 in zebrafish notochond development and biological analysis of the proximal promoter region. Biochem Biophys Res Commun 349, 750-758.

Conrad, A.H., 1971. Thymidylate synthetase activity in cultured mammalian cells. J Biol Chem 246, 1318-1323.

Cunningham, J.T., Rodgers, J.T., Arlow, D.H., Vazquez, F., Mootha, V.K., Puigserver, P., 2007. mTOR controls mitochondrial oxidative function through a YY1-PGC-1alpha transcriptional complex. Nature 450, 736-740.

Dallas, P.B., Gottardo, N.G., Firth, M.J., Beesley, A.H., Hoffmann, K., Terry, P.A., Freitas, J.R., Boag, J.M., Cummings, A.J., Kees, U.R., 2005. Gene expression levels assessed by oligonucleotide microarray analysis and quantitative real-time RT-PCR -- how well do they correlate? BMC Genomics 6, 59.

de Barros, F.R., Goissis, M.D., Caetano, H.V., Paula-Lopes, F.F., Peres, M.A., Assumpcao, M.E., Visintin, J.A., 2010. Serum starvation and full confluency for cell cycle synchronization of domestic cat (felis catus) foetal fibroblasts. Reprod Domest Anim 45, 38-41.

Decker, T., Hipp, S., Ringshausen, I., Bogner, C., Oelsner, M., Schneller, F., Peschel, C., 2003. Rapamycin-induced G1 arrest in cycling B-CLL cells is associated with reduced expression of cyclin D3, cyclin E, cyclin A, and survivin. Blood 101, 278-285.

DeGregori, J., Johnson, D.G., 2006. Distinct and Overlapping Roles for E2F Family Members in Transcription, Proliferation and Apoptosis. Curr Mol Med 6, 739-748.

DeGregori, J., Kowalik, T., Nevins, J.R., 1995a. Cellular targets for activation by the E2F1 transcription factor include DNA synthesis- and G1/S-regulatory genes. Mol Cell Biol 15, 4215-4224.

DeGregori, J., Leone, G., Ohtani, K., Miron, A., Nevins, J.R., 1995b. E2F-1 accumulation bypasses a G1 arrest resulting from the inhibition of G1 cyclin-dependent kinase activity. Genes Dev 9, 2873-2887.

Demidenko, Z.N., Blagosklonny, M.V., 2008. Growth stimulation leads to cellular senescence when the cell cycle is blocked. Cell Cycle 7, 3355-3361.

Dennis, G., Jr., Sherman, B.T., Hosack, D.A., Yang, J., Gao, W., Lane, H.C., Lempicki, R.A., 2003. DAVID: Database for Annotation, Visualization, and Integrated Discovery. Genome Biol 4, P3.

Dennis, P.B., Jaeschke, A., Saitoh, M., Fowler, B., Kozma, S.C., Thomas, G., 2001. Mammalian TOR: a homeostatic ATP sensor. Science 294, 1102-1105.

DiBella, L.M., Park, A., Sun, Z., 2009. Zebrafish Tsc1 reveals functional interactions between the cilium and the TOR pathway. Hum Mol Genet 18, 595-606.

Driever, W., Rangini, Z., 1993. Characterization of a cell line derived from zebrafish (Brachydanio rerio) embryos. In Vitro Cell Dev Biol Anim 29A, 749-754.

Driever, W., Solnica-Krezel, L., Schier, A.F., Neuhauss, S.C., Malicki, J., Stemple, D.L., Stainier, D.Y., Zwartkruis, F., Abdelilah, S., Rangini, Z., Belak, J., Boggs, C., 1996. A genetic screen for mutations affecting embryogenesis in zebrafish. Development 123, 37-46.

Drummond, I.A., Majumdar, A., Hentschel, H., Elger, M., Solnica-Krezel, L., Schier, A.F., Neuhauss, S.C., Stemple, D.L., Zwartkruis, F., Rangini, Z., Driever, W., Fishman, M.C., 1998. Early development of the zebrafish pronephros and analysis of mutations affecting pronephric function. Development 125, 4655-4667.

Du, C., Niu, R., Chu, E., Zhang, P., Lin, X., 2006. Sequence analysis and functional study of thymidylate synthase from zebrafish, Danio rerio. J Biochem 139, 913-920.

Dufner, A., Thomas, G., 1999. Ribosomal S6 kinase signaling and the control of translation. Exp Cell Res 253, 100-109.

Dupin, E., Le Douarin, N.M., 2003. Development of melanocyte precursors from the vertebrate neural crest. Oncogene 22, 3016-3023.

Durinck, S., Moreau, Y., Kasprzyk, A., Davis, S., De Moor, B., Brazma, A., Huber, W., 2005. BioMart and Bioconductor: a powerful link between biological databases and microarray data analysis. Bioinformatics 21, 3439-3440.

Duronio, R.J., O'Farrell, P.H., Xie, J.E., Brook, A., Dyson, N., 1995. The transcription factor E2F is required for S phase during Drosophila embryogenesis. Genes Dev 9, 1445-1455.

Dyson, N., 1998. The regulation of E2F by pRB-family proteins. Genes Dev 12, 2245-2262.

Edinger, A.L., Thompson, C.B., 2002. Akt maintains cell size and survival by increasing mTOR-dependent nutrient uptake. Mol Biol Cell 13, 2276-2288.

Eisen, M.B., Spellman, P.T., Brown, P.O., Botstein, D., 1998. Cluster analysis and display of genome-wide expression patterns. Proc Natl Acad Sci U S A 95, 14863-14868.

Ekker, M., Speevak, M.D., Martin, C.C., Joly, L., Giroux, G., Chevrette, M., 1996. Stable transfer of zebrafish chromosome segments into mouse cells. Genomics 33, 57-64.

Ellies, D.L., Langille, R.M., Martin, C.C., Akimenko, M.A., Ekker, M., 1997. Specific craniofacial cartilage dysmorphogenesis coincides with a loss of dlx gene expression in retinoic acid-treated zebrafish embryos. Mech Dev 61, 23-36.

Essers, J., Theil, A.F., Baldeyron, C., van Cappellen, W.A., Houtsmuller, A.B., Kanaar, R., Vermeulen, W., 2005. Nuclear dynamics of PCNA in DNA replication and repair. Mol Cell Biol 25, 9350-9359.

Fedi, P., Bafico, A., Nieto Soria, A., Burgess, W.H., Miki, T., Bottaro, D.P., Kraus, M.H., Aaronson, S.A., 1999. Isolation and biochemical characterization of the human Dkk-1 homologue, a novel inhibitor of mammalian Wnt signaling. J Biol Chem 274, 19465-19472.

Feitsma, H., Cuppen, E., 2008. Zebrafish as a cancer model. Mol Cancer Res 6, 685-694.

Feuerstein, N., Huang, D., Prystowsky, M.B., 1995. Rapamycin selectively blocks interleukin-2-induced proliferating cell nuclear antigen gene expression in T lymphocyte. Evidence for inhibition of CREB/ATF binding activities. J Biol Chem 270, 9454-9458.

Filippi, A., Mahler, J., Schweitzer, J., Driever, W., 2010. Expression of the paralogous tyrosine hydroxylase encoding genes th1 and th2 reveals the full complement of dopaminergic and noradrenergic neurons in zebrafish larval and juvenile brain. J Comp Neurol 518, 423-438.

Fingar, D.C., Salama, S., Tsou, C., Harlow, E., Blenis, J., 2002. Mammalian cell size is controlled by mTOR and its downstream targets S6K1 and 4EBP1/eIF4E. Genes Dev 16, 1472-1487.

Flores, M.V., Hall, C.J., Crosier, K.E., Crosier, P.S., 2010. Visualization of embryonic lymphangiogenesis advances the use of the zebrafish model for research in cancer and lymphatic pathologies. Dev Dyn 239, 2128-2135.

Folling, A., 1934. Uber Ausscheidung von Phenylbrenztraubensaure in den Ham als Stoffwechselanomalie in Verbindung mit Imbezillitat. Ztschr Physiol Chem, 227:169.

Fournier, M.L., Paulson, A., Pavelka, N., Mosley, A.L., Gaudenz, K., Bradford, W.D., Glynn, E., Li, H., Sardiu, M.E., Fleharty, B., Seidel, C., Florens, L., Washburn, M.P., 2010. Delayed correlation of mRNA and protein expression in rapamycin-treated cells and a role for Ggc1 in cellular sensitivity to rapamycin. Mol Cell Proteomics 9, 271-284.

Freeman, A., Morris, L.S., Mills, A.D., Stoeber, K., Laskey, R.A., Williams, G.H., Coleman, N., 1999. Minichromosome maintenance proteins as biological markers of dysplasia and malignancy. Clin Cancer Res 5, 2121-2132.

Fukami-Kobayashi, J., Mitsui, Y., 1999. Overexpression of proliferating cell nuclear antigen in mammalian cells negates growth arrest by serum starvation and cell contact. Jpn J Cancer Res 90, 286-293.

Garg, R., Geng, C.D., Miller, J.L., Callens, S., Tang, X., Appel, B., Xu, B., 2004. Molecular cloning and characterization of the catalytic domain of zebrafish homologue of the ataxia-telangiectasia mutated gene. Mol Cancer Res 2, 348-353.

Gautier, L., Cope, L., Bolstad, B.M., Irizarry, R.A., 2004. affy--analysis of Affymetrix GeneChip data at the probe level. Bioinformatics 20, 307-315.

Genolet, R., Araud, T., Maillard, L., Jaquier-Gubler, P., Curran, J., 2008. An approach to analyse the specific impact of rapamycin on mRNA-ribosome association. BMC Med Genomics 1, 33.

Gentleman, R.C., Carey, V.J., Bates, D.M., Bolstad, B., Dettling, M., Dudoit, S., Ellis, B., Gautier, L., Ge, Y., Gentry, J., Hornik, K., Hothorn, T., Huber, W., Iacus, S., Irizarry, R., Leisch, F., Li, C., Maechler, M., Rossini, A.J., Sawitzki, G., Smith, C., Smyth, G., Tierney, L., Yang, J.Y., Zhang, J., 2004. Bioconductor: open software development for computational biology and bioinformatics. Genome Biol 5, R80.

Gingras, A.C., Kennedy, S.G., O'Leary, M.A., Sonenberg, N., Hay, N., 1998. 4E-BP1, a repressor of mRNA translation, is phosphorylated and inactivated by the Akt(PKB) signaling pathway. Genes Dev 12, 502-513.

Glinka, A., Wu, W., Delius, H., Monaghan, A.P., Blumenstock, C., Niehrs, C., 1998. Dickkopf-1 is a member of a new family of secreted proteins and functions in head induction. Nature 391, 357-362.

Goissis, M.D., Caetano, H.V., Marques, M.G., de Barros, F.R., Feitosa, W.B., Milazzotto, M.P., Binelli, M., Assumpcao, M.E., Visintin, J.A., 2007. Effects of serum deprivation and cycloheximide on cell cycle of low and high passage porcine fetal fibroblasts. Reprod Domest Anim 42, 660-663.

Gold, D.L., Miecznikowski, J.C., Liu, S., 2009. Error control variability in pathway-based microarray analysis. Bioinformatics 25, 2216-2221.

Goldsmith, M.I., Iovine, M.K., O'Reilly-Pol, T., Johnson, S.L., 2006. A developmental transition in growth control during zebrafish caudal fin development. Dev Biol 296, 450-457.

Golub, T.R., Slonim, D.K., Tamayo, P., Huard, C., Gaasenbeek, M., Mesirov, J.P., Coller, H., Loh, M.L., Downing, J.R., Caligiuri, M.A., Bloomfield, C.D., Lander, E.S., 1999. Molecular classification of cancer: class discovery and class prediction by gene expression monitoring. Science 286, 531-537.

Gonzalez-Sancho, J.M., Aguilera, O., Garcia, J.M., Pendas-Franco, N., Pena, C., Cal, S., Garcia de Herreros, A., Bonilla, F., Munoz, A., 2005. The Wnt antagonist DICKKOPF-1 gene is a downstream target of beta-catenin/TCF and is downregulated in human colon cancer. Oncogene 24, 1098-1103.

Goppelt-Struebe, M., Hahn, A., Iwanciw, D., Rehm, M., Banas, B., 2001. Regulation of connective tissue growth factor (ccn2; ctgf) gene expression in human mesangial cells: modulation by HMG CoA reductase inhibitors (statins). Mol Pathol 54, 176-179.

Gorshtein, A., Rubinfeld, H., Kendler, E., Theodoropoulou, M., Cerovac, V., Stalla, G.K., Cohen, Z.R., Hadani, M., Shimon, I., 2009. Mammalian target of rapamycin inhibitors rapamycin and RAD001 (everolimus) induce anti-proliferative effects in GH-secreting pituitary tumor cells in vitro. Endocr Relat Cancer 16, 1017-1027.

Grolleau, A., Bowman, J., Pradet-Balade, B., Puravs, E., Hanash, S., Garcia-Sanz, J.A., Beretta, L., 2002. Global and specific translational control by rapamycin in T cells uncovered by microarrays and proteomics. J Biol Chem 277, 22175-22184.

Gruber, J., Manninga, H., Tuschl, T., Osborn, M., Weber, K., 2005. Specific RNAi mediated gene knockdown in zebrafish cell lines. RNA Biol 2, 101-105.

Gstraunthaler, G., 2003. Alternatives to the use of fetal bovine serum: serum-free cell culture. ALTEX 20, 275-281.

Guba, M., Koehl, G.E., Neppl, E., Doenecke, A., Steinbauer, M., Schlitt, H.J., Jauch, K.W., Geissler, E.K., 2005. Dosing of rapamycin is critical to achieve an optimal antiangiogenic effect against cancer. Transpl Int 18, 89-94.

Hacia, J.G., Fan, J.B., Ryder, O., Jin, L., Edgemon, K., Ghandour, G., Mayer, R.A., Sun, B., Hsie, L., Robbins, C.M., Brody, L.C., Wang, D., Lander, E.S., Lipshutz, R., Fodor, S.P., Collins, F.S., 1999. Determination of ancestral alleles for human single-nucleotide polymorphisms using high-density oligonucleotide arrays. Nat Genet 22, 164-167.

Hancock, J.D., Lessnick, S.L., 2008. A transcriptional profiling meta-analysis reveals a core EWS-FLI gene expression signature. Cell Cycle 7, 250-256.

Hashemolhosseini, S., Nagamine, Y., Morley, S.J., Desrivieres, S., Mercep, L., Ferrari, S., 1998. Rapamycin inhibition of the G1 to S transition is mediated by effects on cyclin D1 mRNA and protein stability. J Biol Chem 273, 14424-14429.

Hashimoto, H., Itoh, M., Yamanaka, Y., Yamashita, S., Shimizu, T., Solnica-Krezel, L., Hibi, M., Hirano, T., 2000. Zebrafish Dkk1 functions in forebrain specification and axial mesendoderm formation. Dev Biol 217, 138-152.

Hay, N., Sonenberg, N., 2004. Upstream and downstream of mTOR. Genes Dev 18, 1926-1945.

He, C., Bartholomew, C.R., Zhou, W., Klionsky, D.J., 2009. Assaying autophagic activity in transgenic GFP-Lc3 and GFP-Gabarap zebrafish embryos. Autophagy 5, 520-526.

He, S., Salas-Vidal, E., Rueb, S., Krens, S.F., Meijer, A.H., Snaar-Jagalska, B.E., Spaink, H.P., 2006. Genetic and transcriptome characterization of model zebrafish cell lines. Zebrafish 3, 441-453.

Henry, T.B., Menn, F.M., Fleming, J.T., Wilgus, J., Compton, R.N., Sayler, G.S., 2007. Attributing effects of aqueous C60 nano-aggregates to tetrahydrofuran decomposition products in larval zebrafish by assessment of gene expression. Environ Health Perspect 115, 1059-1065.

Hidalgo, M., Rowinsky, E.K., 2000. The rapamycin-sensitive signal transduction pathway as a target for cancer therapy. Oncogene 19, 6680-6686.

Hirata, M., Nakamura, K., Kanemaru, T., Shibata, Y., Kondo, S., 2003. Pigment cell organization in the hypodermis of zebrafish. Dev Dyn 227, 497-503.

Hoffmann, J.L., Torontali, S.P., Thomason, R.G., Lee, D.M., Brill, J.L., Price, B.B., Carr, G.J., Versteeg, D.J., 2006. Hepatic gene expression profiling using Genechips in zebrafish exposed to 17alpha-ethynylestradiol. Aquat Toxicol 79, 233-246.

Hogg, N., Browning, J., Howard, T., Winterford, C., Fitzpatrick, D., Gobe, G., 1999. Apoptosis in vascular endothelial cells caused by serum deprivation, oxidative stress and transforming growth factor-beta. Endothelium 7, 35-49.

Hosoi, H., Dilling, M.B., Shikata, T., Liu, L.N., Shu, L., Ashmun, R.A., Germain, G.S., Abraham, R.T., Houghton, P.J., 1999. Rapamycin causes poorly reversible inhibition of mTOR and induces p53-independent apoptosis in human rhabdomyosarcoma cells. Cancer Res 59, 886-894.

Hsieh, J.C., Kodjabachian, L., Rebbert, M.L., Rattner, A., Smallwood, P.M., Samos, C.H., Nusse, R., Dawid, I.B., Nathans, J., 1999. A new secreted protein that binds to Wnt proteins and inhibits their activities. Nature 398, 431-436.

Hu, M.C., Gong, H.Y., Lin, G.H., Hu, S.Y., Chen, M.H., Huang, S.J., Liao, C.F., Wu, J.L., 2007. XBP-1, a key regulator of unfolded protein response, activates transcription of IGF1 and Akt phosphorylation in zebrafish embryonic cell line. Biochem Biophys Res Commun 359, 778-783.

Hu, Y.A., Gu, X., Liu, J., Yang, Y., Yan, Y., Zhao, C., 2008. Expression pattern of Wnt inhibitor factor 1(Wif1) during the development in mouse CNS. Gene Expr Patterns 8, 515-522.

Huang da, W., Sherman, B.T., Lempicki, R.A., 2009. Systematic and integrative analysis of large gene lists using DAVID bioinformatics resources. Nat Protoc 4, 44-57.

Huang, S., Bjornsti, M.A., Houghton, P.J., 2003. Rapamycins: mechanism of action and cellular resistance. Cancer Biol Ther 2, 222-232.

Huang, S., Liu, L.N., Hosoi, H., Dilling, M.B., Shikata, T., Houghton, P.J., 2001. p53/p21(CIP1) cooperate in enforcing rapamycin-induced G(1) arrest and determine the cellular response to rapamycin. Cancer Res 61, 3373-3381.

Hubbell, E., Liu, W.M., Mei, R., 2002. Robust estimators for expression analysis. Bioinformatics 18, 1585-1592.

Hurford, R.K., Jr., Cobrinik, D., Lee, M.H., Dyson, N., 1997. pRB and p107/p130 are required for the regulated expression of different sets of E2F responsive genes. Genes Dev 11, 1447-1463.

Irizarry, R.A., Bolstad, B.M., Collin, F., Cope, L.M., Hobbs, B., Speed, T.P., 2003. Summaries of Affymetrix GeneChip probe level data. Nucleic Acids Res 31, e15.

Ishida, S., Huang, E., Zuzan, H., Spang, R., Leone, G., West, M., Nevins, J.R., 2001. Role for E2F in control of both DNA replication and mitotic functions as revealed from DNA microarray analysis. Mol Cell Biol 21, 4684-4699.

Ivkovic, S., Yoon, B.S., Popoff, S.N., Safadi, F.F., Libuda, D.E., Stephenson, R.C., Daluiski, A., Lyons, K.M., 2003. Connective tissue growth factor coordinates chondrogenesis and angiogenesis during skeletal development. Development 130, 2779-2791.

Javier, A.F., Bata-Csorgo, Z., Ellis, C.N., Kang, S., Voorhees, J.J., Cooper, K.D., 1997. Rapamycin (sirolimus) inhibits proliferating cell nuclear antigen expression and blocks cell cycle in the G1 phase in human keratinocyte stem cells. J Clin Invest 99, 2094-2099.

Jefferies, H.B., Fumagalli, S., Dennis, P.B., Reinhard, C., Pearson, R.B., Thomas, G., 1997. Rapamycin suppresses 5'TOP mRNA translation through inhibition of p70s6k. EMBO J 16, 3693-3704.

Jervis, G.A., 1947. Studies on phenylpyruvic oligophrenia; the position of the metabolic error. J Biol Chem 169, 651-656.

Jimenez, R.H., Boylan, J.M., Lee, J.S., Francesconi, M., Castellani, G., Sanders, J.A., Gruppuso, P.A., 2009. Rapamycin response in tumorigenic and non-tumorigenic hepatic cell lines. PLoS One 4, e7373.

Jimenez, R.H., Lee, J.S., Francesconi, M., Castellani, G., Neretti, N., Sanders, J.A., Sedivy, J., Gruppuso, P.A., 2010. Regulation of gene expression in hepatic cells by the mammalian Target of Rapamycin (mTOR). PLoS One 5, e9084.

Jin, A., Itahana, K., O'Keefe, K., Zhang, Y., 2004. Inhibition of HDM2 and activation of p53 by ribosomal protein L23. Mol Cell Biol 24, 7669-7680.

Johansson, G., Mahller, Y.Y., Collins, M.H., Kim, M.O., Nobukuni, T., Perentesis, J., Cripe, T.P., Lane, H.A., Kozma, S.C., Thomas, G., Ratner, N., 2008. Effective

in vivo targeting of the mammalian target of rapamycin pathway in malignant peripheral nerve sheath tumors. Mol Cancer Ther 7, 1237-1245.

Johnson, D.G., Schwarz, J.K., Cress, W.D., Nevins, J.R., 1993. Expression of transcription factor E2F1 induces quiescent cells to enter S phase. Nature 365, 349-352.

Jones, L., Goldstein, D.R., Hughes, G., Strand, A.D., Collin, F., Dunnett, S.B., Kooperberg, C., Aragaki, A., Olson, J.M., Augood, S.J., Faull, R.L., Luthi-Carter, R., Moskvina, V., Hodges, A.K., 2006. Assessment of the relationship between pre-chip and post-chip quality measures for Affymetrix GeneChip expression data. BMC Bioinformatics 7, 211.

Kan, N.G., Junghans, D., Izpisua Belmonte, J.C., 2009. Compensatory growth mechanisms regulated by BMP and FGF signaling mediate liver regeneration in zebrafish after partial hepatectomy. FASEB J 23, 3516-3525.

Kawano, Y., Kypta, R., 2003. Secreted antagonists of the Wnt signalling pathway. J Cell Sci 116, 2627-2634.

Kelsh, R.N., Brand, M., Jiang, Y.J., Heisenberg, C.P., Lin, S., Haffter, P., Odenthal, J., Mullins, M.C., van Eeden, F.J., Furutani-Seiki, M., Granato, M., Hammerschmidt, M., Kane, D.A., Warga, R.M., Beuchle, D., Vogelsang, L., Nusslein-Volhard, C., 1996. Zebrafish pigmentation mutations and the processes of neural crest development. Development 123, 369-389.

Khammanit, R., Chantakru, S., Kitiyanant, Y., Saikhun, J., 2008. Effect of serum starvation and chemical inhibitors on cell cycle synchronization of canine dermal fibroblasts. Theriogenology 70, 27-34.

Kherrouche, Z., Blais, A., Ferreira, E., De Launoit, Y., Monte, D., 2006. ASK-1 (apoptosis signal-regulating kinase 1) is a direct E2F target gene. Biochem J 396, 547-556.

Khoo, Y.T., Ong, C.T., Mukhopadhyay, A., Han, H.C., Do, D.V., Lim, I.J., Phan, T.T., 2006. Upregulation of secretory connective tissue growth factor (CTGF) in keratinocyte-fibroblast coculture contributes to keloid pathogenesis. J Cell Physiol 208, 336-343.

Kim, E., Arnould, T., Sellin, L.K., Benzing, T., Fan, M.J., Gruning, W., Sokol, S.Y., Drummond, I., Walz, G., 1999. The polycystic kidney disease 1 gene product modulates Wnt signaling. J Biol Chem 274, 4947-4953.

Kim, J.H., You, K.R., Kim, I.H., Cho, B.H., Kim, C.Y., Kim, D.G., 2004. Over-expression of the ribosomal protein L36a gene is associated with cellular proliferation in hepatocellular carcinoma. Hepatology 39, 129-138.

Kim, S.K., Novak, R.F., 2007. The role of intracellular signaling in insulin-mediated regulation of drug metabolizing enzyme gene and protein expression. Pharmacol Ther 113, 88-120.

Kittleson, M.M., Ye, S.Q., Irizarry, R.A., Minhas, K.M., Edness, G., Conte, J.V., Parmigiani, G., Miller, L.W., Chen, Y., Hall, J.L., Garcia, J.G., Hare, J.M., 2004. Identification of a gene expression profile that differentiates between ischemic and nonischemic cardiomyopathy. Circulation 110, 3444-3451.

Kobayashi, H., Butler, J.M., O'Donnell, R., Kobayashi, M., Ding, B.S., Bonner, B., Chiu, V.K., Nolan, D.J., Shido, K., Benjamin, L., Rafii, S., 2010a. Angiocrine factors from Akt-activated endothelial cells balance self-renewal and differentiation of haematopoietic stem cells. Nat Cell Biol 12, 1046-1056.

Kobayashi, I., Ono, H., Moritomo, T., Kano, K., Nakanishi, T., Suda, T., 2010b. Comparative gene expression analysis of zebrafish and mammals identifies common regulators in hematopoietic stem cells. Blood 115, e1-9.

Kobe, B., Jennings, I.G., House, C.M., Michell, B.J., Goodwill, K.E., Santarsiero, B.D., Stevens, R.C., Cotton, R.G., Kemp, B.E., 1999. Structural basis of autoregulation of phenylalanine hydroxylase. Nat Struct Biol 6, 442-448.

Koch, P.B., Keys, D.N., Rocheleau, T., Aronstein, K., Blackburn, M., Carroll, S.B., ffrench-Constant, R.H., 1998. Regulation of dopa decarboxylase expression during colour pattern formation in wild-type and melanic tiger swallowtail butterflies. Development 125, 2303-2313.

Kononen, J., Bubendorf, L., Kallioniemi, A., Barlund, M., Schraml, P., Leighton, S., Torhorst, J., Mihatsch, M.J., Sauter, G., Kallioniemi, O.P., 1998. Tissue microarrays for high-throughput molecular profiling of tumor specimens. Nat Med 4, 844-847.

Krishan, A., 1975. Rapid flow cytofluorometric analysis of mammalian cell cycle by propidium iodide staining. J Cell Biol 66, 188-193.

Krupnik, V.E., Sharp, J.D., Jiang, C., Robison, K., Chickering, T.W., Amaravadi, L., Brown, D.E., Guyot, D., Mays, G., Leiby, K., Chang, B., Duong, T., Goodearl, A.D., Gearing, D.P., Sokol, S.Y., McCarthy, S.A., 1999. Functional and structural diversity of the human Dickkopf gene family. Gene 238, 301-313.

Kues, W.A., Anger, M., Carnwath, J.W., Paul, D., Motlik, J., Niemann, H., 2000. Cell cycle synchronization of porcine fetal fibroblasts: effects of serum deprivation and reversible cell cycle inhibitors. Biol Reprod 62, 412-419.

Lam, S.H., Wu, Y.L., Vega, V.B., Miller, L.D., Spitsbergen, J., Tong, Y., Zhan, H., Govindarajan, K.R., Lee, S., Mathavan, S., Murthy, K.R., Buhler, D.R., Liu, E.T., Gong, Z., 2006. Conservation of gene expression signatures between zebrafish and human liver tumors and tumor progression. Nat Biotechnol 24, 73-75.

Langenau, D.M., Keefe, M.D., Storer, N.Y., Guyon, J.R., Kutok, J.L., Le, X., Goessling, W., Neuberg, D.S., Kunkel, L.M., Zon, L.I., 2007. Effects of RAS on the genesis of embryonal rhabdomyosarcoma. Genes Dev 21, 1382-1395.

Law, B.K., Chytil, A., Dumont, N., Hamilton, E.G., Waltner-Law, M.E., Aakre, M.E., Covington, C., Moses, H.L., 2002. Rapamycin potentiates transforming growth factor beta-induced growth arrest in nontransformed, oncogene-transformed, and human cancer cells. Mol Cell Biol 22, 8184-8198.

Lee, H.H., Chiang, W.H., Chiang, S.H., Liu, Y.C., Hwang, J., Ng, S.Y., 1995. Regulation of cyclin D1, DNA topoisomerase I, and proliferating cell nuclear antigen promoters during the cell cycle. Gene Expr 4, 95-109.

Lee, K.H., Hur, H.S., Im, S.A., Lee, J., Kim, H.P., Yoon, Y.K., Han, S.W., Song, S.H., Oh, D.Y., Kim, T.Y., Bang, Y.J., 2010. RAD001 shows activity against gastric cancer cells and overcomes 5-FU resistance by downregulating thymidylate synthase. Cancer Lett 299, 22-28.

Lee, L.M., Seftor, E.A., Bonde, G., Cornell, R.A., Hendrix, M.J., 2005. The fate of human malignant melanoma cells transplanted into zebrafish embryos: assessment of migration and cell division in the absence of tumor formation. Dev Dyn 233, 1560-1570.

Lemeer, S., Jopling, C., Naji, F., Ruijtenbeek, R., Slijper, M., Heck, A.J., den Hertog, J., 2007. Protein-tyrosine kinase activity profiling in knock down zebrafish embryos. PLoS One 2, e581.

Leung, A.Y., Leung, J.C., Chan, L.Y., Ma, E.S., Kwan, T.T., Lai, K.N., Meng, A., Liang, R., 2005. Proliferating cell nuclear antigen (PCNA) as a proliferative marker during embryonic and adult zebrafish hematopoiesis. Histochem Cell Biol 124, 105-111.

Lewis, J.L., Bonner, J., Modrell, M., Ragland, J.W., Moon, R.T., Dorsky, R.I., Raible, D.W., 2004. Reiterated Wnt signaling during zebrafish neural crest development. Development 131, 1299-1308.

Li, C., Hung Wong, W., 2001. Model-based analysis of oligonucleotide arrays: model validation, design issues and standard error application. Genome Biol 2, RESEARCH0032.

Li, M., Zhao, C., Wang, Y., Zhao, Z., Meng, A., 2002. Zebrafish sox9b is an early neural crest marker. Dev Genes Evol 212, 203-206.

Linhart, C., Elkon, R., Shiloh, Y., Shamir, R., 2005. Deciphering transcriptional regulatory elements that encode specific cell cycle phasing by comparative genomics analysis. Cell Cycle 4, 1788-1797.

Lipshutz, R.J., Fodor, S.P., Gingeras, T.R., Lockhart, D.J., 1999. High density synthetic oligonucleotide arrays. Nat Genet 21, 20-24.

Lister, J.A., 2002. Development of pigment cells in the zebrafish embryo. Microsc Res Tech 58, 435-441.

Liu, G., Loraine, A.E., Shigeta, R., Cline, M., Cheng, J., Valmeekam, V., Sun, S., Kulp, D., Siani-Rose, M.A., 2003. NetAffx: Affymetrix probesets and annotations. Nucleic Acids Res 31, 82-86.

Liu, H., Feng, G., Wu, L., Fu, S., Liu, P., Yang, W., Zhang, X., 2010. The effects of rapamycin on lens epithelial cell proliferation, migration, and matrix formation: an in vitro study. Mol Vis 16, 1646-1653.

Liu, Y.C., Chen, G.S., Liu, W.L., Wen, S.F., 1995. Estimation of PCNA mRNA stability in cell cycle by a serum-deprivation method. J Cell Biochem 57, 641-646.

Lock, C., Hermans, G., Pedotti, R., Brendolan, A., Schadt, E., Garren, H., Langer-Gould, A., Strober, S., Cannella, B., Allard, J., Klonowski, P., Austin, A., Lad, N., Kaminski, N., Galli, S.J., Oksenberg, J.R., Raine, C.S., Heller, R., Steinman, L., 2002. Gene-microarray analysis of multiple sclerosis lesions yields new targets validated in autoimmune encephalomyelitis. Nat Med 8, 500-508.

Long, Y., Li, Q., Li, J., Cui, Z., 2011. Molecular analysis, developmental function and heavy metal-induced expression of ABCC5 in zebrafish. Comp Biochem Physiol B Biochem Mol Biol 158, 46-55.

Lopez, C.D., Martinovsky, G., Naumovski, L., 2002. Inhibition of cell death by ribosomal protein L35a. Cancer Lett 180, 195-202.

Lovenberg, W., Weissbach, H., Udenfriend, S., 1962. Aromatic L-amino acid decarboxylase. J Biol Chem 237, 89-93.

MacBeath, G., Schreiber, S.L., 2000. Printing proteins as microarrays for high-throughput function determination. Science 289, 1760-1763.

MacInnes, A.W., Amsterdam, A., Whittaker, C.A., Hopkins, N., Lees, J.A., 2008. Loss of p53 synthesis in zebrafish tumors with ribosomal protein gene mutations. Proc Natl Acad Sci U S A 105, 10408-10413.

Makky, K., Tekiela, J., Mayer, A.N., 2007. Target of rapamycin (TOR) signaling controls epithelial morphogenesis in the vertebrate intestine. Dev Biol 303, 501-513.

Martel, R.R., Klicius, J., Galet, S., 1977. Inhibition of the immune response by rapamycin, a new antifungal antibiotic. Can J Physiol Pharmacol 55, 48-51.

Martyniuk, C.J., Gerrie, E.R., Popesku, J.T., Ekker, M., Trudeau, V.L., 2007. Microarray analysis in the zebrafish (Danio rerio) liver and telencephalon after exposure to low concentration of 17alpha-ethinylestradiol. Aquat Toxicol 84, 38-49.

Mayerhofer, M., Aichberger, K.J., Florian, S., Krauth, M.T., Hauswirth, A.W., Derdak, S., Sperr, W.R., Esterbauer, H., Wagner, O., Marosi, C., Pickl, W.F., Deininger, M., Weisberg, E., Druker, B.J., Griffin, J.D., Sillaber, C., Valent, P., 2005. Identification of mTOR as a novel bifunctional target in chronic myeloid leukemia: dissection of growth-inhibitory and VEGF-suppressive effects of rapamycin in leukemic cells. FASEB J 19, 960-962.

McCurley, A.T., Callard, G.V., 2008. Characterization of housekeeping genes in zebrafish: male-female differences and effects of tissue type, developmental stage and chemical treatment. BMC Mol Biol 9, 102.

Meijer, A.H., Verbeek, F.J., Salas-Vidal, E., Corredor-Adamez, M., Bussman, J., van der Sar, A.M., Otto, G.W., Geisler, R., Spaink, H.P., 2005. Transcriptome profiling of adult zebrafish at the late stage of chronic tuberculosis due to Mycobacterium marinum infection. Mol Immunol 42, 1185-1203.

Metcalfe, S.M., Canman, C.E., Milner, J., Morris, R.E., Goldman, S., Kastan, M.B., 1997. Rapamycin and p53 act on different pathways to induce G1 arrest in mammalian cells. Oncogene 15, 1635-1642.

Mirnics, K., Middleton, F.A., Marquez, A., Lewis, D.A., Levitt, P., 2000. Molecular characterization of schizophrenia viewed by microarray analysis of gene expression in prefrontal cortex. Neuron 28, 53-67.

Morey, J.S., Ryan, J.C., Van Dolah, F.M., 2006. Microarray validation: factors influencing correlation between oligonucleotide microarrays and real-time PCR. Biol Proced Online 8, 175-193.

Moriyama, Y., Ohata, Y., Mori, S., Matsukawa, S., Michiue, T., Asashima, M., Kuroda, H., 2010. Rapamycin treatment causes developmental delay, pigmentation defects, and gastrointestinal malformation on Xenopus embryogenesis. Biochem Biophys Res Commun.

Mosley, J.D., Poirier, J.T., Seachrist, D.D., Landis, M.D., Keri, R.A., 2007. Rapamycin inhibits multiple stages of c-Neu/ErbB2 induced tumor progression in a transgenic mouse model of HER2-positive breast cancer. Mol Cancer Ther 6, 2188-2197.

Mosmann, T., 1983. Rapid colorimetric assay for cellular growth and survival: application to proliferation and cytotoxicity assays. J Immunol Methods 65, 55-63.

Moussad, E.E., Brigstock, D.R., 2000. Connective tissue growth factor: what's in a name? Mol Genet Metab 71, 276-292.

Mousses, S., Wagner, U., Chen, Y., Kim, J.W., Bubendorf, L., Bittner, M., Pretlow, T., Elkahloun, A.G., Trepel, J.B., Kallioniemi, O.P., 2001. Failure of hormone therapy in prostate cancer involves systematic restoration of androgen responsive genes and activation of rapamycin sensitive signaling. Oncogene 20, 6718-6723.

Muller, H., Bracken, A.P., Vernell, R., Moroni, M.C., Christians, F., Grassilli, E., Prosperini, E., Vigo, E., Oliner, J.D., Helin, K., 2001. E2Fs regulate the expression of genes involved in differentiation, development, proliferation, and apoptosis. Genes Dev 15, 267-285.

Muller, H., Helin, K., 2000. The E2F transcription factors: key regulators of cell proliferation. Biochim Biophys Acta 1470, M1-12.

Nakashima, T., Kuratomi, Y., Yasumatsu, R., Masuda, M., Koike, K., Umezaki, T., Clayman, G.L., Nakagawa, T., Komune, S., 2005. The effect of cyclin D1 overexpression in human head and neck cancer cells. Eur Arch Otorhinolaryngol 262, 379-383.

Nakatani, T., Honda, E., Hayakawa, S., Sato, M., Satoh, K., Kudo, M., Munakata, H., 2008. Effects of decorin on the expression of alpha-smooth muscle actin in a human myofibroblast cell line. Mol Cell Biochem 308, 201-207.

Navalgund, L.G., Rossana, C., Muench, A.J., Johnson, L.F., 1980. Cell cycle regulation of thymidylate synthetase gene expression in cultured mouse fibroblasts. J Biol Chem 255, 7386-7390.

Nelsen, C.J., Rickheim, D.G., Tucker, M.M., Hansen, L.K., Albrecht, J.H., 2003. Evidence that cyclin D1 mediates both growth and proliferation downstream of TOR in hepatocytes. J Biol Chem 278, 3656-3663.

Neuhauss, S.C., Solnica-Krezel, L., Schier, A.F., Zwartkruis, F., Stemple, D.L., Malicki, J., Abdelilah, S., Stainier, D.Y., Driever, W., 1996. Mutations affecting craniofacial development in zebrafish. Development 123, 357-367.

Neumann, F., Krawinkel, U., 1997. Constitutive expression of human ribosomal protein L7 arrests the cell cycle in G1 and induces apoptosis in Jurkat T-lymphoma cells. Exp Cell Res 230, 252-261.

Nevins, J.R., 2001. The Rb/E2F pathway and cancer. Hum Mol Genet 10, 699-703.

Nicoli, S., Ribatti, D., Cotelli, F., Presta, M., 2007. Mammalian tumor xenografts induce neovascularization in zebrafish embryos. Cancer Res 67, 2927-2931.

Nishigaki, F., Sakuma, S., Ogawa, T., Miyata, S., Ohkubo, T., Goto, T., 2002. FK506 induces chondrogenic differentiation of clonal mouse embryonic carcinoma cells, ATDC5. Eur J Pharmacol 437, 123-128.

Nomura, N., Takahashi, M., Matsui, M., Ishii, S., Date, T., Sasamoto, S., Ishizaki, R., 1988. Isolation of human cDNA clones of myb-related genes, A-myb and B-myb. Nucleic Acids Res 16, 11075-11089.

Oh, C.D., Kim, S.J., Ju, J.W., Song, W.K., Kim, J.H., Yoo, Y.J., Chun, J.S., 2001. Immunosuppressant rapamycin inhibits protein kinase C alpha and p38 mitogen-activated protein kinase leading to the inhibition of chondrogenesis. Eur J Pharmacol 427, 175-185.

Oldham, S., Montagne, J., Radimerski, T., Thomas, G., Hafen, E., 2000. Genetic and biochemical characterization of dTOR, the Drosophila homolog of the target of rapamycin. Genes Dev 14, 2689-2694.

Olson, N.E., 2006. The microarray data analysis process: from raw data to biological significance. NeuroRx 3, 373-383.

Osman, B., Doller, A., Akool el, S., Holdener, M., Hintermann, E., Pfeilschifter, J., Eberhardt, W., 2009. Rapamycin induces the TGFbeta1/Smad signaling cascade in renal mesangial cells upstream of mTOR. Cell Signal 21, 1806-1817.

Pack, M., Solnica-Krezel, L., Malicki, J., Neuhauss, S.C., Schier, A.F., Stemple, D.L., Driever, W., Fishman, M.C., 1996. Mutations affecting development of zebrafish digestive organs. Development 123, 321-328.

Panwalkar, A., Verstovsek, S., Giles, F.J., 2004. Mammalian target of rapamycin inhibition as therapy for hematologic malignancies. Cancer 100, 657-666.

Parichy, D.M., 2006. Evolution of danio pigment pattern development. Heredity 97, 200-210.

Parker, C.E., 1979. Diseases of phenylalanine metabolism. West J Med 131, 285-297.

Patil, M.A., Chua, M.S., Pan, K.H., Lin, R., Lih, C.J., Cheung, S.T., Ho, C., Li, R., Fan, S.T., Cohen, S.N., Chen, X., So, S., 2005. An integrated data analysis approach to characterize genes highly expressed in hepatocellular carcinoma. Oncogene 24, 3737-3747.

Peterson, S.M., Freeman, J.L., 2009. Global gene expression analysis using a zebrafish oligonucleotide microarray platform. J Vis Exp.

Pfaffl, M.W., 2001. A new mathematical model for relative quantification in real-time RT-PCR. Nucleic Acids Res 29, e45.

Polager, S., Kalma, Y., Berkovich, E., Ginsberg, D., 2002. E2Fs up-regulate expression of genes involved in DNA replication, DNA repair and mitosis. Oncogene 21, 437-446.

Pollack, J.R., Perou, C.M., Alizadeh, A.A., Eisen, M.B., Pergamenschikov, A., Williams, C.F., Jeffrey, S.S., Botstein, D., Brown, P.O., 1999. Genome-wide analysis of DNA copy-number changes using cDNA microarrays. Nat Genet 23, 41-46.

Popat, S., Matakidou, A., Houlston, R.S., 2004. Thymidylate synthase expression and prognosis in colorectal cancer: a systematic review and meta-analysis. J Clin Oncol 22, 529-536.

Porter, D., Weremowicz, S., Chin, K., Seth, P., Keshaviah, A., Lahti-Domenici, J., Bae, Y.K., Monitto, C.L., Merlos-Suarez, A., Chan, J., Hulette, C.M., Richardson, A., Morton, C.C., Marks, J., Duyao, M., Hruban, R., Gabrielson,

E., Gelman, R., Polyak, K., 2003. A neural survival factor is a candidate oncogene in breast cancer. Proc Natl Acad Sci U S A 100, 10931-10936.

Preiss, T., Baron-Benhamou, J., Ansorge, W., Hentze, M.W., 2003. Homodirectional changes in transcriptome composition and mRNA translation induced by rapamycin and heat shock. Nat Struct Biol 10, 1039-1047.

Pullen, N., Thomas, G., 1997. The modular phosphorylation and activation of p70s6k. FEBS Lett 410, 78-82.

Pyati, U.J., Webb, A.E., Kimelman, D., 2005. Transgenic zebrafish reveal stage-specific roles for Bmp signaling in ventral and posterior mesoderm development. Development 132, 2333-2343.

Rajeevan, M.S., Vernon, S.D., Taysavang, N., Unger, E.R., 2001. Validation of array-based gene expression profiles by real-time (kinetic) RT-PCR. J Mol Diagn 3, 26-31.

Ramaswamy, S., Tamayo, P., Rifkin, R., Mukherjee, S., Yeang, C.H., Angelo, M., Ladd, C., Reich, M., Latulippe, E., Mesirov, J.P., Poggio, T., Gerald, W., Loda, M., Lander, E.S., Golub, T.R., 2001. Multiclass cancer diagnosis using tumor gene expression signatures. Proc Natl Acad Sci U S A 98, 15149-15154.

Ravikumar, B., Berger, Z., Vacher, C., O'Kane, C.J., Rubinsztein, D.C., 2006. Rapamycin pre-treatment protects against apoptosis. Hum Mol Genet 15, 1209-1216.

Reddy, M.K., Vasir, J.K., Sahoo, S.K., Jain, T.K., Yallapu, M.M., Labhasetwar, V., 2008. Inhibition of apoptosis through localized delivery of rapamycin-loaded nanoparticles prevented neointimal hyperplasia and reendothelialized injured artery. Circ Cardiovasc Interv 1, 209-216.

Ren, B., Yu, G., Tseng, G.C., Cieply, K., Gavel, T., Nelson, J., Michalopoulos, G., Yu, Y.P., Luo, J.H., 2006. MCM7 amplification and overexpression are associated with prostate cancer progression. Oncogene 25, 1090-1098.

Rizwani, W., Alexandrow, M., Chellappan, S., 2009. Prohibitin physically interacts with MCM proteins and inhibits mammalian DNA replication. Cell Cycle 8, 1621-1629.

Roca, F.J., Mulero, I., Lopez-Munoz, A., Sepulcre, M.P., Renshaw, S.A., Meseguer, J., Mulero, V., 2008. Evolution of the inflammatory response in vertebrates: fish TNF-alpha is a powerful activator of endothelial cells but hardly activates phagocytes. J Immunol 181, 5071-5081.

Ross, D.T., Scherf, U., Eisen, M.B., Perou, C.M., Rees, C., Spellman, P., Iyer, V., Jeffrey, S.S., Van de Rijn, M., Waltham, M., Pergamenschikov, A., Lee, J.C., Lashkari, D., Shalon, D., Myers, T.G., Weinstein, J.N., Botstein, D., Brown, P.O., 2000. Systematic variation in gene expression patterns in human cancer cell lines. Nat Genet 24, 227-235.

Ryu, S., Driever, W., 2006. Minichromosome maintenance proteins as markers for proliferation zones during embryogenesis. Cell Cycle 5, 1140-1142.

Ryu, S., Holzschuh, J., Erhardt, S., Ettl, A.K., Driever, W., 2005. Depletion of minichromosome maintenance protein 5 in the zebrafish retina causes cell-cycle defect and apoptosis. Proc Natl Acad Sci U S A 102, 18467-18472.

Sabers, C.J., Martin, M.M., Brunn, G.J., Williams, J.M., Dumont, F.J., Wiederrecht, G., Abraham, R.T., 1995. Isolation of a protein target of the FKBP12-rapamycin complex in mammalian cells. J Biol Chem 270, 815-822.

Saldanha, A.J., 2004. Java Treeview--extensible visualization of microarray data. Bioinformatics 20, 3246-3248.

Sanchez, C.P., He, Y.Z., 2009. Bone growth during rapamycin therapy in young rats. BMC Pediatr 9, 3.

Sarkaria, J.N., Tibbetts, R.S., Busby, E.C., Kennedy, A.P., Hill, D.E., Abraham, R.T., 1998. Inhibition of phosphoinositide 3-kinase related kinases by the radiosensitizing agent wortmannin. Cancer Res 58, 4375-4382.

Saxena, U.H., Powell, C.M., Fecko, J.K., Cacioppo, R., Chou, H.S., Cooper, G.M., Hansen, U., 2009. Phosphorylation by cyclin C/cyclin-dependent kinase 2 following mitogenic stimulation of murine fibroblasts inhibits transcriptional activity of LSF during G1 progression. Mol Cell Biol 29, 2335-2345.

Schallreuter, K.U., Wood, J.M., 1999. The importance of L-phenylalanine transport and its autocrine turnover to L-tyrosine for melanogenesis in human epidermal melanocytes. Biochem Biophys Res Commun 262, 423-428.

Schena, M., Shalon, D., Davis, R.W., Brown, P.O., 1995. Quantitative monitoring of gene expression patterns with a complementary DNA microarray. Science 270, 467-470.

Schonborn, I., Zschiesche, W., Minguillon, C., Spitzer, E., Mohner, M., Ebeling, K., Grosse, R., 1995. Prognostic value of proliferating cell nuclear antigen and c-erbB-2 compared with conventional histopathological factors in breast cancer. J Cancer Res Clin Oncol 121, 115-122.

Schroeder, A., Mueller, O., Stocker, S., Salowsky, R., Leiber, M., Gassmann, M., Lightfoot, S., Menzel, W., Granzow, M., Ragg, T., 2006. The RIN: an RNA integrity number for assigning integrity values to RNA measurements. BMC Mol Biol 7, 3.

Scortechini, A.R., Rupoli, S., Piccinini, G., Luchetti, M.M., Cantori, I., Gabrielli, A., Leoni, P., 1999. Expression of c-myb and B-myb oncogenes on myelofibrotic marrow fibroblasts. Leuk Lymphoma 33, 295-304.

Scott, P.H., Brunn, G.J., Kohn, A.D., Roth, R.A., Lawrence, J.C., Jr., 1998. Evidence of insulin-stimulated phosphorylation and activation of the mammalian target of rapamycin mediated by a protein kinase B signaling pathway. Proc Natl Acad Sci U S A 95, 7772-7777.

Shepard, J.L., Amatruda, J.F., Stern, H.M., Subramanian, A., Finkelstein, D., Ziai, J., Finley, K.R., Pfaff, K.L., Hersey, C., Zhou, Y., Barut, B., Freedman, M., Lee, C., Spitsbergen, J., Neuberg, D., Weber, G., Golub, T.R., Glickman, J.N., Kutok, J.L., Aster, J.C., Zon, L.I., 2005. A zebrafish bmyb mutation causes genome instability and increased cancer susceptibility. Proc Natl Acad Sci U S A 102, 13194-13199.

Shigematsu, H., Yoshida, K., Sanada, Y., Osada, S., Takahashi, T., Wada, Y., Konishi, K., Okada, M., Fukushima, M., 2010. Rapamycin enhances chemotherapy-induced cytotoxicity by inhibiting the expressions of TS and ERK in gastric cancer cells. Int J Cancer 126, 2716-2725.

Shin, D., Shin, C.H., Tucker, J., Ober, E.A., Rentzsch, F., Poss, K.D., Hammerschmidt, M., Mullins, M.C., Stainier, D.Y., 2007. Bmp and Fgf signaling are essential for liver specification in zebrafish. Development 134, 2041-2050.

Shinya, M., Eschbach, C., Clark, M., Lehrach, H., Furutani-Seiki, M., 2000. Zebrafish Dkk1, induced by the pre-MBT Wnt signaling, is secreted from the prechordal plate and patterns the anterior neural plate. Mech Dev 98, 3-17.

Smith, E.J., Leone, G., DeGregori, J., Jakoi, L., Nevins, J.R., 1996. The accumulation of an E2F-p130 transcriptional repressor distinguishes a G0 cell state from a G1 cell state. Mol Cell Biol 16, 6965-6976.

Smolowitz, R., Hanley, J., Richmond, H., 2002. A three-year retrospective study of abdominal tumors in zebrafish maintained in an aquatic laboratory animal facility. Biol Bull 203, 265-266.

Song, H.D., Sun, X.J., Deng, M., Zhang, G.W., Zhou, Y., Wu, X.Y., Sheng, Y., Chen, Y., Ruan, Z., Jiang, C.L., Fan, H.Y., Zon, L.I., Kanki, J.P., Liu, T.X., Look, A.T., Chen, Z., 2004. Hematopoietic gene expression profile in zebrafish kidney marrow. Proc Natl Acad Sci U S A 101, 16240-16245.

Stevaux, O., Dyson, N.J., 2002. A revised picture of the E2F transcriptional network and RB function. Curr Opin Cell Biol 14, 684-691.

Stoeber, K., Tlsty, T.D., Happerfield, L., Thomas, G.A., Romanov, S., Bobrow, L., Williams, E.D., Williams, G.H., 2001. DNA replication licensing and human cell proliferation. J Cell Sci 114, 2027-2041.

Suzuki, S., Adachi, A., Hiraiwa, A., Ohashi, M., Ishibashi, M., Kiyono, T., 1998. Cloning and characterization of human MCM7 promoter. Gene 216, 85-91.

Takahashi, Y., Rayman, J.B., Dynlacht, B.D., 2000. Analysis of promoter binding by the E2F and pRB families in vivo: distinct E2F proteins mediate activation and repression. Genes Dev 14, 804-816.

Takeuchi, H., Kondo, Y., Fujiwara, K., Kanzawa, T., Aoki, H., Mills, G.B., Kondo, S., 2005. Synergistic augmentation of rapamycin-induced autophagy in malignant glioma cells by phosphatidylinositol 3-kinase/protein kinase B inhibitors. Cancer Res 65, 3336-3346.

Tamura, K., Dudley, J., Nei, M., Kumar, S., 2007. MEGA4: Molecular Evolutionary Genetics Analysis (MEGA) software version 4.0. Mol Biol Evol 24, 1596-1599.

Taylor, K.L., Grant, N.J., Temperley, N.D., Patton, E.E., 2010. Small molecule screening in zebrafish: an in vivo approach to identifying new chemical tools and drug leads. Cell Commun Signal 8, 11.

Thompson, J.D., Higgins, D.G., Gibson, T.J., 1994. CLUSTAL W: improving the sensitivity of progressive multiple sequence alignment through sequence weighting, position-specific gap penalties and weight matrix choice. Nucleic Acids Res 22, 4673-4680.

Tian, E., Zhan, F., Walker, R., Rasmussen, E., Ma, Y., Barlogie, B., Shaughnessy, J.D., Jr., 2003. The role of the Wnt-signaling antagonist DKK1 in the development of osteolytic lesions in multiple myeloma. N Engl J Med 349, 2483-2494.

Tirado, O.M., Mateo-Lozano, S., Notario, V., 2005. Rapamycin induces apoptosis of JN-DSRCT-1 cells by increasing the Bax : Bcl-xL ratio through concurrent

mechanisms dependent and independent of its mTOR inhibitory activity. Oncogene 24, 3348-3357.

Tominaga, K., Magee, D.M., Matzuk, M.M., Pereira-Smith, O.M., 2004. PAM14, a novel MRG- and Rb-associated protein, is not required for development and T-cell function in mice. Mol Cell Biol 24, 8366-8373.

Trofimova-Griffin, M.E., Juchau, M.R., 2002. Developmental expression of cytochrome CYP26B1 (P450RAI-2) in human cephalic tissues. Brain Res Dev Brain Res 136, 175-178.

Tsang, C.K., Qi, H., Liu, L.F., Zheng, X.F., 2007. Targeting mammalian target of rapamycin (mTOR) for health and diseases. Drug Discov Today 12, 112-124.

Ung, C.Y., Lam, S.H., Gong, Z., 2009. Comparative transcriptome analyses revealed conserved biological and transcription factor target modules between the zebrafish and human tumors. Zebrafish 6, 425-431.

Vackova, I., Engelova, M., Marinov, I., Tomanek, M., 2003. Cell cycle synchronization of porcine granulosa cells in G1 stage with mimosine. Anim Reprod Sci 77, 235-245.

van Boxtel, A.L., Kamstra, J.H., Cenijn, P.H., Pieterse, B., Wagner, J.M., Antink, M., Krab, K., van der Burg, B., Marsh, G., Brouwer, A., Legler, J., 2008. Microarray analysis reveals a mechanism of phenolic polybrominated diphenylether toxicity in zebrafish. Environ Sci Technol 42, 1773-1779.

Vezina, C., Kudelski, A., Sehgal, S.N., 1975. Rapamycin (AY-22,989), a new antifungal antibiotic. I. Taxonomy of the producing streptomycete and isolation of the active principle. J Antibiot (Tokyo) 28, 721-726.

Walker, S.J., Wang, Y., Grant, K.A., Chan, F., Hellmann, G.M., 2006. Long versus short oligonucleotide microarrays for the study of gene expression in nonhuman primates. J Neurosci Methods 152, 179-189.

Wang, C., Tao, W., Wang, Y., Bikow, J., Lu, B., Keating, A., Verma, S., Parker, T.G., Han, R., Wen, X.Y., 2010. Rosuvastatin, identified from a zebrafish chemical genetic screen for antiangiogenic compounds, suppresses the growth of prostate cancer. Eur Urol 58, 418-426.

Wanner, K., Hipp, S., Oelsner, M., Ringshausen, I., Bogner, C., Peschel, C., Decker, T., 2006. Mammalian target of rapamycin inhibition induces cell cycle arrest in diffuse large B cell lymphoma (DLBCL) cells and sensitises DLBCL cells to rituximab. Br J Haematol 134, 475-484.

Wardle, F.C., Odom, D.T., Bell, G.W., Yuan, B., Danford, T.W., Wiellette, E.L., Herbolsheimer, E., Sive, H.L., Young, R.A., Smith, J.C., 2006. Zebrafish promoter microarrays identify actively transcribed embryonic genes. Genome Biol 7, R71.

Weinmann, A.S., Yan, P.S., Oberley, M.J., Huang, T.H., Farnham, P.J., 2002. Isolating human transcription factor targets by coupling chromatin immunoprecipitation and CpG island microarray analysis. Genes Dev 16, 235-244.

Wenzlau, J.M., Garl, P.J., Simpson, P., Stenmark, K.R., West, J., Artinger, K.B., Nemenoff, R.A., Weiser-Evans, M.C., 2006. Embryonic growth-associated protein is one subunit of a novel N-terminal acetyltransferase complex essential for embryonic vascular development. Circ Res 98, 846-855.

White, J.A., Ramshaw, H., Taimi, M., Stangle, W., Zhang, A., Everingham, S., Creighton, S., Tam, S.P., Jones, G., Petkovich, M., 2000. Identification of the human cytochrome P450, P450RAI-2, which is predominantly expressed in the adult cerebellum and is responsible for all-trans-retinoic acid metabolism. Proc Natl Acad Sci U S A 97, 6403-6408.

Wilson, C.L., Pepper, S.D., Hey, Y., Miller, C.J., 2004. Amplification protocols introduce systematic but reproducible errors into gene expression studies. Biotechniques 36, 498-506.

Wirths, O., Waha, A., Weggen, S., Schirmacher, P., Kuhne, T., Goodyer, C.G., Albrecht, S., Von Schweinitz, D., Pietsch, T., 2003. Overexpression of human Dickkopf-1, an antagonist of wingless/WNT signaling, in human hepatoblastomas and Wilms' tumors. Lab Invest 83, 429-434.

Wissmann, C., Wild, P.J., Kaiser, S., Roepcke, S., Stoehr, R., Woenckhaus, M., Kristiansen, G., Hsieh, J.C., Hofstaedter, F., Hartmann, A., Knuechel, R., Rosenthal, A., Pilarsky, C., 2003. WIF1, a component of the Wnt pathway, is down-regulated in prostate, breast, lung, and bladder cancer. J Pathol 201, 204-212.

Witte, F., Dokas, J., Neuendorf, F., Mundlos, S., Stricker, S., 2009. Comprehensive expression analysis of all Wnt genes and their major secreted antagonists during mouse limb development and cartilage differentiation. Gene Expr Patterns 9, 215-223.

Wixon, J., 2000. Featured organism: Danio rerio, the zebrafish. Yeast 17, 225-231.

Wright, G.W., Simon, R.M., 2003. A random variance model for detection of differential gene expression in small microarray experiments. Bioinformatics 19, 2448-2455.

Wu, W., Glinka, A., Delius, H., Niehrs, C., 2000. Mutual antagonism between dickkopf1 and dickkopf2 regulates Wnt/beta-catenin signalling. Curr Biol 10, 1611-1614.

Wullschleger, S., Loewith, R., Hall, M.N., 2006. TOR signaling in growth and metabolism. Cell 124, 471-484.

Xiao, R., Badger, T.M., Simmen, F.A., 2005. Dietary exposure to soy or whey proteins alters colonic global gene expression profiles during rat colon tumorigenesis. Mol Cancer 4, 1.

Xiong, K.M., Peterson, R.E., Heideman, W., 2008. Aryl hydrocarbon receptor-mediated down-regulation of sox9b causes jaw malformation in zebrafish embryos. Mol Pharmacol 74, 1544-1553.

Yamabuki, T., Takano, A., Hayama, S., Ishikawa, N., Kato, T., Miyamoto, M., Ito, T., Ito, H., Miyagi, Y., Nakayama, H., Fujita, M., Hosokawa, M., Tsuchiya, E., Kohno, N., Kondo, S., Nakamura, Y., Daigo, Y., 2007. Dikkopf-1 as a novel serologic and prognostic biomarker for lung and esophageal carcinomas. Cancer Res 67, 2517-2525.

Yamaguchi, Y., Itami, S., Watabe, H., Yasumoto, K., Abdel-Malek, Z.A., Kubo, T., Rouzaud, F., Tanemura, A., Yoshikawa, K., Hearing, V.J., 2004. Mesenchymal-epithelial interactions in the skin: increased expression of dickkopf1 by palmoplantar fibroblasts inhibits melanocyte growth and differentiation. J Cell Biol 165, 275-285.

Yamaguchi, Y., Passeron, T., Hoashi, T., Watabe, H., Rouzaud, F., Yasumoto, K., Hara, T., Tohyama, C., Katayama, I., Miki, T., Hearing, V.J., 2008. Dickkopf 1 (DKK1) regulates skin pigmentation and thickness by affecting Wnt/beta-catenin signaling in keratinocytes. FASEB J 22, 1009-1020.

Yamaguchi, Y., Passeron, T., Watabe, H., Yasumoto, K., Rouzaud, F., Hoashi, T., Hearing, V.J., 2007. The effects of dickkopf 1 on gene expression and Wnt signaling by melanocytes: mechanisms underlying its suppression of melanocyte function and proliferation. J Invest Dermatol 127, 1217-1225.

Yan, Y.L., Miller, C.T., Nissen, R.M., Singer, A., Liu, D., Kirn, A., Draper, B., Willoughby, J., Morcos, P.A., Amsterdam, A., Chung, B.C., Westerfield, M.,

Haffter, P., Hopkins, N., Kimmel, C., Postlethwait, J.H., 2002. A zebrafish sox9 gene required for cartilage morphogenesis. Development 129, 5065-5079.

Yan, Y.L., Willoughby, J., Liu, D., Crump, J.G., Wilson, C., Miller, C.T., Singer, A., Kimmel, C., Westerfield, M., Postlethwait, J.H., 2005. A pair of Sox: distinct and overlapping functions of zebrafish sox9 co-orthologs in craniofacial and pectoral fin development. Development 132, 1069-1083.

Yelick, P.C., Schilling, T.F., 2002. Molecular dissection of craniofacial development using zebrafish. Crit Rev Oral Biol Med 13, 308-322.

Yu, K., Toral-Barza, L., Discafani, C., Zhang, W.G., Skotnicki, J., Frost, P., Gibbons, J.J., 2001. mTOR, a novel target in breast cancer: the effect of CCI-779, an mTOR inhibitor, in preclinical models of breast cancer. Endocr Relat Cancer 8, 249-258.

Zhang, J.F., Liu, J.J., Lu, M.Q., Cai, C.J., Yang, Y., Li, H., Xu, C., Chen, G.H., 2007. Rapamycin inhibits cell growth by induction of apoptosis on hepatocellular carcinoma cells in vitro. Transpl Immunol 17, 162-168.

Zhao, Q., Dobbs-McAuliffe, B., Linney, E., 2005. Expression of cyp26b1 during zebrafish early development. Gene Expr Patterns 5, 363-369.

Zhou, Y., Capuco, A.V., Jiang, H., 2008. Involvement of connective tissue growth factor (CTGF) in insulin-like growth factor-I (IGF1) stimulation of proliferation of a bovine mammary epithelial cell line. Domest Anim Endocrinol 35, 180-189.

Zinzalla, V., Graziola, M., Mastriani, A., Vanoni, M., Alberghina, L., 2007. Rapamycin-mediated G1 arrest involves regulation of the Cdk inhibitor Sic1 in Saccharomyces cerevisiae. Mol Microbiol 63, 1482-1494.

Zohlnhofer, D., Nuhrenberg, T.G., Neumann, F.J., Richter, T., May, A.E., Schmidt, R., Denker, K., Clauss, M.A., Schomig, A., Baeuerle, P.A., 2004. Rapamycin effects transcriptional programs in smooth muscle cells controlling proliferative and inflammatory properties. Mol Pharmacol 65, 880-889.

Mol Biol Rep
DOI 10.1007/s11033-010-0531-2

Dose- and time-dependent expression patterns of zebrafish orthologs of selected E2F target genes in response to serum starvation/replenishment

Ceren Sucularli · Serif Senturk · Mehmet Ozturk · Ozlen Konu

Received: 13 June 2010 / Accepted: 15 November 2010
© Springer Science+Business Media B.V. 2010

Abstract Targets of E2F transcription factors effectively regulate the cell cycle from worms to humans. Furthermore, the dysregulation of E2F transcription modules plays a highly conserved role in cancers of human and zebrafish. Studying E2F target expression under a given cellular state, such as quiescence, might lead to a better understanding of the conserved patterns of expression in different taxa. In the present study, we used literature searches and phylogeny to identify several targets of E2F transcription factors that are known to be serum-responsive; namely, PCNA, MYBL2, MCM7, TYMS, and CTGF. The transcriptional serum response of zebrafish orthologs of these genes were quantified under different doses (i.e., 0, 0.1, 1, 3, and 10% FBS) and time points (i.e., 6, 24 and 48 hours, h) using quantitative RT-PCR (qRT-PCR) in the zebrafish fibroblast cells (ZF4). Our results indicated that mRNA expression of zebrafish *pcna*, *mybl2*, *mcm7* and *tyms* drastically decreased while that of *ctgf* increased with decreasing serum levels as observed in mammals. These genes responded to serum starvation at 24 and 48 h and to the mitogenic stimuli as early as 6 h except for *ctgf* whose expression was significantly altered at 24 h. The zebrafish Mcm7 protein levels also were modulated by serum starvation/replenishment. The present study provides a foundation for the comparative analysis of quantitative expression patterns for genes involved in regulation of cell cycle using a zebrafish serum response model.

Keywords Cell cycle analysis · MTT analysis · Phylogenetics · Real-time qRT-PCR · Serum/wound response · ZF4

Abbreviations

ZF4	Zebrafish embryonic cell line
FBS	Fetal bovine serum
tyms	Thymidylate synthetase
mybl2	Myeloblastosis oncogene-like 2
pcna	Proliferating cell nuclear antigen
ctgf	Connective tissue growth factor
mcm7	Minichromosome maintenance deficient 7
ef1α	Elongation factor 1-alpha

Electronic supplementary material The online version of this article (doi:10.1007/s11033-010-0531-2) contains supplementary material, which is available to authorized users.

C. Sucularli · S. Senturk · M. Ozturk · O. Konu (✉)
Department of Molecular Biology and Genetics,
Faculty of Science, Bilkent University, 06800 Ankara, Turkey
e-mail: konu@fen.bilkent.edu.tr

M. Ozturk
INSERM—Université Joseph Fourrier,
CRI U823, Grenoble 38042, France

Introduction

The comparison of expression patterns across different taxa helps to identify the extent of the contribution by a particular signaling/transcription module into the regulation of cell cycle and tumor progression [1]. E2F transcription factors are crucially important in cell cycle regulation and share conserved regulatory motifs in worms, insects, fish and mammals [2]. The dysregulation of E2F transcription modules might promote tumors as revealed by the highly conserved signatures obtained from functional gene-set enrichment analyses of the zebrafish and human cancer microarray datasets [1, 3]. Indeed, the zebrafish has recently emerged as a preferable vertebrate model

Published online: 30 November 2010

organism for demonstrating the striking conservation of liver cancer expression profiles between zebrafish and human [1, 4]. Furthermore, zebrafish were used as a promising xenotransplantation model for human malignant cell lines [5, 6].

The quiescent state induced by serum starvation represents a powerful model for studying the mitogen dependency of cancer cells [7, 8]. An increased wound/serum response has already been associated with a worse prognosis in multiple epithelial cancers [9] while microarray studies of human cancer cells and zebrafish cell lines have helped to characterize the global transcriptional signature for serum response [10, 11]. The strong association between the cell cycle, E2F transcription factors and mitogen levels has been well-established for mammals: The reduced serum conditions result in decreased rates of proliferation followed by an arrest in the G1 phase of the cell cycle [12]; and E2F1, among other transcriptional regulators, drives quiescent cells into the S phase [13, 14]. In serum-replenished human cell lines, an increase in E2F1 at the G1 to S phase transition also has been detected [15]. However, the cellular aspects of the quiescent state induced by serum starvation are not well characterized in zebrafish.

Similarly, the expression response of E2F targets to serum starvation/replenishment has been investigated using large scale transcriptional factor binding site and expression studies in mammals [16, 17]. For instance, among others, *PCNA*, *TYMS*, *MCM2-7*, *MYBL2* were shown to be readily induced in mammals by growth-inducing mitogenic stimuli, such as increased serum concentrations and/or by E2F signaling while *CTGF* was repressed by E2F signaling [16–22]. In zebrafish, *pcna*, *tyms*, *mybl2* and *ctgf* were studied previously, yet mostly in the context of embryonic development and tissue expression. *pcna* has been shown as a cell proliferation marker in zebrafish embryonic intermediate cell mass and in the highly proliferating cell subgroup of adult kidney cells [23]. The zebrafish *ctgf* is expressed in the zebrafish embryonic stages [24, 25], while *mybl2* has been shown to be involved in cancer progression as well as cell proliferation, similar to human homolog [26, 27]. Previous studies have shown the importance of Pcna as well as Mcm proteins in zebrafish cell proliferation in zebrafish retina [28, 29]. The expression of *pcna* and *mcm5* were shown to be correlated, and proposed as the markers of cell proliferation also in zebrafish models [28]. Although several components of the minichromosome maintenance (Mcm) complex including *mcm7* have been identified in an insertional mutagenesis screen in zebrafish, only the expression of *mcm5* has been characterized in detail [28, 30]. Accordingly, the time- and dose-dependent serum responses for the abovementioned genes have not been analyzed quantitatively in the literature.

In the present study, we hypothesized that serum starvation might lead to quiescence in zebrafish fibroblasts and thus modulate the strength and magnitude of expression response of E2F target orthologs in a dose- and time-dependent manner [16, 18, 19, 21, 31]. Therefore, we first demonstrated the phylogenetic conservation of the selected orthologs of mammalian E2F targets in zebrafish. Next, we established a serum-response model using zebrafish embryonic fibroblast cells (ZF4) based on cell viability assays. Moreover, the levels of cell proliferation and cell cycle progression were determined when ZF4 cells were serum-replenished based on BrdU incorporation measurements and flow cytometric analyses, respectively. We then performed real-time qRT-PCR analysis of these selected genes under different dose- and time-dependent serum starvation and serum replenishment conditions. Our findings indicated that ZF4 cells went into a reversible state of quiescence upon serum depletion as evidenced by multiple cellular parameters, and thus could be used as a quiescence model for comparative expression studies among vertebrates. In addition, mRNA expression of *mybl2*, *tyms*, *pcna*, *mcm7* and *ctgf* responded to serum starvation/replenishment in a manner comparable to that observed in mammals based on the information from existing literature. This study provides a foundation for the comparative analysis of expression patterns for genes involved in cell cycle regulation using the ZF4 cell line serum response model.

Materials and methods

Selection of the gene set and primer design

To obtain a more comprehensive understanding of the zebrafish serum-dependent cell signaling, we strategically selected a set of genes known to be repressed under serum deprivation and/or upregulated by E2F1 [16, 18, 19, 21, 31, 32]. Accordingly, zebrafish orthologs of *TYMS*, *MYBL2*, *PCNA* and *MCM7* were selected for phylogenetics and qRT-PCR studies. In addition, CTGF, a likely secondary target repressed by E2F also was selected. The decrease in *CTGF* mRNA levels by E2Fs was confirmed with Northern Blot analyses, and the regulation of *CTGF* transcription was likely to be indirect shown by cycloheximide treatment [32]. Primers were designed for real-time qRT-PCR analysis using Primer 3 v.0.4.0 (http://frodo.wi.mit.edu) (Table 1) [33].

Amino acid sequence alignments and phylogenetic analysis

The protein sequences extracted from NCBI (http://www.ncbi.nlm.nih.gov/) and ENSEMBL (http://www.ensembl.org/index.html) databases were aligned using ClustalW

Table 1 List of primer pairs and the amplification efficiencies of the primers

Gene name	Forward primer	Reverse primer	Primer efficiency
mybl2	5′-CCCACACTGAAGGAGGTGAT-3′	5′-CTCCTTTACTGCCCTTGCTG-3′	1.89
pcna	5′-AGCCTGTCATCTGTGGGATT-3′	5′-TGGTAAAGCTAAGGCCCAAA-3′	1.85
mcm7	5′-GAGATTTACGGCCATGAGGA-3′	5′-GGTGTACTGACTGCGTGGAG-3′	2
tyms	5′-TGCTAACGGCTCCAGAGAGT-3′	5′-CATGATGATCCTTCGGTCCT-3′	1.86
ctgf	5′-ACCAATGACAACCGTGAGTG-3′	5′-GGTAGTGGTACAGCCGGAAA-3′	1.78
ef1a	5′-CCCTGGACACAGAGACTTCA-3′	5′-CAGCCTCAAACTCACCAACA-3′	1.81

[34] and the percent amino acid identity was calculated. The amino acid sequences provided in Table S1 for the Tyms, Mybl2, Pcna, Ctgf and Mcm7 proteins were used for generating the bootstrapped neighbor-joining phylogenetic trees using MEGA version 4 [35] for the following species: human (Hs), rat (Rn), mouse (Mm), chicken (Gg), cow (Bt), salmon (Ss), stickleback (Ga), green spotted puffer fish (Tn), zebrafish (Dr), western clawed frog (Xt), fugu (Tr) and medaka (Ol).

Cell culture

The zebrafish embryonic fibroblast (ZF4; ATCC, CRL-2050) [36] cells were cultured in D-MEM/F-12 (1:1) with 10% FBS and 1% Penicillin/Streptomycin (10,000 U/ml Penicillin, 10,000 μg/ml Streptomycin; HyClone, SH30023, CH30160, and SV30010, respectively; Logan, UT, USA) at 28°C.

Three different experimental designs were used for qRT-PCR analyses; each group contained two biological replicates. Treatment groups at each time point were compared with their time-specific control groups (10% FBS). Accordingly, (1) dose-dependent serum starvation experiments were performed using 3×10^6 ZF4 cells (passage number, 13) in T75 flasks incubated with 10% FBS for 24 h followed by the addition of media containing a dose series of FBS (i.e., 0, 1, 3 and 10%) for another 24 h. (2) For the 24 h serum replenishment experiments, 3.75×10^6 ZF4 cells (passage number, 16) in T150 flasks were incubated for 24 h (i.e., time 0) and 48 h with 0.1 or 10% FBS-containing media after an initial seeding period of 24 h; the 24 h serum-starved cells were re-incubated with 10% FBS for another 24 h (serum replenishment). (3) Similarly, for the 6 h serum replenishment experiments, 3×10^6 ZF4 cells (passage number, 20) were incubated in T75 flasks for 24 h with media containing 0.1% FBS and then re-incubated with 0.1 or 10% FBS for 6 h. A 30 h 10% FBS control group also was included. Cells were counted following trypsin (without EDTA; HyClone, SV30037, Logan, UT, USA) treatment and cell pellets were preserved in liquid nitrogen until later use.

MTT analyses were performed at different serum levels, with 2×10^4 ZF4 cells (passage number, 22) cultured in triplicates for 24 h in 96-well microplates. Similarly MTT assays for serum replenishment were performed with 2×10^4 ZF4 cells (passage number, 19) that were starved for 24 h in 96-well plates before replenishment with 10% FBS for the indicated time points. For PI staining, 3×10^6 ZF4 cells (passage numbers, 20–23) were seeded in 100 mm petri dishes and cultured in 0.1 or 10% FBS supplemented media. All samples were prepared in duplicates for testing significance. For BrdU analysis 5×10^5 ZF4 cells (passage number, 22) were cultured in 6-well plates in triplicates and serum starved in 0.1% FBS for 48 h. Effects of 24 h serum replenishment also were tested.

Assays for cell cycle, viability and proliferation

3-(4,5-dimethylthiazole-2-yl)-2,5-diphenyltetrazolium bromide (MTT), reduced to an insoluble formazan dye by mitochondrial enzymes, provides a reliable cellular assay for detecting viable cells. The MTT assay was performed according to the manufacturer's protocols (Vybrant MTT Cell Proliferation Assay Kit, Molecular Probes, V-13154, Germany). The absorbancy at 540 nm was read with a μQuant^{TM} Microplate Spectrophotometer (BioTek, Winooski, VT, USA). The results from triplicate measurements were normalized to the blanks and averaged.

The cell cycle analysis of 24–48 h serum-starved or that of 24 h starved and then replenished ZF4 cells was performed with propidium iodide (PI) staining to assess the percentages of cells at each cell cycle stage [37, 38]. The PI staining was performed as previously described [39]. At each sampling, 3×10^4 cells were analyzed by Becton Dickinson FACScalibur (USA).

The effect of serum starvation on cell proliferation was investigated with 5-bromo-2-deoxyuridine (BrdU) staining as previously described [39]. Briefly, cells were incubated with BrdU adjusted to a final concentration of 0.92 μg/ml for 24 h (Sigma, B9285, St. Louis, MO, USA). Fixed cells were blocked in 10% FBS in PBS for 1 h before incubation with an α-BrdU antibody (1:500 in 2% FBS in PBS; Dako, M0744, Denmark) and α-mouse secondary antibody (1:750

in 2% FBS; Invitrogen, A11029, USA). DAPI was used for counterstaining nuclei. The number of BrdU incorporated cell nuclei was determined by counting multiple fields per group (i.e., approximately 1100–1500 DAPI stained nuclei) on digital fluorescent microscopy images (Zeiss, AX10 Imager A1, Germany).

Real-time qRT-PCR analysis

Total RNA was isolated from 0, 1, 3 and 10% FBS-treated samples as well as those from the serum replenishment experiments (0.1 and 10% FBS samples at 6, 24, 30 and 48 h) using SV total RNA isolation kit (Promega, Z3100, Madison, WI, USA). Reverse-transcription into cDNA was performed by RevertAid First Strand cDNA synthesis kit (Fermentas, K1622, Lithuania). Real-time qRT-PCR analysis was conducted with iCycler (Bio-Rad, Hercules, CA, USA) thermocycler using DyNAmo HS SYBR-green kit (Finnzymes, F-410L, Espoo, Finland). Each cDNA sample was amplified in duplicate by using 20 μM gene-specific primers (Table 1). Amplification conditions were 10 min at 95°C followed by 45 cycles of 30 s at 95°C, 30 s at 62°C (for *tyms*, *mcm7* and *mybl2*) or 60°C (for *ctgf*, *pcna* and *ef1a*). The primer efficiencies (E) were calculated using 10-fold serial dilutions of cDNA where E equals to $10^{[-1/\text{slope of the dilution curve}]}$ (Table 1). The relative expression ratio of target genes were calculated using a modified delta-delta Ct method [40] based on primer pair-specific amplification efficiencies and *ef1a* as the reference gene [41, 42]. The log2 transformed fold change values were plotted in the figures and were used for testing significant differences. For each gene, the real-time qRT-PCR reactions were performed in the same run using biological and technical duplicates.

Western blot

Western blots were performed in order to analyze the serum response of the Mcm7 protein expression. Briefly, cells were lysed with NP-40 lysis buffer containing 50 mM Tris–HCl, pH 8, 150 mM NaCl, 1% NP40 and 1X protease inhibitor complex (Roche, Mannheim, Germany). Protein quantification was performed using Bradford solution (Sigma, B6916, St. Louis, MO, USA). 20 μg of total protein lysate was subjected to gel electrophoresis and transferred (Invitrogen, Carlsbad, USA) as previously described [39]. Western blotting was performed using the primary antibodies, Mcm7 (Santa Cruz Biotechnology, sc9966, Santa Cruz, CA, USA) or α-Tubulin (Calbiochem, CP06, Darmstadt, Germany), following 1 h incubation with the horseradish peroxidase (HRP)-conjugated goat anti-mouse secondary antibody (Sigma, St. Louis, MO, USA). Proteins were detected using ECLplus (Amersham, rpn 2132, Buckinghamshire, UK). Mcm7 protein expression was compared against that of α-Tubulin for the same set of samples.

Statistical analyses

The MTT, BrdU and PI staining results were analyzed by One-way ANOVAs to test for the dose dependency and/or effects of serum replenishment in response to serum in ZF4 cells. The log2 transformed real-time qRT-PCR expression results for dose-dependent serum starvation for *tyms*, *mybl2*, *pcna*, *ctgf*, and *mcm7* and were compared among groups using a One-way ANOVA. The time-dependent serum replenishment data for the same genes were analyzed using a Two-way ANOVA to test for effects of time and dose, simultaneously. For both the starvation and replenishment experiments, pairwise analyses between dose treatments within an ortholog were then performed using Fisher's pairwise comparisons following use of a One-way ANOVA. All analyses were performed in Minitab® and plotted with GraphPad Prism® 5.0 (USA).

Results

Phylogenetic conservation of PCNA, MYBL2, TYMS, MCM7, and CTGF

Phylogenetic analyses of selected genes showed variable degrees of conservation of the zebrafish homologs with their vertebrate orthologs, yet expectedly the mammalian proteins clustered together while the zebrafish orthologs were closer to fish counterparts (Fig. 1a–e).

The zebrafish and mammalian comparisons based on ClustalW indicated that the sequence similarity ranged from low to high depending on the gene under consideration. For example, the zebrafish Mybl2 amino acid sequence was very weakly conserved among taxa (53% between human and zebrafish) whereas Pcna protein sequence identity among species was relatively higher (90% between human and zebrafish). The Tyms, Ctgf and Mcm7 protein sequence similarities between human and zebrafish ranged between 75 and 80% (Table S2).

Analysis of cell cycle and proliferation in serum-starved/replenished ZF4 cells

The cell cycle analysis of 24–48 h serum-starved ZF4 cells was performed with PI staining. Our results revealed that a large fraction of the control ZF4 cells were found at the G0/G1 phase of the cell cycle (Fig. 2). However, serum starvation caused a significant increase in cells at the G0/G1 phase, while decreasing the number of cells entering the S

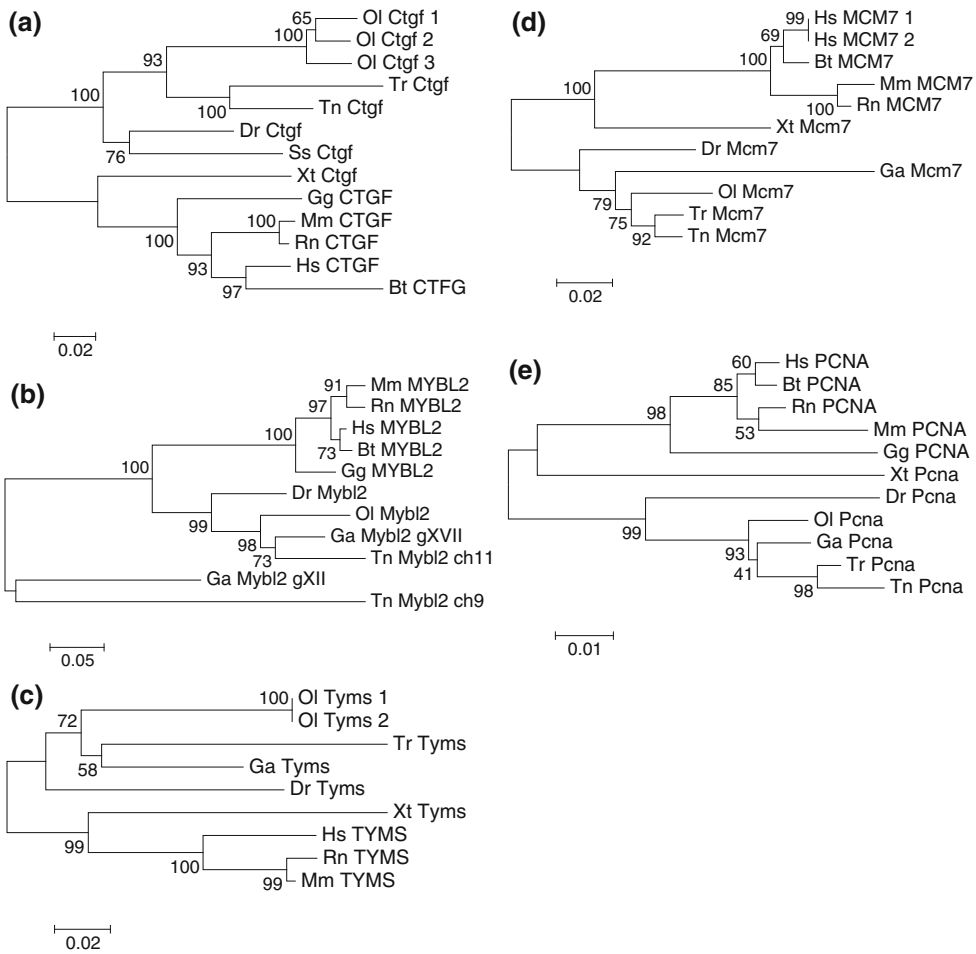

Fig. 1 The phylogenetic analyses of selected E2F target ortholog protein sequences in different species (Table S1). **a** Ctgf; **b** Mybl2; **c** Tyms; **d** Mcm7; **e** Pcna. The bootstrapped neighbor-joining phylogenetic tree was generated using MEGA4. Species: Human (*Hs*), rat (*Rn*), mouse (*Mm*), chicken (*Gg*), western clawed frog (*Xt*), zebrafish (*Dr*), fugu (*Tr*), medaka (*Ol*), cow (*Bt*), salmon (*Ss*), stickleback (*Ga*), green spotted puffer fish (*Tn*). *Scale bar* refers to substitutions per site

and to a lesser degree the G2/M phases for both the 24 and 48 h serum starvation experiments. The treatment with serum for 24 h increased the number of cells entering the S phase, when compared with the serum-starved and non-starved cells; this increase might have reflected a synchronization event induced by serum starvation for cells at the G1 phase of the cell cycle (Fig. 2). When cells were cultured at a lower confluency, a similar trend was observed such that serum starvation resulted in an increase in G0/G1 and a decrease in S phases (Fig. S1). However, our findings suggest that the number of 10% FBS-treated cells at G0/G1 might be influenced by the level of confluency while the serum-starved cell numbers did not vary with confluency levels (Fig. 2 vs. Fig. S1).

Our results also showed that serum starvation caused a significant decrease in cell proliferation such that the rate of BrdU incorporation was 99% in the control ZF4 cells cultured with 10% FBS for 48 h, while only 11% of the cells incorporated BrdU upon 48 h serum starvation (Fig. 3). The ZF4 cells that were serum-starved and then replenished for 24 h reentered a state of proliferation. This indicated that the effect of 24 h serum starvation on DNA synthesis was reversible.

Dose-dependent response to serum starvation

The increase in cell viability of ZF4 cells was directly correlated with the increased serum levels. The pairwise comparisons showed that the 0, 1 and 3% FBS groups responded to reduced serum levels by a significant decrease in cell viability (Fig. 4a, One-way ANOVA; $P \leq 0.001$ for % FBS).

One-way ANOVA performed on real-time qRT-PCR results showed that *mybl2*, *mcm7* and *tyms* expression levels decreased significantly under serum starvation in a dose-dependent manner while the level of change approached significance in *pcna* (Fig. 4b). Pairwise tests based on Fisher's multiple comparisons indicated that the expressions of *mybl2*, *mcm7*, *tyms* and *pcna* genes were significantly down regulated at the 0% FBS treatment but only for *mybl2* and *mcm7*, the change in expression was significant also at the 1% FBS level when compared to control levels. *ctgf* showed a significant dose-dependent response to serum starvation; *ctgf* expression steadily increased at the 3 and 1% FBS treatments, while there was no significant difference between the 10 and 0% FBS treatments (Fig. 4b).

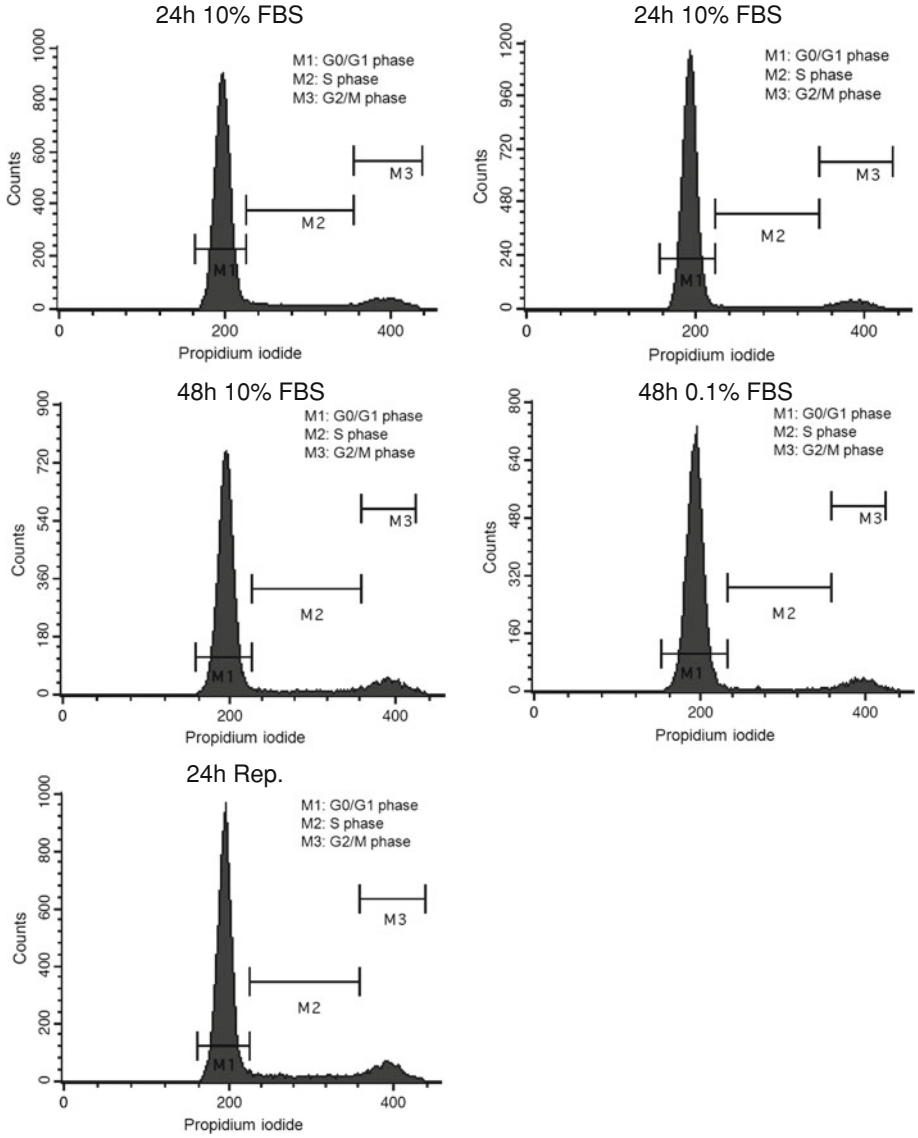

Fig. 2 Cell cycle analysis of ZF4 cells in response to serum fluctuations. The mean percentage of cells at the G0/G1, S, G2/M for the 24 h and 48 h serum starvation and 24 h serum replenishment (24 h 0.1% FBS following 24 h 10% FBS) experiments were shown along with ± standard deviation. *indicates a significant difference from the 10% FBS group while # refers to a significant difference between the 48 h 0.1% FBS and 24 h replenishment groups at $P \leq 0.05$

	24h 10% FBS	24h 0.1% FBS	48h 10% FBS	48h 0.1% FBS	24h Replenishment
G0/G1	85.40 ± 0.12	91.48 ± 0.26*	85.24 ± 0.86	91.22 ± 0.02*	80.66 ± 0.28#*
S	6.44 ± 0.60	2.25 ± 0.05*	5.90 ± 0.28	2.32 ± 0.42*	8.27 ± 0.24#*
G2/M	8.35 ± 0.49	6.35 ± 0.21*	8.75 ± 1.04	6.28 ± 0.45	11.25 ± 0.11#

Time-dependent response to serum replenishment

Serum replenishment for 6 h was adequate for recovery of the cells from reduced cell viability caused by serum starvation (Fig. 5a, One-way ANOVA; $P \leq 0.001$), while the 24 h serum replenishment allowed for complete recovery of cell viability (Fig. 5b, One-way ANOVA; $P \leq 0.001$).

The expressions of *tyms, mybl2*, *mcm7* and *pcna* were significantly different in at least one of the groups tested (i.e., 24 or 48 h serum-starved (0.1% FBS) or control (10% FBS) groups). A Two-way ANOVA showed that the starvation associated decrease observed in the expression of these genes was significant and independent of time (Fig. 6a, Two-way ANOVA according to log2 transformed fold change difference; *tyms*, $P_{dose} = 0.001$, $P_{time} = 0.558$; *mybl2*, $P_{dose} \leq 0.001$, $P_{time} = 0.212$; *pcna*, $P_{dose} = 0.001$, $P_{time} = 0.276$; *mcm7*, $P_{dose} \leq 0.001$, $P_{time} = 0.576$). Serum-starved cells at both the 24 and 48 h showed significant decreases in the mRNA levels of *mybl2*, *mcm7* and *pcna* whereas that of *tyms* was only significantly different from the 24 h 10% FBS

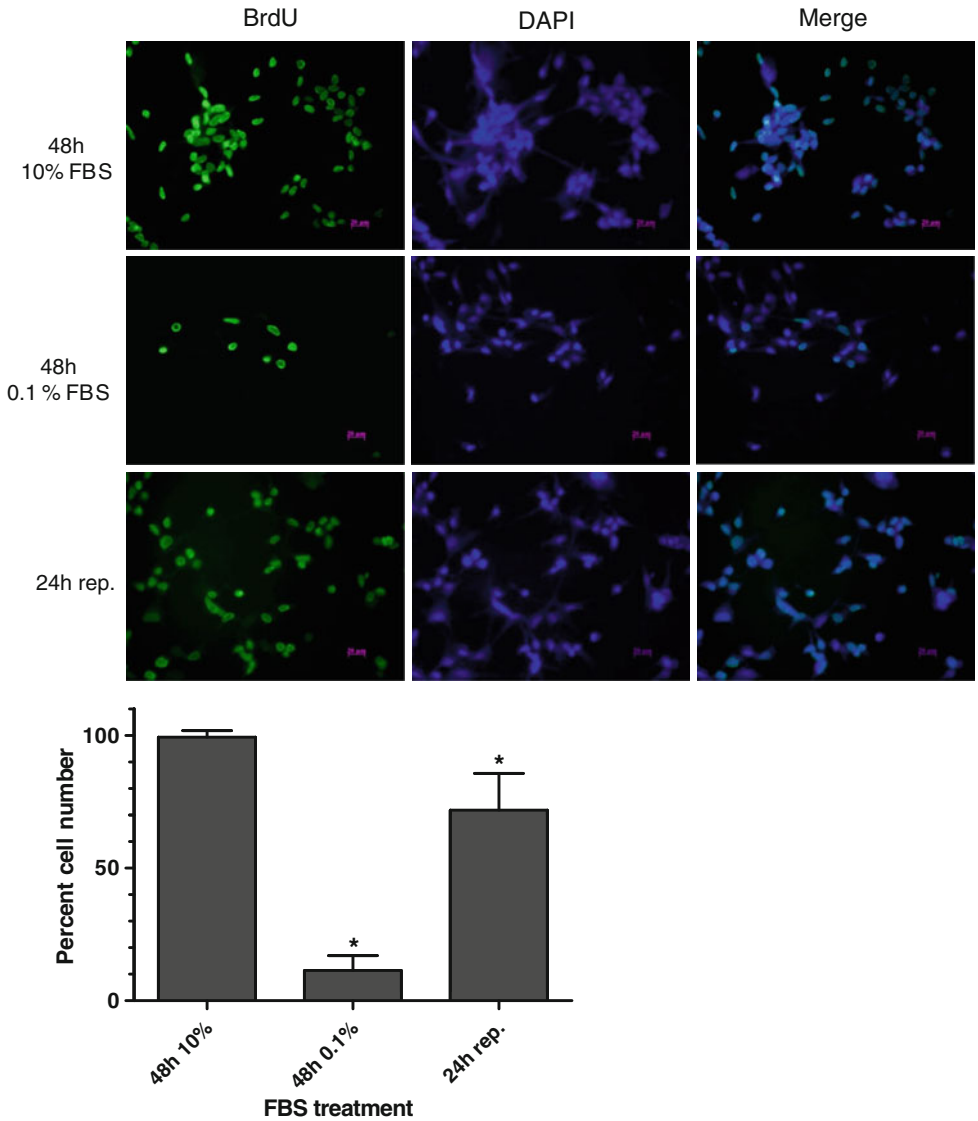

Fig. 3 BrdU incorporation in serum-starved/replenished ZF4 cells. ZF4 cells treated with 0.1% FBS for 48 h were compared with those in control group cultured in 10% FBS for 48 h. In the replenishment group, cells recovered from starvation for 24 h (24 h rep.). Nuclei were stained by DAPI where BrdU incorporating cell nuclei were observed using the green filter. *Scale bars* represented a distance of 20 µm and the magnification was set at ×40. The mean number of BrdU positive nuclei corrected against the total number of nuclei per group was plotted, whiskers correspond to ± std. *indicates significance at $P \leq 0.05$

treatment. Strikingly, the serum replenishment restored expression to the original levels (Fig. 6a). The transcriptional change in *ctgf*, on the other hand, was time-dependent, yet highly significant at both the 24 and 48 h time-points (Fig. 6a, Two-way ANOVA according to log2 transformed fold change difference; *ctgf*, $P_{\text{dose}} \leq 0.001$, $P_{\text{time}} = 0.01$). The level of protein expression of Mcm7 also exhibited a significant decrease under the 24 h serum starvation regime (Fig. 6b) suggesting that changes observed at the mRNA levels also were reflected in the protein synthesis.

We also quantitatively analyzed the change in mRNA levels for cells replenished with 10% FBS for 6 h upon serum starvation (Fig. 7a). The expression levels of *tyms*, *mybl2* and *pcna* increased significantly with serum at 6 h as they did at 24 h, while the expression of *ctgf* was unaffected. The change in *mcm7* mRNA expression approached significance at 6 h while it was highly significant at 24 h. *mcm7* gene expression was also studied at the protein level. There was a consistent decrease in the Mcm7 protein levels by serum starvation at the 24 and 48 h treatments. The serum replenishment, particularly for the 24 h, was highly effective in restoring the original level of protein expression for Mcm7 (Fig. 7b).

Discussion

In the present study, we investigated the expression patterns of the zebrafish orthologs of the known mammalian direct or secondary targets of E2F transcription factors; *tyms*, *mybl2*, *pcna*, *ctgf* and *mcm7* in serum-starved/replenished ZF4 cells using real-time qRT-PCR analyses. Moreover, we demonstrated for the first time that in ZF4 cells serum starvation and replenishment treatments

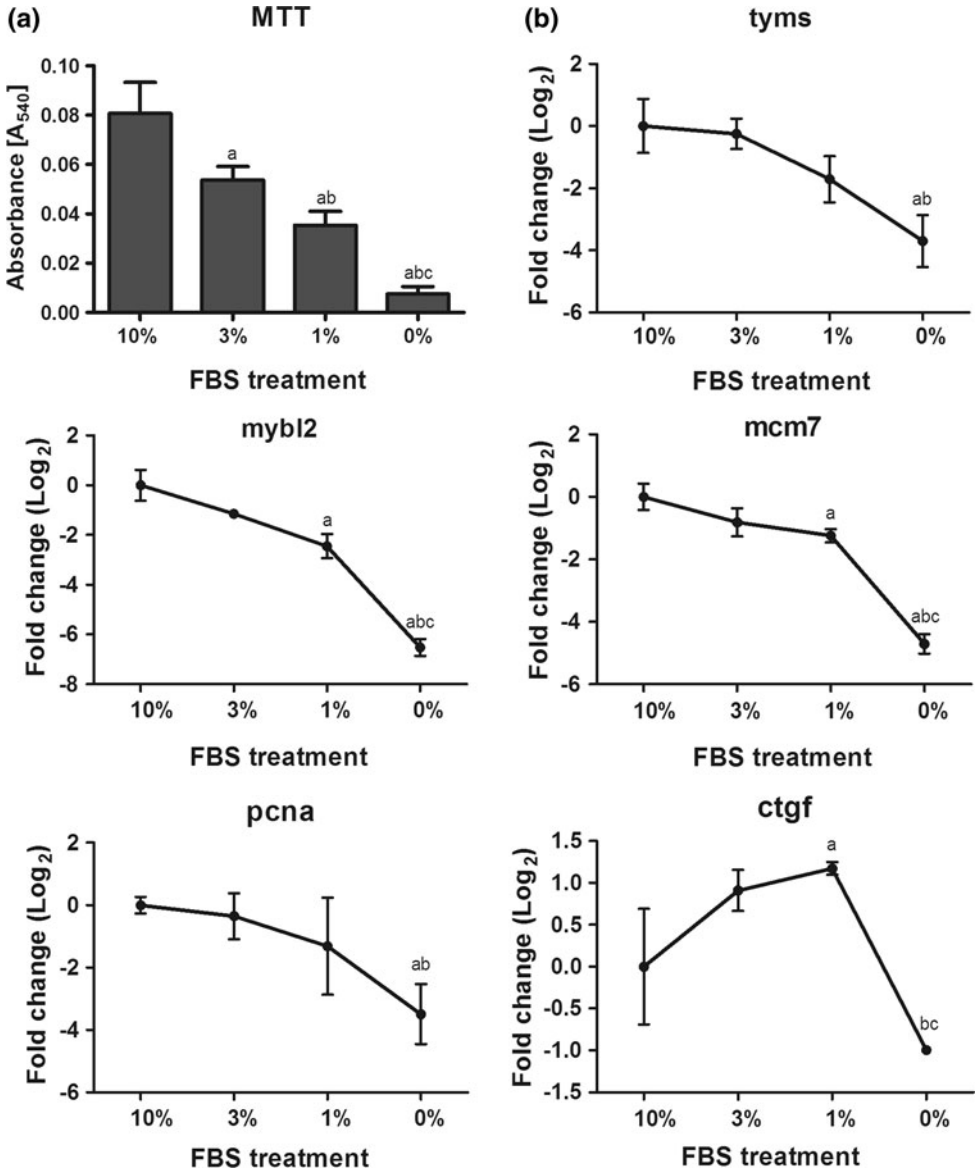

Fig. 4 Dose-dependency of ZF4 serum response **a** MTT assay results of ZF4 grown under different serum concentrations, i.e., 0, 1, 3 or 10% FBS-supplemented media, for 24 h, **b** The real-time qRT-PCR results of selected genes in response to serum starvation. The ZF4 cells were grown in 0, 1, 3 or 10% FBS-supplemented media for 24 h. Data were normalized to the 10% FBS treatment. (One-way ANOVA according to log2 transformed fold change difference; *tyms*, $P = 0.024$; *mybl2*, $P \leq 0.001$; *pcna*, $P = 0.077$; *ctgf*, $P = 0.013$; *mcm7*, $P = 0.001$). [a, b, c] refers to significance at $P \leq 0.05$ from 10, 3, and 1% FBS, respectively, based on Fisher's multiple comparisons

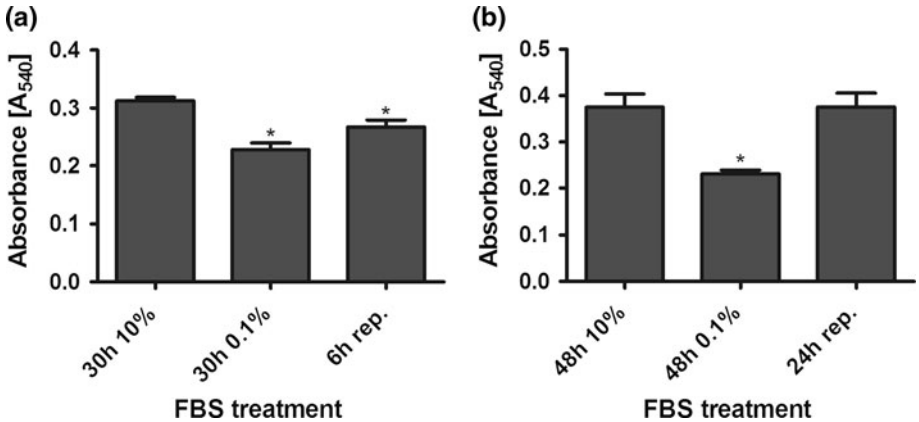

Fig. 5 MTT assay results of serum-replenished cells **a** 6 h serum replenishment with 10% FBS (6 h rep.), **b** 24 h serum replenishment with 10% FBS (24 h rep.). * refers to significance at $P \leq 0.05$ where only a two-group comparison was made

significantly affected cells at different cell cycle phases in ZF4 cells. In the literature, there are a few examples showing that the serum response might be dose- and time-dependent [20, 43–46]. Herein we showed that the effects of serum starvation/replenishment on gene expression of E2F target orthologs were dose- and time-dependent in

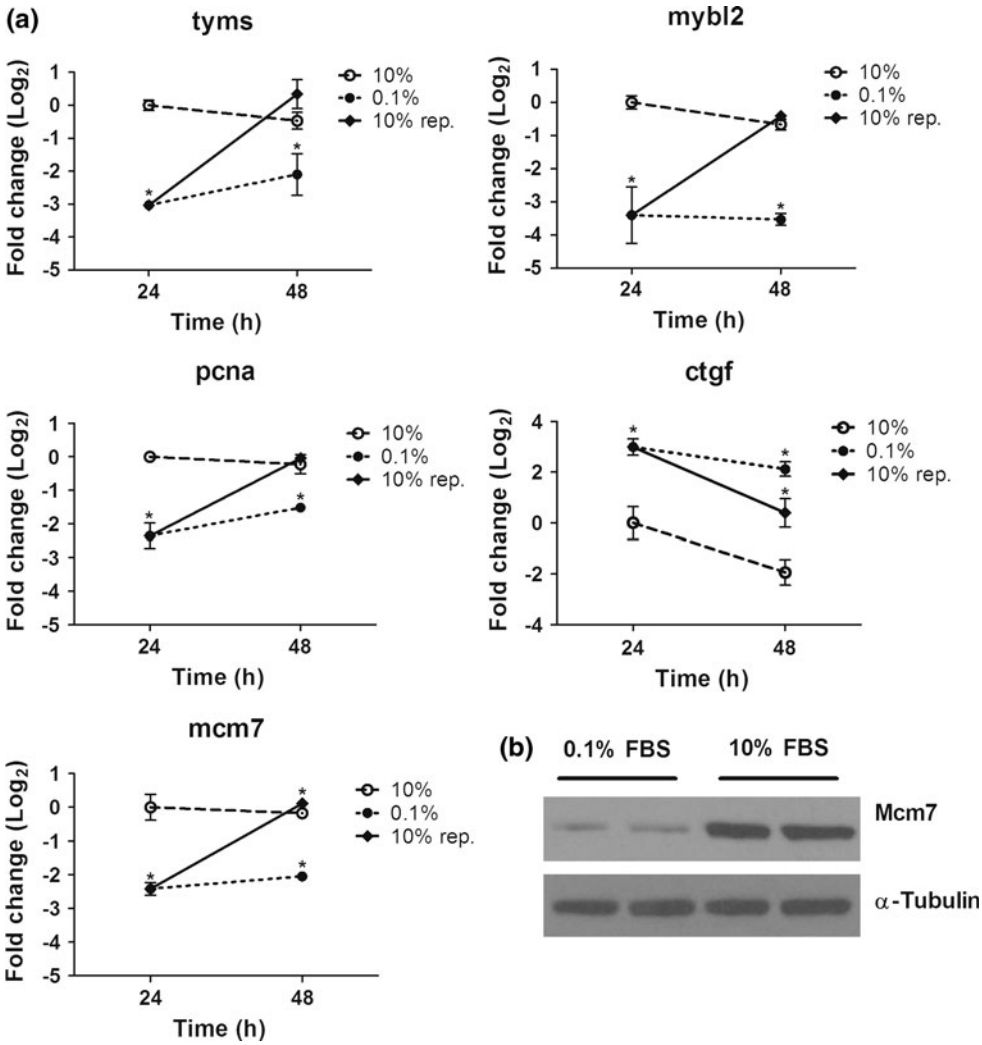

Fig. 6 **a** The real-time qRT-PCR results of selected genes under 24 h serum replenishment regime. The real-time qRT-PCR results were normalized to the 24 h 10% FBS-treatment. One-way ANOVA results were, for 24 h: *tyms*, $P = 0.002$; *mybl2*, $P = 0.031$; *pcna*, $P = 0.013$, *ctgf*, $P = 0.028$; *mcm7*, $P = 0.015$ for 48 h: *tyms*, $P = 0.03$; *mybl2*, $P \leq 0.001$; *pcna*, $P = 0.005$; *ctgf*, $P = 0.007$; *mcm7*, $P \leq 0.001$. * refers to a group significantly different from the 10% control at the given time point. 10% rep. refers to the treatment of 24 h serum starvation followed by 24 h serum replenishment. **b** Protein expression of Mcm7 gene for the 24 h starved versus asynchronized ZF4 cells

ZF4 cells. In the present study, ZF4 cells arrested at G0/G1 upon serum starvation served as a model for quiescence. The transcriptional serum responses of the selected genes were in accord with findings from studies performed with mammalian cells.

The characterization of proliferative properties of ZF4 cells in response to serum

The asynchronized mammalian fibroblasts accumulate in G0/G1 phase of the cell cycle after serum starvation and reenter the S phase upon serum stimulation [47]. Herein, we described the cellular serum response of the ZF4 fibroblast cell line, a frequently used in vitro model in zebrafish [48–52]. Our results showed that (a) the serum starvation significantly decreased the viable cell numbers, which were later on rescued by serum replenishment; and (b) the viable ZF4 cells that have survived the serum starvation stopped proliferating and became arrested at the G0/G1 phase of cell cycle as previously shown in the mammalian fibroblast cells [47, 53–56]. Most strikingly, the serum-replenished cells reentered the S phase of cell cycle and commenced proliferation as the mammalian fibroblasts [57]. The high percentage of ZF4 cells entering the S phase after serum stimulation represented a likely synchronization process caused by serum starvation.

The expression response to serum fluctuations in ZF4 cells in comparison to that in mammals

Recent studies emphasize the role of comparative models in understanding the functional conservation of important cell signaling components. Our findings indicated that the zebrafish *pcna*, *tyms*, *mcm7* and *mybl2* genes were highly responsive to serum in the direction observed in mammalian cells [18, 20, 21].

The real-time qRT-PCR results showed that the zebrafish *pcna* expression was highly responsive to serum starvation and replenishment as previously shown for mouse embryonic fibroblast (MEF) [21, 58] and in the Chinese

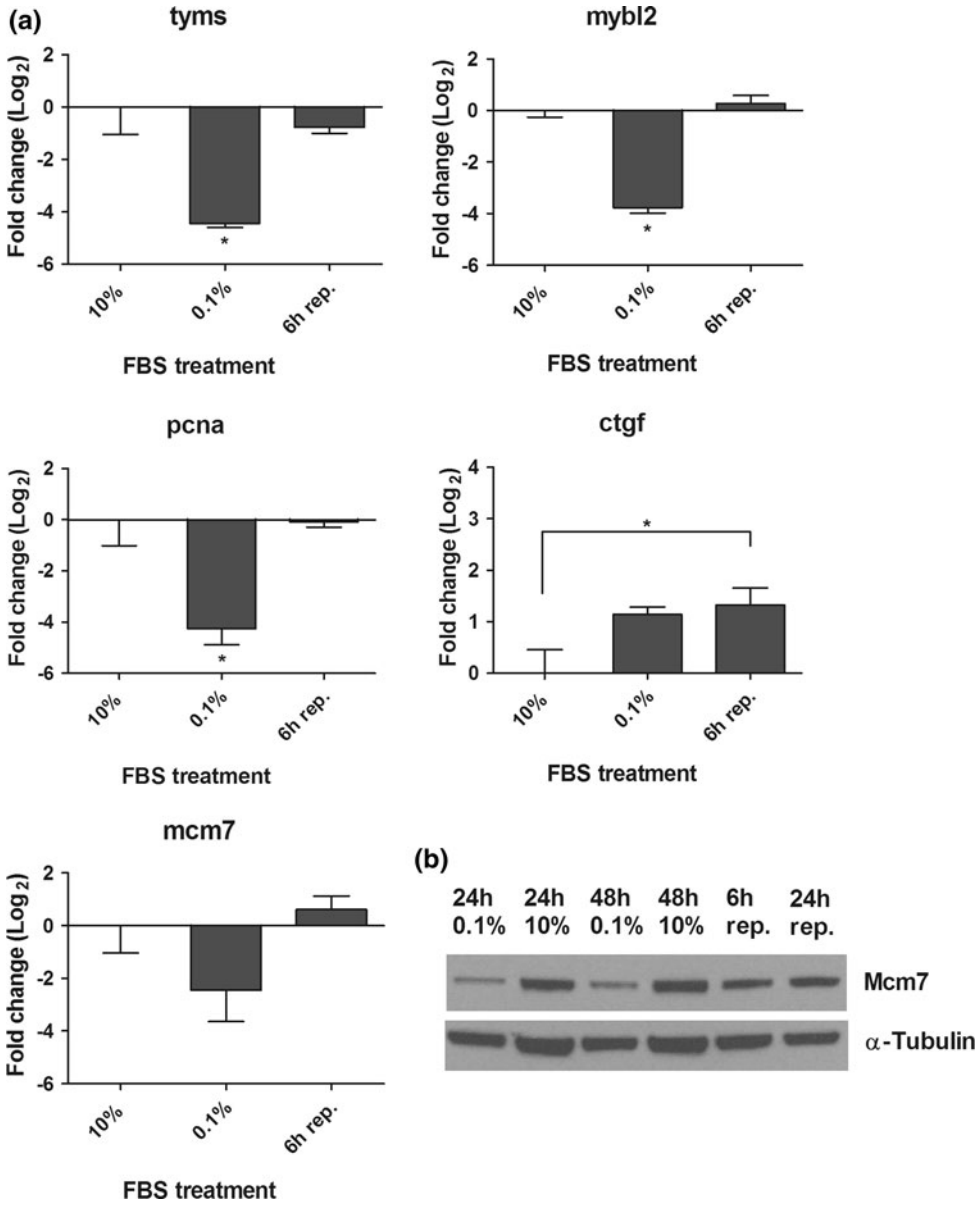

Fig. 7 **a** The real-time qRT-PCR results for 6 h serum-replenished cells. The real-time qRT-PCR results were normalized to the 30 h 10% FBS-treatment. One-way ANOVA results were: *tyms*, $P = 0.011$; *mybl2*, $P = 0.001$; *pcna*, $P = 0.014$; *ctgf*, $P = 0.053$; *mcm7*, $P = 0.095$. The significance at $P \leq 0.05$ was represented as * **b** Protein expression of Mcm7 under serum starvation and replenishment

hamster ovary cell line (CHOK1) [59]. Serum starvation resulted in a highly significant decrease in the expression of the zebrafish *mybl2* in our study as in the normal human bone marrow fibroblasts [19]. We observed an increase in *mybl2* expression starting from 6 h of serum stimulation. In quiescent mouse embryonic fibroblast cells the *Mybl2* mRNA increased gradually after serum stimulation starting at the 12 h of serum replenishment [60].

We detected a significant increase in the *tyms* expression even within 6 h of serum replenishment. A similar increase in the *Tyms* expression following serum stimulation also was observed in NIH 3T3 cells between the 8 h-10 h of serum treatment [61] yet in mouse 3T6 fibroblasts, the Tyms activity showed a decrease under long-term serum starvation [31].

We have found that *ctgf* expression was serum-responsive in a time-dependent manner and most drastically increased at the 24 h 0.1% FBS treatment; the expression was reduced following serum recovery between the 6–24 h. Human *CTGF* expression also responded to serum in the same direction based on the GEO microarray expression profile analysis of human T98G cells [11]. Stimulatory effects of serum starvation on zebrafish *ctgf* thus suggest significant functional conservation across vertebrate taxa. However, the direction of the effects might be species as well as cell-type specific, as in contrast to our findings, a decrease in the *CTGF* mRNA was detected after serum stimulation in a human mesangial cell line [22].

In mouse and human cells, the prolonged quiescent state caused the downregulation of all the mcm proteins

(MCM2-7), while reentering into the G1 phase led to upregulation of Mcm transcripts and proteins [18]. We have shown that *mcm7* expression in ZF4 cells was serum-responsive, while the changes observed at the mRNA levels were linearly reflected at the protein level; similar changes were observed in the serum-stimulated MCF7 breast cancer cells [62]. The mRNA and protein expression of the *mcm7* gene have been characterized in zebrafish model for the first time in the present study. However, to better assess the correlation between mRNA and protein levels under serum starvation, further studies focusing on other genes are needed.

In conclusion, our findings indicated that the level of serum incorporated into the media has been reflected in the cellular characteristics as well as the transcriptional response the ZF4 cells displayed, suggesting a significant dose- and time-dependency in serum response. Furthermore, we showed that the fibroblast serum response in zebrafish was highly similar to that in mammals with respect to the genes under investigation. Serum starvation was as effective at the 48th h as at the 24th h for *pcna*, *tyms*, *mcm7*, *mybl2*, and *ctgf*. 6 h serum replenishment experiments on the other hand showed that only the expression of *tyms*, *mybl2* and *pcna* returned to near normal levels while the *mcm7* and *ctgf* responded to increased serum levels relatively later. Moreover, the mammalian orthologs of the selected genes examined in the present study are known to be regulated by different transcription factors in addition to E2F family members, i.e., c-myc, p53, and/or TFG-β2 [16, 63–68]. It will be interesting to further test whether these zebrafish orthologs also share common transcriptional regulatory signatures.

Acknowledgments This study was supported by research Grants from TUBITAK, The Scientific and Technological Research Council of Turkey (to MO and OK). This project partially contributes to the fulfillment of requirements for the PhD thesis of Ceren Sucularli. We thank to Dr. Ali O. Gure, Ms. Rana Nelson and Dr. Michelle Adams for valuable suggestions in reviewing the manuscript. We also kindly thank Gizem Olmezer for her help in protein preparation for western blot analysis.

References

1. Lam SH, Wu YL, Vega VB, Miller LD, Spitsbergen J et al (2006) Conservation of gene expression signatures between zebrafish and human liver tumors and tumor progression. Nat Biotechnol 24:73–75
2. Linhart C, Elkon R, Shiloh Y, Shamir R (2005) Deciphering transcriptional regulatory elements that encode specific cell cycle phasing by comparative genomics analysis. Cell Cycle 4:1788–1797
3. Ung CY, Lam SH, Gong Z (2009) Comparative transcriptome analyses revealed conserved biological and transcription factor target modules between the zebrafish and human tumors. Zebrafish 6:425–431
4. Feitsma H, Cuppen E (2008) Zebrafish as a cancer model. Mol Cancer Res 6:685–694
5. Stoletov K, Klemke R (2008) Catch of the day: zebrafish as a human cancer model. Oncogene 27:4509–4520
6. Lee LM, Seftor EA, Bonde G, Cornell RA, Hendrix MJ (2005) The fate of human malignant melanoma cells transplanted into zebrafish embryos: assessment of migration and cell division in the absence of tumor formation. Dev Dyn 233:1560–1570
7. Porter D, Weremowicz S, Chin K, Seth P, Keshaviah A, et al. (2003) A neural survival factor is a candidate oncogene in breast cancer. Proceedings of the National Academy of Sciences of the USA 100: 10931–10936
8. Nakashima T, Kuratomi Y, Yasumatsu R, Masuda M, Koike K et al (2005) The effect of cyclin D1 overexpression in human head and neck cancer cells. Eur Arch Otorhinolaryngol 262:379–383
9. Chang HY, Sneddon JB, Alizadeh AA, Sood R, West RB et al (2004) Gene expression signature of fibroblast serum response predicts human cancer progression: similarities between tumors and wounds. PLoS Biol 2:E7
10. He S, Salas-Vidal E, Rueb S, Krens SF, Meijer AH et al (2006) Genetic and transcriptome characterization of model zebrafish cell lines. Zebrafish 3:441–453
11. Cam H, Balciunaite E, Blais A, Spektor A, Scarpulla RC et al (2004) A common set of gene regulatory networks links metabolism and growth inhibition. Mol Cell 16:399–411
12. Dorner D, Vlcek S, Foeger N, Gajewski A, Makolm C et al (2006) Lamina-associated polypeptide 2alpha regulates cell cycle progression and differentiation via the retinoblastoma-E2F pathway. J Cell Biol 173:83–93
13. Weinberg RA (1996) E2F and cell proliferation: a world turned upside down. Cell 85:457–459
14. Johnson DG, Schwarz JK, Cress WD, Nevins JR (1993) Expression of transcription factor E2F1 induces quiescent cells to enter S phase. Nature 365:349–352
15. Kherrouche Z, Blais A, Ferreira E, De Launoit Y, Monte D (2006) ASK-1 (apoptosis signal-regulating kinase 1) is a direct E2F target gene. Biochem J 396:547–556
16. Bracken AP, Ciro M, Cocito A, Helin K (2004) E2F target genes: unraveling the biology. Trends Biochem Sci 29:409–417
17. Arata Y, Fujita M, Ohtani K, Kijima S, Kato JY (2000) Cdk2-dependent and -independent pathways in E2F-mediated S phase induction. J Biol Chem 275:6337–6345
18. Stoeber K, Tlsty TD, Happerfield L, Thomas GA, Romanov S et al (2001) DNA replication licensing and human cell proliferation. J Cell Sci 114:2027–2041
19. Scortechini AR, Rupoli S, Piccinini G, Luchetti MM, Cantori I et al (1999) Expression of c-myb and B-myb oncogenes on myelofibrotic marrow fibroblasts. Leuk Lymphoma 33:295–304
20. Le Francois BG, Maroun JA, Birnboim HC (2007) Expression of thymidylate synthase in human cells is an early G(1) event regulated by CDK4 and p16INK4A but not E2F. Br J Cancer 97:1242–1250
21. Hurford RK Jr, Cobrinik D, Lee MH, Dyson N (1997) pRB and p107/p130 are required for the regulated expression of different sets of E2F responsive genes. Genes Dev 11:1447–1463
22. Goppelt-Struebe M, Hahn A, Iwanciw D, Rehm M, Banas B (2001) Regulation of connective tissue growth factor (ccn2; ctgf) gene expression in human mesangial cells: modulation by HMG CoA reductase inhibitors (statins). Mol Pathol 54:176–179
23. Leung AY, Leung JC, Chan LY, Ma ES, Kwan TT et al (2005) Proliferating cell nuclear antigen (PCNA) as a proliferative marker during embryonic and adult zebrafish hematopoiesis. Histochem Cell Biol 124:105–111
24. Dickmeis T, Plessy C, Rastegar S, Aanstad P, Herwig R et al (2004) Expression profiling and comparative genomics identify a

conserved regulatory region controlling midline expression in the zebrafish embryo. Genome Res 14:228–238
25. Chiou MJ, Chao TT, Wu JL, Kuo CM, Chen JY (2006) The physiological role of CTGF/CCN2 in zebrafish notochond development and biological analysis of the proximal promoter region. Biochem Biophys Res Commun 349:750–758
26. Stern HM, Murphey RD, Shepard JL, Amatruda JF, Straub CT et al (2005) Small molecules that delay S phase suppress a zebrafish bmyb mutant. Nat Chem Biol 1:366–370
27. Shepard JL, Amatruda JF, Stern HM, Subramanian A, Finkelstein D, et al. (2005) A zebrafish bmyb mutation causes genome instability and increased cancer susceptibility. Proceedings of the National Academy of Sciences of the USA 102: 13194–13199
28. Ryu S, Holzschuh J, Erhardt S, Ettl AK, Driever W (2005) Depletion of minichromosome maintenance protein 5 in the zebrafish retina causes cell-cycle defect and apoptosis. Proceedings of the National Academy of Sciences of the USA 102: 18467–18472
29. Ryu S, Driever W (2006) Minichromosome maintenance proteins as markers for proliferation zones during embryogenesis. Cell Cycle 5:1140–1142
30. Golling G, Amsterdam A, Sun Z, Antonelli M, Maldonado E et al (2002) Insertional mutagenesis in zebrafish rapidly identifies genes essential for early vertebrate development. Nat Genet 31:135–140
31. Navalgund LG, Rossana C, Muench AJ, Johnson LF (1980) Cell cycle regulation of thymidylate synthetase gene expression in cultured mouse fibroblasts. J Biol Chem 255:7386–7390
32. Muller H, Bracken AP, Vernell R, Moroni MC, Christians F et al (2001) E2Fs regulate the expression of genes involved in differentiation, development, proliferation, and apoptosis. Genes Dev 15:267–285
33. Rozen S, Skaletsky H (2000) Primer3 on the WWW for general users and for biologist programmers. Methods Mol Biol 132:365–386
34. Thompson JD, Higgins DG, Gibson TJ (1994) CLUSTAL W: improving the sensitivity of progressive multiple sequence alignment through sequence weighting, position-specific gap penalties and weight matrix choice. Nucleic Acids Res 22:4673–4680
35. Tamura K, Dudley J, Nei M, Kumar S (2007) MEGA4: molecular evolutionary genetics analysis (MEGA) software version 4.0. Mol Biol Evol 24:1596–1599
36. Driever W, Rangini Z (1993) Characterization of a cell line derived from zebrafish (*Brachydanio rerio*) embryos. In Vitro Cell Dev Biol Anim 29A:749–754
37. Krishan A (1975) Rapid flow cytofluorometric analysis of mammalian cell cycle by propidium iodide staining. J Cell Biol 66:188–193
38. Abu Bakar MF, Mohamad M, Rahmat A, Burr SA, Fry JR (2010) Cytotoxicity, cell cycle arrest, and apoptosis in breast cancer cell lines exposed to an extract of the seed kernel of Mangifera pajang (bambangan). Food Chem Toxicol 48:1688–1697
39. Senturk S, Gursoy-Yuzugullu O, Cingoz B, Akcali KC, Ozturk M (2010) Transforming growth factor-beta induces senescence in hepatocellular carcinoma cells and inhibits tumor growth. Hepatology 52:966–974
40. Pfaffl MW (2001) A new mathematical model for relative quantification in real-time RT-PCR. Nucleic Acids Res 29:e45
41. Tang R, Dodd A, Lai D, McNabb WC, Love DR (2007) Validation of zebrafish (*Danio rerio*) reference genes for quantitative real-time RT-PCR normalization. Acta Biochim Biophys Sin (Shanghai) 39:384–390
42. McCurley AT, Callard GV (2008) Characterization of housekeeping genes in zebrafish: male-female differences and effects of tissue type, developmental stage and chemical treatment. BMC Mol Biol 9:102
43. Zhang J, Wang X, Zhao Y, Chen B, Suo G et al (2006) Neoplastic transformation of human diploid fibroblasts after long-term serum starvation. Cancer Lett 243:101–108
44. Yabuta N, Onda H, Watanabe M, Yoshioka N, Nagamori I et al (2006) Isolation and characterization of the TIGA genes, whose transcripts are induced by growth arrest. Nucleic Acids Res 34:4878–4892
45. Quinn CM, Kagedal K, Terman A, Stroikin U, Brunk UT et al (2004) Induction of fibroblast apolipoprotein E expression during apoptosis, starvation-induced growth arrest and mitosis. Biochem J 378:753–761
46. Osabe M, Sugatani J, Takemura A, Kurosawa M, Yamazaki Y et al (2009) Up-regulation of CAR expression through Elk-1 in HepG2 and SW480 cells by serum starvation stress. FEBS Lett 583:885–889
47. Brooks RF (1976) Regulation of fibroblast cell cycle by serum. Nature 260:248–250
48. Schaaf MJ, Koopmans WJ, Meckel T, van Noort J, Snaar-Jagalska BE et al (2009) Single-molecule microscopy reveals membrane microdomain organization of cells in a living vertebrate. Biophys J 97:1206–1214
49. Roca FJ, Mulero I, Lopez-Munoz A, Sepulcre MP, Renshaw SA et al (2008) Evolution of the inflammatory response in vertebrates: fish TNF-alpha is a powerful activator of endothelial cells but hardly activates phagocytes. J Immunol 181:5071–5081
50. Luo Y, Weng S, Wang Q, Shi X, Dong C et al (2009) Tiger frog virus can infect zebrafish cells for studying up- or down-regulated genes by proteomics approach. Virus Res 144:171–179
51. Hu MC, Gong HY, Lin GH, Hu SY, Chen MH et al (2007) XBP-1, a key regulator of unfolded protein response, activates transcription of IGF1 and Akt phosphorylation in zebrafish embryonic cell line. Biochem Biophys Res Commun 359:778–783
52. Burns JC, Friedmann T, Driever W, Burrascano M, Yee JK (1993) Vesicular stomatitis virus G glycoprotein pseudotyped retroviral vectors: concentration to very high titer and efficient gene transfer into mammalian and nonmammalian cells. Proceedings of the National Academy of Sciences of the USA 90: 8033–8037
53. Khammanit R, Chantakru S, Kitiyanant Y, Saikhun J (2008) Effect of serum starvation and chemical inhibitors on cell cycle synchronization of canine dermal fibroblasts. Theriogenology 70:27–34
54. Goissis MD, Caetano HV, Marques MG, de Barros FR, Feitosa WB et al (2007) Effects of serum deprivation and cycloheximide on cell cycle of low and high passage porcine fetal fibroblasts. Reprod Domest Anim 42:660–663
55. de Barros FR, Goissis MD, Caetano HV, Paula-Lopes FF, Peres MA et al (2010) Serum starvation and full confluency for cell cycle synchronization of domestic cat (*felis catus*) foetal fibroblasts. Reprod Domest Anim 45:38–41
56. Dalman A, Eftekhari-Yazdi P, Valojerdi M, Shahverdi A, Gourabi H et al (2009) Synchronizing cell cycle of goat fibroblasts by serum starvation causes apoptosis. Reprod Domest Anim 45(5):e46–e53
57. Kues WA, Anger M, Carnwath JW, Paul D, Motlik J et al (2000) Cell cycle synchronization of porcine fetal fibroblasts: effects of serum deprivation and reversible cell cycle inhibitors. Biol Reprod 62:412–419
58. Fukami-Kobayashi J, Mitsui Y (1999) Overexpression of proliferating cell nuclear antigen in mammalian cells negates growth arrest by serum starvation and cell contact. Jpn J Cancer Res 90:286–293
59. Liu YC, Chen GS, Liu WL, Wen SF (1995) Estimation of PCNA mRNA stability in cell cycle by a serum-deprivation method. J Cell Biochem 57:641–646

60. Tominaga K, Magee DM, Matzuk MM, Pereira-Smith OM (2004) PAM14, a novel MRG- and Rb-associated protein, is not required for development and T-cell function in mice. Mol Cell Biol 24:8366–8373
61. Saxena UH, Powell CM, Fecko JK, Cacioppo R, Chou HS et al (2009) Phosphorylation by cyclin C/cyclin-dependent kinase 2 following mitogenic stimulation of murine fibroblasts inhibits transcriptional activity of LSF during G1 progression. Mol Cell Biol 29:2335–2345
62. Rizwani W, Alexandrow M, Chellappan S (2009) Prohibitin physically interacts with MCM proteins and inhibits mammalian DNA replication. Cell Cycle 8:1621–1629
63. Xu J, Morris GF (1999) p53-mediated regulation of proliferating cell nuclear antigen expression in cells exposed to ionizing radiation. Mol Cell Biol 19:12–20
64. Scian MJ, Carchman EH, Mohanraj L, Stagliano KE, Anderson MA et al (2008) Wild-type p53 and p73 negatively regulate expression of proliferation related genes. Oncogene 27:2583–2593
65. Lee Y, Chen Y, Chang LS, Johnson LF (1997) Inhibition of mouse thymidylate synthase promoter activity by the wild-type p53 tumor suppressor protein. Exp Cell Res 234:270–276
66. Leask A, Holmes A, Black CM, Abraham DJ (2003) Connective tissue growth factor gene regulation. Requirements for its induction by transforming growth factor-beta 2 in fibroblasts. J Biol Chem 278:13008–13015
67. Iizuka N, Tsunedomi R, Tamesa T, Okada T, Sakamoto K et al (2006) Involvement of c-myc-regulated genes in hepatocellular carcinoma related to genotype-C hepatitis B virus. J Cancer Res Clin Oncol 132:473–481
68. Guida T, Salvatore G, Faviana P, Giannini R, Garcia-Rostan G et al (2005) Mitogenic effects of the up-regulation of minichromosome maintenance proteins in anaplastic thyroid carcinoma. J Clin Endocrinol Metab 90:4703–4709